Technical Report Documentation Page

1. Report No. FHWA/TX-12/0-6435-1	2. Government Accession No.	3. Recipient's Catalog No.
4. Title and Subtitle CAM Mix Design with Local Aggregates		5. Report Date October 2011
		6. Performing Organization Code
7. Author(s) Andre de Fortier Smit, Sivaram Prasad, Jorge Prozzi, and Maghsoud Tahmoressi		8. Performing Organization Report No. 0-6435-1
9. Performing Organization Name and Address Center for Transportation Research The University of Texas at Austin 1616 Guadalupe Street, Suite 4.202 Austin, TX 78701		10. Work Unit No. (TRAIS) 11. Contract or Grant No. 0-6435
12. Sponsoring Agency Name and Address Texas Department of Transportation Research and Technology Implementation Office P.O. Box 5080 Austin, TX 78763-5080		13. Type of Report and Period Covered Technical Report September 2009–August 2011 14. Sponsoring Agency Code
15. Supplementary Notes Project performed in cooperation with the Texas Department of Transportation and the Federal Highway Administration.		

16. Abstract

This study provides revised mix design recommendations for crack attenuating mixtures (CAM) with local aggregates. The use of lower quality aggregates is cost beneficial but limits the application of these mixes in terms of reduced performance. Aggregate guidelines and aggregate quality criteria are provided to enhance the rutting and cracking performance of these mixes. It is recommended to design CAM using local aggregates with the Superpave gyratory compactor with the capability of measuring the shear stress of the mix during compaction. CAM is susceptible to shear failure if the voids in these mixes become over filled with asphalt to the point that hydrostatic pore pressures negate the shear strength of the mix. CAM with local aggregates are very susceptible to stripping and the Hamburg wheel tracking test is useful test to mobilize pore pressures in these mixtures to address stripping. The overlay tester is used to evaluate cracking performance but was found to be highly variable even for these fine-graded mixes. The semi-circular bending (SCB) test is evaluated as an alternative and SCB cracking parameters are recommended to characterize cracking performance. The overall poor performance of CAM with local aggregates prompted the evaluation of alternative rut-resistant crack attenuating mixes, specifically stone-matrix asphalt (SMA) and coarse matrix high binder (CMHB) stone skeleton mixes using local aggregates, which were less susceptible to rutting and cracking compared to CAM. The mix design recommendations as well as aggregate guidelines and quality criteria provided in the report are based on laboratory investigations and field validation is strongly recommended before implementation.

17. Key Words crack attenuating asphalt, Hamburg, overlay, aggregate, criteria guidelines		18. Distribution Statement No restrictions. This document is available to the public through the National Technical Information Service, Springfield, Virginia 22161; www.ntis.gov.	
19. Security Classif. (of report) Unclassified	20. Security Classif. (of this page) Unclassified	21. No. of pages 198	22. Price

Form DOT F 1700.7 (8-72) Reproduction of completed page authorized

CAM Mix Design with Local Aggregates

Andre de Fortier Smit
Sivaram Prasad
Jorge Prozzi
Maghsoud Tahmoressi

CTR Technical Report:	0-6435-1
Report Date:	October 2011
Project:	0-6435
Project Title:	CAM Mix Design with Local Materials in Texas
Sponsoring Agency:	Texas Department of Transportation
Performing Agency:	Center for Transportation Research at The University of Texas at Austin

Project performed in cooperation with the Texas Department of Transportation and the Federal Highway Administration.

Center for Transportation Research
The University of Texas at Austin
1616 Guadalupe Street, Suite 4.202
Austin, TX 78701

www.utexas.edu/research/ctr

Disclaimers

Author's Disclaimer: The contents of this report reflect the views of the authors, who are responsible for the facts and the accuracy of the data presented herein. The contents do not necessarily reflect the official view or policies of the Federal Highway Administration or the Texas Department of Transportation (TxDOT). This report does not constitute a standard, specification, or regulation.

Patent Disclaimer: There was no invention or discovery conceived or first actually reduced to practice in the course of or under this contract, including any art, method, process, machine manufacture, design or composition of matter, or any new useful improvement thereof, or any variety of plant, which is or may be patentable under the patent laws of the United States of America or any foreign country.

Engineering Disclaimer

NOT INTENDED FOR CONSTRUCTION, BIDDING, OR PERMIT PURPOSES.

Research Supervisor: Jorge A. Prozzi

Acknowledgments

The authors acknowledge the project director Michael Bolin and Richard Izzo from the Flexible Pavements branch for their input and direction during the course of the project. The authors thank Tommy Blackmore from the Austin District office for his input and assistance with the collection of materials as well as providing design information for the CMHB mixture evaluated in the study. Finally, the authors are grateful to TxDOT personnel in the districts that provided information and photographs on the performance of CAM in their districts.

Table of Contents

List of Figures

List of Tables

Chapter 1. Introduction

1.1 Background

Crack Attenuating Mixtures (CAM) are relatively new hot-mix asphalt (HMA) applications being used by the Texas Department of Transportation (TxDOT). These mixtures are fine graded, designed using relatively small stone-sized aggregates and screenings with a high asphalt content, specifically for retarding the reflective cracking in thin asphalt overlays without sacrificing rutting resistance. CAM is being designed and constructed in Texas based on special specifications (e.g., TxDOT Special Specification 3165). These mixtures are *typically* placed as an interlayer between an existing pavement and a surface layer of HMA, although they are increasingly being placed as a thin surface course overlaying concrete and asphalt pavements to mitigate reflection cracking.

As a surface course, a CAM mix must be designed to meet both demanding structural and functional requirements. These mixes must have sufficient tensile strength to resist cracking, adequate stability to resist shear failure and permanent deformation, as well as skid resistance, particularly when used on roads with higher posted speed limits. These requirements and the fact that CAM, being a fine graded mix, generally lacks surface macrotexture, suggest the use of high quality aggregates. This together with the high asphalt binder content used for these mixes results in an expensive mix, more so if aggregates available from local sources do not meet current specification requirements, which would require the shipment of acceptable aggregates from other states or TxDOT Districts.

When used as an interlayer or as a surface course on roads with low posted speeds, it may be justified to relax the aggregate quality requirements relating to durability and friction, as currently specified for CAM. Furthermore, when used as a surface course, CAM will not necessarily be subjected to the same structural demands required of stone-matrix asphalt (SMA) or porous friction course (PFC) mixtures and consequently the aggregate quality requirements for CAM should be less stringent compared to these mixes. Evidence does suggest, however, that CAM designed with high quality aggregates and PG 76-22 binders are performing well, whereas some problems are reported for CAM designed using local aggregates and softer PG 70-22 binders. Hence, TxDOT saw the need to optimize the use of local aggregate resources to cost-effectively improve the performance of CAM in Texas.

1.2 Study objectives

The primary objective of the research was to develop a mix design procedure for CAM with local aggregates. These mixes should comply with minimum acceptance criteria in terms of rutting and cracking. Local aggregate sources should be surveyed and characterized for potential use with CAM towards the development of aggregate quality criteria and guidelines to optimize performance.

Secondary objectives include the development of alternative mix design strategies that could serve as CAM and the development of alternative laboratory tests to characterize the rutting and cracking performance of CAM.

1.3 Methodology and scope

The focus of this study was on the use of CAM designed using local aggregates. By characterizing the critical properties of the aggregates influencing the rutting and cracking response of CAM, it will be possible to predict or anticipate the relative performance of CAM designed using local or new aggregate sources. A laboratory program was designed to characterize the properties of aggregates for CAM from local sources. Current performance criteria in terms of the Hamburg Wheel Tracker (HWT) using Tex-242-F and the Overlay Tester (OT) using Tex-248-F were initially applied to assess current mix design procedures (TxDOT Special Specification 3165) and to develop minimum aggregate quality criteria. During the application of the research, it became evident that the current HWT and OT requirements may be too stringent; they eliminated most if not all of the local aggregates as potential candidates for use with CAM. For this reason, the researchers re-evaluated the HWT and OT requirements for CAM with local aggregates and relaxed these requirements, based on an overall assessment of the laboratory performance of the CAM tested as part of the study. Revised mix design and minimum aggregate quality criteria and guidelines were developed based on the relaxed performance requirements.

1.4 Report outline

The report is divided into the following chapters documenting the various aspects addressed in the study:

Literature review: The report begins by reviewing previous CAM studies including its initial development and current mix design procedures with emphasis on local aggregate characterization and how aggregate properties influence mixture performance. The aggregate imaging system (AIMS) was used as part of the study to measure the angularity and texture of the local aggregates used and the AIMS concepts and criteria are briefly discussed. An overview of thin HMA overlays using fine mixes is provided. Literature on test protocols suitable for CAM performance testing is reviewed, including a summary of alternative tests used in the study to characterize the rutting and cracking performance of CAM.

Project survey: Mix design information of current CAM projects constructed in Texas was reviewed and compiled into a database. Projects from this database in north, south, and central Texas were selected and visually surveyed. Results and commentary of the surveys and a discussion of the performance of existing CAM projects in Texas are provided.

Aggregate characterization: The identification of potential local aggregate sources and their characterization thorough numerous aggregate tests and properties are then discussed. In addition to aggregate properties currently specified for CAM, the study evaluated the AIMS properties of the aggregates and the filler component through Rigden voids and hydrometer tests.

CAM mix design: The mix design procedures previously recommended for CAM were evaluated and efforts to refine these procedures to incorporate local aggregates in CAM are provided. The research investigated the influence of high binder content on the volumetric properties of the CAM mixtures and the shear strength component of these mixes. Recommendations for volumetric mix design criteria are provided in this regard.

Performance testing: The mix design criteria as well as aggregate quality criteria and guidelines as provided in the report are based on the rutting and cracking performance of the CAM tested as part of the study using the HWT and overlay tester respectively. The results of

these laboratory performance tests provided key information regarding the failure mechanisms of CAM and in particular the sensitivity of these mixes to moisture damage.

Alternative designs: To address the overall poor performance of CAM with local aggregates as observed during the study, various alternative CAM with local aggregates—as well as strategies to improve the performance of CAM—were investigated, including the use of stone skeleton mixes, blending local aggregates with high quality aggregates, and optimizing the filler-binder component of the mixes. Although the alternative mixtures as evaluated do not strictly classify as CAM per TxDOT Special Specification 3165, these mixtures show promise and are briefly discussed as alternatives for crack attenuating mixes that may be deployed in thin overlays.

Aggregate quality criteria and guidelines: Criteria and guidelines were developed based on a correlation study of the aggregates and CAM mixes tested as part of the study by relating the aggregate properties of the mixes tested to their rutting and cracking performance. In addition to aggregate properties typically specified for HMA, recommendations regarding AIMS parameters and filler characteristics to optimize mixture performance are provided.

Semi-circular bending test: A by-product of the research study included the further development of the semi-circular bending (SCB) test to evaluate the cracking performance of CAM. Results of SCB testing at ambient and low temperatures are provided and the benefits of the SCB are briefly discussed.

Finally, conclusions are drawn and recommendations are made towards the continued development and use of CAM with local aggregates in Texas.

Chapter 2. Literature Review

2.1 CAM development

CAM essentially evolved from rich bottom layer (RBL) mixes designed specifically to attenuate reflective cracking resulting from high tensile stresses that develop beneath asphaltic layers in pavement structures. If the stiffness of an underlying layer is lower than the overlay, the latter will bend under loading. Repeated flexure of the layer will eventually lead to crack initiation and ultimately propagation. Thus, the life of the pavement can be extended by ensuring that the layer subjected to tensile stresses is sufficiently resilient to resist these. If the tensile strength of this layer is considerably greater than the tensile stresses to which it will be subjected, then theoretically the pavement will last ad infinitum—the perpetual pavement concept. This was the purpose of Kock's "Strata" product and RBL, a derivative thereof, is one such underlying layer that provides the required resilience and resists the crack propagation.

In Texas, RBL is designed using Item 344 (TxDOT, 2004) as a fine dense-graded Superpave Type F mix to 98% maximum theoretical density at 50 gyrations in the Superpave gyratory compactor (SGC). The gradations of these mixes do not pass below the Superpave reference or restricted zone and are only designated as the bottom lift on perpetual pavement designs. Typically these mixes have 0.5 percentage extra asphalt above optimum to improve tensile strength.

As indicated, RBL was developed in part as a surrogate for the propriety asphalt mixture Strata, developed by Koch Pavement Solutions. Strata is composed of a highly polymer-modified asphalt binder at a high asphalt content in a dense fine aggregate mixture, resulting in an elastic and impermeable layer typically used as an interlayer. This mix has a percentage passing the #4 sieve ranging from 80–100 percent. Zhou and Scullion (2005) report on the performance of SH3 in Houston that included a Strata section. They found that, while Strata has superior crack retarding properties, it has very low rutting resistance.

CAM was originally applied in the Bryan District (TxDOT, 2007). CAM has similar properties as RBL except that it has an additional rut resistance that qualifies the mix for surface applications as well. While the rut-resistant CAM can be used in lieu of RBL, the reverse is not recommended, as RBL is not validated for rutting performance. CAM development thus grows from the need for a mixture that is also rut resistant. Current TxDOT Special Specifications 3165 for CAM include the same HWT requirements imposed on Item 341 and 344 mixes.

2.2 Fine-graded mixes for thin overlays

The stringent rutting requirements imposed on CAM are a result of these mixes being used as either surfaces courses or interlayers beneath relatively thin overlays. The use of CAM as a thin overlay option is attractive from a cost point of view. The use of fine-graded HMA for thin overlay applications is well documented. Thin-lift HMA layers placed at thicknesses ranging from approximately 0.25 inch to 2 inch have been used for maintenance and rehabilitation applications (Acott, 1992). Typically, thin-lift HMA layers have been used to extend pavement life, improve ride quality, correct surface defects (leveling), improve safety characteristics, enhance appearance, and reduce road-tire noise. In order to provide the required road user safety and riding comfort, the following engineering properties of the surfacing layers are essential (Oliver, 1998; Pretorius et al., 2004):

- **Skid resistance:** Low speed skid resistance is determined mainly by the resistance to polishing under traffic of the coarse aggregate used in the surfacing. High-speed skid resistance is determined both by surface texture (a coarse texture, helped further by interconnected interlayer voids allowing water to escape from beneath vehicle tires and so minimizes the risk of hydroplaning) and the polish resistance of the coarse aggregate.
- **Spray generation:** Water on the road surface is atomized by the action of vehicle tires and the droplets are thrown into the air. This results in considerable volumes of water being deposited on vehicle windscreens and as a general fog surrounding fast moving vehicles. Both these effects reduce driver visibility. Spray can be almost entirely eliminated if water can be rapidly drained through the surfacing (interconnected voids) and is expelled at the sides. Some relief can also be obtained by having high surface voids, i.e., good surface texture.
- **Road noise:** Porous surfaces, originally developed for spray reduction, have been found to appreciably reduce tire noise. Where a conventional porous (open-graded) asphalt cannot be used, then a surfacing with a negative texture is preferable. Surfacings where positive surface texture is obtained by particles protruding upwards from the surface (such as sprayed seals) produce noisier surfacings. The level of noise tends to increase as the maximum size of the aggregate particle and macrotexture of the surface increases.
- **Conspicuity of road markings and glare/reflection:** The two factors of importance for good conspicuity are texture and color. If surface texture is too low, a film of water may cover the markings during rain. Specular reflection from the water film surface can then totally obscure the markings.
- **Windscreen breakage:** Windscreen breakage is almost exclusively related to surface seals that can be eliminated using thin HMA applications.
- **Smooth ride:** The ride smoothness that can be achieved is controlled largely by the curvature of the underlying layers but may be smoothed or leveled using thin HMA overlays.
- **Low construction and maintenance costs:** The factors important in the construction cost of a surfacing are the price of the materials and the thickness of the layer. Maintenance costs are determined by the properties and durability of the surfacing, hence the trend to use high quality materials that provide improved surfacing performance, and to control costs by reducing layer thickness.
- **Avoidance of delays during construction and maintenance:** Emulsion seals can, under certain conditions, take many hours to build sufficient strength to avoid stone loss under traffic. HMA can generally be traveled on within an hour.
- **Fuel consumption and wear and tear on vehicle:** The main factor affecting vehicle wear and tear is pavement roughness (texture and undulations).

The Texas array of asphalt mixes that could be used for relatively thin overlays includes a number of alternatives, each with specific applications. These are summarized in Table 2.1,

which shows the nominal maximum aggregate size of the mixes (NMAS) and the breakdown in composition for the stone, sand (passing #8 sieve), and dust (passing #200 sieve) fractions of dense-graded HMA, Superpave (SP), coarse matrix high binder (CMHB), and SMA used in Texas. The minimum design VMA criteria and recommended minimum thicknesses of layers of these mixes are also shown.

Table 2.1 Composition of TxDOT fine dense-graded, CMHB, and SMA mixes

Spec Item	341		344		346		
Mix	Type D	Type F	SP D	CMHB F	SMA D	SMA F	SMAR F
NMAS	1/2"	3/8"	1/2"	1/2"	3/4"	3/8"	3/8"
Stone, %	54–65	52–62	33–68	73–83	72–84	70–80	73–83
Sand, %	33–39	36–41	30–57	12–18	8–16	12–16	12–18
Dust, %	2–7	2–7	2–10	5–9	8–12	8–14	5–9
Min VMA, %	15	16	16	15	17.5	17.5	19
Min Thick, in	1.5	1.25	1.25	1.5	1.5	1.25	1.5

The minimum asphalt layer thickness is dictated by the maximum size of the aggregate. Minimum lift thickness should be at least three times the nominal maximum aggregate size to ensure the aggregate can align during compaction to achieve the required density and also to ensure that the mix is impermeable. The thickness of the layer does influence its compactability. Too thin a mat does not always have sufficient workability. The Texas mixes shown in Table 2.1 are designed to a target laboratory-modeled density of 96 percent and consequently have relatively low asphalt contents. In contrast, CAM is currently designed to 98 percent with a minimum asphalt content of 7 percent.

Ultra-thin HMA mixes are developed in Michigan, Georgia, and Maryland, the gradations of which are shown in Table 2.2. The lift thickness of these mixes is generally less than 1 inch. The mix-design requirements of the Michigan DOT include a Marshall air void of 4.5 to 5.0 percent, VMA $\leq$ 15.5 percent, a maximum fines/binder ratio of 1.4, a Marshall flow (0.01 inch) of 8 to 16, and a Marshall stability of at least 1,200 lbs (Walubita et al., 2008). Superpave mixes with #4 NMAS constitute a potential option for very thin HMA overlays equal to or less than 1 inch (Cooley et al., 2002). Georgia DOT has used a No. 4 NMAS HMA mix for over 30 years for low volume highways and leveling purposes with reportedly good field performance results; it is placed in thin lift thicknesses of not more than 1 inch (Cooley et al., 2002). Maryland uses these mixes as part of their pavement management program for typical lift thickness of 0.75 to 1 inch with excellent rutting and cracking resistance performance (Cooley et al., 2002).

Ohio has been evaluating a mix termed *Smooth Seal* that was originally developed as an alternative to the propriety *Ralumac* product. Smooth Seal is recommended for aged and raveled pavements with no appreciable rutting, which are also structurally adequate with no fatigue damage. The latter is critical because Smooth Seal is not used to retard reflection cracks and is not promoted as a CAM. Smooth Seal has two types: A and B. The Type B mix is similar to the TxDOT CAM mix but with a lower asphalt content, about 6.5 percent. The Type A mix is a lot finer than TxDOT CAM with 80 to 100 percent passing the #16 sieve. The high skid and good

reported performance of these mixes may warrant further investigation for possible application in Texas.

Table 2.2 Gradation bands for various thin overlay mixes (Cooley et al., 2002)

Sieve Size (English/metric)		Michigan	Georgia	Maryland	Ohio Smooth Seal Type A	Ohio Smooth Seal Type B
NMAS		#4	#4	#4 or 3/8"	3/8"	1/2"
3/4"	**19.0**	100	100	100	100	100
½"	**12.5**	100	100	100	100	100
⅜"	**9.5**	99–100	90–100	100	100	95–100
#4	**4.75**	75–95	75–95	80–100	95–100	85–95
#8	**2.36**	55–75	60–65	36–76	90–100	53–63
#16	**1.18**	-	-	-	80–100	37–47
#30	**0.6**	25–45	-	-	60–90	25–35
#50	**0.3**	-	20–50	-	30–65	9–19
#100	**0.15**		-	-	10–30	-
#200	**0.075**	3–8	4–12	2–12	3–10	3–8

The National Center for Asphalt Technology (NCAT) has investigated the use of fine dense-graded HMA and SMA mixtures for use as maintenance options in thin overlays (Cooley et al., 2002a and 2002b; Cooley and James, 2003; Cooley and Brown, 2003). These mixtures have a nominal maximum aggregate size of 4.75 mm (#4 sieve or 0.2 inches) and are somewhat finer than the current CAM specified in Texas having 20 to 50 percent passing the #30 sieve. Binder contents used for these mixes ranged from 6 to 7.5 percent. The fine-graded HMA mixes evaluated by NCAT are based on those used by Georgia and Maryland. Voids in the mineral aggregate (VMA) requirements of these mixes are established to ensure sufficient asphalt at a design air void of 4 percent.

In one study, NCAT evaluated the use of manufactured aggregate screenings as the sole aggregate portion of an HMA. Factors included in this research study were aggregate screenings type, binder type, fiber, and design air void content. They concluded that mixes having screenings as the sole aggregate portion can be successfully designed in the laboratory for some screenings but may be difficult for others. Binder contents of the screening mixes evaluated ranged from 4.5 to 8.5 percent. Screenings type, the existence of cellulose fiber, and design air void content all significantly affected optimum binder content of the mix, although screenings type had the largest impact. They found that mixes designed at 4 percent air voids had significantly higher rut depths than mixes designed at 5 or 6 percent air voids. This important finding suggests fine-graded HMA designed at too low air voids may be susceptible to shear flow and rutting.

In another study, Cooley and Brown (2003) reported on the design of fine SMA mixes. They concluded that these could successfully be designed in the laboratory and were a viable option for thin overlays. The fine SMA mixes offered excellent rut resistance and were less permeable than conventional SMA mixes, at similar air void levels, and thus should be more durable. Generally, fibers or modified binders are used to prevent drainage of the mixes with relatively high binder content (6 to 8.3 percent) during transport and placing. High quality fine

aggregates with polymer modified binders (Walubita et al., 2008) are recommended for overlay SMA mixes to ensure adequate skid resistance, ride quality, and durability. The German experience, where SMA was first developed, indicates a service life of up to 18 years for thin SMA overlay surfacing (Belin, 1998).

NovaChip, which originated in France in the 1980s, is a proprietary and trademarked thin pavement management HMA mix that was initially developed to increase skid resistance and to seal old pavement surfaces. In the USA, it is licensed through Koch Materials, Inc. (now SemGroup Inc.), but currently non-trademarked names and mix-design specifications, such as ultrathin HMA wearing course or ultrathin bonded wearing course, are in use. *NovaChip* is a gap-graded HMA mix with high quality aggregates typically with 3/8-inch NMAS and a minimum of 5 percent asphalt content, placed usually in thin lift applications with a thickness ranging from 0.75 inch to 1 inch. The gap grading ensures good stone on stone contact which improves the rut resistance and skid performance. The *NovaChip* application process consists of applying a thin liquid polymer modified membrane followed by the HMA mix application. The reported expected service life of *NovaChip* is at least 10 years (Uhlmeyer, 2003; Cooper and Mohammad, 2004). The gap-graded *NovaChip* is a rut-resistant surface mix that with increased binder content could serve as a crack attenuating surface mix. However, it is relatively expensive and requires specially trained contractors.

2.3 CAM mix design

Walubita and Scullion (2008) report on the initial work done on the mix design and performance of CAM in Texas. They indicate the following mix design attributes required to improve thin HMA overlay performance and durability:

- Use of high modified (polymer) asphalt-binder content (6 to 8.5 percent) to improve cracking resistance and durability characteristics. Polymer modified binders such as PG 76-22S are also less temperature-susceptible.
- Use of high quality fine (such as granite or crushed gravel), preferably gap-graded aggregates with a good interlock and stone-on-stone contact matrix for improved rutting resistance and durability properties.
- Hard, durable, non-polishing, and well macro-textured low absorptive aggregates for improved skid resistance and surface texture.
- High VMA and low air voids (i.e., high compaction target density of around 98 percent) in the mix-design matrix. Low air voids minimizes water and air ingress, consequently minimizing the potential for moisture damage and binder oxidative aging. On top of promoting stone-on-stone contact, high VMA also decreases mix permeability.
- Increased asphalt-binder film thickness for improved durability and cracking resistance properties. Most literature recommends at least 10 to 12 micron film thickness.
- Use of additives such as lime (about 0.3 to 1.5 percent) and silicon dioxide to improve moisture damage and skid resistance, respectively.

The optimum asphalt content of CAM is determined as that which provides a laboratory bulk relative density of 98 percent of maximum theoretical density (Rice's density) after 50 gyrations using the SGC, which is similar to that of RBL. Special specification 3165 imposes a minimum asphalt content requirement of 7 percent and design VMA of 17 percent. CAM is compacted in the field to in-place air voids from 2 to 6 percent per specification requirement. Figure 2.1 illustrates the relative volumes of the aggregate fractions and binder making up a typical CAM mixture.

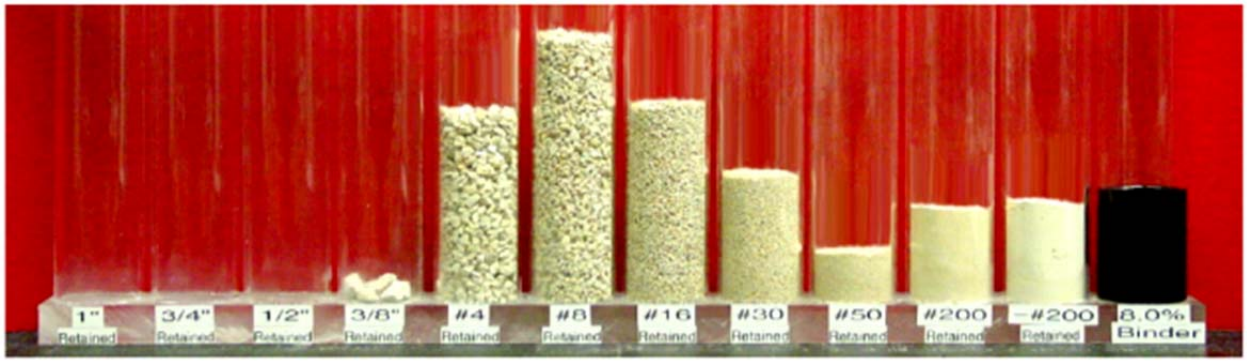

Figure 2.1 CAM volumetric components (courtesy of the TxDOT Flexible Pavements Branch)

The gradation of CAM, generally made by blending crushed screenings and Type F rock, is shown in Figure 2.2, which compares CAM to other fine mixtures used by TxDOT including RBL, SMA, and CMHB. Although not specified in the plans, a PG 76-22 binder is usually required to meet both the HWT and OT specification requirements. Surface Aggregate Class (SAC) A aggregate is not required unless CAM is used as a surface course and desired by the district; however, most contractors have found that SAC A aggregates are needed to meet the Hamburg and overlay requirements.

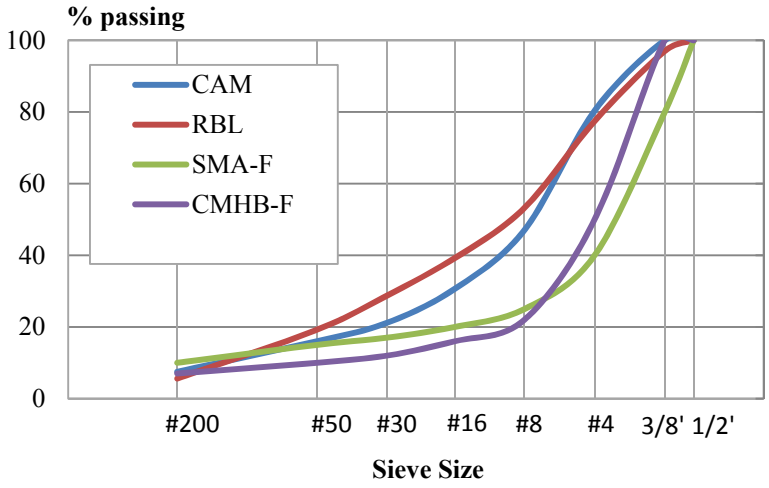

Figure 2.2 Gradations of fine-graded HMA used in Texas

The current mix design procedure for CAM is discussed by Walubita and Scullion (2008) as part of TxDOT Project 0-5598: *Development of Very Thin Overlay Systems*. This procedure attempts to select the optimum asphalt content (OAC) to balance the rutting and fatigue performance of the CAM mix. Specimens are compacted using 50 gyrations in the SGC at four trial AC contents. HWT and OT tests are performed using these specimens. A "window" of acceptable OAC is determined such that HWT rutting is less than 20,000 cycles (for PG 76-22 binders) and OT cycles exceed 750 for a 93 percent stress reduction. The selected OAC is then verified by compacting specimens to 93 percent density and repeating the HWT and OT tests. Zhou et al. (2007) report that this "balanced" procedure generally works for CAM design, although problems have been experienced when using lower PG binders and when designing with low quality aggregates such as absorptive limestone.

For the balanced design OAC selection, it is recommended, as a rule of the thumb, to pick the OAC at the third-quarter point of the window of acceptable OAC. Walubita and Scullion indicate that this OAC level reasonably allows for construction variability while satisfactorily meeting the HWT rutting and OT cracking requirements. They found it difficult in some cases (e.g., for limestone mixes) to meet the 98 percent target density at 50 gyrations during the balanced mix-design and OAC selection process and recommend reviewing and/or increasing the number of gyrations. They also found that while a limited number of mixes could not satisfy the OAC verification requirements at 93 percent density, it was apparent that satisfactory results were, in almost all cases, obtained at 96 percent density. Therefore, they recommend reviewing the verification compaction density as these mixes are typically compacted to a density of 96 percent in the field.

The current CAM mix design procedure does not address some important considerations usually accounted for in asphalt mixture design. Unlike the Superpave mixture design method, no consideration is given to design traffic or the temperature in which the mix will be used. For example, Prozzi et al. (2006) developed guidelines to adjust the design level (N_{des}) for Superpave mixes in Texas based on traffic and climate as shown in Figure 2.3. The low number of gyrations (50) currently specified for CAM suggests that these mixes are only appropriate for low to medium traffic volume roads. Furthermore, designing the mixture at 98 percent will ensure higher asphalt contents and low voids in the mix but may leave the mixture susceptible to flushing, shear failure and rutting if it is subjected to higher than expected volumes of traffic or temperatures.

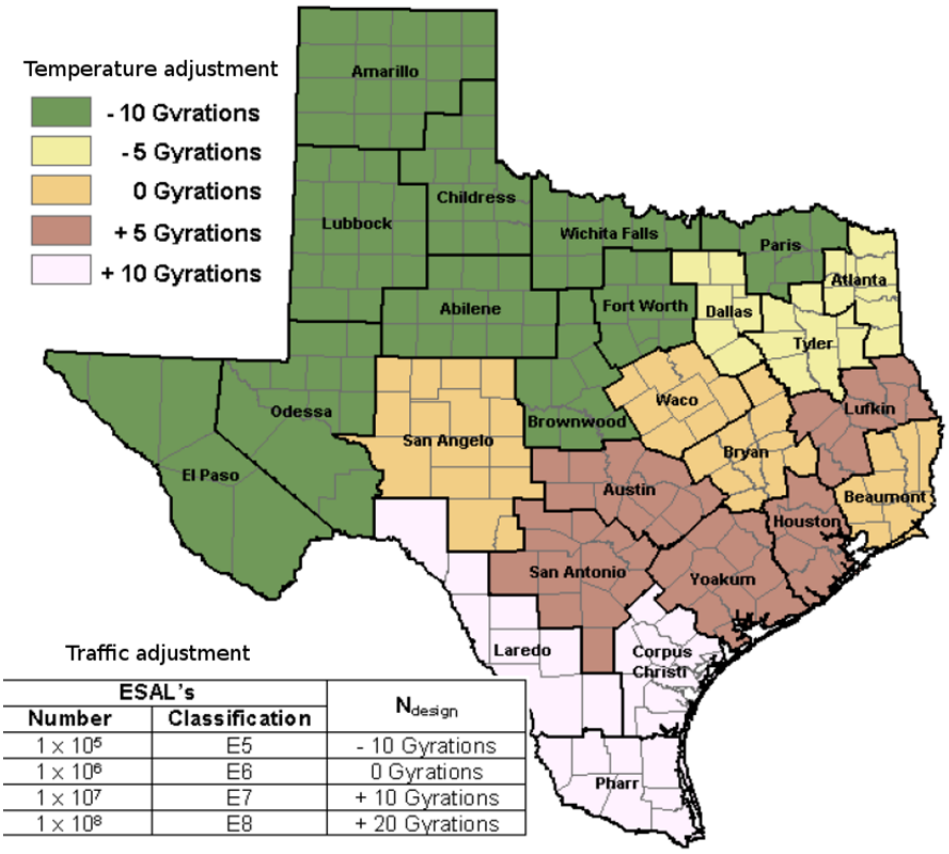

Traffic adjustment

ESAL's		N_{design}
Number	Classification	
1×10^5	E5	- 10 Gyrations
1×10^6	E6	0 Gyrations
1×10^7	E7	+ 10 Gyrations
1×10^8	E8	+ 20 Gyrations

Figure 2.3 Guidelines for selection of N_{des} for Texas districts (after Prozzi et al.,2006)

Low air voids may be desirable to prevent or reduce oxidative aging of the binder in the mix. This, however, leaves very little room to accommodate extra binder that may occur given that the thermal coefficient of expansion of asphalt binder is considerably larger than that of the aggregate. The voids in the mix must also accommodate possible higher than optimum AC contents, given the normal variability associated with the manufacturing process (±0.3%), as well as over-compaction during construction or further in-situ densification of the mixture in the field under traffic. Furthermore, while these problems may be addressed, to an extent, using stiffer binders, this may not be desirable and may negatively impact the workability and compactability of the mixture during construction.

Verifying the OAC at 93 percent is also questionable because these mixtures are compacted to between 94 and 98 percent in the field. Poor performance at 93 percent density does not necessarily translate to poor performance at 96 percent density although the opposite may be true.

CAM presents an interesting mixture design problem. These mixtures can be defined as dense-graded, clearly having sand skeletons as shown in the Richardson triangle in Figure 2.4. This diagram is used to classify asphalt mixtures based on the dust (filler), sand, and coarse aggregate components in the mix. Mixtures with coarse skeletons (such as SMA and PFC) generate aggregate interlock through stone-on-stone contact. Mixtures with filler skeletons have high filler contents.

Filler mixtures are rarely used in Texas and are more commonly used to accommodate studded tires or for dam cores, for example. The most commonly used mixtures are those with

sand skeletons, e.g., dense-graded and Superpave mixtures. CAM also falls into this category. The red line in the figure demarcates these three categories.

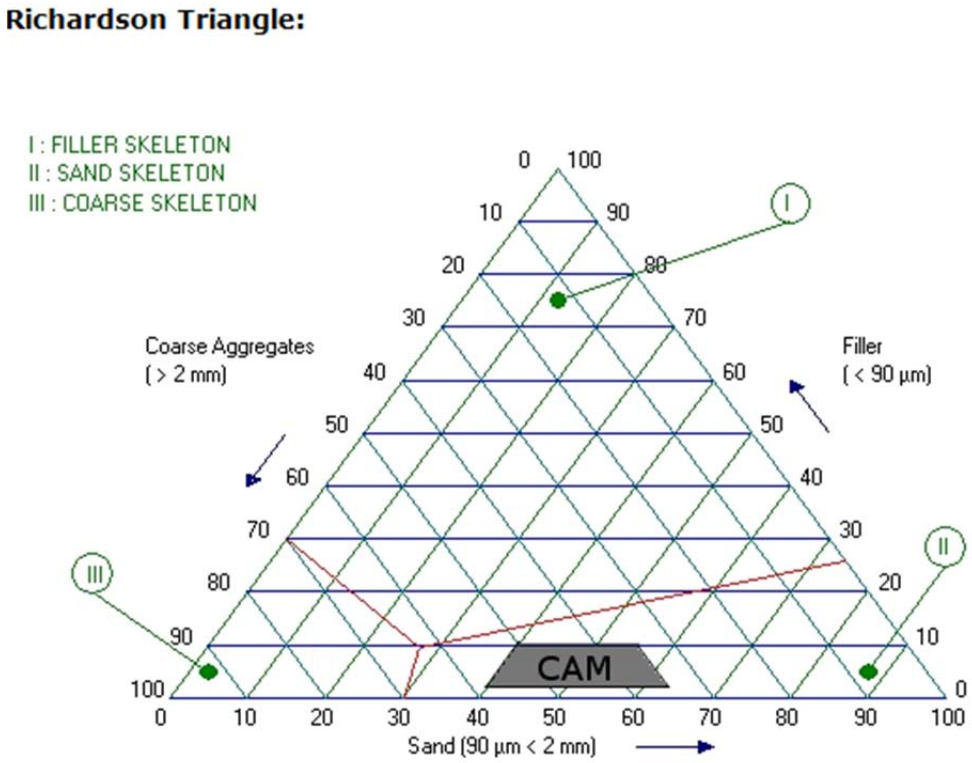

Figure 2.4 CAM aggregate structure

CAM mixtures develop strength or stability from sand-on-stone contact, which emphasizes the need for high fine aggregate angularity to resist permanent deformation. Given the relatively high AC contents of CAM, the coarse aggregates essentially "float" in a matrix/mastic of fine aggregates and the asphalt binder. Therefore, in these mixes, strength properties of coarse aggregates are generally less important, while the characteristics of the fine aggregates, the binder, and the mastic of the mix will control its rutting and fatigue properties. Higher AC and filler (passing #200 sieve) contents for CAM mixes also emphasizes the need to address filler-binder interaction to ensure durability and workability of these mixtures. A limit on maximum filler content will ensure durability by providing sufficient coating of binder over the aggregates.

2.4 Rutting performance

For CAM, the HWT is specified to ensure rutting performance. The required HWT performance is related to asphalt binder grade, thus for PG 76-22 binder, the maximum rutting after the application of 20,000 cycles must be less than 0.5 inches. Given the high binder contents used in CAM, cracking is generally not the primary concern for these mixtures, but rather rutting susceptibility and flushing. This was emphasized in the TxDOT 0-5598 study on thin overlays (Walubita and Scullion, 2008), where all of the mixtures evaluated passed OT criteria but some failed in the HWT.

As mentioned, the high binder contents and low air voids associated with CAM serve to mitigate reflective cracking but could increase the rutting susceptibility and flushing potential of the mixture. The HWT is used by TxDOT to assess HMA rutting and specifications have been established that limit allowable rutting depending on the PG grade of the binder in the mixture. A great number of specimens were tested as part of the project and the HWT can run for up to 7 hours on a single test. Therefore, it was deemed necessary to find an alternative test that could accurately and rapidly assess the rutting performance of CAM. Kim's rutting test was evaluated as an alternative to screen CAM mixes for rutting performance.

The concept behind Kim's rutting test is illustrated in Figure 2.5. In this test, a rod having a diameter (D) of 40 mm (1.6 inch) is pressed into a gyratory compacted specimen at a constant deformation rate. What makes the test interesting is that the loading head has rounded edges (radius, r of 10 mm) that generate both vertical compressive and shear stresses within the specimen in a manner analogous to the tire loading of an asphalt pavement. Specimens are conditioned under water at 60 °C (140 °F) for 30 minutes prior to testing.

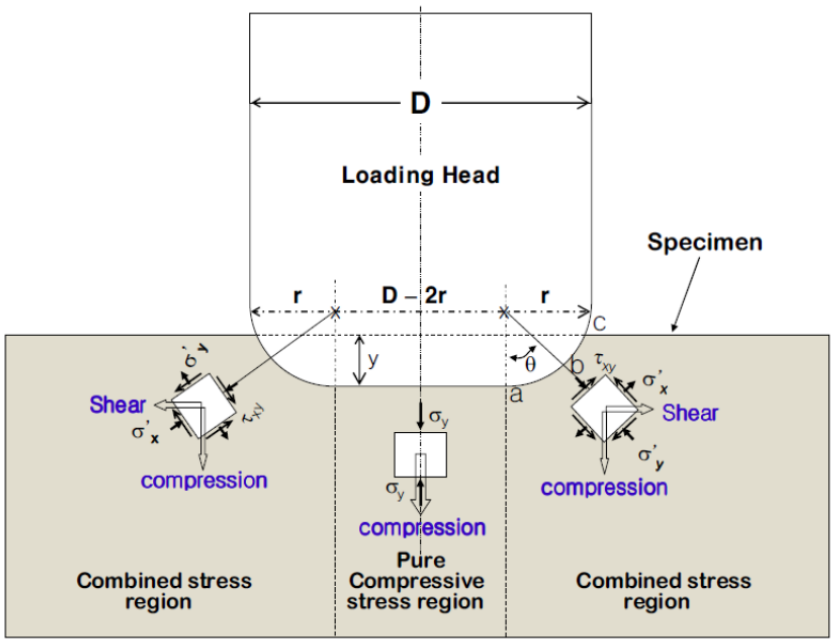

Figure 2.5 States of stress in specimen under loading head

Figure 2.6 shows a gyratory compacted specimen under loading in Kim's test as well as a typical specimen after testing, with the indentation of the loading head clearly visible on the top surface. Also evident are shear cracks distributed throughout the length of the specimen as the material is displaced under the loading head.

Figure 2.6 Kim's test setup and failed specimen

A deformation strength (SD) parameter is calculated based on the results of the test as a function of the deformation (y) into the specimen and the maximum compressive strength (P) of the specimen before it fails.

$$S_D = \frac{0.32P}{(10+\sqrt{20y-y^2})^2} \qquad \textbf{Eq. 2.1}$$

This rutting parameter (SD) has been shown to correlate very well with wheel tracking (WT) and asphalt pavement analyzer (APA) tests as shown in Figure 2.7.

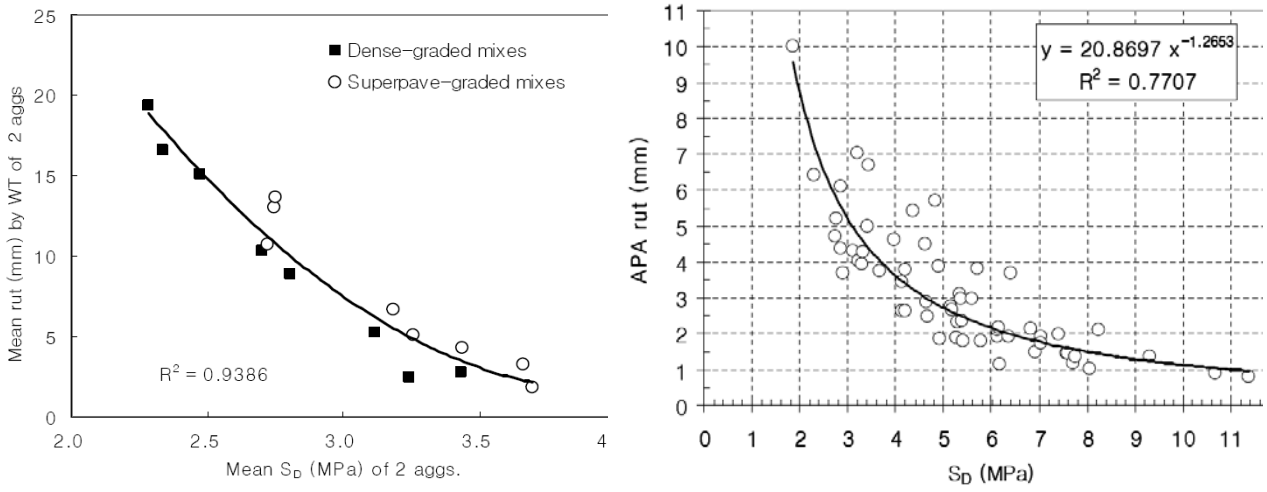

Figure 2.7 Comparison of Kim's SD with wheel tracking and APA test results

It must be emphasized that the use of Kim's test as part of the project was primarily for screening purposes. Kim's test takes a couple of minutes to perform compared to hours in the HWT. Kim's test may also be ideally suited for the testing of CAM mixtures because there are not large aggregates in the CAM mix and no stone-on-stone contact obstructing the passage of

the ram. As the loading head will essentially be pushed into a mastic rich mixture, in a sense it is not unlike a penetration test on asphalt binder, but on a much larger scale. Given the simplicity of the test and the fact that it can easily be used by TxDOT with current equipment (only a Marshall press is required), the test was further investigated as part of the study. Based on preliminary findings, recommendations to improve this test are also provided.

2.5 Cracking performance

Although rutting is considered the critical performance parameter for CAM, a study of the cracking potential of CAM was included in the project as it provides a unique opportunity to investigate the cracking mechanism and failure modes of asphalt mixes. Crack testing of CAM comprised of fine aggregate with high binder contents will result in reduced variability compared to conventional HMA, thus allowing a better assessment of cracking mechanisms and the crack potential of HMA in general. Therefore, the use of fine-graded CAM is deemed beneficial for developing and evaluating cracking test protocols, and it provided an opportunity to investigate the sensitivity of various cracking parameters as part of the study. These included parameters such as tensile strength, stress intensity factor, J-integral, and force-displacement area, which are discussed in more detail later in the report.

Reflective cracking is now arguably the most common distress associated with flexible pavements in Texas. This failure is commonly defined as the upward propagation of existing cracks from the base or the existing pavement into and through the newly constructed asphalt overlay. Reflective cracks are caused by a number of factors including traffic, temperature variations, and uneven soil movements. The site conditions, pavement structure, traffic volume, the climate, and the construction materials together decide which of these forces is predominant for a particular site. CAM mixtures were introduced to mitigate these types of failures. Evaluating the cracking performance of CAM is therefore a critical component of the research project. The cracking performance of CAM was assessed using the overlay tester, the indirect tension test, and the SCB strength test. These are briefly discussed.

2.5.1 Overlay tester

The OT was developed in the late 1970s to simulate the opening and closing of joints or cracks, which is one of the main forces inducing reflective cracking in asphalt overlays on jointed concrete pavements. Zhou and Scullion (2005) and Zhou et al. (2007) report that the results from the overlay tester are sensitive to temperature, opening displacement, asphalt content, air voids, asphalt grade and aggregate.

Fatigue cracking is a two-stage process that is generally initiated with the formation of micro-cracks. These later converge to form macro-cracks, which will then propagate through the pavement structure, i.e., crack initiation and crack propagation. The overlay tester focuses on the crack propagation component as the crack is initiated on the first cycle of the testing procedure.

OT is performed by applying cyclic triangular loading to specimen glued to the OT frame. Testing continues until a 93 percent reduction or more of the maximum load measured from the first opening cycle occurs. If a 93 percent reduction is not reached, then the test is run to 1,200 cycles. TxDOT maintains a database of OT test results of all HMA tested by the Department. The three figures that follow summarize results from the OT database, showing the median and average number of cycles to failure for different HMA types tested. Figure 2.8 compares the OT performance of different asphalt mixtures used in Texas; clearly CAM exhibits superior cracking resistance. Figure 2.9 shows OT performance in terms of binder performance

grade (PG) and Figure 2.10 in terms of aggregate type. Interestingly, superior cracking resistance is seen for crumb-rubber modified binders but binder PG does not appear to influence cracking performance. Quartzite aggregates clearly exhibit better cracking performance than other aggregate types. Limestone aggregates, which are the typical local aggregates available in Texas, show the lowest cracking performance.

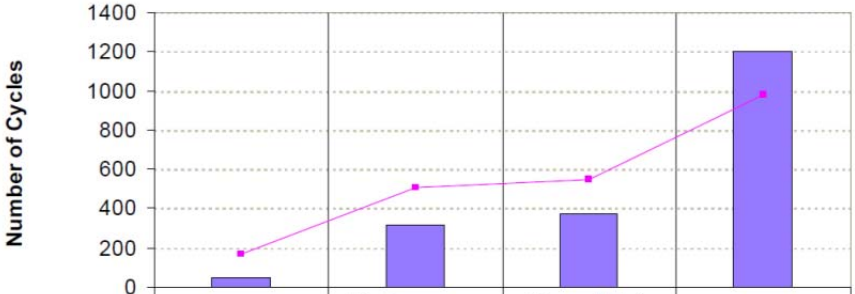

	Dense Graded	Performance Designed	Stone-Matrix Asphalt	RBL/CAM
Median	47	317	374	1200
Count	417	76	39	58
Minimum	1	3	24	83
Maximum	1200	1200	1200	1200
Average	172	507	548	978

Figure 2.8 OT performance of different HMA used in Texas (after Rand, 2007)

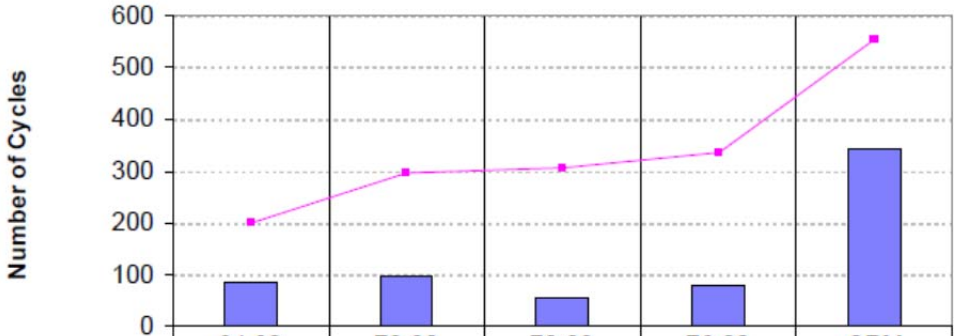

	64-22	70-22	70-28	76-22	CRM
Median	84	96	55	80	344
Count	119	156	69	172	21
Minimum	2	1	2	2	14
Maximum	1200	1200	1200	1200	1200
Average	199	297	306	336	555

Figure 2.9 Influence of binder type on OT performance (after Rand, 2007)

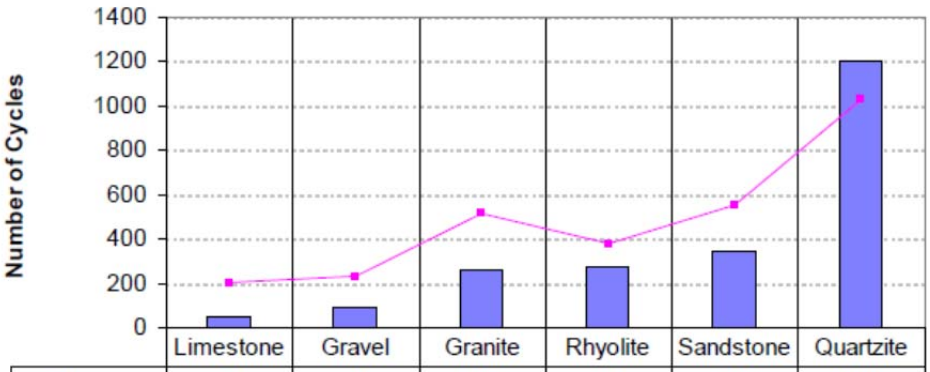

	Limestone	Gravel	Granite	Rhyolite	Sandstone	Quartzite
Median	53	90	262	271	344	1200
Count	147	62	80	15	25	14
Minimum	2	2	2	80	10	457
Maximum	1200	1200	1200	1200	1200	1200
Average	204	232	512	378	555	1030

Figure 2.10 Influence of aggregate type on OT performance (after Rand, 2007)

The main criticism directed towards the OT is the variability in the test results, which is evident when comparing the difference in minimum and maximum cycles to failure shown in the figures above. Walubita et al. (2009) address options to reduce the high variability in the OT typically associated with coarse dense-graded HMA. This project includes OT testing to evaluate the cracking potential of CAM and provides an opportunity to better assess the variability of the OT in relation to fine-graded HMA.

2.5.2 Indirect tensile test

The indirect tensile test (IDT) is one of the oldest and most popular tests for evaluating HMA specimens in the laboratory for fatigue as well as low temperature thermal cracking (Kennedy and Hudson, 1968). It can be run both as a static as well as a dynamic test and can be used to determine parameters such as resilient and dynamic modulus, tensile strength, and compliance. The main advantage of this test is its simplicity. The fatigue response of HMA measured using the IDT is correlated to field performance (Tangella et al., 1990). The IDT applies an indirect tensile force to the asphalt specimen along the diametrical plane in a cylindrical specimen that is loaded along its length. The complex stress distribution within the specimen under loading makes the test very sensitive to loading conditions and temperatures.

The permanent deformation at the loading strips is one of the major concerns with this test that reduces the energy available to crack the specimen. Hence, the work done to fail a specimen is not completely utilized for cracking of the specimen alone, which complicates the analysis of the test results when evaluating cracking resistance. Furthermore, the indirect tension state of stress in an IDT specimen does not simulate direct tension stresses apparent in actual HMA pavement layers under loading. These shortcomings prompted the development of the semi-circular bending test.

2.5.3 Semi-circular bending test

The SCB test, pictured in Figure 2.11, has been used extensively to evaluate the cracking and fatigue of asphalt mixtures (Van de Ven et al., 1997; Smit, 2002; Hofman et al., 2003;

Arabani and Ferdowsi, 2006; Mull et al., 2006). An advantage of the SCB is that regular gyratory compacted specimens or field cores can be used. Halved specimens effectively double the number of specimens that are tested and the loading configuration generates a uniaxial tensile stress at the bottom of the specimen that propagates upwards, simulating actual cracking response in the field. The variability of the SCB is comparable to that of the IDT and some researchers indicate that this variability can be further reduced by notching the base of the SCB specimen. Notching to the SCB specimen was applied as part of this study, which demonstrated that, under loading, cracking in the SCB specimen consistently originates at the notch tip and grows upwards towards the point of loading.

Figure 2.11 SCB test

The tensile strength (σ_t) of materials tested using the SCB may be estimated based on Eq. 2.2, which was derived using finite element methods (FEM) using elastic isotropic elements for unnotched specimen under plane stress conditions in a three-point loading configuration with roller supports at 0.8 times the diameter of the specimen (Van de Ven et al., 2007).

$$\sigma_t = \frac{4.263 \cdot P}{t \cdot D} \qquad \textbf{Eq. 2.2}$$

Because the formulation shown above is based on elastic analysis, a reasonable estimate of tensile strength can only be determined at either low temperatures or high loading speeds. This equation is not valid for notched SCB specimen. Notching the SCB specimen results in a concentration of stresses at the notch tip and a redistribution of stresses within the specimen under loading. For this reason, it was necessary to reformulate tensile strength estimates; three-dimensional FEM methods were again applied to allow an estimate of tensile strength at varying notch depths. The FEM applied is discussed in more detail later in the report. In addition to tensile strength measurements, alternative fracture mechanics cracking parameters were investigated to evaluate the sensitivity of the SCB test to mixture type.

Fracture mechanics deals with methods to calculate how a crack is initiated, propagates, and ends. Depending on the stress and corresponding strain states in a material, a crack can occur

as a result of three different modes as shown in Figure 2.12. Mixed cracking refers to the state when more than one type of crack mode occurs.

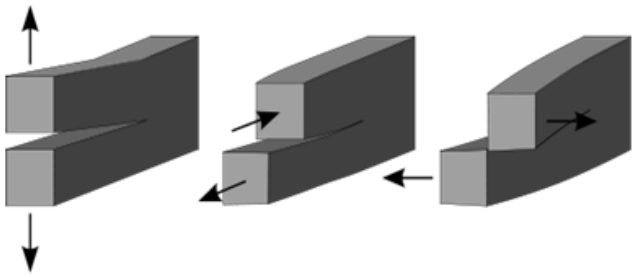

Figure 2.12 Cracking modes I, II, and III

In Mode I cracking, the stresses are perpendicular to the crack, pulling the crack open. In Mode II, the shear stresses are acting parallel to the plane of the crack and perpendicular to the crack front. This generates a shear crack, where the crack slides along itself. Additionally, the stresses do not cause the material to move out of its original plane. Finally, in Mode III the stresses are acting parallel to the plane of the crack and parallel to the crack front. This causes the material to separate and slide along itself while moving out of its original plane. In pavement engineering the focus is generally on Mode I and II cracking.

Mode I cracking is the most prevalent in pavement structures as tensile stresses are a dominating cause of cracking. In order to understand what happens to the HMA mix during Mode I cracking, the stress intensity factor (K_I) is normally used. Simply stated, K_I is a measure of how likely it is that a crack will grow in an unstable manner when tensile stresses are applied to the material. The solutions for K_I are dependent on test and loading configurations; in the current study, the relationship developed by Lim et al. (1993) between applied load (P) and stress intensity factor for the notched SCB configuration was used as given by:

$$K_I = Y_I \cdot \sigma_0 \cdot \sqrt{\pi \cdot a} \qquad \textbf{Eq. 2.3}$$

$$\sigma_0 = \frac{P}{2 \cdot r \cdot t} \qquad \textbf{Eq. 2.4}$$

$$Y_I = 4.782 - 1.219 \cdot \frac{a}{r} + 0.63 \cdot \exp\left(7.045 \cdot \frac{a}{r}\right) \qquad \textbf{Eq. 2.5}$$

where a is the notch depth, r is the radius and t the thickness of the SCB specimen.

Tensile strength and stress intensity factor are elastic material parameters and cannot be accurately estimated if materials undergo plastic deformation or flow as is the case when HMA specimen are tested at ambient temperatures. The high stress concentration at the notch tip in the SCB specimens results in a degree of plastic failure at these temperatures. To address this, the researchers evaluated the concept of J-integral.

The concept of J-integral was first introduced by Rice (1968). Rice defined the J-integral as the potential energy *difference* between two identically loaded bodies having different crack sizes. Figure 2.13 illustrates this concept, showing force-displacement curves of two different

specimens with different crack sizes. The energy required to displace the specimen is the area beneath the curve. More energy will be required to displace the specimen with the smaller crack. The shaded area indicates the potential energy difference between the two specimens.

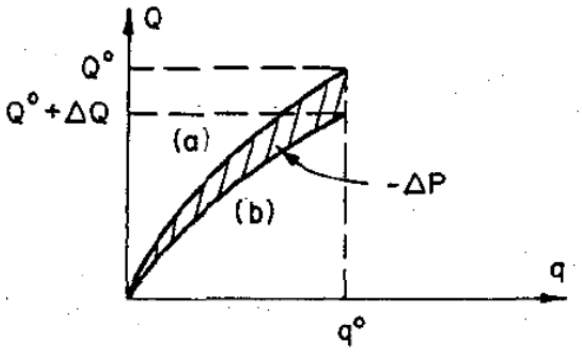

Figure 2.13 J-integral concept

Thus, by testing specimen with different notch depths and comparing the relative areas beneath the force-displacement curves of these specimens, a J-integral parameter for the material may be calculated that provides an indication of the resistance of the material to cracking, i.e., the larger the area difference between notch depths, the more potential energy required to propagate the crack and therefore the more crack resistant the material. Because the concept of J-integral considers the total energy required for displacement regardless of whether the specimen undergoes plastic deformation, it may be a better cracking parameter to evaluate HMA mixtures tested at ambient temperatures. This assumption was evaluated using the SCB by testing CAM specimen with different notch depths as part of the study.

2.6 CAM with local aggregates

Today there is an incentive to use more marginal aggregates while still providing long-lasting quality roads and structures. This is due to the depletion of, and consequent competition for, natural aggregate resources. Furthermore, there is an increasing public resistance to the opening of new quarries. The increasing cost of these materials is a serious issue and road engineers are now tasked with optimizing the use of available resources.

Walubita and Scullion (2008) report on the mix design of a number of mixes for pilot projects as part of their study. They indicate that, of the CAM mixes designed, all passed (and exceeded) overlay test requirements but some failed in the HWT. CAM with granite aggregate having SAC A performed considerably better in the HWT than CAM with limestone aggregate and SAC B. They recommend the use of high quality aggregates with a preferred SAC A and low soundness value (< 20 percent) for thin overlays mixes. They also discourage the use of absorptive aggregates (> 2 percent absorption) that can lead to a loss of effective binder in the mix. Walubita and Scullion (2008) concluded that current CAM specifications appear to be satisfactory for the thin overlay aggregates, including the gradation characteristics. For the materials and mixes evaluated in their study, the order of decreasing superior laboratory performance was (1) granite, (2) sandstone, (3) trap rock, and (4) limestone.

2.6.1 Aggregate quality

The quality of aggregates used in asphalt mixtures is specified to ensure long-term performance. Extensive research in this regard has been done on Texan aggregates (Gandhi and Lytton, 1984; Kandhal and Parker, 1998; Chowdhury et al., 2001; Cooley and James, 2003; Mahmoud, 2005; Masad et al., 2006; Fowler et al., 2006). A number of qualification tests are applied to discriminate between satisfactory and unsatisfactory aggregates. The toughness of aggregates is the ability to resist abrasion and degradation and is measured by the Los Angeles abrasion test, the micro-Deval, and magnesium sulfate soundness loss. Polish value (Tex 438-A) determined using the British pendulum is an indicator of the wearing characteristics of aggregates over time. The acid insoluble residue test (Tex 612-J) is used to determine the percentage of the non-carbonate particles present in the aggregate sample.

Figure 2.14 shows abrasion (magnesium soundness and micro-Deval) properties of commonly used aggregates in Texas, determined as part of TxDOT Project 1707: *Long-Term Research on Bituminous Coarse Aggregate*. The greater the aggregate loss from abrasion tests, the more susceptible an aggregate is to breakdown and degradation. From Figure 2.14 it can be seen that, in general, sandstone and limestone (i.e., local aggregates) are susceptible to abrasion while non-carbonate (siliceous) gravel show the best overall performance.

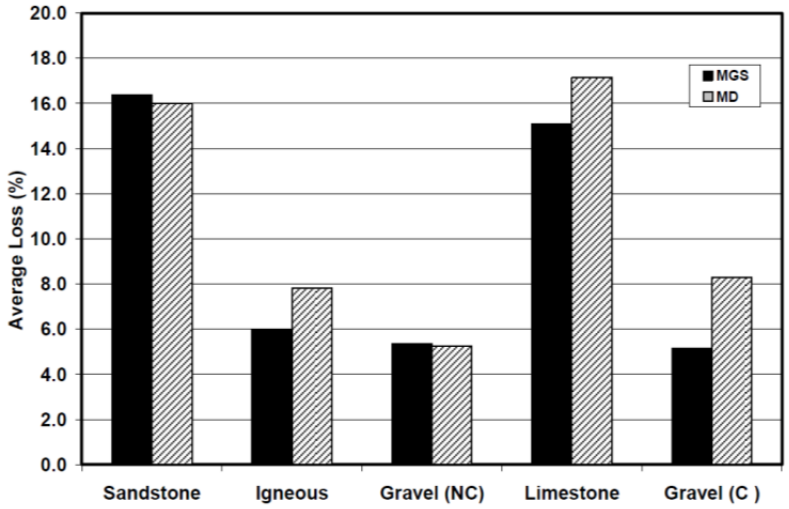

Figure 2.14 Abrasion of Texan aggregates (after Jayawickrama and Madhira, 2008)

Although there are questions and debate regarding the accuracy and consistency of some of the tests used to characterize aggregates (Fowler et al., 2006), they do serve to rank the general quality of aggregates in terms of strength, friction and durability properties. An evaluation of the various test methods to assess the quality of aggregates is beyond the scope of this project but specification testing that is applied was supplemented as part of the research with other tests such as the relatively new aggregate imaging system (AIMS) to characterize the shape and texture properties of aggregates.

2.6.2 Surface aggregate classification system

Jayawickrama and Madhira (2008) recently reviewed the aggregate classification system used by TxDOT. They compared the results of laboratory aggregate tests such as the British pendulum polish value test, the acid insoluble residue test, the micro-Deval abrasion test, and the magnesium sulfate soundness test to field skid measurements using the locked wheel skid trailer with a smooth tire tested at 50 mph. The analysis of field skid data clearly showed that synthetic aggregates, sandstone, and igneous materials consistently provided very good to excellent skid resistance. The gravel category was less consistent but nevertheless provided good overall skid resistance performance. Among all different aggregate categories, the limestone and the dolomite-limestone showed the greatest variability, i.e., some performing well, others very poorly. Because a very large fraction of the aggregate sources in Texas belong to this category, Jayawickrama and Madhira emphasize that it is important to develop reliable methods of classifying these borderline materials as satisfactory or unsatisfactory. They found, for example, that all sources with an acid insoluble residue of no less than 80 percent provided terminal skid resistance of at least 35, i.e., good skid resistance. These aggregate are also characterized by micro-Deval losses of less than 8 percent or magnesium sulfate soundness losses of less than 5 percent.

An important conclusion from the above-mentioned research is that aggregate characterization tests do not consistently distinguish between good and poor performers, particularly for "borderline" materials, which blurs the distinction between the aggregate classification categories. In the same study, Masad et al. (2006) used the AIMS to measure aggregate resistance to polishing, abrasion, and breakage. AIMS was used to measure the angularity, texture, and shape of coarse aggregates before and after the micro-Deval test in order to compute the change in physical characteristics of the aggregates due to the induced abrasion. The AIMS was used to supplement the micro-Deval results. They found, for example, that a decrease in sphericity indicates that the aggregate has the potential to experience particle breakage. AIMS results can also be used to set maximum values for loss of texture in order for the mix to have the necessary friction between particles. They concluded that this method is more sensitive than the current methods and allows the aggregates to be spread more evenly in the four different categories. They recommended (and provided) revised procedures to classify Texan aggregates as shown in Figure 2.15.

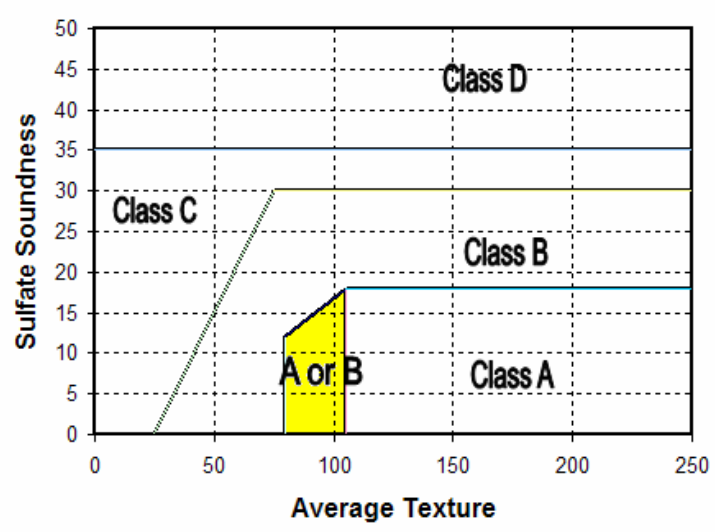

Figure 2.15 New aggregate classification system (Masad et al., 2006)

2.6.3 Aggregate imaging system

AIMS was used to further characterize the local aggregates used in the study. AIMS is designed to analyze the form, angularity, and texture of coarse aggregates (as illustrated in Figure 2.16) as well as angularity and form of fine aggregates. The three fundamental characteristics that constitute particle geometry are described as follows (Masad, 2004). Form reflects variations in the proportions of a particle. Angularity reflects variations at the corners, that is, variations superimposed on shape. Surface texture is used to describe the surface irregularity at a scale that is too small to affect the overall shape. The above three properties are independent of each other and can vary independently.

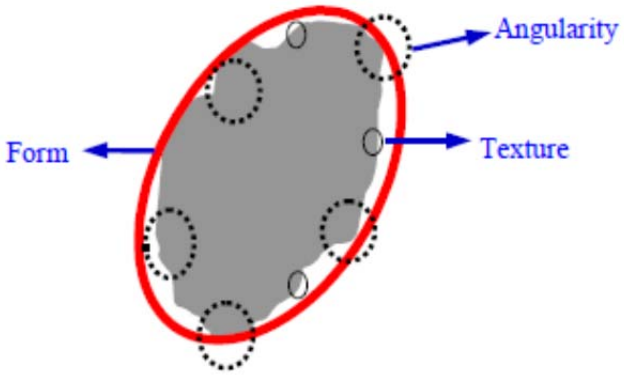

Figure 2.16 Components of an aggregate shape: form, angularity, and texture (Masad, 2004)

A high sphericity is generally desirable for HMA as it indicates more cubical particles. Figure 2.17 shows a chart that describes the form of aggregate particles based on AIMS parameters. It can be used to distinguish among flat, elongated, and flat and elongated particles.

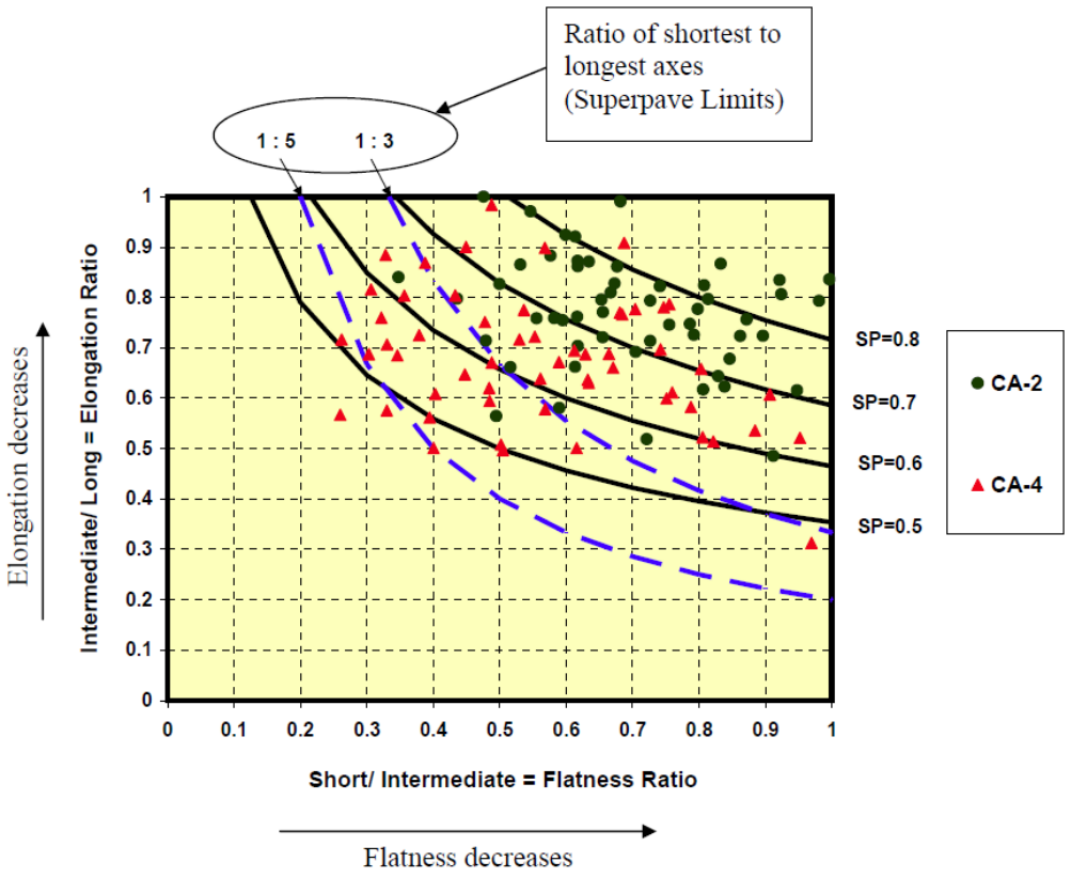

Figure 2.17 Identifying flat and elongated aggregates (Masad, 2005)

Superimposed on this chart are the 3:1 and 5:1 limits for the longest to shortest dimension ratio. Particles with a 1:1 ratio are cubical and particles exceeding the 5:1 ratio are classified by Superpave as being flat and elongated. Special specification 3165 for CAM has a maximum limit of flat and elongated particles (5:1) of 10 percent. Table 2.3 shows the classification of angularity and surface texture based on the AIMS parameters.

Table 2.3 Aggregate angularity and texture classifications categories (Masad, 2005)

Angularity		Surface texture	
Rounded	< 2,100	**Polished**	< 185
Sub-rounded	2,100–4,000	**Smooth**	185–275
Sub-angular	4,000–5,400	**Low roughness**	275–350
Angular	5,400–10,000	**Moderate roughness**	350–460
		High roughness	460–800

Chapter 3. Survey and Database of CAM Projects in Texas

The past and current work on CAM in Texas is reviewed and summarized in this chapter. Information pertaining to the design and construction of existing and past CAM projects was gathered. The chapter also summarized a database of these projects established to track the design, construction, and performance information of CAM in Texas.

3.1 Current CAM projects

Table 3.1 shows a listing of CAM projects constructed in Texas. The table indicates whether the CAM is applied as a surface course or underlayer as well as the high temperature asphalt PG and SAC of the aggregates used for the CAM mix.

Figure 3.1 summarizes the application of CAM in Texas, indicating the distribution by facility, layer course, and binder grade. The majority of the CAM projects in Texas have been produced using aggregate with SAC A. The figure shows that CAM is used on Interstate Highway (IH), State Highway (SH), US Highway (US), and Farm-to-Market (FM) roadway facilities as both surface course and underlayers, although no CAM surface courses have been used on SH facilities.

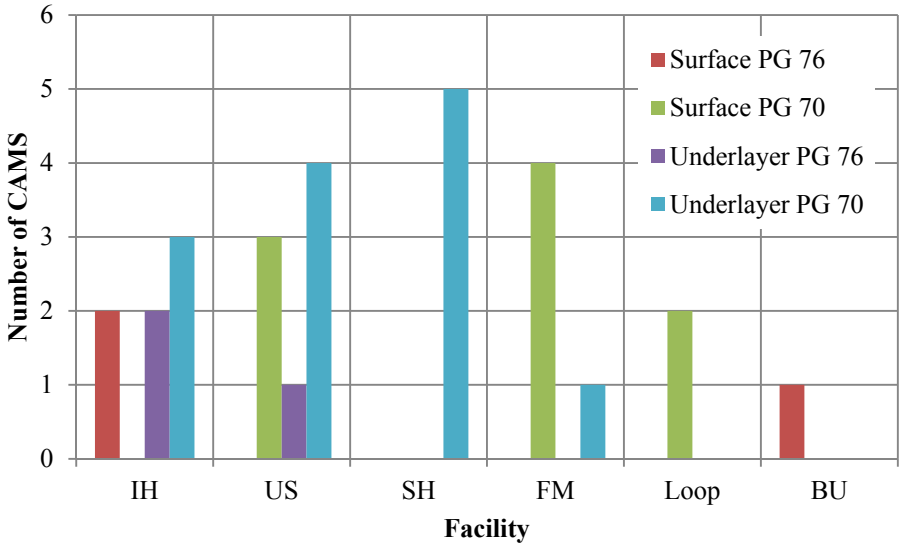

Figure 3.1 Summary of Texas CAM Projects by Facility, Application and Binder Grade

Table 3.1 Current CAM projects in Texas

DISTRICT	COUNTY	ROUTE	LAYER	PG	SAC
ABILENE	SHACKELFORD	US 180	Underlayer	70	B
ATLANTA	TITUS	SH 49	Underlayer	70	A
AUSTIN	BURNET	US 281	Surface	70	A
BEAUMONT	HARDIN	FM 770	Underlayer	70	A
BEAUMONT	JASPER	US 96	Underlayer	70	A
BEAUMONT	CHAMBERS	IH 10	Underlayer	70	A
BRYAN	FREESTONE	US 84	Underlayer	70	A
BRYAN	BRAZOS	SH 21	Underlayer	70	A
BRYAN	LEON	IH 45	Surface	76	A
BRYAN	BRAZOS	FM 2154	Surface	70	A
BRYAN	BRAZOS	FM 60	Surface	70	A
BRYAN	LEON	IH 45	Underlayer	76	A
BRYAN	BRAZOS	FM 1179	Surface	70	A
DALLAS	DALLAS	US 67	Underlayer	76	A
DALLAS	DALLAS	SH 114	Underlayer	70	A
LAREDO	WEBB	LP 20	Surface	76	A
LAREDO[1]	LA SALLE	IH 35	Surface	76	A
LUFKIN	ANGELINA	BU 59-G	Surface	76	A
PARIS	GRAYSON	US 69	Surface	70	A
PARIS	HOPKINS	FM 499	Surface	70	A
PARIS	LAMAR	LP286	Surface	70	A
SAN ANTONIO	UVALDE	US 90	Surface	70	A
TYLER	GREGG	SH 135	Underlayer	70	A
TYLER	HENDERSON	SH 31	Underlayer	70	A
TYLER	RUSK	US 259	Underlayer	70	A
WACO	BELL	IH 35	Underlayer	76	B
WACO	MCLENNAN	IH 35	Underlayer	70	B
WACO	HILL	IH 35E	Underlayer	76	B

Table 3.2 includes a summary of CAM design information retrieved from research and TxDOT construction projects listed in the SiteManager database. It also provides gradations, OAC, and material information if available and indicates if the mix passed the HWT and OT tests. In general the CAM designs comprise two or three stockpiles including coarse aggregate (SAC A), manufactured sand, and screenings. In general, 1 percent lime is added to the mix. The compositions of the mixes vary in the following ranges: coarse aggregate (21–54 percent), manufactured sand (20–33 percent), and screenings (25–60 percent). Asphalt contents used for CAM range from 7 percent to 8.5 percent.

[1] This CAM surface construction was halted when the mix failed HWT criteria.

Table 3.2 CAM project designs

	Amarillo	Abilene	Lubbock	EE Hood	Research	Bryan	Odessa	Wichita	Lufkin	Cumby	Denison
1/2"	100.0	100.0	100.0	100.0	100.0	100.0	100.0	100.0	100.0	100.0	100.0
3/8"	100.0	99.9	100.0	100.0	99.8	98.7	100.0	100.0	100.0	99.8	99.8
#4	74.3	77.8	79.6	73.2	73.9	73.6	80.5	84.6	79.4	75	73
#8	41.5	42.5	42.1	53.2	47.7	55.3	49.5	43.3	47.6	42	44
#16	29.7	25.9	27.1	40.7	32.3	37.5	35.2	21.9	31.0	30	30.4
#30	21.2	16.7	19.7	22.4	22.7	22.2	24.5	13.7	20.1	23.6	23.9
#50	14.3	11.4	15.5	14.6	16.3	10.7	13.4	10.2	12.2	19.9	19.9
#200	4.3	6.9	6.9	7.7	9.9	4.4	3.7	2.0	4.2	6.3	7.1
PG Binder	70-22	76-22	70-28	70-22	70-22	70-22	76-22	70-22	76-22	70-22	70-22
Aggregate	Gravel	Limestone	Gravel	Trap Rock	NA	Limestone	Gravel	Gravel	Igneous	NA	NA
SAC	A	A	A	A	NA	A	A	A	A	NA	NA
OAC, %	7.5	7.5	7.5	7.1	7.0	7.1	8.0	8.5	8.3	7.7	7.5
Quarry	Highcard Ranch	Eastland	Matador	Knippa	NA	Delta Marble Falls	Hoban	Zack Burkett	Jones Mill	NA	NA
HWT	Passed	Failed	Failed	Failed	Passed	Passed	Passed	NA	Passed	Passed	NA
OT	Passed	Passed	Passed	Passed	Failed	Passed	Passed	NA	Passed	NA	NA
Anti-strip	1% Lime	1% Lime	1% Lime	0.5% ArrMaz HP+	1.5% Lime	1% Lime	None	1% Lime	1% Lime	NA	NA

3.2 Visual survey of CAM performance

A visual survey was conducted on selected CAM projects constructed in Texas to ascertain their performance and condition. Photographs were taken of distresses observed on these CAM sections and are included in Appendix A. Information and photographs regarding the performance of CAM of other sections were also relayed by some TxDOT area offices.

District: Laredo, County: La Salle, Route: IH 35	
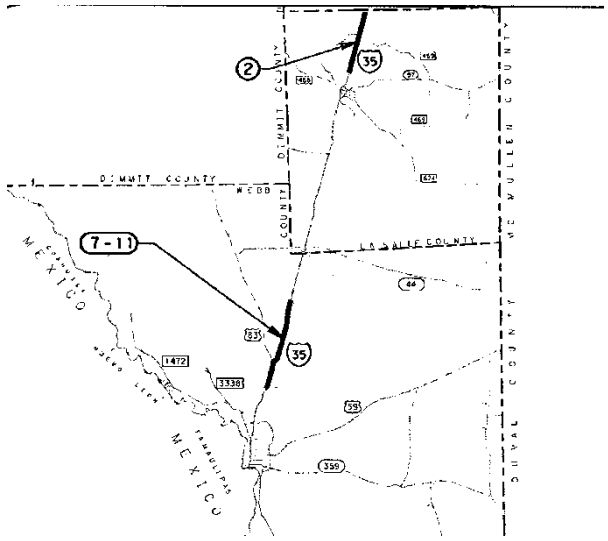	A problem reported during the construction of this CAM surface course was blistering of the asphalt mix as pictured in Figure A.1 and Figure A.2 in Appendix A. It is believed that this phenomenon results from the evapo-migration of moisture and air trapped beneath the impervious CAM layer as it heats during the day. The bulge or blister that develops is severe as shown in the figures but reportedly settles when the surface cools. It was indicated to the researchers that the intended construction of the surface course using CAM was halted after the mix failed to meet required HWT test criteria. The CAM that was paved up until this point was left in place and the construction was continued using an SMA-F mix.

District: Laredo, County: Webb, Route: Loop 20	
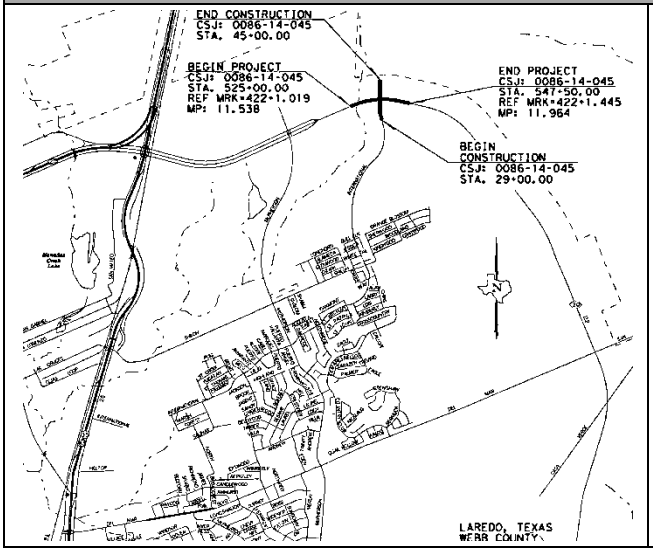	Figure A.3 shows the cracking of the old section on Loop 20 that was overlaid using CAM. This photo shows the end of the CAM construction, which is visible in the foreground. Localized longitudinal cracking was evident on the CAM overlay as shown in Figure A.4 and Figure A.5. Indications are that these are not necessarily reflection cracks but may be edge- or shoulder-related. Overall the performance of this CAM appears excellent and no visible rutting is apparent even though this is a heavily trafficked roadway. This is a good example of a CAM mix performing well.

District: Bryan, County: Brazos, Route: SH 21	
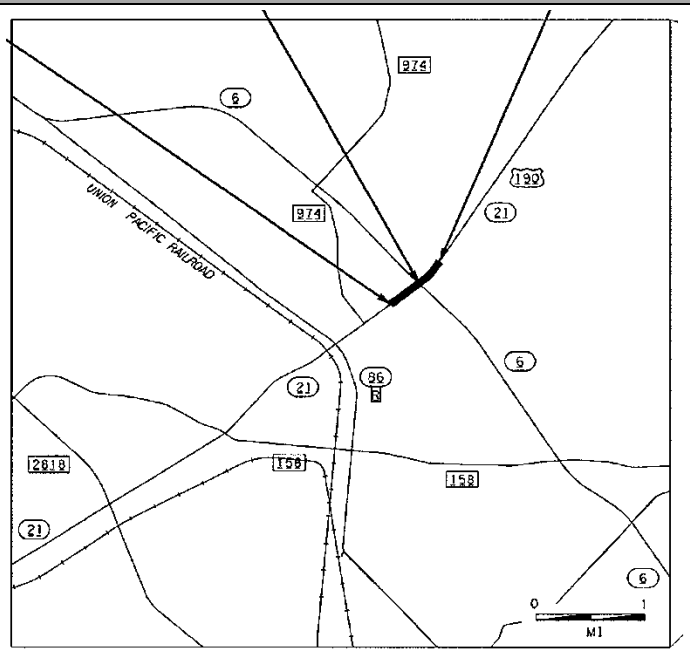 CITY OF BRYAN	Localized shoving of the CAM underlayer was apparent at the intersection of SH 21 and SH 6 in Bryan as shown in Figure A.6. This shoving was relatively deep (~ 3 inches) with bulging around the depression indicative of shear flow. Some surface cracking was also evident in the vicinity of the intersection but this is not necessarily related to the underlying CAM. Overall the performance of this roadway appears satisfactory.

District: Bryan, County: Brazos, Route: FM 60	
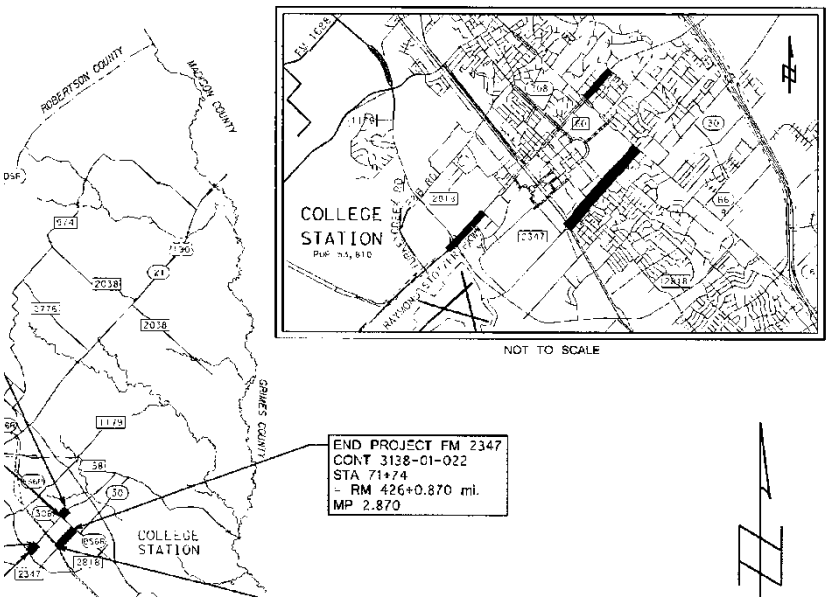	Sections of CAM surface course were paved on FM 60 in Bryan as shown in Figure 3.5. This CAM was relatively new at the time of the survey and appeared to be in excellent condition with no visible rutting at intersections. A rough surface finish was apparent throughout the paved sections as shown in Figure A.7. The surface did appear slick and reflections off the surface from vehicle head lights were clearly visible as shown in Figure A.8. Figure A.9 also shows the light reflection off the CAM surface on the section of roadway opposite the Texas A&M Research Park building.

District: Bryan, County: Brazos, Route: FM 2154	
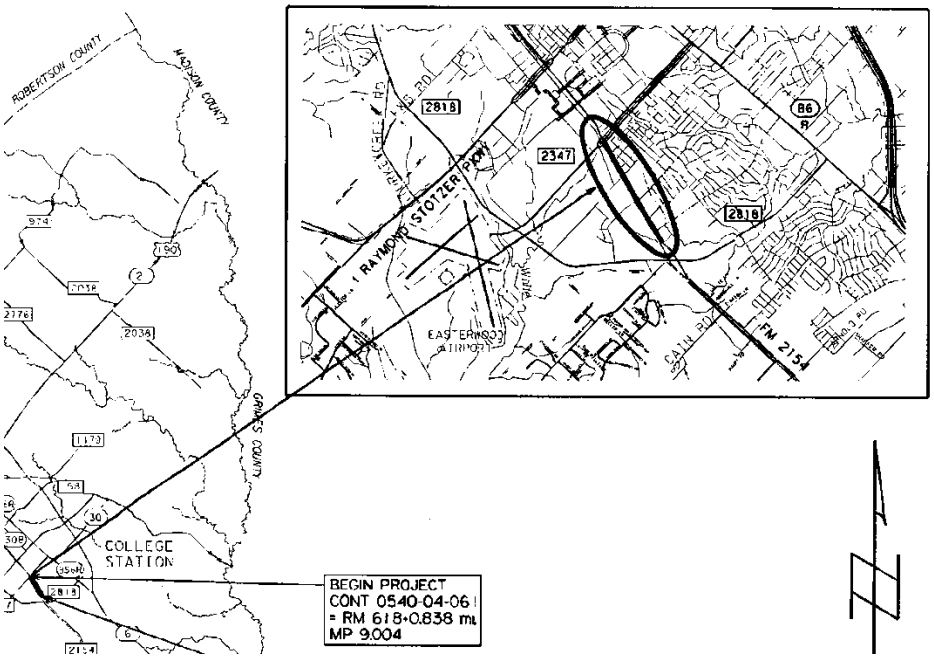	Very severe to moderate rutting and shoving of the CAM surface was apparent at intersections on FM 2154 as shown in Figure A.10 and Figure A.11. This surface also appeared slick and reflected light from oncoming vehicles as shown in Figure A.12

District: Bryan, County: Brazos, Route: FM 1179	
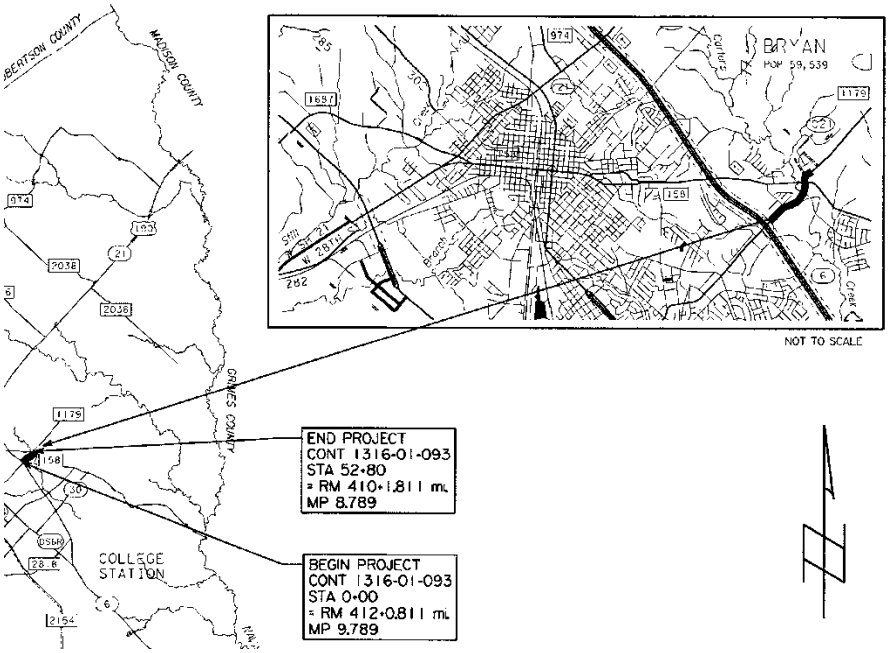	TxDOT took photographs and reported excessive shoving resulting from vehicle turning movements on the CAM surface paved on FM 1179 and FM 2347 in Bryan as shown in Figure A.13 and Figure A.14. This particular surface distress was subsequently repaired and was believed to have resulted from the CAM being paved too thickly in the curve. A subsequent survey by the researchers shows excessive shoving at intersections on this roadway as shown in Figure A.15 and Figure A.16. The slick appearance and light reflection of the surface is also apparent in Figure A.16. The rough surface finish previously seen on the CAM on FM 60 was also apparent on this roadway as shown in Figure A.17.

District: Paris, County: Hopkins, Route: FM 449	
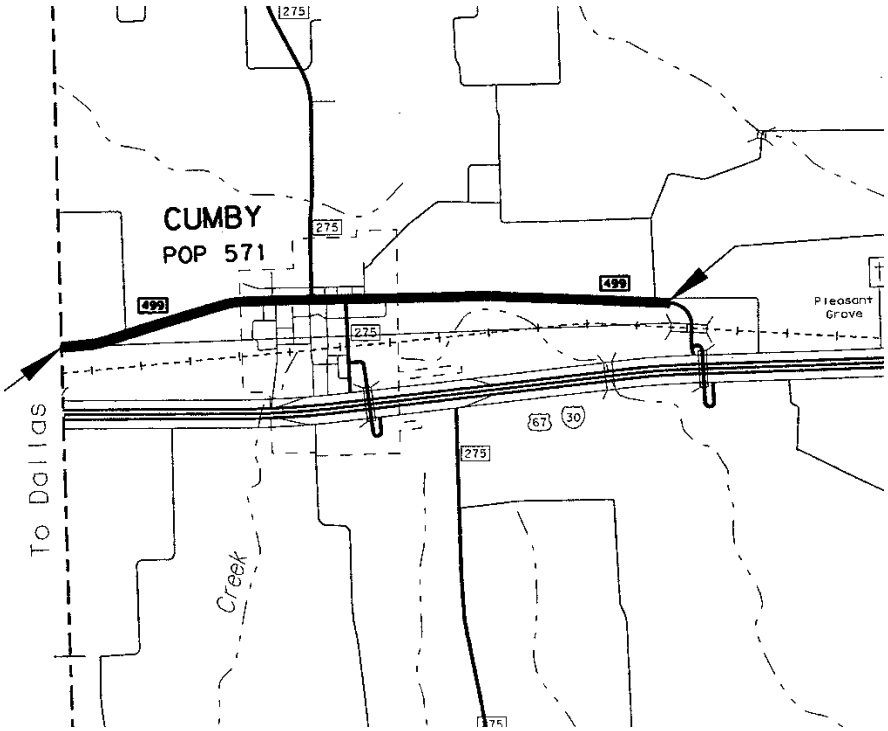	This mix is paved on the main road running through the city of Cumby. The CAM overlay was placed over a severely cracked surface. The reflection cracks running transversely and longitudinally as shown on the surface originated from the underlying jointed concrete pavement. The new CAM overlay, although aesthetically improving the appearance of the roadway, did not impede the reflection of the cracks. Transverse cracking of the CAM surface was apparent at regular spacing distances along the roadway as shown in Figure A.18, Figure A.19, and Figure A.20.

District: Paris, County: Grayson, Route: US 69	
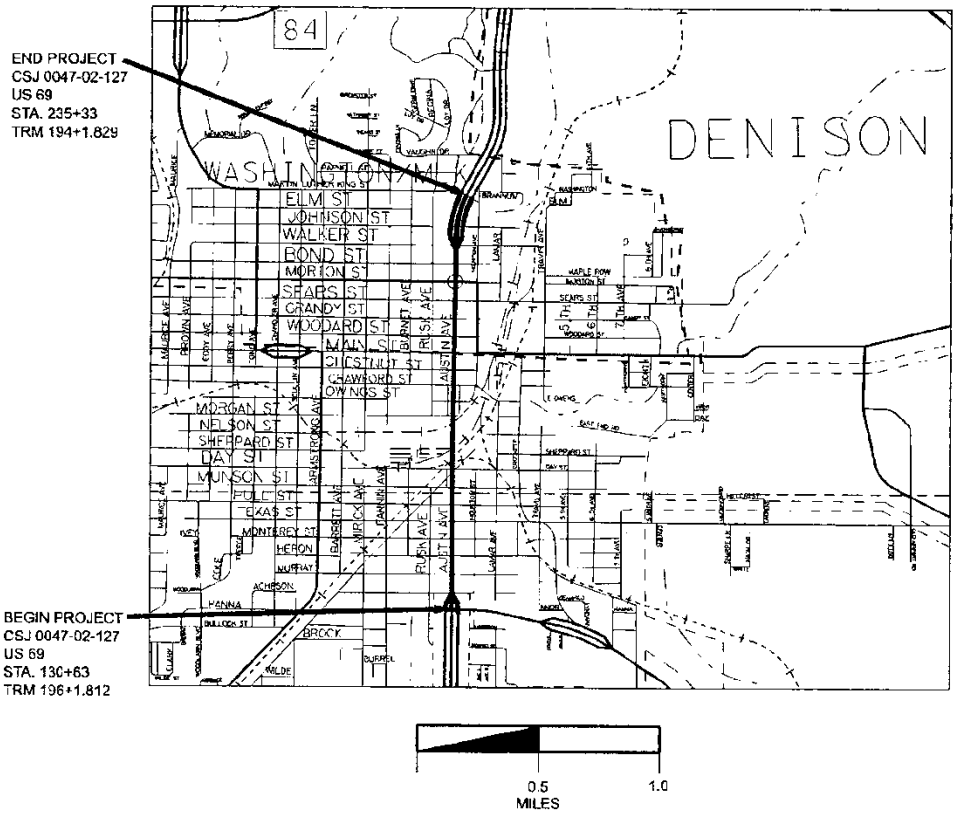	This mix appeared to be performing well overall, although evidence of both longitudinal and transverse cracking was seen, as shown in Figure A.21 and Figure A.22 respectively. Slight shoving of the CAM surface was also apparent at some of the intersections as shown in Figure A.23.

District: San Antonio, County: Uvalde, Route: US 90
TxDOT provided photos and indicated blemishes in the form of flushing or bleeding of binder apparent on the CAM paved on US 90 in Uvalde County as shown in Figure A.24 and Figure A.25. The photos suggest that this problem may be related to uneven tack coat distribution probably from a few nozzles on the binder distributor. It is interesting to see how this excess binder has bled through the CAM surface, itself rich in asphalt.

3.3 Summary of Texas CAM performance

Although the photographs included in this report emphasize the distresses observed in the field, the condition of the CAM projects as observed was, in general, reasonable with localized failures at various locations along the construction.

The predominant failure or distress observed in the field for the CAM surface and underlayer mixes was rutting in the form of shoving and shear failure. The rutting observed was localized and predominantly at intersections in the form of depressions with no volume change, i.e., the mix bulged alongside the rut instead of consolidating. This is indicative of mixes that are over-asphalted with low air voids. Although no physical evidence was collected, the survey indicates the potential for problems regarding the skid resistance, light reflection, and tire-pavement noise of some of the CAM projects visited. CAM is promoted as a crack attenuating mix but reflective cracking was observed on a number of CAM projects where the underlying layer was cracked. This may suggest that pre-treatment of the underlying layer may be necessary before applying CAM overlays. It was reported by the Fort Worth district that cracking of CAM evident after winter appeared to heal during the summer. While this is a possible benefit of using CAM, it does suggest that water ingress may occur.

The application of CAM is still relatively new in Texas with most sections less than 3 years old. Some of the projects surveyed in the study were less than 1 year old. It is therefore recommended that the performance of these projects continue to be monitored to better realize the long-term performance of CAM.

3.4 CAM database

A database of the CAM projects constructed in Texas was prepared as a product of this research and submitted to TxDOT in Microsoft Access format on a CDROM. This database includes a listing of the CAM projects as well as tables summarizing the design and QCQA data collected on these projects as documented in SiteManager. A data dictionary accompanies the database outlining the fields in each of the database tables.

Chapter 4. Characterization of Local Aggregates

This chapter addresses the characterization of aggregates collected from different quarries in Texas as part of the study. Results of characterization tests are provided that were later used to establish aggregate quality criteria and guidelines for CAM with local aggregates.

4.1 Local aggregate sources

Table 4.1 indicates the quarries identified for the collection of aggregate used for the CAM mixes in the study. Materials from 14 quarries were collected, consisting of both coarse and fine fractions sampled from stockpiles on site. The coarse stockpile was typically a 3/8-inch rock and the fine stockpile comprised either manufactured sand and/or crusher screenings. Gradations of the coarse and fine fractions were determined via sieving—the coarse fractions were generally quite uniform. One SAC A source was included to serve as a reference for performance comparisons with the local aggregate sources.

Table 4.1 Project aggregate sources

Quarry	Producer	Type	SAC
Murphy	Fordyce	Gravel	A
Marble Falls	Capitol	Limestone	B
Beckmann	Martin Marietta	Limestone	B
Solms Road	Martin Marietta	Limestone	B
Spicewood	Vulcan	Limestone	B
Yearwood	R.T.I.	Limestone	B
Feld	Texas Crushed Stone	Limestone	B
Burnet	Hanson	Limestone	B
1604	Vulcan	Limestone	B
Lone Star	Dean Word	Limestone	B
Mico # 68	Lattimore	Limestone	B
Pit 365	Mine Service	Gravel	B
Tehuacana	Vulcan	Limestone/Dolomite	B
Luckett	Trinity	Gravel (partly crushed)	B

4.2 Aggregate specification criteria

TxDOT special specification 3165 requires that aggregates used for CAM are furnished from sources that conform to the requirements shown in Table 4.2. The criteria shown in this table match those specified for Item 346 SMA mixtures. Aggregates for CAM must be mechanically crushed gravel or stone and the use of reclaimed asphalt pavement (RAP) is not

permitted. These criteria emphasize the need for high quality aggregates that will (1) not crush under surface loads, (2) be durable, (3) provide and maintain acceptable frictional characteristics, and (4) will ensure high mixture stability.

Selecting aggregates that meet all of these requirements is often difficult. For example, aggregates with high porosity and rough surface texture frequently are not hard and durable. Particles that are hard and have high resistance to abrasion and degradation may tend to have poor bond strength and be highly susceptible to polishing. The high cost and shortage of quality aggregate drives the incentive to use more marginal and/or local aggregates while still providing long-lasting quality roads and structures.

Table 4.2 SS 3165 aggregate quality criteria

Property	**Test Method**	**Requirement**
Coarse Aggregate		
Surface Aggregate Classification	AQMP	As on plans
Deleterious material, %, max	Tex-217-F, Part I	1.0
Decantation, %, max	Tex-217-F, Part II	1.5
Micro-Deval abrasion, %, max	Tex-461-A	Note 1
Los Angeles abrasion, %, max	Tex-410-A	30
Magnesium sulfate soundness, 5 cycles, %, max	Tex-411-A	20
Coarse aggregate angularity, 2 crushed faces, %, min	Tex 460-A, Part I	95 (Note 2)
Flat and elongated particles @ 5:1, %, max	Tex-280-F	10
Fine Aggregate		
Linear shrinkage, %, max	Tex-107-E	3
Combined Aggregate (Note 3)		
Sand equivalent, %, min	Tex-203-F	45

Notes:
1. Not used for acceptance purposes. Used by the Engineer as an indicator of the need for further investigation.
2. Only applies to crushed gravel.
3. Aggregates, without mineral filler, or additives, combined as used in the job-mix formula (JMF).

SAC addresses aggregate texture and frictional characteristics for bituminous *coarse* aggregates as part of the TxDOT's Wet Weather Accident Reduction Program (WWARP). Aggregates are classified based on the criteria listed in Table 4.3 and are related to the skid resistance properties of the aggregates. The higher the class, the better the long-term skid resistance offered.

Table 4.3 Surface aggregate classification criteria

Property	Test Method	SAC A	SAC B	SAC C
Acid insoluble residue, % min	Tex-612-J	55	----	----
5-cycle Mg, % max	Tex-411-A	25	30	35
Crushed Faces, 2 or more, % min	Tex-460-A	85	85	85

4.3 Aggregate characterization properties

Various tests are used to characterize the properties of aggregates:

- **Los Angeles abrasion** measures aggregate toughness and resistance to degradation and abrasion under load. This test is specified to ensure that the aggregate will not break down excessively during production, under construction equipment, or from traffic loading. The specification requirements for LA abrasion are the most stringent for stone skeleton mixes that have significant stone-on-stone contact, suggesting that this criterion may be relaxed somewhat for sand-skeleton mixes such as CAM.
- **micro-Deval** measures an aggregate's durability and resistance to abrasion by subjecting the aggregate to polishing and grinding with steel balls and water. The results from this test cannot be used for acceptance purposes.
- **Coarse aggregate angularity** determines the number of mechanically induced crushed faces on individual aggregate particles. Coarse aggregate angularity affects the bond between aggregate and binder as well as mix stability and workability.
- **Flat and elongated particles** are undesirable because they can hinder the packing ability of the aggregate, break easily under load, and can affect mix workability, strength, and compactibility. The current test procedure determines whether an aggregate particle is flat and elongated by determining the ratio of the particle's longest dimension to its shortest dimension.
- **Magnesium sulfate soundness** measures an aggregate's durability and resistance to weathering by subjecting the aggregate to alternating cycles of soaking in a magnesium sulfate solution and then drying. It is also a good indicator of how an aggregate will perform when subjected to freeze/thaw cycles. Using durable aggregates results in mixtures that are less prone to develop raveling, potholes, and pop outs. Hard, durable aggregates typically have low soundness loss values.
- **Acid insoluble residue** on both coarse and fine aggregates is used to determine the percent of non-carbonate material contained within an aggregate sample by dissolving the sample in hydrochloric acid. Non-carbonate aggregates have been shown to provide better long-term wet skid resistance than carbonate aggregates. Carbonate aggregates such as limestone will almost completely dissolve when placed in hydrochloric acid, whereas non-carbonate aggregates will dissolve only slightly when placed in hydrochloric acid. The typical acid insoluble residue from

limestone aggregates ranges from 0 percent to about 10 percent. Non-carbonate aggregates have acid insoluble residue values ranging from 50 percent to 100 percent.

- For the fine aggregates, **linear shrinkage** is an indicator of the amount of clay fines in the mineral filler and the **sand equivalent** test determines the relative proportion of detrimental fine dust or clay-like particles in the fine aggregates.
- **Polish value** (Tex 438-A) determined using the British pendulum is an indicator of the wearing characteristics of aggregates over time.

Table 4.4 shows the characterization properties of the aggregates used in the study, including the SAC, Los Angeles abrasion (LA), magnesium sulfate soundness loss (SM), micro-Deval abrasion (MD) and acid insoluble residue (AI).

Table 4.4 Aggregate characterization properties

Quarry	Producer	SAC	LA	SM	MD	AI
Murphy	Fordyce	A	19	5	6	84
Marble Falls	Capitol	B	28	9	10	1
Beckmann	Martin Marietta	B	30	30	25	1
Solms Road	Martin Marietta	B	27	10	18	1
Spicewood	Vulcan	B	22	8	8	4
Yearwood	R.T.I.	B	27	16	19	1
Feld	Texas Crushed Stone	B	33	24	25	2
Burnet	Hanson	B	26	4	9	5
1604	Vulcan	B	37	30	30	1
Lone Star	Dean Word	B	29	23	22	1
Mico # 68	Lattimore	B	29	10	18	1
Pit 365	Mine Service	B	24	28	20	4
Tehuacana	Vulcan	B	35	17	24	12
Luckett	Trinity	B	23	14	12	35

Table 4.2 indicated that a maximum magnesium sulfate soundness loss of 20 percent is permitted for CAM, which would disqualify five aggregate sources. The Los Angeles abrasion maximum criterion of 30 percent disqualifies two aggregates sources. With the exception of the aggregates from Trinity Materials, all are crushed stone, which qualifies in terms of coarse aggregate angularity. The table highlights that a wide range of different aggregate properties were covered in the study. It is interesting to see that most of the aggregate sources meet the current CAM specification requirements.

4.4 AIMS results

AIMS testing were conducted on all the aggregate types used in the study. The results of various AIMS parameter estimations are summarized below.

Table 4.5 shows the AIMS sphericity results for the coarse aggregate stockpiles used in the study. Higher sphericity values indicate more cubical particles and lower values indicate flaky aggregates. The aggregate from the Spicewood quarry was the flakiest of the aggregates tested. The coarse aggregate from the Vulcan Tehuacana quarry was too large for CAM and only the fine aggregate from this quarry was used in the study (by blending with coarse aggregate from the Luckett and Feld quarries).

Table 4.5 AIMS sphericity of coarse aggregates

Quarry	Producer	AVG	STDEV
Murphy	Fordyce	0.71	0.11
Marble Falls	Capitol	0.70	0.12
Beckmann	Martin Marietta	0.69	0.09
Solms Road	Martin Marietta	0.66	0.10
Spicewood	Vulcan	0.65	0.12
Yearwood	R.T.I.	0.68	0.09
Feld	Texas Crushed Stone	0.68	0.09
Burnet	Hanson	0.62	0.09
1604	Vulcan	0.69	0.12
Lone Star	Dean Word	0.67	0.10
Mico # 68	Lattimore	0.69	0.12
Pit 365	Mine Service	0.72	0.10
Tehuacana	Vulcan	-	-
Luckett	Trinity	0.68	0.13

Table 4.6 and Table 4.7 summarize the AIMS *gradient* angularity results from image analysis of the coarse and fine stockpiles respectively. The gradations of the fine aggregate stockpiles from the Feld, Lone Star, and Luckett quarries were not suitable for use with CAM. With reference to Table 2.3, the CAM aggregates used in the study class as either sub-rounded or sub-angular in terms of angularity. Aggregate angularity significantly influences the stability and rutting performance of HMA (Meier et al., 1979; Kalcheff et al., 1982). It was anticipated that fine aggregate angularity is probably more critical for CAM given the larger proportion of fine aggregates in these mixes.

Table 4.6 AIMS angularity of coarse aggregates

Quarry	Producer	AVG	STDEV
Murphy	Fordyce	3220	1681
Marble Falls	Capitol	3555	1273
Beckmann	Martin Marietta	3052	1384
Solms Road	Martin Marietta	3544	1614
Spicewood	Vulcan	3373	1041
Yearwood	R.T.I.	3009	1172
Feld	Texas Crushed Stone	4785	1835
Burnet	Hanson	4573	1841
1604	Vulcan	4626	2275
Lone Star	Dean Word	4612	2030
Mico # 68	Lattimore	3631	1794
Pit 365	Mine Service	2525	797
Tehuacana	Vulcan	-	-
Luckett	Trinity	1882	1375

Table 4.7 AIMS angularity of fine aggregates

Quarry	Producer	AVG	STDEV
Murphy	Fordyce	3382	1584
Marble Falls	Capitol	4578	1666
Beckmann	Martin Marietta	4186	1997
Solms Road	Martin Marietta	3848	1694
Spicewood	Vulcan	3716	1420
Yearwood	R.T.I.	3906	1585
Feld	Texas Crushed Stone	-	-
Burnet	Hanson	4983	2096
1604	Vulcan	3663	1633
Lone Star	Dean Word	-	-
Mico # 68	Lattimore	4652	2075
Pit 365	Mine Service	2818	1512
Tehuacana	Vulcan	4640	1779
Luckett	Trinity	-	-

Table 4.8 shows the coarse aggregate AIMS surface texture results. All the values are less than 185, which places all aggregates into the category of "polished" as per Table 2.3.

Table 4.8 AIMS surface texture of coarse aggregates

Quarry	Producer	AVG	STDEV
Murphy	Fordyce	66.8	54.1
Marble Falls	Capitol	72.6	26.6
Beckmann	Martin Marietta	47.4	26.9
Solms Road	Martin Marietta	46.8	21.0
Spicewood	Vulcan	160.8	69.8
Yearwood	R.T.I.	72.6	19.1
Feld	Texas Crushed Stone	71.1	39.7
Burnet	Hanson	133.8	47.4
1604	Vulcan	64.8	39.4
Lone Star	Dean Word	66.6	39.4
Mico # 68	Lattimore	87.5	68.2
Pit 365	Mine Service	70.7	24.6
Tehuacana	Vulcan	-	-
Luckett	Trinity	40.7	21.0

In addition to the above results, AIMS flakiness distribution plots for all the aggregates are shown in Appendix B.

4.4.2 Superpave fine aggregate angularity

Method C of ASTM C 1252 was used to determine the fine aggregate angularity (FAA) of the aggregate sources. This is a measure of the uncompacted voids of the fine aggregates that are generally positively correlated with the angularity of the aggregates. The results of the FAA tests are shown in Table 4.9. The Hanson aggregate from the Burnet quarry has the highest FAA—this aggregate also had the highest AIMS angularity (Table 4.7). The Marble Falls aggregate on the other hand has the lowest FAA but had very high AIMS angularity. Recent experience with the current Superpave criterion for fine aggregate angularity shows that there are cases where this test does not discern poor quality from high quality aggregates (Huber et al., 1998; Chowdhury et al., 2001). The FAA test measures angularity based on the packing properties of the aggregates. Packing of aggregates is generally a function of surface texture, shape, and gradation in addition to angularity. Masad et al. (2003) also reported that uncompacted voids do not relate to the AIMS angularities or surface textures measured on the fine aggregate.

Table 4.9 Fine aggregate angularity (uncompacted voids)

Quarry	Producer	FAA
Murphy	Fordyce	51
Marble Falls	Capitol	36
Beckmann	Martin Marietta	46
Solms Road	Martin Marietta	47
Spicewood	Vulcan	46
Yearwood	R.T.I.	53
Feld	Texas Crushed Stone	-
Burnet	Hanson	77
1604	Vulcan	39
Lone Star	Dean Word	-
Mico # 68	Lattimore	42
Pit 365	Mine Service	47
Tehuacana	Vulcan	46
Luckett	Trinity	-

4.5 Filler characterization

Filler is defined as that fraction of the aggregate passing the #200 sieve. It interacts with the binder to form a mastic or mortar that provides cohesion to the mix. The amount of filler in a mix should be controlled because too much filler may result in lean mixes with workability and durability issues and too low filler content does not provide the mortar stiffness necessary to counter permanent deformation.

Traxler (1937) assumed that any stiffening of mortars should be related to the physical properties of fillers, such as particle size, grain-size distribution, and shape. Anderson et al. (1982) investigated the influence of dust in HMA and found that fineness is not always a measure of the magnitude of stiffening that will result when a dust is added to bitumen. The stiffening that occurs in filler-bitumen mixtures is more apparent in the softening point test results than in viscosity or penetration test results. They concluded that fine mineral dusts may act as a bitumen extender even though they stiffen the bitumen. When fine dusts are used as a bitumen extender, the mix properties can be very sensitive to changes in bitumen content. Maximum and minimum filler:binder ratios must be based on the effect of the fine dust on fatigue, creep, compactibility, and other mixture properties.

Anderson (1987) developed guidelines for the use of dust and presented spatial models for filler-bitumen mastics as shown in Figure 4.1. The gradation of the dust fraction should be measured. He suggested that the percentage free bitumen in the dust fraction should be maintained at 40 percent or less, based on mechanical properties and workability.

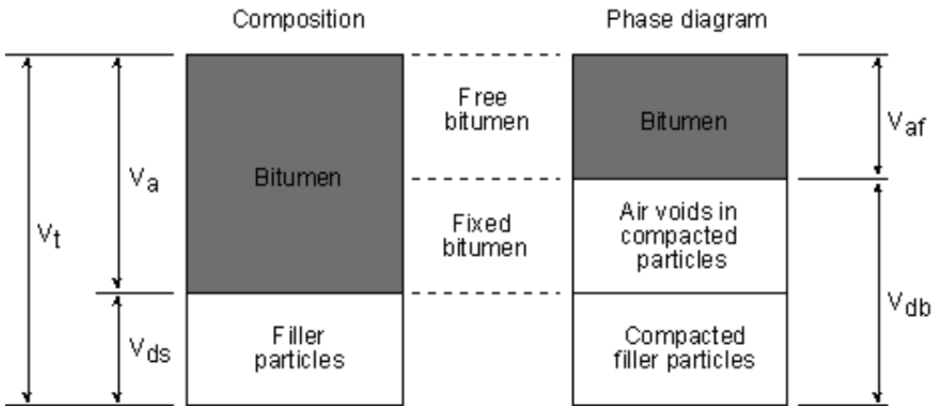

Figure 4.1 Filler-binder spatial model (Anderson, 1987)

Cooley at al. (1998) reported that a property derived from the dry compaction test on fillers (the percent bulk volume) has been shown to be an indicator of filler's stiffening potential. A limiting value of bulk volume was selected as 55 percent based on tests at both high service temperatures (softening point) and mixing/transport/compaction temperatures. Figure 4.2 shows a relation between the percent bulk volume and ring and ball temperature.

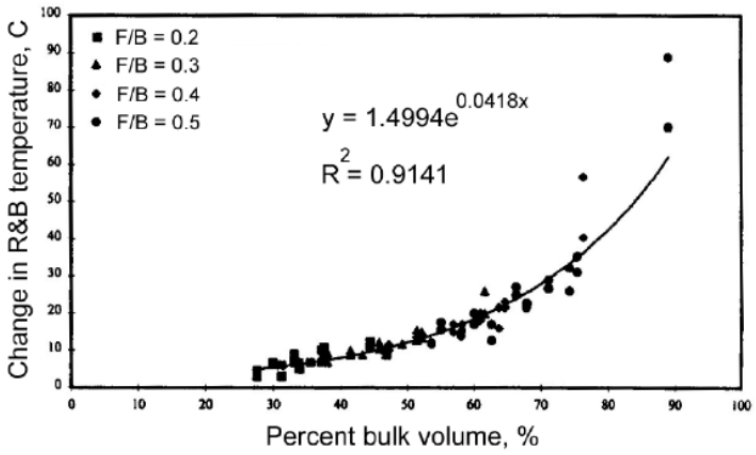

Figure 4.2 Relationship illustrating stiffening of filler-bindermortar (Cooley et al., 1998)

A study in Argentina (Recasens et al., 2005) addressed the critical concentration of filler in HMA. They suggest that this critical concentration corresponds to a dispersion of filler particles in the bitumen moving as freely as possible but in contact with each other, i.e., when applied stresses in the viscous deformation of the continuous filler-bitumen medium is such that frictional resistance between particles is at a minimum. This particle arrangement is what is expected in a sediment and is obtained by settling a dispersion of filler. The critical concentration is calculated with the following equation:

$$C_s = \frac{P}{V \cdot \gamma} \qquad \textbf{Eq. 4.1}$$

where

C_s = critical concentration of filler,
P = dry weight of filler (g),
V = settled volume of filler in anhydrous kerosene after 24 h (cm^3), and,
γ = specific gravity of the filler (g/cm^3).

Rigden (1947) described the volumetric properties of dry compacted fillers. Fillers compacted to maximum density without crushing the particles have air voids in the aggregate structure as illustrated in Figure 4.1. The binder required to fill these voids is called *fixed binder*. The binder in excess of the fixed binder (so-called *free bitumen*) is used to lubricate the filler particles and enables it to move freely in the viscous binder medium. Rigden hypothesized that mastic with a binder content less than that of the fixed binder content, which is a bare minimum binder required to fill the voids inside the filler structure, becomes stiffer and results in dry mastic. Availability of free bitumen allows the mastic to be more fluid and enables the binder filler medium to coat the coarser aggregates.

The apparatus shown in Figure 4.3 is used to compact filler to allow the calculation of fixed and free binder volumes. The apparatus consists of a small 100g compaction hammer and mold. About 1g of filler is compacted using the hammer falling freely from a height of an inch and 25 blows.

Figure 4.3 Rigden compaction apparatus

The following filler properties are defined:

$$\%V_{dv} = \frac{V_{db} - V_{ds}}{V_{db}} \qquad \textbf{Eq. 4.2}$$

$$\%V_{db} = \frac{V_{db}}{V_a + V_{ds}} \cdot 100 \qquad \textbf{Eq. 4.3}$$

$$\%V_{af} = 100 - \%V_{db} \qquad \textbf{Eq. 4.4}$$

where,

V_{ds} = volume of filler,
V_{af} = volume of free binder,
$\%V_{db}$ = percent bulk volume of filler,
V_a = volume of binder,
V_{db} = bulk volume of compacted filler,
$\%V_{dv}$ = percent voids in compacted filler (Rigden's voids), and,
$\%V_{af}$ = percent free binder.

Table 4.10 shows Rigden's voids determined for all the fillers used in the CAM mixes prepared from the various aggregate sources used in the study.

Table 4.10 Rigden's voids of CAM fillers

Quarry	Producer	AVG
Murphy	Fordyce	29.72
Marble Falls	Capitol	34.00
Beckmann	Martin Marietta	38.89
Solms Road	Martin Marietta	34.22
Spicewood	Vulcan	42.44
Yearwood	R.T.I.	38.91
Feld	Texas Crushed Stone	-
Burnet	Hanson	36.66
1604	Vulcan	31.70
Lone Star	Dean Word	-
Mico # 68	Lattimore	30.16
Pit 365	Mine Service	37.81
Tehuacana	Vulcan	37.81
Luckett	Trinity	-

The Belgium mix design method includes an expression for the increase in softening point of filler-binder mortars as a function of the voids in filler (Rigden's voids) and filler-binder ratio expressed in volume units as shown in Figure 4.4. Based on their experience, the optimum filler-binder ratio depends on the Rigden's voids of the filler and is selected such that an increase in softening point of between 12 and 16 °C (54 and 61 °F) is achieved in order to satisfy both durability and stability requirements.

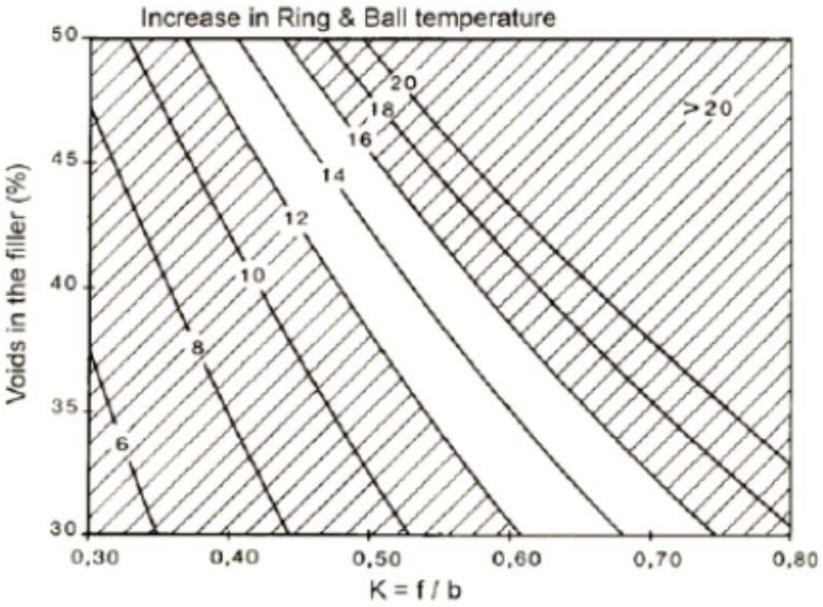

Figure 4.4 Increase in softening point as a function of filler properties

In an attempt to improve the performance of CAM with local aggregates, the researchers explored the option of optimizing the filler-binder ratio of CAM. The Superpave mix design method, for example, recommends filler binder ratios of between 0.6–1.2 on a mass basis. With asphalt contents typically above 7 percent and filler contents that ranged from 2–7 percent, the filler binder ratio of the CAMs initially evaluated typically varied from 0.3–1.0. The higher the filler content the stiffer the mastic, which could improve the stability and rutting performance of CAM. Too high a filler content, however, leads to mixes with low workability and durability problems.

To optimize the filler-binder ratio of CAM, the researchers ran ring and ball softening point tests (ASTM D36) on filler-binder mastics at varying ratios. Based on the results of this testing and using the Belgium method illustrated in Figure 4.4 as a guide, it was found that the filler-binder ratio of CAM could be increased to 1.3 without compromising workability. An aggregate stockpile high in filler content was obtained from the Marble Falls quarry and a new CAM designed to achieve the filler-binder ratio of 1.3. This is the Marble Falls II mix, the design of which is discussed in the next chapter.

HWT tests were run on this mix using a PG 76-22 binder, which failed prematurely before the application of 7,000 cycles. Attempts to improve the performance of the mix using a stiffer PG 82-22 binder also failed. The results of the HWT tests on these mixes are shown in Figure 4.5.

Another aspect influencing the characteristic of the filler component in the mix is the particle size distribution of the dust. The hydrometer test (ASTM D 422) may be used to establish the particle size distribution in fine soils (clays and silts). The test uses the technique of sedimentation in a long vertical cylinder of specific diameter with the settlement of the particles monitored over time. This test was run on the CAM fillers and the size distributions obtained for the various fillers tested are shown in Figure 4.6. The percentage of particles in suspension with less than 10 micron size was selected as a filler characterizing parameter. It is interesting to see a

significant difference in the hydrometer particle distribution for fillers from the Burnet and Marble Falls quarries compared with the other fillers.

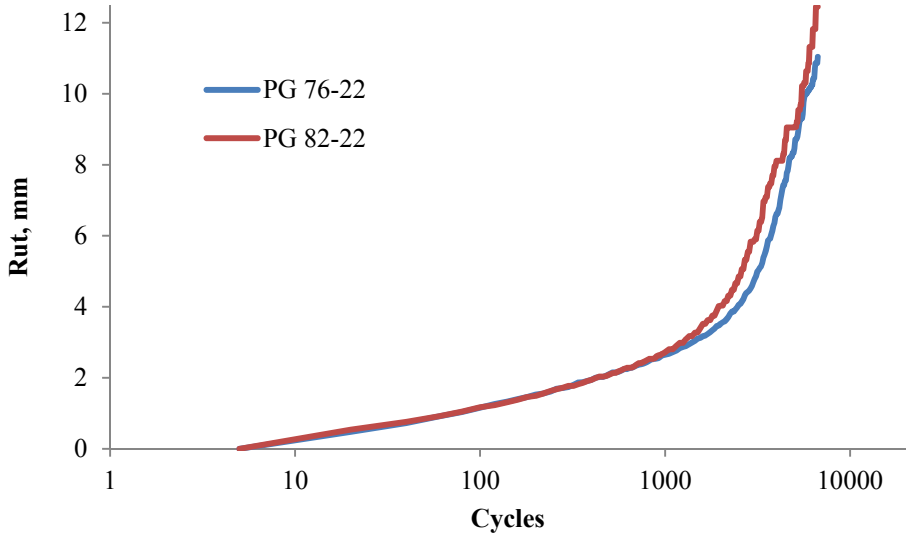

Figure 4.5 HWT testing of Marble Falls II gradation

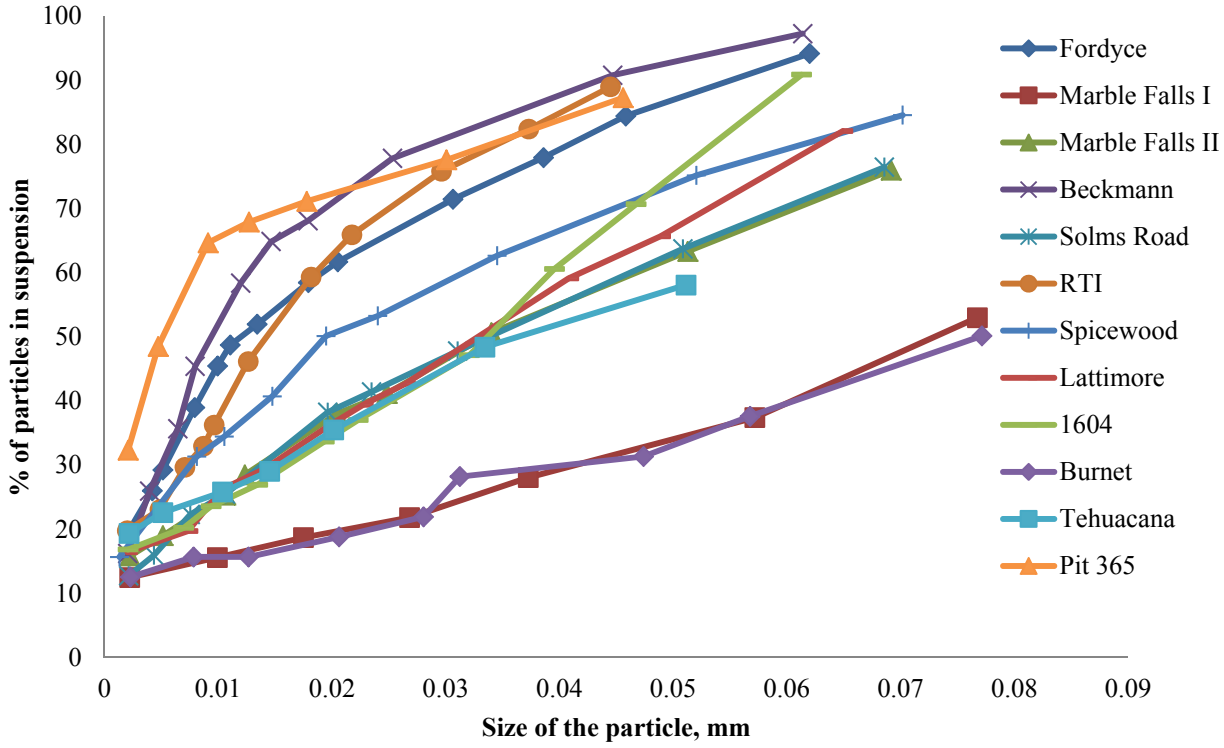

Figure 4.6 Hydrometer particle distribution of CAM fillers

Chapter 5. CAM Mix Design with Local Aggregates

This chapter discusses the volumetric mix design of CAM with local aggregates. Initially the current CAM specifications were applied and the volumetric properties and shear characteristics of these mixes were evaluated. Based on the rutting and cracking performance of these mixes together with the volumetric criteria, revised mix design recommendations were established and additional CAM were designed based on these new recommendations. The revised mix design recommendations are provided in a later chapter following a discussion of CAM rutting and cracking performance.

5.1 CAM gradations

The gradations of the various CAM mixes initially evaluated as part of the study are shown in Table 5.1. Following an evaluation of the volumetric and performance properties of these mixes, additional CAM were designed, the gradations of which are shown in Table 5.2. A total of 14 mixes were designed. All of the mixes fall within the special specification 3165 gradation limits.

In general the coarse and fine stockpiles collected from individual quarries were blended to obtain the required gradations. However, in three selected cases, either the coarse or the fine stockpiles were replaced, as shown in Table 5.2, to obtain the required gradations. The two Marble Falls mixes had different fine stockpiles—one having higher filler content than the other, but both from the same source.

Table 5.1 Initial CAM gradation designs

Sieve	CAM Specification	Fordyce	Marble Falls I	Marble Falls II	Beckmann	Solms Road	RTI	Spicewood
1/2 "	100	100.0	100.0	100.0	100.0	100.0	100.0	99.9
3/8"	98-100	98.6	99.8	99.8	100.0	99.9	100.0	97.4
#4	70-90	82.3	83.4	82.1	78.6	77.5	79.0	74.0
#8	40-65	52.7	54.6	50.7	62.6	52.2	52.8	57.7
#16	20-45	34.2	38.3	35.9	36.6	35.2	36.4	33.0
#30	10-30	20.9	26.4	25.7	19.0	22.2	22.2	19.9
#50	10-20	12.3	16.8	19.8	10.0	12.3	13.7	14.0
#200	2-10	6.2	2.7	8.9	4.1	2.3	5.4	7.2

Table 5.2 Secondary CAM gradation designs

Sieve	CAM Specification	Lattimore	1604	Burnet	Pit 365	Luckett/ Tehuacana	Feld/ Tehuacana	Lone Star/ Pit 365
1/2 "	100	100.0	100.0	100.0	100.0	100.0	100.0	100.0
3/8"	98-100	99.8	99.7	99.3	99.4	100.0	100.0	99.9
#4	70-90	70.7	81.1	74.9	71.9	76.0	74.7	71.8
#8	40-65	46.0	41.8	46.5	49.6	49.1	50.4	43.4
#16	20-45	30.9	29.6	30.0	36.0	37.4	37.2	31.6
#30	10-30	20.3	21.5	18.6	24.7	27.7	27.4	21.9
#50	10-20	12.1	14.6	10.4	17.0	19.4	19.6	15.3
#200	2-10	3.3	5.2	2.2	7.6	5.6	6.7	7.0

5.2 Volumetric design

Special specification 3165 was used for the initial mix design of CAM with local aggregates. The OAC were initially established by testing at different asphalt contents with each aggregate blend and selecting the OAC to achieve 98 percent relative density after 50 gyrations. The *Servopac* SGC with the capability to measure the shear stress applied to the mix during compaction was used. All mixtures were subjected to short term oven aging (STOA) for 2 hours prior to compaction as per Tex-241-F. Lime was added to each mix at 1 percent by mass. A PG 76-22 from Valero was used throughout the study. In Appendix C, volumetric plots showing the change in relative density, VMA, and voids filled with asphalt (VFA) with compaction are shown for each of the mixes evaluated in the study. Also shown on these plots is the shear stress with gyratory compaction. The legends of these figures indicate the percentage asphalt content at which the mixes were compacted.

Apparent in the gyratory compaction characteristic plots shown in Appendix C is the decreased rate of compaction for many of the designed mixes, particularly at the higher AC contents. This is clear from the change in the slope of the relative density curves with compaction indicating a resistance to compaction. This resistance to compaction occurs as a result of the voids in the mix becoming filled with asphalt. The compressed asphalt in these voids builds hydrostatic or pore pressures that negates further compaction of the mix. This behavior was assumed from a *visual* assessment of the specimens after compaction, where excess asphalt was noticeable on the surface and sides of specimen after compaction, being forced and squeezed from the mix, while no excessive crushing of the aggregate was apparent during compaction; however, no extractions were performed to confirm this.

The increase in pore pressures in the mix (u) would reduce the effective strength of the mix based on the Terzaghi principle:

$$\sigma' = \sigma - u \qquad \textbf{Eq. 5.1}$$

This is confirmed from the decrease in shear stress apparent for many of the CAM designed, particularly for those at higher asphalt contents. This decrease in shear stress is not the characteristic behavior for asphalt mixes, which would typically exhibit an increase in shear stress to an upper bound based on the cohesive strength and aggregate internal friction. This

upper bound is maintained throughout compaction unless the mix undergoes shear failure, which is the case for many of the CAM designed.

The loss in shear stress for these CAM is an indication that the voids in the mix have become overfilled with asphalt. The figures that follow (Figure 5.1 through 5.9) compare the loss in shear stress to the VFA for most of the CAM designed at varying asphalt contents. The optimum asphalt contents (OAC) of the mixes is shown. It is interesting to note that shear failure occurs when the VFA in the mix increases beyond a certain limit. The reader is reminded of the Superpave mix design restriction placed on VFA from 65 to 75 percent to prevent the mix from overfilling with asphalt. This is analogous, although from the figures it is clear that there is no single limit at which shear failure occurs. For the Fordyce gravel mix with PG 76-22 binder as shown in Figure 5.1, shear failure of the mix occurs at a VFA of approximately 65 percent for an AC of 7 percent but at 80 percent for the other AC levels. In general, the higher the AC content, the higher the VFA of the mix at shear failure. This could indicate that the additional binder serves to further lubricate the mix to facilitate further compaction. Figure C.11 shows an example of CAM (Burnet aggregate source) that does not exhibit a loss in shear strength. Shear failure is apparent, however, in all mixes where VFA has increased beyond 80 percent, but there is a risk of shear failure when VFA is beyond 65 percent. As such, VFA is probably not the best criterion to indicate overfilling of the mix. The researchers therefore recommend that the gyratory shear stress be measured during the design of CAM to ensure that the mix does not undergo excessive shear failure at optimum asphalt content.

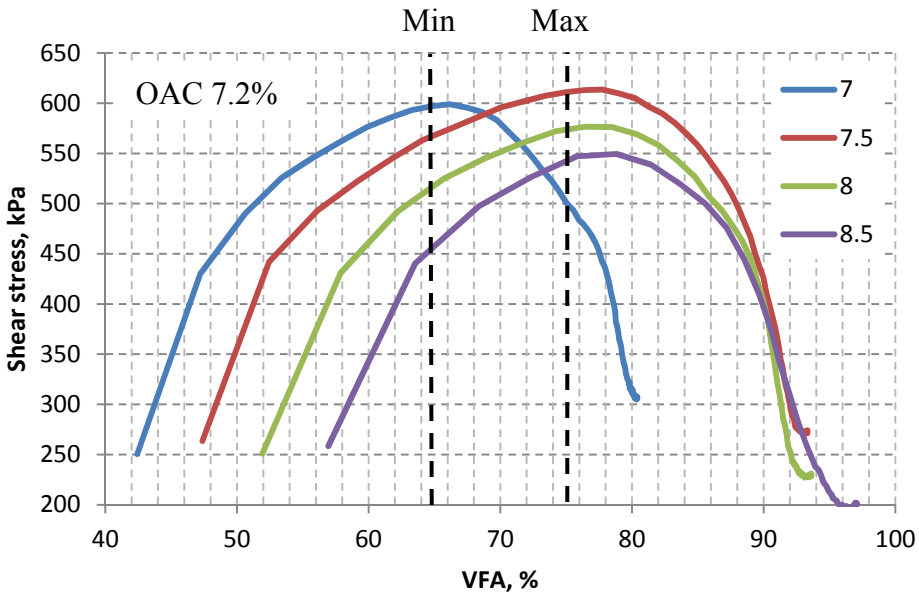

Figure 5.1 VFA vs. shear stress for Fordyce gravel PG 76-22 mix

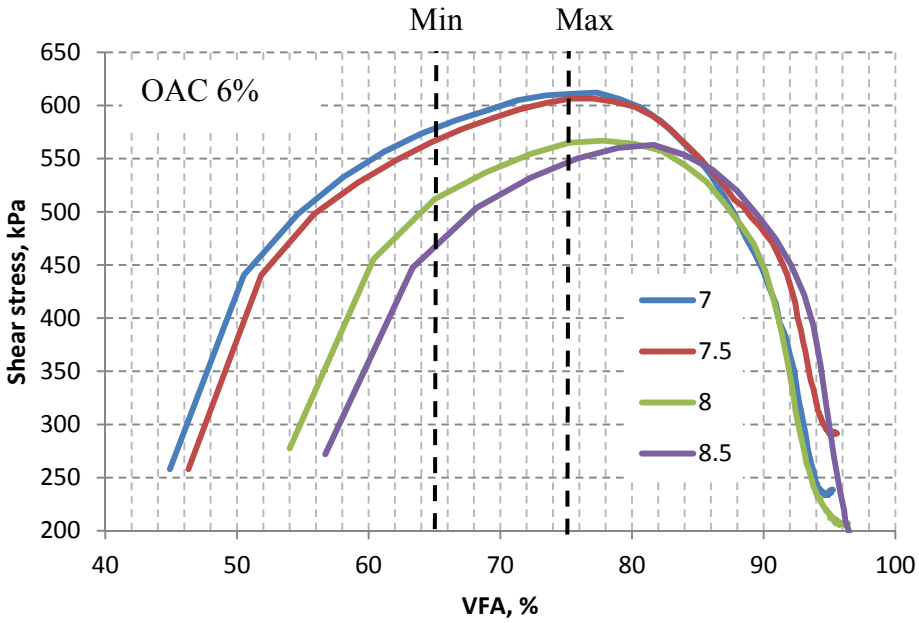

Figure 5.2 VFA vs. shear stress for Fordyce gravel PG 70-22 mix

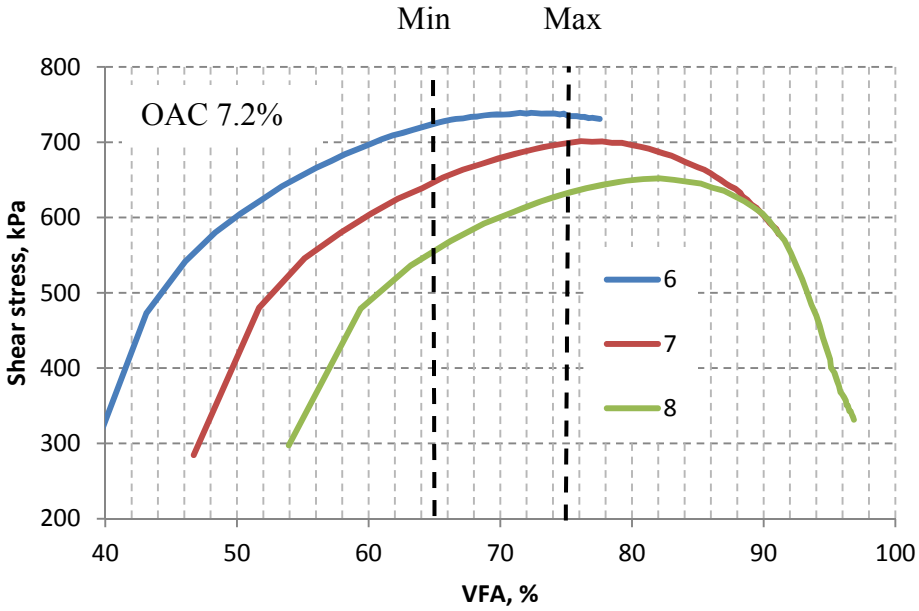

Figure 5.3 VFA vs. shear stress for Marble Falls I mix

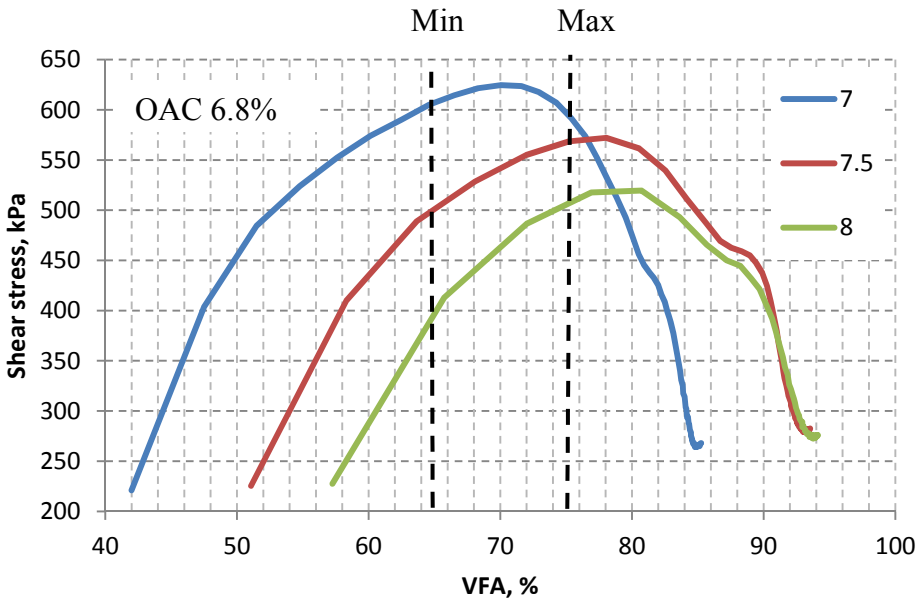

Figure 5.4 VFA vs. shear stress for Marble Falls II mix

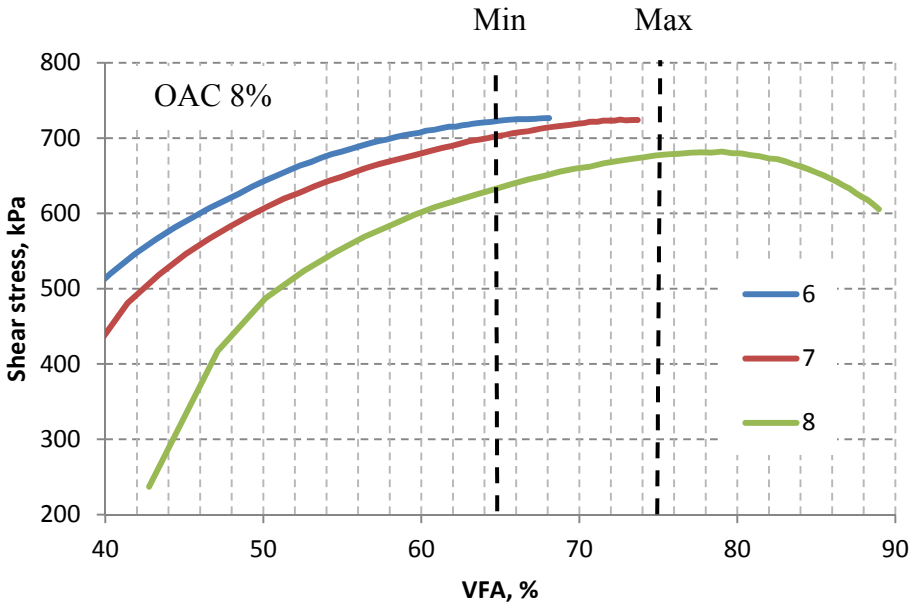

Figure 5.5 VFA vs. shear stress for Beckmann mix

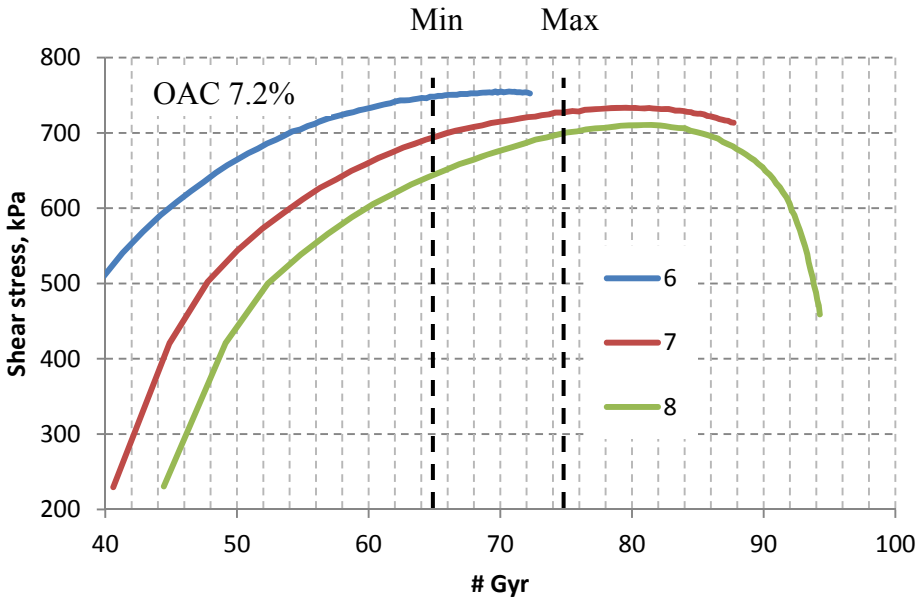

Figure 5.6 VFA vs. shear stress for Solms Road mix

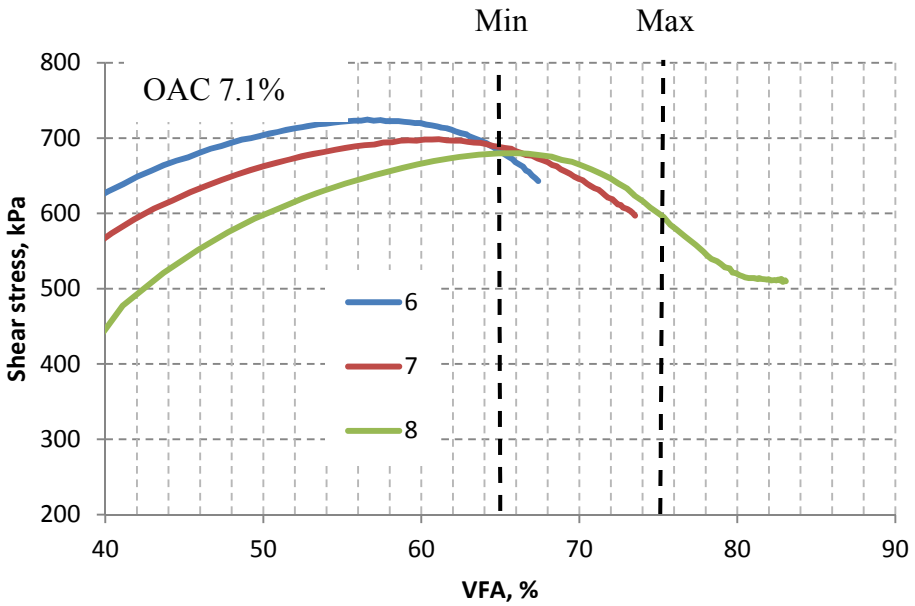

Figure 5.7 VFA vs. shear stress for RTI mix

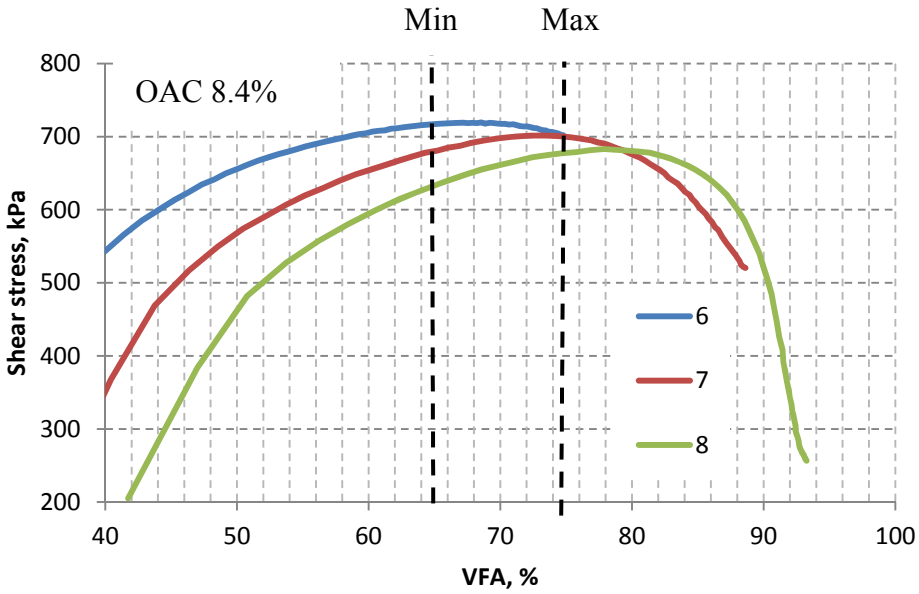

Figure 5.8 VFA vs. shear stress for Spicewood mix

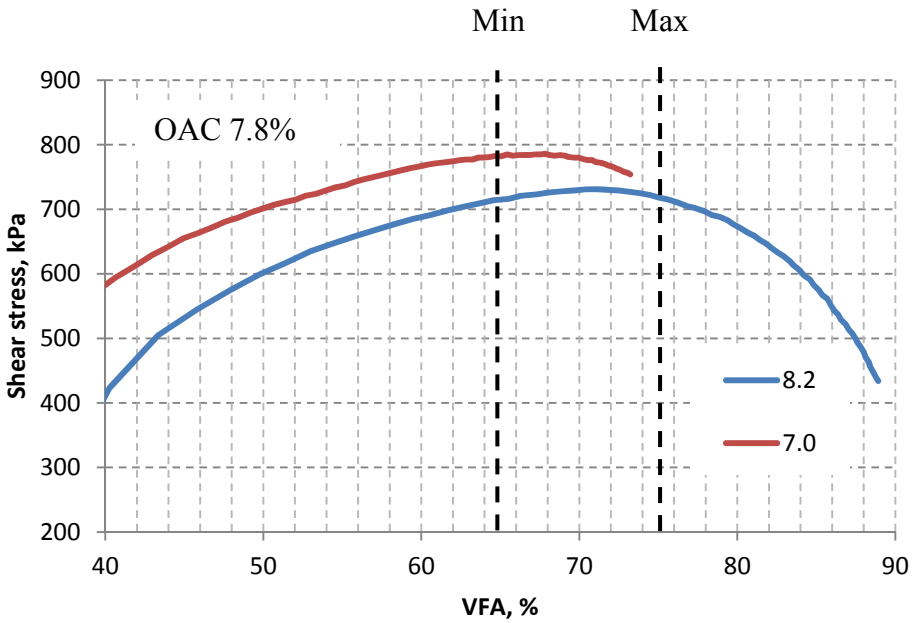

Figure 5.9 VFA vs. shear stress for Lattimore mix

The use of the less stiff PG 70-22 binder exacerbated the densification of the Fordyce gravel CAM mix, requiring less compactive effort to over-densify, even at the lower AC levels.

From an evaluation of the volumetric properties of these mixes at varying asphalt contents, the design of CAM to 98 percent relative density poses a risk of selecting optimum asphalt contents that would result in overfilling of these mixes with subsequent shear failure. Following an evaluation of the rutting and cracking performance of CAM, revised mix design recommendations are provided in a later chapter to improve the performance of CAM designed using local aggregates.

Chapter 6. Performance Testing of CAM

This chapter discusses the performance testing of CAM to evaluate its resistance to cracking, rutting, and moisture susceptibility. The applicability of the current CAM performance criteria are also evaluated towards developing minimum failure criterion for CAM mixes with local aggregates.

6.1 HWT rutting performance

The HWT was used to evaluate the rutting and stripping performance of the CAM mixes as specified in special specification 3165 using Tex-242-F. The results of the HWT tests on the project mixes are summarized in Table 6.1, with cycles to failure determined at a 0.5 inch rut. In addition to cycles to failure, the table includes other HWT parameters such as the creep and stripping slopes, cycles at the stripping inflection point (SIP), the deformation after 5,000 cycles (D5K), and the deformation at the SIP (DSIP). Figure 6.1 illustrates these parameters. The SIP is defined as the number of cycles at the intersection of the creep and stripping slopes.

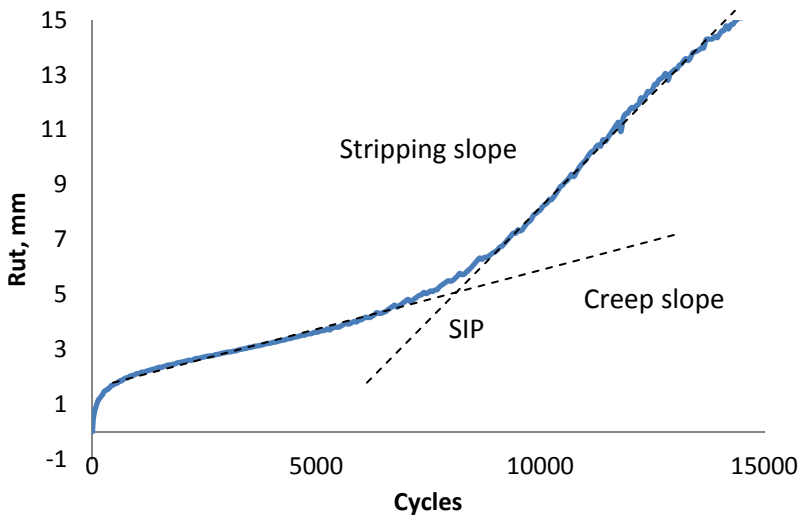

Figure 6.1 HWT parameter definitions

Not all of the CAM mixes designed could be tested in the HWT. Despite the fact that prepared specimens were left in the mold for a significant amount of time, some of these mixes would fall apart on cooling after being compacted at high optimum asphalt contents at the 7 percent air voids level required for HWT testing. The HWT results highlight the poor rutting performance of the CAM mixes with local aggregates. The majority of the CAM mixes evaluated failed before achieving 10,000 cycles. Stripping of the binder from both the coarse and fine aggregate components was evident in the majority of the mixes tested. The figures in Appendix D show the average HWT curves for the mixes tested. These are plotted in log-scale to accentuate the stripping slopes.

Table 6.1 CAM HWT results

Mix	AC, %	Cycles	Creep*	Stripping **	SIP	D5K	DSIP
Fordyce	6.0	10,800	0.0004	0.0016	4,800	3.747	3.522
	7.0	9,433	0.0005	0.0016	3,500	5.441	3.493
	8.0	7,550	0.0007	0.0021	3,600	7.049	4.798
Marble Falls I	6.0	20,000	0.0002	0.0013	11,350	2.098	3.472
	7.0	12,550	0.0004	0.0014	7,350	3.618	4.989
	8.0	10,300	0.0007	0.0013	5,400	5.936	6.256
Beckmann	6.0	11,250	0.0004	0.0014	4,050	3.632	2.861
	7.0	10,250	0.0004	0.0016	3,150	2.629	5.501
	8.0	8,750	0.0006	0.0015	2,150	6.67	2.66
Solms Road	7.2	7,150	0.0009	0.0018	2,950	8.928	4.459
RTI	7.1	6,050	0.0008	0.002	1,150	9.244	2.374
Spicewood	8.4	7,800	0.001	0.0017	3,900	7.458	5.803
Lattimore	7.8	8,100	0.0006	0.0017	2,000	2.27	6.402
1604	7.1	10,500	0.0005	0.0014	2,600	5.505	2.541
Burnet	7.6	20,000	0.0003	0.0006	11,200	3.787	5.811
Luckett/Tehuacana	7.3	10,200	0.001	0.001	NA	6.957	NA

* Number of passes for 1mm rut depth due to rutting alone
** Number of passes for 1mm rut depth due to rutting and stripping

The photographs that follow (Figures 6.2 through 6.4) illustrate the stripping of the coarse and fine aggregates apparent after testing the CAM mixes in the HWT. Observing some of the CAM specimen during HWT testing it was apparent that the mix is pushed and kneaded backwards and forwards under the action of the wheel load. Maximum deformation in the HWT was not in the center between the two HWT specimens tested but rather at the edges of the specimen where the test wheel reverses direction. Material was also shoved out from under the wheel as shown in the photographs.

It is clear that the CAM mixtures tested are particularly moisture susceptible and prone to stripping. It is hypothesized that the mechanism of failure in the HWT is as a result of rapid initial densification of these mixes under the HWT wheel load. With initial trafficking the voids on the surface of the specimen, which are filled with water, would rapidly reduce to low levels. At this point, pressure on the surface of the specimen would result in extremely high hydrostatic pressures confined within the low voids within the specimen that results in the binder being stripped from the aggregates. It is doubtful whether anti-stripping agents would be beneficial under these conditions.

The HWT testing emphasized the stripping potential of CAM with local aggregates and is the right tool to evaluate the moisture susceptibility of these mixes. CAM also have a high percentage of fine aggregates that are likely hydrophilic with the potential for attracting moisture. Thus, not only are these mixtures susceptible to rutting, given the high asphalt contents used, but are also susceptible to moisture and stripping through the combined action of low air voids and the potential to mobilize high pore-water pressures.

Figure 6.2 HWT testing of RTI mix

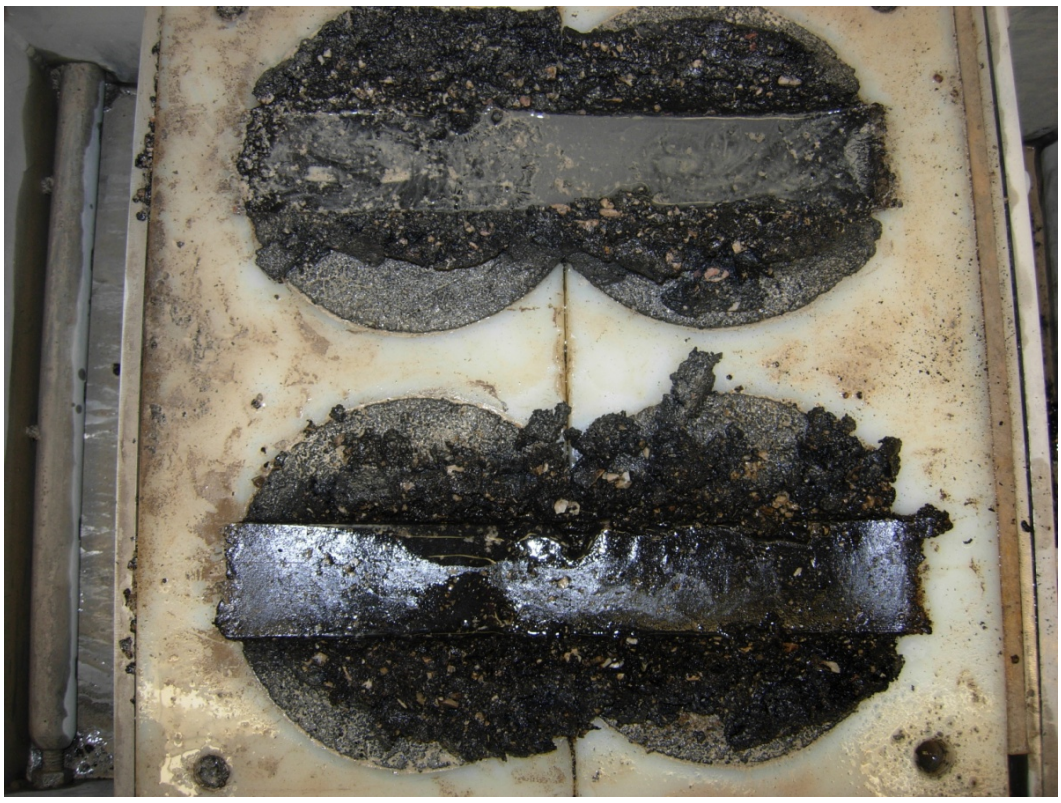

Figure 6.3 HWT testing of Solms Road mix

Figure 6.4 HWT testing of Spicewood mix

CAM mixes in the field are compacted to 96 percent relative density in thin lifts, often in the order of 1 inch. The HWT test criteria based on Tex 242-F require specimen thicknesses of 63±1 mm and a relative density of 93±1 percent. To evaluate the response of CAM compacted to 96 percent relative density and 1 inch in height, HWT tests were run on thin 1 inch specimen supported by rigid underlying bases trimmed to provide the required thickness in the HWT mold. Specimens compacted to 96 percent relative density were also tested. Figure 6.5 shows the results of these tests.

From the figure it can be seen that there was no significant difference in the two specimens with different densities but the thinner specimen failed sooner. Stripping is again evident in all cases. Although based on limited testing, these results do support the hypothesis that the CAM mixes densify rapidly under the HWT, such that it is irrelevant whether HWT testing is done at 93 or 96 percent relative density. It is interesting to note that the thin CAM specimen failed more rapidly, as it suggests that the HWT as currently run on thicker specimen may not be appropriate to evaluate the rutting performance of mixes in thin overlays. These mixtures, particularly if supported by stiff underlying bases, would be subjected to very high compressive stresses with an increased potential for rutting failure. This warrants the development of alternative testing protocols to evaluate HMA mixes used in thin overlays.

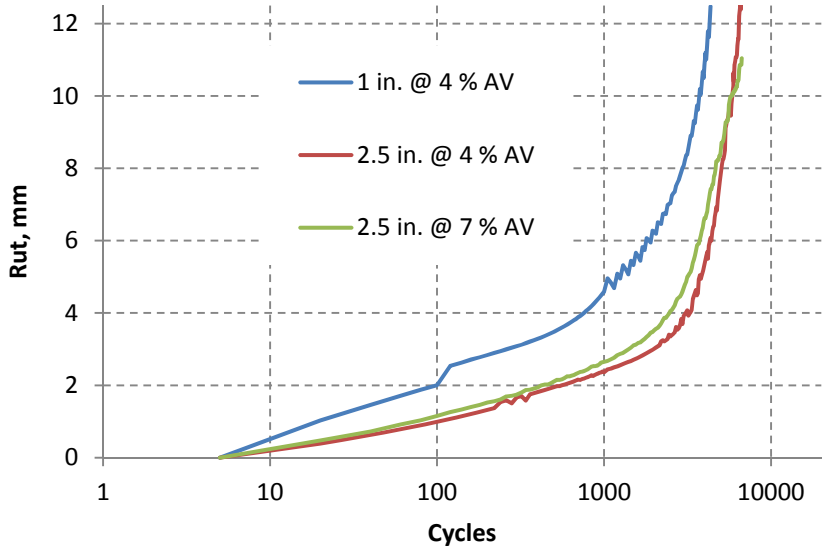

Figure 6.5 HWT of Marble Falls II with varying thickness and density

6.2 Kim's rutting test

Kim's rutting test was previously discussed in the literature review section of this report. In this test a 40 mm diameter ram is pushed into the surface of a 150 mm diameter gyratory compacted specimen at a constant displacement rate of 50 mm/min. To evaluate this test, CAM specimen were prepared to 93 percent relative density and conditioned in water at 50 °C/122 °F for at least 30 minutes prior to testing. For illustrative purposes, plots of the load-deformation curves of specimen tested to failure in Kim's test are shown in Figure 6.6 for different CAM mixes prepared and tested at different AC contents.

From the figure it can be seen that the more rut-resistant Marble Falls I limestone mix undergoes lower deformation at a higher load compared to the Fordyce gravel mix at the higher AC content. It is important to note that the strength parameter is calculated based on the deformation at maximum load. After this point the mix loses lateral confinement due to failure of the specimen.

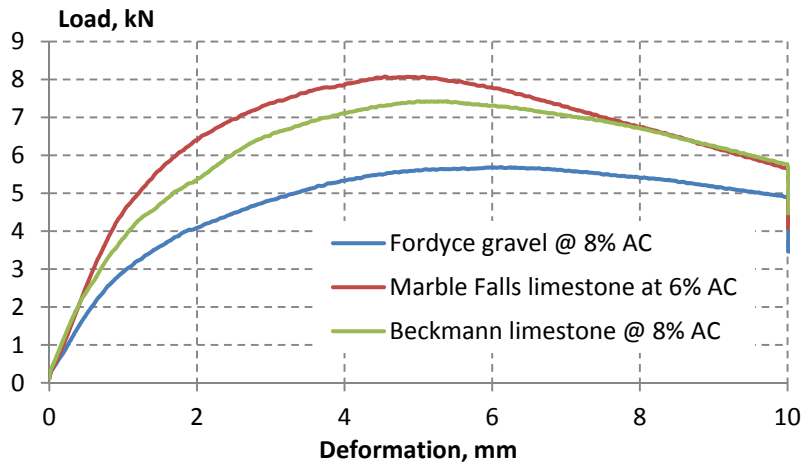

Figure 6.6 Kim's test load-deformation plots

Table 6.2 summarizes the results of the Kim's tests on the CAM mixes tested, showing the number of tests as well as the mean, standard deviation and coefficient of variation (COV) of the rutting strength parameter (SD) calculated using Eq. 2.1 for the mixes at three asphalt contents.

Table 6.2 Kim's test results (SD)

Mix	AC, %	# Tests	Mean, MPa	Stdev, MPa	COV, %
Fordyce	6	2	7.9	0.2	3.0
	7	2	6.7	0.1	1.2
	8	2	4.8	0.2	3.9
Marble Falls I	6	2	7.7	0.0	0.1
	7	2	5.1	0.2	4.7
	8	2	4.3	0.1	1.4
Beckmann	6	2	9.9	0.4	4.5
	7	2	9.4	0.4	4.7
	8	2	6.8	0.2	2.2

No rutting criteria have been developed to assess the rutting potential of asphalt mixes based on Kim's test. However, the higher the strength parameter, the better the expected rutting performance. Figure 6.7 and Figure 6.8 compare the Kim's strength parameter to the HWT cycles to failure for the mixes tested. When comparing the Fordyce gravel and Beckmann limestone rutting performances, a linear trend is apparent but the Marble Falls limestone mix does not fit these data. In fact the Marble Falls limestone mixes strength parameter at 6 percent AC is lower than that for the Beckmann limestone at 6 percent AC. However, the former clearly performed better in the HWT.

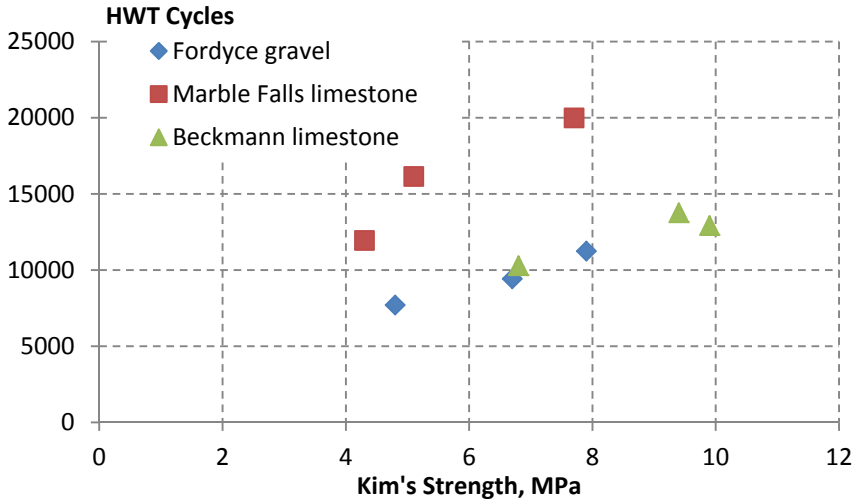

Figure 6.7 Comparing Kim's and HWT test results

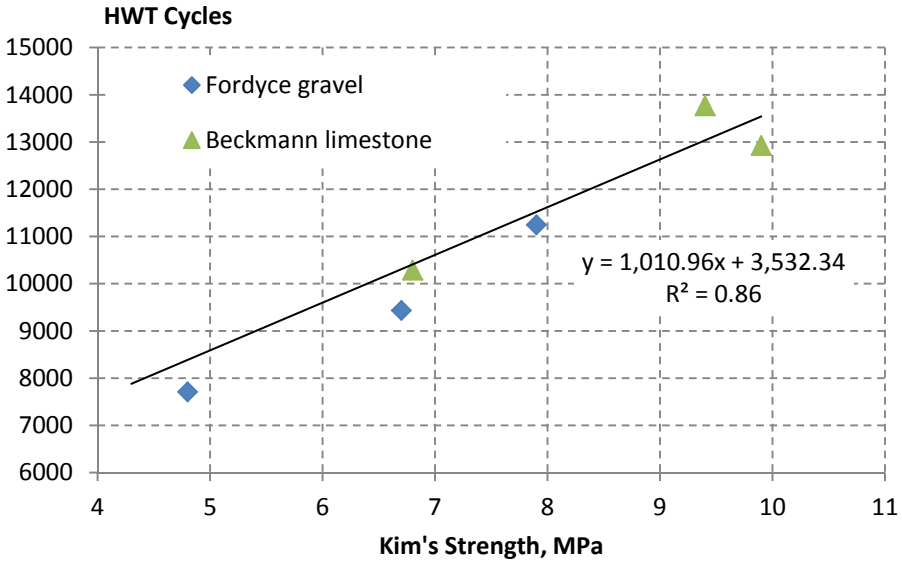

Figure 6.8 Correlation between Kim's test and HWT

Based on the preliminary testing, clearly further research is required to better relate Kim's and HWT testing results. Excluding the Marble Falls data the two tests compare well. Options to explore for Kim's test would be testing at higher temperatures, e.g., 60 °C (140 °F), slower loading rates, and providing a *degree* of lateral confinement to the test specimen analogous to Hveem stabilometer testing. One CAM mix was evaluated using Kim's test by testing the specimen with complete confinement in the gyratory compaction mold. This resulted, however, in very high loading forces. Another option to explore would be to test specimen unconfined but to reduce the diameter of the test ram, thereby increasing the volume of lateral confinement provided by the specimen. The test does show promise, however, particularly for screening fine-graded CAM mixes.

6.3 CAM cracking resistance

The resistance of CAM to cracking was evaluated using the OT, IDT, and SCB tests.

6.3.1 Overlay tester

OT tests on the CAM mixes were done as part of the study in accordance with TxDOT Tex-248-F by Pavetex, Inc. Table 6.3 summarizes the results of these cracking tests. Current CAM criteria require at least 750 cycles for a 93 percent stress reduction. The cracking data indicate that only three of the CAM mixes tested passed the OT criteria, although the OAC of the Marble Falls I mix was closer to 7 percent, at which it fails the OT. The Spicewood and Burnet mixes were tested at OAC. The former failed the HWT criteria at this OAC but the Burnet mix just passed, making it the only CAM mix with SAC B aggregate evaluated as part of the study to pass both the HWT and OT criteria.

Table 6.3 CAM OT test results showing cycles to failure

Mix	AC, %	Tests	Mean	Stdev	COV, %
Fordyce	6	3	5	0	0.0
	7	3	31	2	5.0
	8	3	286	168	58.8
Marble Falls I	6	3	138	101	72.9
	7	3	557	188	33.7
	8	3	1,200	0	0.0
Beckmann	6	3	31	7	21.2
	7	3	125	59	47.1
	8	3	479	241	50.3
Solms Road	7.2	3	573	161	28.1
RTI	7.1	3	167	78	46.8
Spicewood	8.4	3	1,104	166	15.1
Lattimore	7.8	3	386	287	74.3
1604	7.1	3	95	35	36.8
Burnet	7.6	3	1,200	0	0
Luckett/Tehuacana	7.3	3	423	248	58.7

Apparent in Table 6.3 are the very high COV for the OT cycles to failure. High COV values are typically associated with OT testing of dense-graded mixes with larger aggregates. Clearly this test is highly variable even for fine-graded CAM even at the higher AC contents.

6.3.2 Indirect tensile test

Table 6.4 summarizes the results of the IDT test on CAM mixes at varying asphalt contents. The current CAM criteria require tensile strengths in the range of 80–200 psi. The

tensile strengths of the CAM mixes decrease with increasing AC content. These tests are run at 25 °C/77 °F.

Table 6.4 CAM IDT test results

Mix	AC, %	Tests	Mean, psi	Stdev, psi	COV, %
Fordyce	6	2	138.0	1.0	0.7
	7	2	122.0	8.6	7.0
	8	2	106.1	0.5	0.5
Marble Falls I	6	2	143.7	4.8	3.4
	7	2	126.8	3.7	2.9
	8	2	101.0	1.5	1.5
Beckmann	6	2	170.0	1.8	1.0
	7	2	160.7	2.1	1.3
	8	2	110.7	20.6	18.7

In itself, the tensile strengths as determined in the IDT provide no clear indication of the cracking potential of the CAM mixes tested. A better parameter in this regard is the area under the force-displacement curve that indicates the work required to fail the specimen—the more work, the greater the cracking resistance of the mix. The area under the curves until the peak load was determined for the mixes tested and is shown in Table 6.5.

Table 6.5 IDT area under force-displacement curve until peak load (kN.mm)

Mix	AC, %	Tests	Mean	Stdev	COV, %
Fordyce	6	2	34.1	2.4	6.9
	7	2	39.1	1.3	3.4
	8	2	41.2	2.0	4.8
Marble Falls I	6	2	57.0	0.8	1.4
	7	2	47.6	1.9	3.9
	8	2	46.0	1.0	2.2
Beckmann	6	2	36.3	0.6	1.7
	7	2	39.4	1.7	4.4
	8	2	42.9	0.2	0.4

The areas until peak load shown in Table 6.5 generally increase with increasing asphalt content for the different mixes. Thus, as expected, the resistance to cracking would increase accordingly. The exception is the Marble Falls mix that shows a higher area at the lower 6

percent AC level. From the COV values, the variability in the test data associated with the IDT is considerably lower compared to the OT.

6.3.3 Semi-circular bending test

SCB tests were run on the CAM mixes by notching the base of these specimens to a depth of 15 mm. SCB tests were run at a temperature of 25 °C/77 °F. Table 6.6 shows the average and standard deviation of the peak load to failure for the different CAM mixes tested. As for the IDT tests, the peak load decreases with an increase in asphalt content. However, ANOVA analysis on these three sets of data indicates that they are not significantly different (statistically).

Table 6.6 SCB peak load to failure (kN)

Mix	AC, %	Tests	Mean	Stdev	COV, %
Fordyce	6	4	6.6	0.3	4.9
	7	4	6.1	0.2	2.6
	8	4	5.6	0.4	8.0
Marble Falls I	6	4	7.6	0.3	4.4
	7	4	6.8	0.3	5.1
	8	3	5.4	0.2	3.2
Beckmann	6	4	7.0	0.1	1.2
	7	4	6.7	0.1	2.0
	8	4	6.2	0.2	3.8

Figure 6.9 compares the peak loads in the SCB compared to the IDT to fail the specimen. The asphalt contents at which the specimen were tested are shown. Overall, these loads have no clear relationship, although linear trends are evident for Fordyce and Marble Falls mixes. The IDT loads are an order 2 or more greater than corresponding SCB loads.

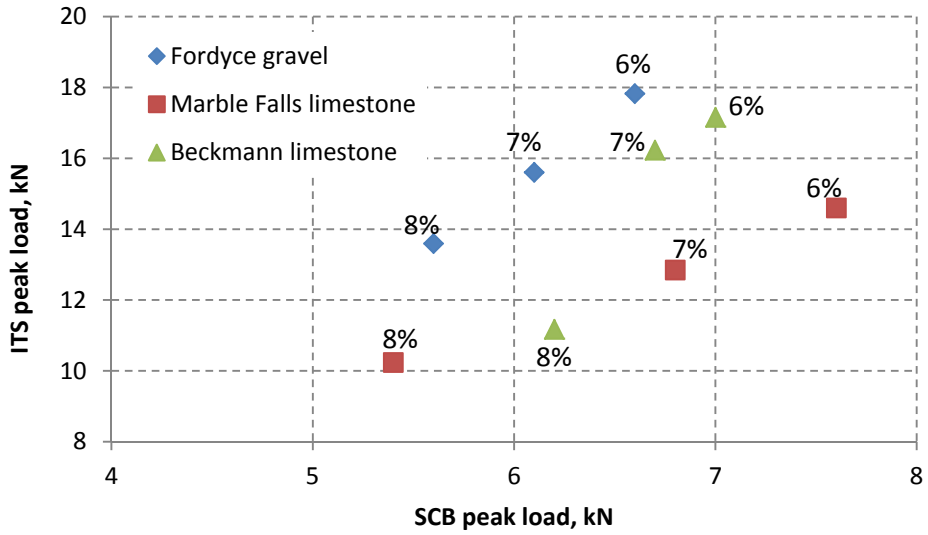

Figure 6.9 Comparison between SCB and ITS peak loads to fail specimen

Each of the SCB specimens tested provided a complete load-deformation curve. Thus, the area beneath the curves before and after the peak load could be calculated accurately. These data are shown in Tables 6.7 through 6.9. In each of these tables, the area (or work required to fail the specimen) increases with an increase in the asphalt content of the mix. This indicates the ability of the SCB to quantify the cracking potential of CAM. In each case, the Marble Falls mix at 8 percent AC has the greater area compared to the other mixes.

The area beneath the curves after the peak loads in the SCB test provide an indication of the work required to propagate the crack through the specimen after crack initiation, thus a viable parameter to measure the crack resistance of the CAM mixes. Figure 6.10 compares the number of cycles to failure as measured in the OT to the area in the SCB following the peak load. Although no clear trends are evident, as shown in Figure 6.11, a power law relationship is apparent if the Beckmann limestone data are excluded. The variability associated with the various SCB parameters are comparable to those measured in the IDT and lower than the variability observed in the OT.

Table 6.7 SCB total area under force-displacement curves (kN.mm)

Mix	AC, %	Tests	Mean	Stdev	COV, %
Fordyce	6	4	9.5	0.5	5.0
	7	4	11.6	0.9	8.0
	8	4	17.1	0.9	5.3
Marble Falls I	6	4	13.9	1.8	12.6
	7	4	19.5	2.8	14.6
	8	3	23.1	0.9	4.0
Beckmann	6	4	8.1	0.3	3.5
	7	4	9.7	1.0	10.6
	8	4	13.5	1.1	8.4

Table 6.8 SCB area before max load (kN.mm)

Mix	AC, %	Tests	Mean	Stdev	COV, %
Fordyce	6	4	4.0	0.2	4.3
	7	4	4.6	1.0	21.9
	8	4	5.8	1.2	20.1
Marble Falls I	6	4	5.2	0.9	16.4
	7	4	6.7	1.1	16.0
	8	3	7.8	0.2	2.0
Beckmann	6	4	3.5	0.3	7.7
	7	4	3.8	0.4	10.6
	8	4	5.2	0.6	10.8

Table 6.9 SCB area after max load (kN.mm)

Mix	AC, %	Tests	Mean	Stdev	COV, %
Fordyce	6	4	5.6	0.6	10.0
	7	4	7.0	0.7	9.5
	8	4	11.3	0.6	5.0
Marble Falls I	6	4	8.7	0.9	10.5
	7	4	12.7	1.9	14.7
	8	3	15.3	0.8	5.2
Beckmann	6	4	4.7	0.5	10.1
	7	4	5.9	0.6	10.9
	8	4	8.3	0.7	8.0

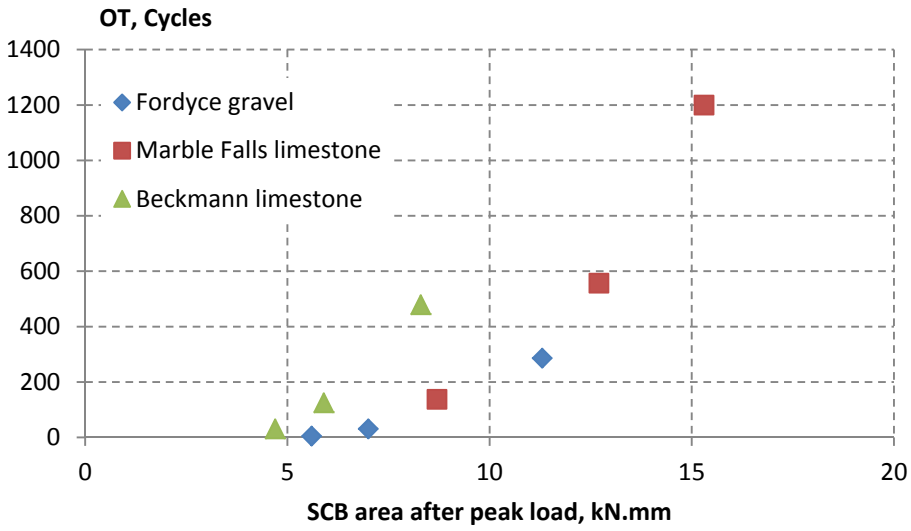

Figure 6.10 Comparison between OT and SCB results

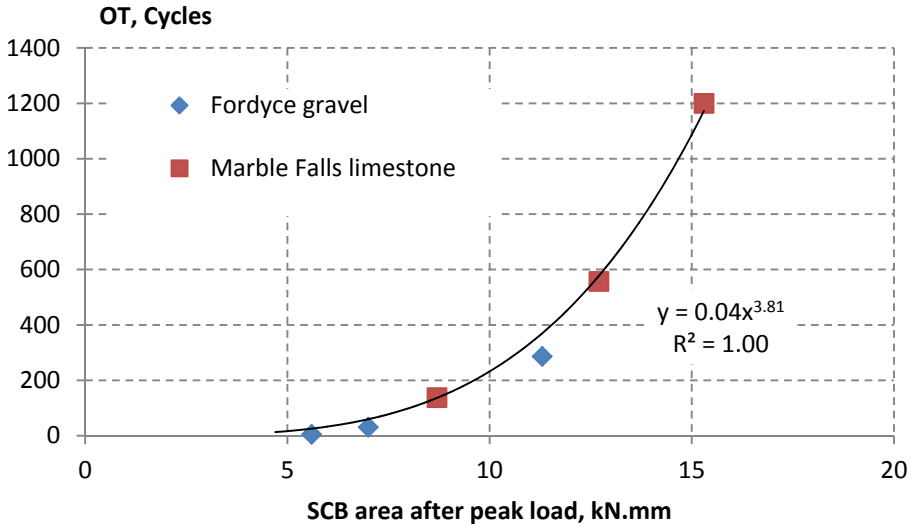

Figure 6.11 Correlation between OT and SCB results

In addition to peak load and area under the force-displacement curves, the stress-intensity factor (SIF) calculated using Eq. 2.5 and tensile strengths of the notched SCB specimens were determined. The latter required formulation of tensile strength equations for notched SCB specimens using finite element methods, which is addressed in a later chapter. A summary of the SCB test results for the CAM mixes is given in Table 6.10.

Table 6.10 SCB evaluation of CAM at 25 °C/77 °F

Mix	%AC	Peak Load, kN	Total Area, mm^2	Area before peak, mm^2	Area after peak, mm2	SIF, $MPa.mm^{0.5}$	Tensile Strength, MPa
Fordyce	6	6.6	9.6	4.0	5.6	223.6	18.4
	7	6.1	11.6	4.7	7.0	207.2	17.0
	8	5.6	17.1	5.8	11.3	190.6	15.7
Marble Falls	6	7.6	14.0	5.2	8.7	258.1	21.2
	7	6.8	19.5	6.8	12.7	227.1	18.7
	8	5.5	23.1	7.8	15.3	181.8	15.0
Beckmann	6	7.0	8.1	3.5	4.7	235.2	19.4
	7	6.7	9.7	3.8	5.9	224.5	18.5
	8	6.2	13.5	5.2	8.3	211.3	17.4
Burnet	7.6	5.8	16.3	7.2	9.1	109.8	10.2
Lattimore	7.8	5.6	12.0	5.5	6.5	107.2	10.0
Luckett/Tehuacana	7.3	7.2	12.4	6.6	5.8	136.4	12.7
1604	7.1	6.8	9.8	5.4	4.4	130.2	12.1

Comparing the SCB results with the OT results shown in Table 6.3, some general trends and similarities are evident. The Marble Falls mix at 8 percent AC and the Burnet mix both performed well in the OT and have higher areas and lower peak loads, SIF, and tensile strengths in the SCB. The performance ranking of the mixes tested in the OT, however, does not match that of the SCB. The lower SIF and tensile strength values determined in the SCB are contradictory to expectations but then a lower IDT tensile strength was also obtained for the better cracking resistant mixtures as shown in Table 6.4. This unexpected behavior is related to the relatively high temperature (25 °C/77 °F) at which the IDT and SCB tests were run. Both SIF and tensile strength formulations are based on elastic theory but at this elevated temperature the material undergoes a degree of plastic deformation under loading.

The response of the CAM mixes to SCB testing and the positive correlations obtained compared to OT prompted further investigation of the SCB as a cracking test to evaluate HMA. Additional SCB tests on the CAM mixes evaluated as part of the study at 5 °C/41 °F as well as tests on other HMA mixes including a dense-graded Type B mix were done to identify the best cracking parameter to evaluate HMA mixes tested using the SCB. These tests and the further research done on the SCB test are discussed in a later chapter.

6.4 Performance criteria for CAM mix with local aggregates

The current performance criteria specified for CAM mixtures in terms of the HWT and OT are applicable, i.e., less than a 12.5 mm rut after 20,000 cycles for PG 76-22 mixtures tested in the HWT and a minimum of 750 cycles for a 93 percent stress reduction in the OT. As previously indicated only one of the CAM mixes tested, the Burnet mix, satisfied both criteria. The HWT results for CAM indicate that the mixes tested, in general, fail before achieving 10,000 cycles. This level of performance is acceptable for dense-graded Item 341 mixes with PG 64-22 binders.

The design recommendation to increase the design voids in the mix to 3 percent at 50 gyrations for CAM with local aggregates will result in lower OAC for these mixes with expected improved rutting resistance. It is recommended, therefore, that the rutting performance of CAM mixes with local aggregates be evaluated against a minimum of 10,000 cycles in the HWT regardless of the PG grade used for these mixes. It is further proposed that the SIP of these mixes be beyond 5,000 cycles to ensure adequate resistance to moisture susceptibility.

These recommendations are based solely on an evaluation of the laboratory performance of the CAM mixes tested as part of the study. In light of current HWT criteria, these recommendations indicate that CAM with local aggregate are only appropriate for applications comparable to dense-graded (Item 341) mixes using PG 64-22 binders. Field evaluation of the performance of the CAM mixes is required for validation of these recommendations.

Only two of the CAM mixes evaluated at OAC passed the OT test requirement and the high variability in failure cycles makes it difficult to select an appropriate level of acceptable performance in the OT for the mixes tested. As such, the OT is indicative of a go/no-go type test; for this reason, the researchers see no reason to lower the current criterion of 750 cycles for a 93 percent stress reduction.

Chapter 7. CAM Mix Design Procedure Using Local Aggregates

Chapter 5 of this report expanded on the volumetric mix design and properties of the CAM designed using local aggregates. The OACs of the mixes were initially selected to achieve 98 percent relative density after 50 gyrations in the Superpave gyratory compactor as per special specification 3165 recommendations. The performance evaluation of these mixes was addressed in Chapter 6, which showed the results of HWT and OT tests on these mixes at OAC. This chapter is a synthesis of these findings towards revising and recommending new mix design criteria for CAM with local aggregates.

7.1 The selection of optimum asphalt content

After the first year of the project, it became increasingly evident that the researchers were unable to satisfactorily design a CAM with local aggregate with acceptable rutting and OT performance. It was clear that a compromise was necessary; hence, the recommendation in Chapter 6 to design these mixtures for low traffic volumes with an acceptable HWT performance of 10,000 cycles regardless of asphalt grade used. Rutting and stripping of these mixes in the HWT was the primary failure concern; this occurs as a direct consequence of overfilling the voids in the mix with binder with densification, either in the compactor or under the HWT wheel load. Shear failure of these mixes was clearly demonstrated and related to the low voids in the mix becoming overfilled with asphalt.

Figure 7.1 shows a mix design chart relating four volumetric properties of HMA mixtures, i.e., air voids, volume of effective binder (Vbe), VMA, and VFA. The x-axis shows the effective volume of asphalt or binder in the mix and the y-axis is the air voids. The dotted lines are lines of equal VMA and the blue solid lines running diagonally across are lines of equal VFA. VMA is the sum of the voids in the mix and the volume of effective asphalt. The thicker solid red line slanted off the vertical shows the path of densification of a typical asphalt mix, the asphalt content selected in this case to allow compaction to 2 percent voids in the mix and a minimum VMA of 17 percent—the volumetric criteria currently specified for CAM under special specification 3165.

This figure indicates that if CAM are compacted to 2 percent air voids, then the VFA of these mixes are between 85 and 90 percent. This is well beyond the VFA level at which shear failure was apparent for the CAM with local aggregate designed as part of the study. The Superpave mix design method provides for the design of HMA at the 4 percent voids in the mix level to reduce the risk of overfilling the mix with asphalt. Clearly a reduction in the relative density of CAM from the 98 percent level is justified; the question is how far can it be reduced to still provide mixes with adequate asphalt to ensure acceptable cracking performance. To answer this question the results of the volumetric designs were compared to the HWT, OT, and gyratory compaction shear strength performance measures of the CAM as designed.

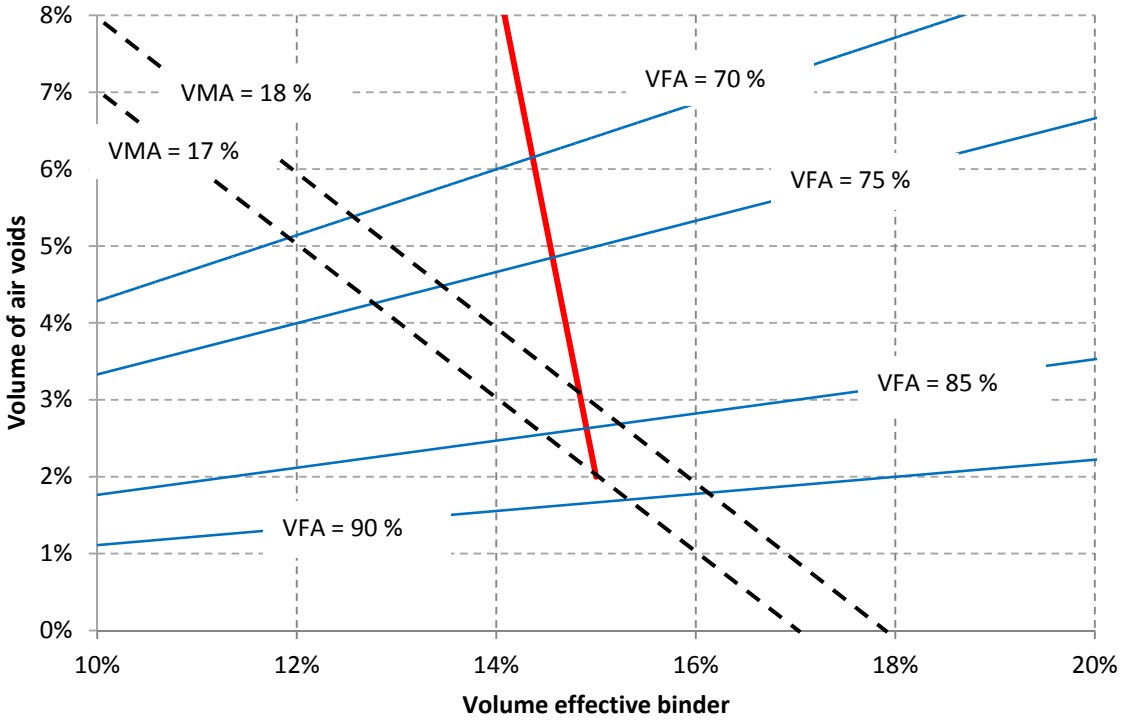

Figure 7.1 Mix design chart

Table 7.1 shows the asphalt contents of the CAM designed and selected volumetric properties of the mixtures compared to performance measures in terms of HWT, OT and gyratory compaction shear strength (SS) parameters. The volumetric properties include the relative density (%Gmm), VMA, and VFA at 50 and 75 gyrations where applicable. To evaluate the influence of density of performance, Figure 7.2 compares the HWT and OT results in terms of relative compaction density after 50 gyrations for these mixes. It can be seen that the OT results are particularly sensitive to compaction level and as expected increase with an increase in density—this is analogous to an increase in binder content. The HWT results, on the other hand, are not sensitive to compaction level although a slight decrease in the trend line is apparent with increased density as expected. A better measure of mixture stability as influenced by compaction level is the gyratory compaction shear strength as shown in Figure 7.3. In this figure, shear failures during compaction were evident when the relative density of the mix exceeded approximately 97.5 percent. In both cases, optimum performance of the CAM mixtures in terms of HWT, OT, and shear strength is obtained when the relative density of the mix is in the order of 97 percent at 50 gyrations. This, therefore, would appear to be the optimum density at which to select the optimum asphalt contents of CAM with local aggregates to 1) optimize rutting and cracking performance and 2) provide a measure of safety against the risk of overfilling the mix with asphalt, which could lead to shear failures.

Table 7.1 Summary of CAM volumetric and performance measures

	AC	%Gmm @50	%Gmm @75	VMA @50	VFA @50	HWT	OT	SS
Fordyce	6	91.2	91.4	21.4	54.4	10,800	5	341
	7	96.2	96.4	18.8	79.7	9,433	31	324
	8	98.7	98.8	18.4	92.9	7,550	286	229
Marble Falls 1	6	96.0	97.3	17.7	77.6	20,000	138	731
	7	98.4	99.6	17.8	91.2	12,550	557	578
	8	99.4	99.8	19.0	96.9	10,300	1200	332
Beckmann	6	94.0	95.9	18.8	68.1	11,250	31	727
	7	94.8	96.8	19.7	73.7	10,250	125	724
	8	97.9	99.8	19.4	89.0	8,750	479	606
Solms Road	7.2	96.4	97.8	21.1	82.9	7,150	573	707
RTI	7.1	94.6	95.9	17.2	68.8	6,050	167	628
Spicewood	8.4	98.4	98.6	20.4	91.9	7,800	1104	315
Lattimore	7.8	96.1	97.4	17.0	77.6	8,100	386	675
1604	7.1	96.3	97.3	17.7	78.9	10,500	95	609
Burnet	7.6	96.3	97.5	19.9	81.3	20,000	1200	726
Luckett/Tehuacana	7.3	97.6	97.7	18.0	86.6	10,200	423	218

Table 7.1 shows that on average the relative densities of the mixtures evaluated after 75 gyrations are in the order of 1 percent higher than the densities determined after 50 gyrations. This provides an additional criterion for the selection of appropriate CAM mixtures, i.e., the relative density of the mix should not exceed the 98 percent level after 75 gyrations. This is analogous to the Superpave N_{max} compaction level to ensure that the mix will not over-densify over its design life.

The mean VMA determined for the mixes after 50 gyrations is in the order of 18.7 percent. With reference to the mix design chart shown in Figure 7.1, by increasing the design compaction level from 92 percent to 93 percent, it is feasible to increase the minimum VMA of CAM from 17 percent to 18 percent to ensure sufficient voids in the mix and encourage the use of higher asphalt contents. The increase in minimum VMA to 18 percent appears feasible in the context of the mixtures evaluated as part of the study and is therefore recommended for the design of CAM with local aggregates.

Comparing the VFA data to the shear strength results, it can be seen that for the mixes tested at optimum asphalt content, a loss in shear strength is on average associated with an increase in VFA above 80 percent. While this level may serve as a criterion to ensure shear stability, as previously discussed, voids filled with asphalt does not appear to be a reliable indicator of shear failure, with some mixes failing at VFA levels as low as 65 percent.

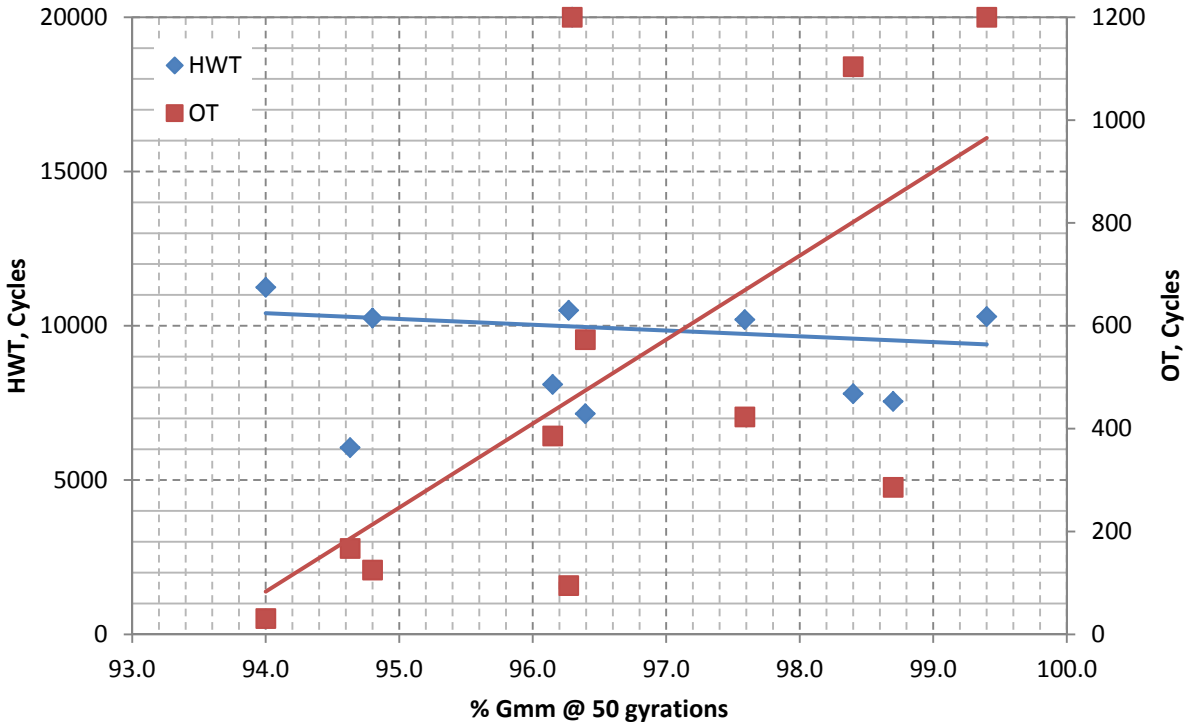

Figure 7.2 Comparison of HWT and OT with compaction density

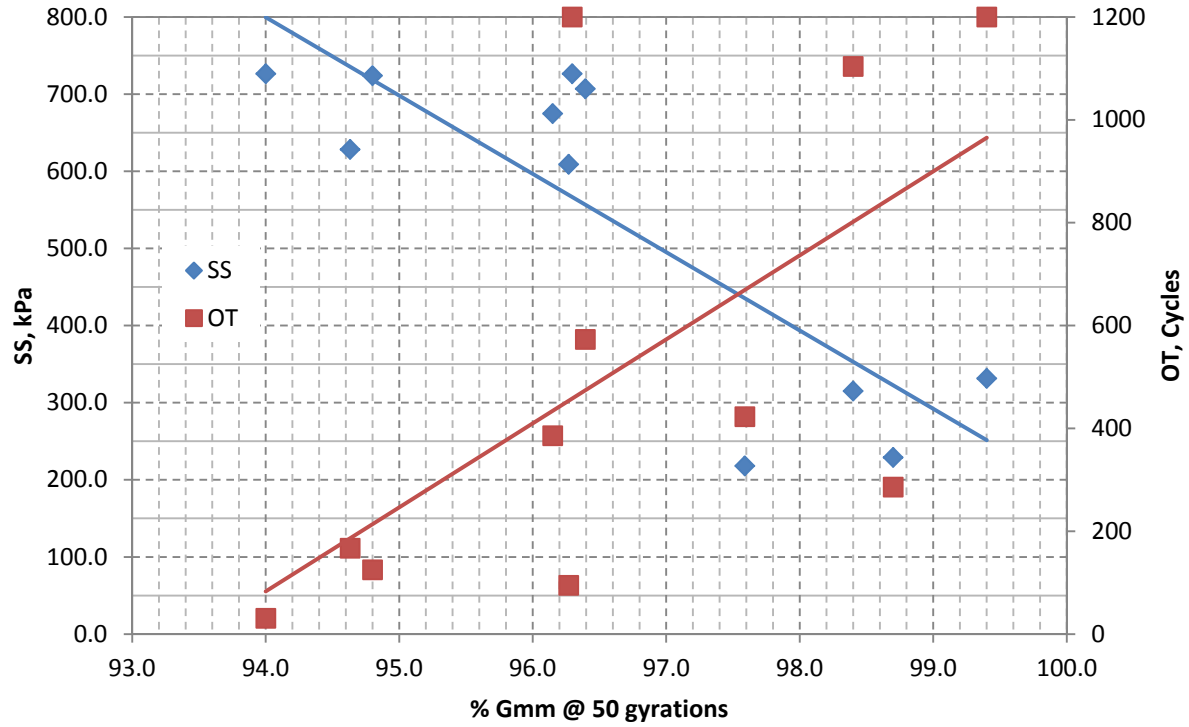

Figure 7.3 Comparison of shear strength and OT with compaction density

7.2 Recommended CAM mix design procedure using local aggregates

In summary, the researchers recommended that CAM with local aggregates be designed using the Superpave gyratory compactor. It is recommended that these mixes be compacted at 3 or more asphalt contents by applying 75 gyrations and measuring the densification and shear strength of these mixes with compaction. The volumetric properties of these mixes should be back-calculated to determine the relative density, VMA, and VFA after 50 gyrations. The compaction levels of 50 and 75 gyrations are the design (N_{des}) and maximum (N_{max}) levels respectively.

This procedure will require determination of the maximum theoretical (Rice's) density of the mixes at the varying asphalt contents and the bulk specific gravity of the aggregate blend. Based on the findings of this study, the criteria shown in Table 7.2 are recommended and should be applied to determine the optimum asphalt content of the CAM mix. The HWT and OT tests should be run on the mix prepared at this OAC per standard procedures. Acceptable performance in the terms of HWT and OT is recommended as shown. As indicated, the shear stress curves from the gyratory compactor should be checked to ensure that the CAM mix does not fail in shear before the application of the N_{des} number of gyrations. If this feature is not available on the compactor, then the maximum VFA criterion as indicated is recommended. A maximum VFA criterion of 80% is recommended to provide mixes with higher asphalt contents that are resistant to shear failure.

Table 7.2 CAM mix design criteria

Criterion	**Level**
Relative density at N_{des} (50 gyr)	= 97 %
Relative density at N_{max} (75 gyr)	<= 98 %
Minimum VMA at N_{des}	>= 18 %
No shear failure before N_{des}	Check shear stress curve
Maximum VFA* at N_{des}	<= 80 %
HWT (regardless of binder PG grade)	>= 10,000 cycles at 12.5 mm rut
OT	>= 750 cycles to 93 % stress reduction

* To be applied if shear stress measurements are not available.

Chapter 8. Alternative Crack Attenuating Mixtures

Various crack attenuating or resistant alternatives to CAM were investigated to address the poor rutting resistance observed for the CAM mixes with local aggregates as evaluated. One option to improve this poor performance was the use of stone skeleton mixes; another was the option of blending high quality SAC A aggregates with the local aggregates.

8.1 Stone-skeleton mixes

Referring back to Richardson's triangle illustrated in Figure 2.4, CAM is classified as a sand skeleton mix. The coarse aggregates in CAM are therefore not in contact, essentially serving to fill the sand matrix without offering structural support. Efforts to increase the stiffness of the CAM matrix by optimizing the filler-binder component as well as the use of stiffer binders did not significantly improve the rutting performance of the CAM evaluated. By opening the gradation of the CAM mixes, it was possible to design fine SMA and CMHB mixes using local aggregates that ensured stone-on-stone contact. This section discusses the design and initial performance evaluation of these stone-on-stone mixes.

8.1.1 SMA design

An SMA design using the coarse aggregate stockpile from the RTI plant and the fine aggregate stockpile from the Solms Road quarry was evaluated. To achieve an SMA gradation, it was necessary to supplement the filler content of the mix using fly-ash. This was also required to provide mastic stability and the amount of fly-ash was varied to ensure specimens would remain intact upon extraction from the gyratory compaction mould. One percent of hydrated lime was added to this blend. Table 8.1 shows the final gradation of this mix, which was gyratory compacted at three different asphalt contents using a PG 76-22 binder.

Table 8.1 Stockpile and blend gradations of SMA

Sieve	RTI coarse	Solms Road	Fly ash	Lime	Blend	SMA-F Specification
1/2	100	100	100	100	100	100
3/8	100	100	100	100	100	70-90
#4	0	100	100	100	28	30-50
#8	0	100	100	100	28	20-30
#16	0	67.1	100	100	22.4	8-30
#30	0	41.7	100	100	18.1	8-30
#50	0	22.3	100	100	14.8	8-30
#200	0	2.7	100	100	11.5	8-14
Volume fractions	**72%**	**17%**	**10%**	**1%**	**100%**	

Cellulose fibers (0.3 percent by mass) were used with this mix to minimize asphalt drain-down. Given the relatively low specific gravity of the fly-ash component, it was necessary to

approach the design of this mix based on volume instead of mass gradations. Figure 8.1 shows the gyratory compaction characteristic of this mix at the three asphalt contents ranging from 6.5 to 7.5 percent. The linear trends apparent in this figure indicate that the mix is not resisting compaction as was the case for the dense-graded CAM.

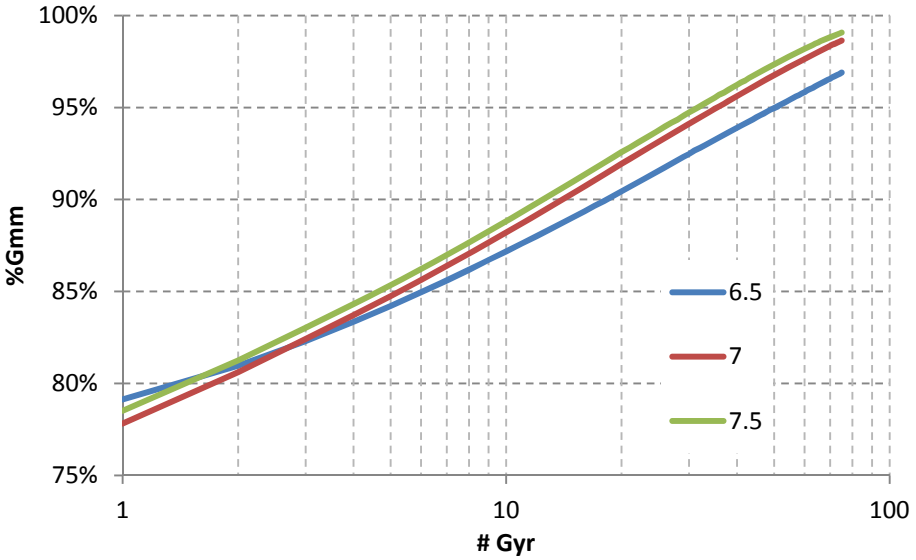

Figure 8.1 Compaction characteristic of SMA mix

Figure 8.2 shows the shear stress variation with compaction. It can be seen that at the two lower AC contents the mix does not undergo shear failure. However, even at the 7.5 percent AC content, the shear failure only occurs after 50 gyrations, whereas shear failures in the CAM mixes generally occurred at relatively low numbers of gyration.

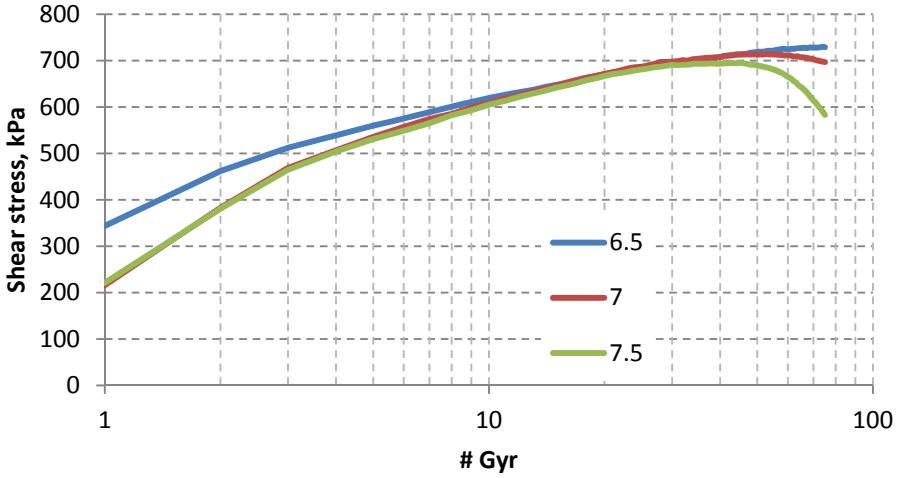

Figure 8.2 Shear stress with compaction of SMA mix

The volumetric properties with compaction indicate that this mix is significantly more stable than the comparative CAM mixes designed. The optimum asphalt content of this mix to

achieve 93 percent relative density after 50 gyrations was selected at 7 percent. HWT tests were run on specimens prepared at this AC level but compacted to 7 percent VIM per Tex-242-F. Figure 8.3 shows the superior rutting performance of this mix, with the total rutting in the order of 6 mm after the application of 20,000 cycles.

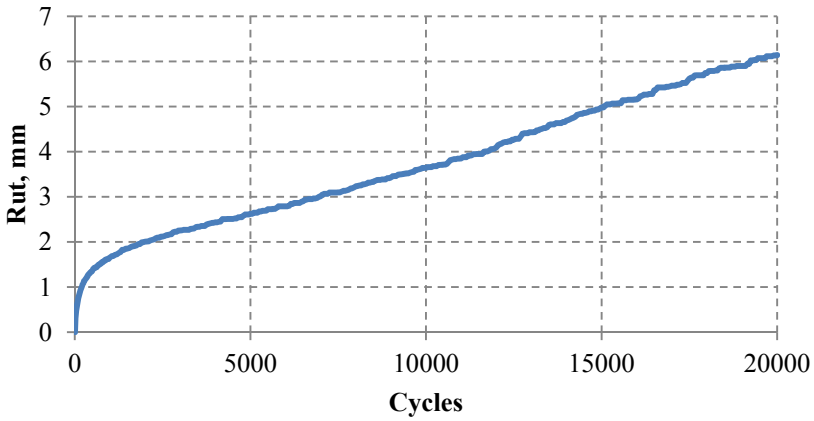

Figure 8.3 HWT test on SMA mix

No stripping of the coarse or fine aggregates was apparent after running the HWT test on the SMA mix and the rutting that developed appeared to be a consequence of densification of the mix, as shown in Figure 8.4.

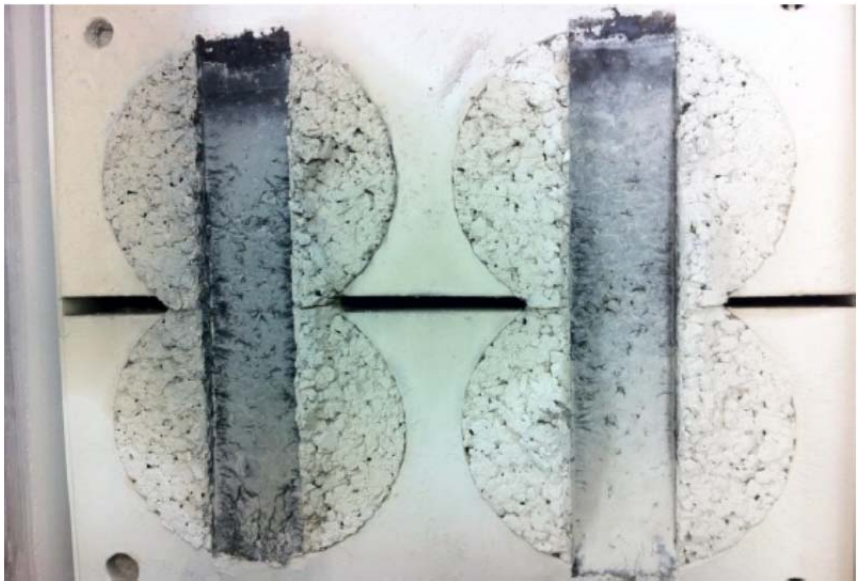

Figure 8.4 Densification of the SMA mix in the HWT

8.1.2 CMHB design

SMA may not be cost-effective; therefore, the design of a CMHB alternative using local aggregates was attempted. These mixes still provide stone-on-stone contact but at a reduced filler content. A CMHB-F design was obtained from the Austin district for a mix being constructed on

IH 35. This mix comprised 77 percent coarse Grade 5 rock from the Delta Capitol Aggregates quarry (SAC A) and 23 percent screenings from the Yearwood RTI North quarry (SAC B). Samples of this mix were also collected during construction and tested for rutting performance.

The Fordyce gravel and Marble Falls limestone aggregate sources were evaluated for the CMHB design. The gradations of the field mix were duplicated using the local aggregate sources. Attempts to design these mixes using the gyratory compactor failed—the voids in the mix even after the application of 75 gyrations exceeded 8 percent, with an asphalt content of 7.5 percent. These mixes are typically designed using the Texas gyratory compactor.

Using the field mix as a guide, specimens for the Fordyce gravel and Marble Falls limestone aggregates where prepared for HWT and OT tests using the SGC to an asphalt content of 7 percent. The optimum asphalt content of the field mix was at 6.8 percent. The specimens for the HWT and OT tests were compacted to 93 percent relative density. Table 8.2 shows the HWT and OT performance of the CMHB mixes tested. The mixes with local aggregates were tested with both PG 70-22 and PG 76-22 Valero binders

Table 8.2 HWT and OT testing of CMHB mixes

Mix	HWT	OT
Field Mix with PG 76-22	2mm @ 20,000	41; 50; 24 (38 cycles)
Fordyce with PG 70-22	3,500 cycles	873; 435; 1,200 (840 cycles)
Marble Falls with PG 70-22	4,650 cycles	1,200; 1,200 (1,200 cycles)
Fordyce with PG 76-22	10,449 cycles	803; 732; 1,153 (896 cycles)
Marble Falls with PG 76-22	7,576 cycles	1,200; 1,200 (1,200 cycles)

From the table it can be seen that the field mix performed particularly well in the HWT with a 2 mm rut after the application of 20,000 cycles. This mix performed poorly in the OT, however, with an average of 38 cycles to failure. The CMHB designs with local aggregates did not perform very well in the HWT, although better performance of the mixes was observed with the stiffer binders as expected. The cracking performance of the CMHB mixes with local aggregates was superior, however.

Figure 8.5 shows the Fordyce mix HWT specimens after testing. Although no excessive crushing or stripping of the aggregates was apparent, the mix did appear to undergo shear failure in the HWT with upheaval displacement of the mix under the wheel load.

Figure 8.5 HWT specimen failure for CMHB Fordyce mix

8.1.3 High quality aggregate blending

Another option considered to improve the rutting performance of crack attenuating mixes was the replacement or blending of the local aggregates used in these mixes with high quality SAC A. From the onset of the project is was apparent that the performance of CAM is highly dependent on the nature of the aggregates, both coarse and fine. It may therefore be feasible to justify the cost of shipping high quality aggregates for blending with CAM comprising predominantly local aggregates if performance is adequately improved.

To evaluate this option, the Marble Falls mix previously designed was reconstituted by firstly replacing 50 percent of the coarse stockpile and then replacing 50 percent of the fine stockpile with SAC A Trap Rock from the Knippa quarry. In addition, the CMHB mix previously designed using the Marble Falls aggregates was reconstituted by replacing 50 percent of the coarse aggregate component with the Knippa rock. All three of these mixes were prepared using a PG 76-22 binder at an AC content of 7 percent and tested in the HWT. The rutting performance of these mixes in terms of cycles to failure and stripping inflection point (SIP) is shown in Table 8.3.

From the table it can be seen that replacing either the coarse or fine gradation component in the mixes with high quality SAC-A did not improve the rutting performance of the CAM mixes. Stripping of both the coarse and fine aggregates was observed in these HWT tests as shown in Figure 8.6 and Figure 8.7. This supports the previously indicated notion that these mixes are high susceptible to stripping and that the HWT device is able to mobilize the high pore pressures in these low voids mixes.

The performance of the CMHB mix did indeed improve significantly with the replacement of the coarse component with SAC-A aggregates. This finding suggests that a blend

of SAC-A and SAC-B aggregates may be used for CMHB mixes to optimize performance at reduced cost.

Table 8.3 HWT evaluation of SAC-A aggregate replacement

Mix gradation	Cycles	SIP
CAM coarse component replaced	6,574	2505
CAM fine component replaced	6,869	3250
CMHB coarse component replaced	13,335	5820

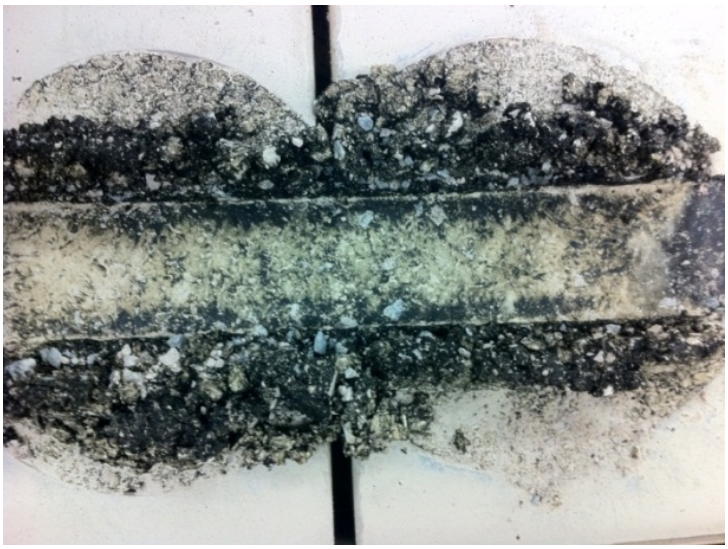

Figure 8.6 HWT of Marble Falls CAM with coarse component replaced with SAC-A

Figure 8.7 HWT of Marble Falls CAM with fine component replaced with SAC-A

Chapter 9. Aggregate Quality Criteria and Guidelines

This chapter relates the aggregate properties determined for the CAM mixtures, as outlined in Chapter 4, together with blend and mixture properties relating to CAM performance with local aggregates in terms of both rutting and cracking, as outlined in Chapter 6. A correlation study was conducted to estimate the strength of the relationships between these properties and corresponding CAM performance. Aggregate quality criteria and guidelines are developed based on these correlations, and recommendations made for the selection of suitable aggregate sources for use with CAM.

9.1 Aggregate performance characterization

Solaimanian et al. (2002) previously evaluated the influence of aggregate properties on the rutting performance of dense-graded asphalt mixtures used in Texas. They classified HWT performance from severe to mild in terms of aggregate properties based on the testing of a variety of different aggregates. Their findings are relevant to the current study and are shown in Table 9.1. Comparing these data to the aggregate classification properties of the CAM mixes shown in Table 4.4, it was anticipated that severe degradation in the HWT could be expected for the CAM with local aggregates used in the current study—as was the case in general.

Table 9.1 HWT performance related to aggregate properties (Solaimanian et al., 2002)

Level of degradation	LA Abrasion Loss, %	Micro-Deval Loss, %	Soundness Loss, %	P.V. Loss, %
Severe	> 25	> 12	> 16	> 40
Moderate	20–25	5–12	7–16	34–40
Mild	< 20	< 5	< 7	< 34

To further investigate the influence of aggregate properties on the performance of the CAM used in the study, a statistical correlation was done comparing HWT and OT performance to various aggregate properties including:

1 **Characterization properties**
   a. Los Angeles abrasion
   b. Magnesium sulfate soundness loss
   c. micro-Deval loss
   d. Acid insoluble residue
2 **AIMS properties**
   a. Sphericity
   b. Surface texture
   c. Coarse aggregate angularity
   d. Fine aggregate angularity
3 **Filler properties**
   a. Rigden's voids
   b. Hydrometer percentage passing 10 micron

c. Filler-binder ratio
d. Free binder content

4 Blend gradation properties

a. Fineness modulus (gradation)
b. Stone content
c. Sand content
d. Filler content
e. Superpave FAA

The results of the performance correlation study are summarized in Table 9.2. The performance indicators include HWT cycles to failure, the creep and stripping slopes, the number of cycles to the SIP, the D5K, the DSIP, and the OT cycles to failure. The Hamburg performance parameters used were previously defined in Figure 6.1.

Table 9.2 Aggregate property vs. performance correlation matrix

Aggregate/blend property	HWT cycles	Creep slope	Strip slope	SIP	D5K	DSIP	OT cycles
Los Angeles Abrasion	0.01	-0.30	0.06	-0.18	-0.12	-0.32	-0.25
Soundness magnesium	-0.23	-0.01	0.03	**-0.48**	0.14	**-0.70**	-0.27
micro-Deval	-0.24	-0.06	0.09	**-0.50**	0.06	**-0.56**	-0.34
Acid insolubility	0.02	-0.06	-0.15	-0.01	-0.08	-0.16	-0.42
AIMS sphericity	**-0.53**	-0.03	**0.48**	-0.57	0.00	-0.44	**-0.74**
AIMS surface texture	0.35	-0.08	-0.17	0.49	-0.22	**0.64**	0.63
AIMS coarse aggregate angularity	**0.46**	**-0.64**	-0.14	**0.54**	-0.37	0.23	-0.13
AIMS fine aggregate angularity	**0.61**	-0.28	**-0.65**	**0.62**	**-0.54**	**0.57**	0.18
Superpave FAA	**0.61**	-0.26	**-0.51**	**0.58**	0.00	0.16	-0.19
Rigden's voids	-0.07	0.54	0.09	0.11	0.53	0.12	0.62
Hydrometer 10 microns	**-0.49**	0.19	0.31	**-0.58**	0.32	**-0.56**	-0.16
Fineness modulus	-0.41	0.34	0.41	-0.24	0.51	-0.37	0.11
Coarse component	0.08	0.27	-0.26	0.04	-0.25	**0.62**	0.45
Sand content	-0.12	0.08	0.06	0.01	0.14	-0.06	**0.48**
Filler content	**-0.51**	0.48	0.54	-0.45	0.52	-0.22	0.04
Filler-binder ratio	**-0.49**	0.41	**0.56**	-0.44	0.53	-0.28	-0.18
Free binder	**0.52**	**-0.49**	**-0.54**	**0.47**	**-0.57**	0.31	0.07

The Pearson correlation coefficients shown in Table 9.2 indicate the strength of the relationships between the aggregate properties and the performance measures; the significant correlations are shaded. The sign on the correlation coefficient is relevant as it indicates the direction of the effect. For example, it can be seen that an increase in AIMS sphericity leads to a decrease in HWT cycles or an increase in AIMS surface texture corresponds to an increase in HWT cycles, etc. The correlation plots comparing each of the aggregate properties with each of the performance parameters are shown in Appendix D.

An overview of the figures in Appendix D indicates that the correlations of certain parameters are heavily biased by a single data point that if removed, significantly changes the correlation coefficient. For example, consider the influence of AIMS sphericity on HWT cycles shown in Figure 9.1. The Burnet mix was an exception and had low AIMS sphericity but performed well in the HWT. The question is whether this point should be considered an outlier—but with no justification to remove the biasing point, the correlations were reported with all data considered. The correlation coefficients (R^2) in the figures showing the fits are the square of the Pearson correlation coefficients shown in Table 9.2.

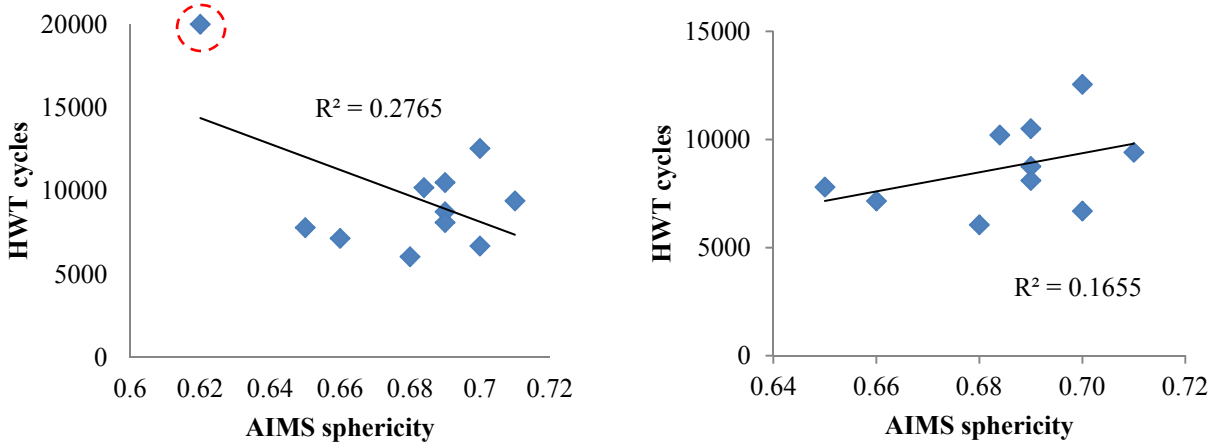

Figure 9.1 Influence of AIMS sphericity on HWT cycles

Los Angeles abrasion and acid insolubility where found to be uncorrelated with any of the CAM performance parameters. In the case of acid insolubility (AI), most of the aggregates in the study were limestone with similar AI values, which explains the low correlation. Contrary to LA abrasion, micro-Deval significantly influences the HWT cycles to the SIP and the DSIP. This is a relevant finding indicating the moisture sensitivity of the CAM mixtures. Magnesium sulfate soundness loss mirrors the effect of micro-Deval. For both of these parameters, an increase in aggregate degradation corresponds to a decrease in SIP and DSIP. This suggests that stripping in CAM may be decreased by using aggregates with low degradation values.

With regard the AIMS parameters, it can be seen that aggregate sphericity (shape) and angularity significantly influence mixture performance. Flakier or elongated aggregates with low sphericity provided better HWT and OT performance. Increased coarse and fine aggregate angularity improved rutting performance but did not affect cracking performance in the OT. Interestingly, the AIMS surface texture parameter does not appear to significantly influence either rutting or cracking performance of CAM. This is probably related to the very low surface texture values of the aggregates used in the study and suggests that aggregates for CAM should preferably have high surface texture to improve rutting and cracking performance. Stripping of binder from aggregates is also exacerbated with low surface texture. The benefit of high angularity and in particular fine aggregate angularity is again emphasized by the positive effect of the Superpave FAA parameter.

An interesting finding in the study was the significant effect of filler on the rutting performance of CAM in particular. The correlation analysis indicates that not only is filler

content significant but also the nature of the filler and its interaction with the binder. The analysis indicates that higher filler contents lead to increased rutting. This was previously demonstrated as shown in Figure 4.5 for the Marble Falls II mix, which exhibited more rutting in the HWT compared to the Marble Falls I mix. Higher filler-binder ratios not only result in increased rutting but also increase the rate of stripping. In addition, fillers with a high percentage of 10 micron particles are detrimental. Very fine clay-like fillers have increased surface area that adsorbs more binder. These findings strongly support restricting the filler contents of CAM mixtures. The significant effect of free binder on performance is another interesting finding. Free binder is defined, as shown in Figure 4.1, as the binder not adsorbed by the filler, which is available to coat the coarser aggregates and lubricate the mix. Fillers for CAM should therefore be selected to increase this free binder content to reduce rutting and stripping of the mix.

Finally, increasing the sand content (passing #8 sieve) of CAM appears to benefit the cracking performance of these mixes.

9.2 Aggregate guidelines and criteria for CAM

This study highlights the benefits of HWT testing to evaluate the stripping potential of CAM. The problem of stripping *can* be addressed through the judicious selection of aggregates. This is necessary to justify the application of anti-stripping agents. Although the effect of stripping on the rutting performance of CAM was evaluated, consideration should also be given to address its effect on the cracking resistance of CAM by water conditioning specimens prior to OT testing.

The AIMS device was effective in distinguishing the texture and angularity characteristics of the aggregates used in the study. Clearly local aggregates of class SAC B differ vastly in properties and the AIMS may be used to better distinguish these.

Efforts to improve the performance of CAM indicated the benefit of characterizing the filler used with these mixes. The calculation of Rigden's voids and particle distribution analysis of the filler is strongly recommended.

Based on the evaluation of the effect of aggregate properties on the performance of CAM, the following guidelines are applicable to improve both the rutting and cracking resistance of CAM. These guidelines are applicable to CAM produced using both local and high quality aggregates:

- Use non-abrasive aggregates.
- Select aggregates with high surface texture.
- Use aggregates with high angularity particularly fine aggregate angularity.
- Restrict the filler content of CAM and aim to reduce the filler-binder ratio.
- Avoid the use of very fine fillers having a high percentage passing 10 microns.

The aggregate specification requirements for CAM per special specification 3165 are indicated in Table 4.2. Based on this study, the following recommended revisions are proposed:

- Micro-Deval testing of CAM aggregates is preferred over LA abrasion and the maximum abrasion loss in the micro-Deval should be restricted to 15 percent.

- The maximum magnesium sulfate soundness loss of CAM aggregates should not exceed 15 percent.
- Retain the current angularity and flakiness requirements for CAM aggregates but introduce an AIMS criterion to require a minimum fine aggregate angularity of 4,500.
- For fillers (passing #200 sieve), the percentage particles finer than 10 micron should not exceed 30 percent.
- The filler content of CAM should not exceed 7 percent.

These guidelines are based on the testing of 14 different aggregate sources to optimize the rutting and cracking performance of CAM. The aggregates tested cover an array of aggregate properties in terms of shape, strength, and durability. Field validation is recommended for implementation of these guidelines.

Chapter 10. Further Development of the SCB

This chapter presents research done as part of the study towards identifying a crack characterizing parameter that can distinguish different asphalt mixes of known cracking performance using the semi-circular bending (SCB) test. The study evaluated different crack parameters obtained from monotonic testing of SCB specimens at 5 °C/41 °F and 25 °C/77 °F. In addition to CAM, a plant-produced dense-graded Type B mix was tested to evaluate the SCB effectiveness for mixes with larger nominal aggregate size. Cracking parameters were identified using fracture mechanics and energy-based concepts. The theoretical significance and efficiency of the SCB in terms of screening asphalt mixes using the cracking parameters is discussed.

10.1 Finite element analysis of notched SCB specimen

A finite element analysis (FEA) was done to formulate the tensile stress distribution within notched SCB specimens. Notching reduces the variability in the SCB by ensuring the crack develops and propagates from the notch under loading. The researchers had previously reported on the tensile stress distribution in unnotched SCB specimens (van de Ven et al., 1997). For the FEA, a 3D model of the current SCB configuration was developed comprising cylindrical loading and support conditions as previously shown in Figure 2.11. Figure 10.1 shows the 3D model and the mesh applied to the specimen using quadrilateral elements.

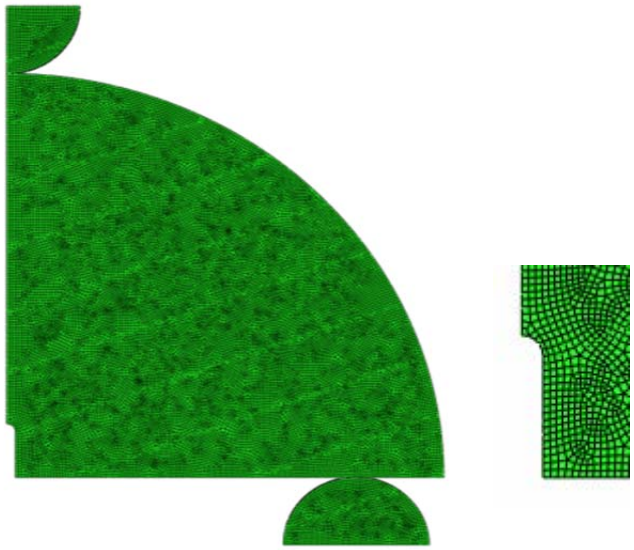

Figure 10.1 Model of notched SCB specimen

Using symmetry, only one-half of the specimen was modeled. The notch was modeled with a 3 mm gap and 1.5 mm circular radius at the tip. The length of the notch was varied to determine the influence on tensile stress. The loading and support conditions were applied using frictionless contacts within the finite element software package *ABAQUS*. Elastic material properties were assumed.

Figure 10.2 shows the horizontal tensile stress distribution in an SCB specimen under loading with a 10 mm notch depth. Very high tensile stresses are apparent at the tip of the notch.

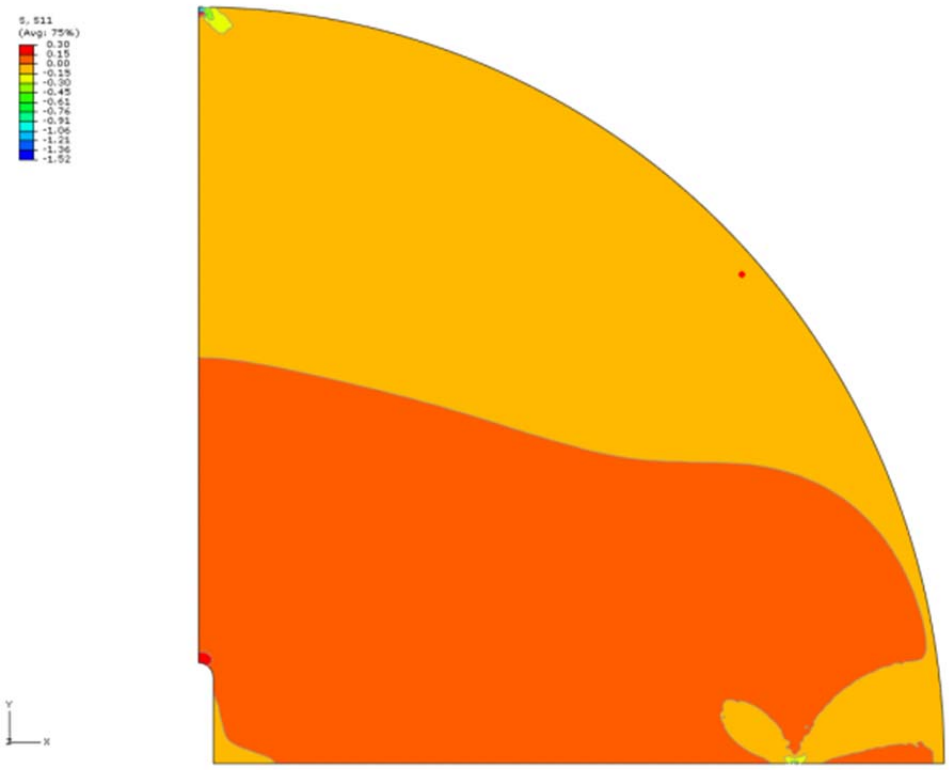

Figure 10.2 Tensile stress distribution in notched SCB specimen

By varying the depth of the notch and running repeated FEA on the model, it was possible to formulate the horizontal tensile stress at the tip of the notch as a function of notch depth. The tensile stress (S_{11}) is a function of the applied load (P) as well as the diameter (D) and thickness (t) of the specimen as shown in Eq. 10.1:

$$S_{11} = \frac{K \cdot P}{D \cdot t} \qquad \textbf{Eq. 10.1}$$

The stress constant, K, was determined as a function of notch depth using FEA as shown in Figure 10.3. An increase in the notch depth results in increased horizontal tensile stress at the notch tip. This equation was used to calculate the tensile strengths reported for notched SCB specimens in the report.

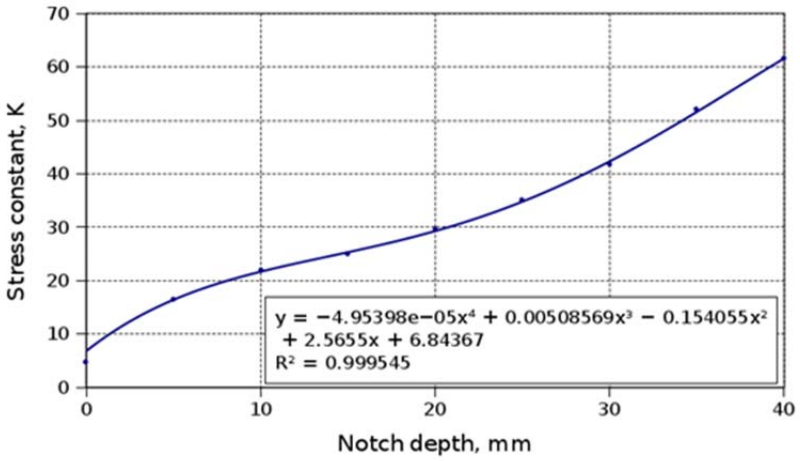

Figure 10.3 Variation of SCB stress constant with notch depth

10.2 Cracking parameters

In addition to tensile strength, various other cracking parameters were evaluated to assess the sensitivity of the SCB test. The SIF was previously discussed and the formulation of SIF for the SCB shown in Eq. 2.5. SIF is a material property and independent of specimen geometry but only valid when the material is tested under elastic conditions, i.e., at low temperatures and/or high frequencies. Plane strain conditions are also essential for validity of the stress intensity factor, thus the requirement to test thinner specimens.

The area beneath the force-displacement curve from a monotonic SCB test was previously shown in Figure 6.11 to correlate with the overlay tester cycles to failure. This area is the energy input into the system to fail the specimen from crack initiation through crack propagation. The concept of the J-integral was previously introduced as the potential energy difference between two identically loaded bodies having different crack sizes, as illustrated in Figure 2.13. This potential energy difference is an indicator of cracking resistance. To demonstrate the J-integral concept, consider multiple SCB specimens tested with different notch depths. Figure 10.4 shows force displacement curves for a CAM mix and a Type B mix tested with notch depths of 10, 15, and 20 mm. These tests were run on specimen gyratory compacted to 7 percent air voids at a temperature of 5 °C/41 °F and a constant deformation rate of 50 mm/min.

The figure shows that the energy required to fail the specimen decreases with an increase in the notch depth. This is expected because with a greater notch depth, less material needs to be cracked. Figure 10.5 compares the area under the force displacement curves up until the peak load and plots this against the notch depth. The steeper slope for the CAM mixtures indicate the increased resistance to cracking for these mixes compared to the Type B mix. While the slopes indicate the difference in cracking resistance between the mixes, the area under the slopes appears to be a more robust cracking parameter.

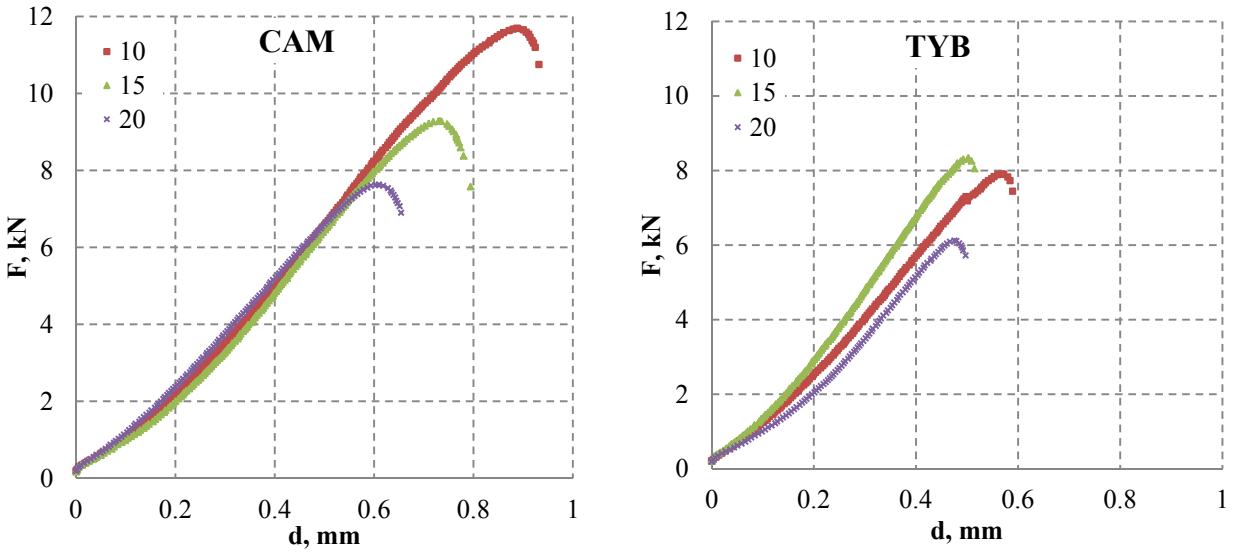

Figure 10.4 SCB strength tests on CAM and Type B mixes with varying notch depths at 5 °C/41 °F

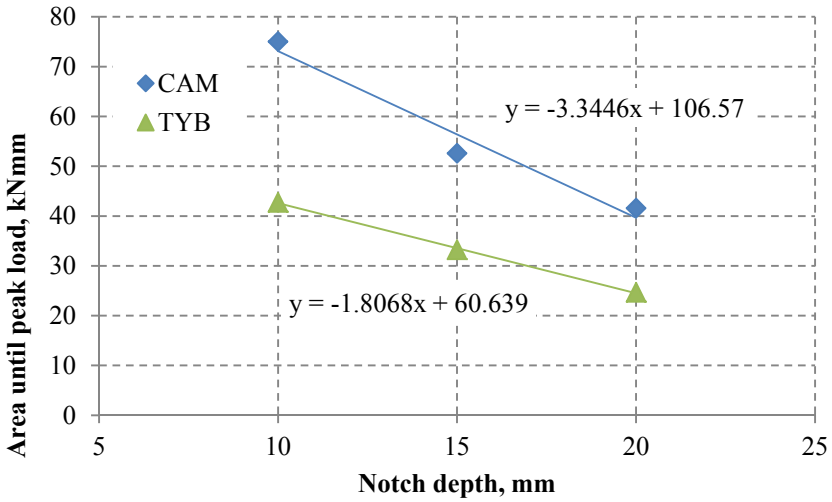

Figure 10.5 Area concept indicating cracking resistance of CAM and Type B mixes

Table 10.1 compares various SCB cracking parameters determined for a CAM mix compared with a Type B mix based on monotonic testing done at a temperature of 5 °C/41 °F. Table 10.2 compares cracking parameters for two identical CAM mixtures that only varied by asphalt content, one with a 6 percent AC content and the other at 8 percent. These latter tests were run at 25 °C/77 °F. The tables show the peak load and peak load displacement with the various notch depths used, the slopes of the peak load areas and the slope area under the peak load area curves illustrated in Figure 10.5, the SIF calculated using Eq. 2.5, and tensile strength (TS) calculated using Eq. 10.1.

Table 10.1 SCB test parameters determined at 5 °C/41 °F

Mix	Notch mm	Peak kN	Disp. mm	Slope kN	Slope Area kN.mm^2	SIF Mpa. mm$^{0.5}$	AVG SIF	TS MPa	AVG TS
Type B @ OAC	10	9.4	0.6	1.8	335.4	25.3	26.7	20.9	21.1
	15	8.2	0.5			28.8		22.4	
	20	6.4	0.5			26.1		20.1	
CAM @ OAC	10	11.3	0.8	3.3	564.0	30.1	31.8	24.9	25.1
	15	9.0	0.7			32.6		25.2	
	20	7.9	0.6			32.8		25.3	

Table 10.2 SCB test parameters determined at 25 °C/77 °F

Mix	Notch mm	Peak kN	Disp. mm	Slope kN	Slope Area kN.mm^2	SIF Mpa. mm$^{0.5}$	AVG SIF	TS MPa	AVG TS
CAM 6%	10	9.9	1.9	0.41	149.7	28.3	27.9	23.1	22.5
	15	8.1	2.0			28.6		22.2	
	20	6.8	1.4			27.6		21.2	
	25	6.1	1.4			28.8		23.3	
	30	4.8	1.3			26.2		22.7	
CAM 8%	10	6.9	2.8	0.44	161.7	19.6	19.7	16.0	15.9
	15	5.8	2.6			20.3		15.7	
	20	5.0	2.1			20.3		15.6	
	25	4.3	1.9			20.4		16.4	
	30	3.3	2.0			17.9		15.5	

Comparing the test parameters determined at 5 °C/41 °F with those determined at 25 °C/77 °F, some interesting trends are observed. Peak loads at the lower temperature tests are higher for the more crack resistant mixes but lower for these mixes at the higher test temperature. The same trend is observed for SIF and tensile strength. The reason for the difference in response can be directly related to the test temperature. At 25 °C/77 °F the material is no longer elastic and energy applied at this temperature is used not only for cracking but also permanent deformation of the specimen. Thus, at 25 °C/77 °F, the SCB test is not a particularly sensitive test to evaluate the cracking potential of different asphalt mixes. At the lower temperature, however, a clear difference in all of the parameters evaluated is evident, because most of the energy applied to the specimen is used for cracking. Further investigation of the SCB using different mixes would be beneficial in identifying the best cracking parameter.

Chapter 11. Research Findings and Recommendations

This report addressed the mix design and evaluation of crack attenuating mixtures (CAM) with local aggregates. By characterizing the critical properties of the aggregates influencing the performance of CAM, it was possible to develop criteria and guidelines for the design of these mixtures using local or new aggregate sources. The mix design procedure was evaluated and refined to incorporate the use of these local aggregates towards optimizing rutting and cracking performance.

The application of CAM is still relatively new in Texas. A database of existing projects was developed as part of the study and a visual survey of selected projects in north, central, and south Texas was undertaken, some of these having been constructed within a year of the survey. CAM in Texas is used as both a surface- and under-layer. The survey indicated that the primary failure of CAM in Texas was localized rutting due to shoving and shear failures, predominantly at intersections under the action of stop-and-go traffic. The survey indicated the potential for problems regarding the skid resistance and light reflection off particularly smooth surfaces. Reflective cracking through a thin CAM overlay paved over a jointed concrete pavement was observed on a pavement in the Paris district. Indications from the Districts are that reflection cracks that open up in CAM during the winter heal during the summer. Overall, the performance of CAM in Texas as surveyed appeared reasonable with excellent performance observed for some, such as the SAC-A CAM mix (with PG 76-22) on Loop 20 in the Laredo District. It is recommended that the performance of these projects continue to be monitored to better realize the long-term performance of CAM.

Local aggregates from 14 different sources in Texas were evaluated as part of the study. Characterization of these aggregates was a critical component of the study. In this regard, the Aggregate Imaging System (AIMS) was very useful to distinguish the surface texture and angularity properties of these aggregates, which varied considerably, even within the same surface aggregate class (SAC). Characterization of the local aggregates used in the study included evaluation of the classification properties, AIMS sphericity, surface texture and angularity, and properties of the filler component, including Rigden voids, filler-binder ratio, and hydrometer particle distribution. A correlation analysis was done relating the aggregate properties to the rutting and cracking performance of the CAM mixes. It was found that Los Angeles abrasion and acid insolubility were uncorrelated with any of the CAM performance parameters evaluated. The micro-Deval abrasion and magnesium sulfate soundness loss significantly influenced HWT performance, indicating that stripping in CAM may be decreased by using aggregates with low degradation values. Increased coarse and fine aggregate angularity, as measured using AIMS, improved rutting performance but did not affect cracking performance in the Overlay Tester (OT). The rutting and cracking performance as well as the stripping resistance of CAM may be improved by using aggregates with increased surface texture. An interesting finding in the study was the significant effect of filler on the rutting performance of CAM in particular. In this regard, filler content, the nature of the filler, and its interaction with the binder significantly influenced rutting performance. These findings strongly support restricting the filler contents of CAM mixtures. The report includes guidelines and aggregate quality criteria for the use of local aggregates with CAM.

In general, the aggregate characterizing tests reflected the very poor quality of local aggregates that are typically low in angularity, having little or no surface texture. This adversely affects the rutting resistance of CAM and renders these mixes prone to stripping. The very poor

rutting and cracking performance of all CAM designed as part of the study required a compromise in terms of establishing limits for acceptable performance. Based on an overview of the general performance of these mixes, it is recommended that the rutting performance of CAM with local aggregates be evaluated using the Hamburg wheel tracker (HWT) per current procedures but that the required number of cycles to a 0.5 inch rut be reduced from 20,000 to 10,000 regardless of the performance grade of the asphalt used. Hence, it is anticipated that these mixes may be appropriate only for applications similar to those for dense-graded hotmix with PG 64-22 binders. The HWT mobilizes pore water pressures in CAM that aggravates the stripping of these mixes. As such, it is the right test to evaluate the performance of CAM. To address the stripping of CAM, it is recommended that an additional criterion be imposed to ensure that no stripping inflection point (SIP) occurs before the application of 5,000 cycles in the HWT. It is further recommended that the current OT cracking criterion of 750 cycles to failure remain in effect, although wet conditioning of OT specimens prior to testing is strongly recommended.

It is recommended that the mix design of CAM be done by using a Superpave gyratory compactor capable of measuring the shear stress of the mix during compaction. The optimum asphalt content of CAM should be selected to achieve a relative density of 97 percent at the N_{des} number of gyrations (50 gyrations). To ensure that the mix does not overfill with asphalt with further compaction, a restriction of 98 percent relative density is imposed at the N_{max} level (75 gyrations). The mix must not fail in shear before the application of the N_{des} number of gyrations during compaction. If shear stress measurements are not available, the voids filled with asphalt (VFA) of the mix at N_{des} must be less than 80 percent. The reduction in the required density at N_{des} from 98 percent to 97 percent as recommended supports an increase in required minimum VMA from 17 percent to 18 percent to allow sufficient binder in these mixes.

Kim's test was evaluated as an alternative to HWT testing to rapidly screen the rutting performance of CAM. This test correlated well with the HWT but further development of the test is recommended to provide a degree of confinement to test specimens during testing, either directly or by using a loading ram with a smaller diameter. The variability in the results of OT cracking tests on the CAM was very high, even for these fine-graded mixes. The semi-circular bending (SCB) test was evaluated as an alternative measure of cracking performance. Specifically the study evaluated various cracking parameters to investigate the sensitivity of the SCB in distinguishing the cracking resistance of different mixtures. In this regard, the area beneath force-displacement curves from monotonic tests on notched specimens, stress intensity factor, and tensile strength proved to be useful parameters. The study included a finite element analysis to determine the tensile stress distribution in notched specimen. Based on initial evaluations, the best SCB cracking parameter appeared to be the slope area under the peak load area curves determined based on the testing of multiple SCB specimens with varying notch depths. Based on a comparison of the cracking performance of CAM and other mixes, it is recommended that SCB testing be done at a temperature of 5 °C/41 °F to diminish permanent deformation during testing towards better cracking characterization.

The report includes a chapter discussing alternatives to CAM for cracking attenuating surface mixtures. In this regard, both fine-graded stone matrix asphalt (SMA) and coarse matrix high binder (CMHB) mixes were evaluated using local aggregates. Also investigated was the influence of blending the local aggregates in both the coarse and fine components of the CMHB mix as well as in CAM with high quality aggregates. The SMA mix with local aggregates proved to have acceptable rutting performance but would probably be a very costly alternative to CAM. The CMHB mix with local aggregates had similar rutting performance compared to CAM but

excellent cracking performance in the OT. Blending with higher quality aggregates improved the performance of CMHB but not CAM.

Based on the study, the report provides revised recommendations for the mix design of CAM using local aggregates. Guidelines for the use of local aggregates and aggregate quality criteria are also recommended to enhance the rutting and cracking performance of CAM with local aggregates. These recommendations are based on laboratory investigations and field validation of these is strongly recommended before implementation.

References

Acott, M. (1991), Thin Hot Mix Asphalt Surfacings. National Asphalt Pavement Association, Information Series 110. Lanham, MD.

Anderson R. M., P. A. Turner, R. L. Peterson and R. B. Mallick (2002), Relationship of Superpave Gyratory Compaction Properties to HMA Rutting Behavior, NCHRP 9-16 Report 478, pg 19.

Anderson, D. A., J. P. Tarris and J. D. Brock (1982), Dust Collector Fines and their Influence On Mixture Design, Proceedings of the Association of Asphalt Paving Technologists, Vol. 51, pg 363.

Anderson, D. A. (1987), Guidelines for Use of Dust In Hot-Mix Asphalt Concrete Mixtures, Proceedings Association of Asphalt Paving Technologists, Vol. 56, pg 492.

Arabani, M. and B. Ferdowsi (2006), Characterization of Tensile Fracture Resistance of Hot Mix Asphalt Using Semi-Circular Bend Test, ISSA International Congress, Beijing, China.

Bayomy, F. M, M. A. Mull-Aglan, A. A. Abdo and M. J. Santi (2006), Evaluation of Hot Mix Asphalt (HMA) Fracture Resistance Using the Critical Strain Energy Release Rate, Jc, 85th Annual Meeting Compendium of Papers CD-ROM, Transportation Research Board, Washington, DC.

Chowdhury, A., J. W. Button, V. Kohale and D. Jahn (2001), Evaluation of Superpave Fine Aggregate Angularity Specification, ICAR Report 201-1, International Center for Aggregates Research, TTI, Texas A&M University, College Station, Texas.

Cocurullo, A., G.D. Airey, A.C. Collop and C. Sangiorgi (2007). Indirect Tensile Versus Two Point Bending Fatigue Testing, Proceedings of Institute of Civil Engineers, Transport 161, pp. 207–220.

Cooley, L. A., R. S. James and M. S. Buchanan (2002), Development of Mix Design Criteria for 4.75 mm Mixes, NCAT Report 02-04, National Center for Asphalt Technology, Auburn University, AL.

Cooley, L., M. Stroup-Gardiner, E. R. Brown, D. Hanson and M. Fletcher (1998), Characterization Of Asphalt-Filler Mortars With Superpave Binder Tests, Proceedings Association of Asphalt Paving Technologists, Vol. 67.

Cooley, L.A. and E.R. Brown (2003), Potential Of Using Stone Matrix Asphalt (SMA) For Thin Overlays, NCAT Report 03-01, National Center for Asphalt Technology, Auburn University, AL.

Cooley, L.A., and R.S. James (2003), Micro-Deval Testing of Aggregates in the Southeast, Transportation Research Record No. 1837, National Research Council, Washington, D.C.

Cooley, L.A., M. H. Huner and E.R. Brown (2002a), Use of Screenings to Produce HMA Mixtures, NCAT Report 02-04, National Center for Asphalt Technology, Auburn University, AL.

Cooley, L.A., R. S. James and M.S. Buchanan (2002b), Development Of Mix Design Criteria For 4.75 mm Superpave Mixes – Final Report, NCAT Report 02-10, National Center for Asphalt Technology, Auburn University, AL.

Cooper, S. B. and L. N. Mohammad (2004), NovaChipTM Surface Treatment - Six Year Evaluation, Louisiana Transportation Research Center, Louisiana.

Di Benedetto, H., C. De La Roche, H. Baaj, A. Pronk and R. LundStrom (1997), Fatigue of Bituminous Mixtures: Material and Structures 37 - Different Approaches and RILEM Group Contribution.

Fletcher, T., C. Chandan, E. Masad and K. Sivakumar (2003), Aggregate Imaging System (AIMS) for Characterizing the Shape of Fine and Coarse Aggregates, Transportation Research Record 1832, Transportation Research Board, Washington D.C., pp. 67-77.

Fowler, D.W., J. J. Allen, A. Lange and P. Range (2006), The Prediction of Coarse Aggregate Performance by Micro-Deval and Other Aggregate Tests, Research Report ICAR 507-1F, International Center for Aggregates Research, The University of Texas at Austin, TX.

Gandhi, P.M. and R. L. Lytton (1984), Evaluation of Aggregates for Acceptance in Asphalt Paving Mixtures, Proceedings of the Association of Asphalt Paving Technologists, Vol. 53, Scottsdale, AZ.

Hofman, R., B. Oosterbaan, S. M. J. G Erkens and J. Van der Kooij (2003), Semi-Circular Bending Test to Assess the Resistance against Crack Growth. Proceedings of the Sixth International RILEM Symposium on Performance Testing and Evaluation of Bituminous Materials, pp. 257–263.

Howson, J., E. A. Masad, A. Bhasin V. C. Branco, E. Arambula, R. L. Lytton and D. Little (2007), System for the Evaluation of Moisture Damage Using Fundamental Material Properties, Report 0-4524-1, Texas Transportation Institute, The Texas A&M University System, College Station, TX.

Huang, B., X. Shu and Y. Tang (2005), Comparison of Semi-Circular Bending and Indirect Tensile Strength Tests for HMA Mixtures. Advances in Pavement Engineering (GSP 130). Austin, TX.

Huber G. A., J. C. Jones and N.M. Jackson (1998), Contribution of Fine Aggregate Angularity and Particle Shape to Superpave Mixture Performance, Transportation Research Record, Journal of the Transportation Research Board 1609, Washington, D.C., 28–35.

Jacobs, M.M.J. (1995), Crack Growth in Asphalt Mixes, Ph.D Dissertation, Delft University of Technology, Delft, Netherlands.

Jayawickrama, P.W. and P. Madhira (2008), Review of TxDOT WWARP Aggregate Classification System, Report No. 0-1707-8, Texas Tech University, College of Engineering, Lubbock, TX.

Kalcheff I. V. and D. G. Tunnicliff (1982), Effects of Crushed Stone Aggregate Size and Shape on Properties of Asphalt Concrete. Proc., AAPT, Vol. 51.

Kandhal, P., and F. Parker (1998), Aggregate Tests Related to Asphalt Concrete Performance in Pavement, Report No. 405, NCHRP, Washington, D.C.

Kennedy, T. W. and W.R. Hudson (1968), Application of the Indirect Tensile Test to Stabilized Materials. Highway Research Record 235, Highway Research Board. Washington, D.C.

Kim, Y.R., D. N. Little and R.L. Lytton (2003), Fatigue and Healing Characterization of Asphalt Mixtures, Journal of Materials in Civil Engineering, American Society of Civil Engineers, Vol. 15, No. 1, 2003, pp 75-83.

Lim, I.L., I. W. Johnston and S. K. Choi (1993), Stress Intensity Factors for Semi Circular Specimens under Three Point Bendin, Engineering Fracture Mechanics Vol.44, No.3, pp. 363-382.

Lytton, R.L., E. A. Masad, C. Zollinger, R. Bulut and D. Little (2005), Measurements of Surface Energy and Its Relationship to Moisture Damage, Report 0-4524-2, Texas Transportation Institute, The Texas A&M University System, College Station, TX.

Mahmoud, E (2005), Development of Experimental Methods for the Evaluation of Aggregate Resistance to Polishing, Abrasion, and Breakage, M.Sc. Thesis, Department of Civil Engineering, Texas A&M University, College Station, TX.

Mallat, S. G. (1989), A Theory for Multiresolution Signal Decomposition: The Wavelet Representation, IEEE Transactions on Pattern Analysis and Machine Intelligence, Vol. II, No. 7.

Masad, E. A., J. Button and T. Papagiannakis (2000), Fine Aggregate Angularity: Automated Image Analysis Approach, Transportation Research Record 1721, Transportation Research Board, Washington D.C., pp. 66–72.

Masad, E. A., A. Luce and E. Mahmoud (2006), Implementation Of Aims In Measuring Aggregate Resistance To Polishing, Abrasion And Breakage, Report 5-1707-03-1, Texas Transportation Institute, The Texas A&M University System, College Station, TX.

Masad, E. A., D. Olcott, T. White and L. Tashman (2001), Correlation of Fine Aggregate Imaging Shape Indices with Asphalt Mixture Performance, Transportation Research Record, Journal of the Transportation Research Board 1757, pp. 148–156.

Masad, E.A., D. N. Little, L. Tashman, S. Saadeh, T. Al-Rousan and R. Sukhwani (2003), Evaluation Of Aggregate Characteristics Affecting HMA Concrete Performance, Research Report ICAR 203-1, Texas Transportation Institute, The Texas A&M University System, College Station, TX.

McLean, D. B (1974), Permanent Deformation Characteristics of Asphalt Concrete, Ph.D. Thesis, University of California, Berkeley.

Meier W. R., E. J. Elnicky and B. R. Schuster (1979), Fine Aggregate Shape and Surface Texture, FHWA – A288-229. DOT Arizona, Lansing.

Mohammad, N. L., Z. Wu and M. Aglan (2004), Characterization of Fracture and Fatigue Resistance on Recycled Polymer-Modified Asphalt Pavements, 5th RILEM conference on Pavement Cracking, France.

Mull, M.A., A. Othman and L. Mohammad (2005), Fatigue Crack Growth Analysis of HMA Employing the Semi-Circular Notched Bend Specimen, TRB 2006 Annual Meeting Conference Proceedings. Washington, DC.

Oliver R (1998), Thin Bituminous Surfacings And Desirable Road User Performance, ARRB Research Report ARR325, AARB Transport Research, Australia.

Paris, P.C., and F. Erdogan (1963), A Critical Analysis of Crack Progression Laws, Transactions of the ASME, Journal of Basic Engineering, Series D, 85, No. 3.

Pretorius, F.J., J.C. Wise and M. Henderson (2004), Development Of Application Differentiated Ultra-Thin Asphalt Friction Courses For Southern African Application, Proceedings of the 8th Conference on Asphalt Pavements for Southern Africa, South Africa.

Prozzi, J.A., J. P. Aguiar-Moya, A. d. F. Smit, M. Tahmoressi and K. Fults (2006), Recommendations for Reducing Superpave Compaction Effort to Improve Mixture Durability and Fatigue Performance, FHWA/TX-07/0-5132-1, Center for Transportation Research, University of Texas at Austin, Austin, TX.

Rand, D. (2007), Update on the Overlay Tester for Use in Designing Crack Resistant Asphalt Mixes, Presentation made at the 2007 Transportation Short Course, TX.

Recasens R. Miró, A. Martínez, and F. Pérez Jiménez (2005), Technical University of Catalonia, Jordi Girona 1–3, Módulo B1, 08034 Barcelona, Spain. H. Bianchetto, Universidad Nacional de La Plata, Calle 7 entre 47 y 48, 1900 La Plata, Argentina., Transportation Research Record: Journal of the Transportation Research Board, No. 1901, Transportation Research Board of the National Academies, Washington, D.C., pg. 10–17

Rice, J. R. (1968), A Path Independent Integral and the Approximate Analysis of Strain Concentration by Notches and Cracks. Journal of Applied Mechanics, Vol. 35, pg 379-386.

Rigden, P.J. (1947), The Use Of Fillers In Bituminous Road Surfacings - A Study Of Filler Binder Systems In Relation To Filler Characteristics, Journal of the Society of Chemical Industry, Vol. 66.

Smit, A.d.F. (2002), The Probabilistic and Volumetric Design of HMA, Ph.D Dissertation, University of Stellenbosch, South Africa.

Solaimanian, M., G. R. Pendola and T.W. Kennedy (2002), Relationship Between Aggregate Properties and Hamburg Wheel Tracking Results, Report 4977-1, Center for Transportation Research, University of Texas, TX.

Sousa, J.B., J. C. Pais, M. Prates, R. Barros, P. Langlois, and A.M. Leclerc (1998), Effect of Aggregate Gradation on Fatigue Life of Asphalt Concrete Mixes, Transportation Research Record 1630, pp 62–68. Washington, D.C.

Tangella, S.C.S.R., J. Craus, J. A. Deacon and C.L. Monismith (1990), Fatigue Response of Asphalt Mixtures, Report TM-UCB-A-003A-89-3, Institute of Transportation Studies, University of California. Berkeley, CA.

Traxler, R.N. (1937), The Evaluation Of Mineral Powders As Fillers For Asphalt, Proceedings of the Association of Asphalt Paving Technologists, Vol. 8.

TxDOT (2004), Standard Specifications for Construction and Maintenance of Highways, Streets, and Bridges, Texas Department of Transportation, Austin, TX.

Uhlmeyer, J. S. (2003), Tech Notes - The Use of NovaChipTM as a Surface Treatment, Washington State Department of Transportation (WSDOT).

Van de Ven, M., A. d. F. Smit and R. L. Krans (1997), Possibilities of a Semi-Circular Bending Test, Proceedings of the Eighth International Conference on Asphalt Pavements, Vol. II. Seattle, WA.

Walubita L. Lubinda and T. Scullion (2008), Thin HMA Overlays In Texas: Mix Design And Laboratory Material Property Characterization, Texas Transportation Institute, Report 0-5598-1, The Texas A&M University System, College Station, TX.

Walubita, L.F., V. Umashankar, X. Hu, B. Jamison, F. Zhou, T. Scullion, A. Epps Martin and S. Dessouky (2009), New Generation Mix-Designs: Laboratory Testing and Construction of the APT Test Sections. Texas Department of Transportation Project Interim Report FHWA/TX-10/0-6132-1, Texas A&M University. College Station, TX.

Wu, Z., L. N. Mohammad, L. B. Wang and M.A. Mull (2005), Fracture Resistance Characterization of Superpave Mixtures Using the Semi-Circular Bending. Test Journal of ASTM International (JAI), Volume 2, Issue 3.

Zhou, F. and T. Scullion (2005), Overlay Tester: A Rapid Performance Related Crack Resistance Test, FHWA/TX-05/0-4467-2, TTI, College Station, TX.

Zhou, F., S. Hu and T. Scullion (2007), Development and Verification of the Overlay Tester Based Fatigue Cracking Prediction Approach, FHWA/TX-07/9-1502-01-8, Texas Transportation Institute, The Texas A&M University System, College Station, TX.

Appendix A: Survey Photos

Figure A.1: CAM blistering (IH35, LaSalle, Laredo)

Figure A.2: CAM blistering extent (IH35, LaSalle, Laredo)

Figure A.3: Cracking on Loop 20

Figure A.4: Longitudinal cracking of CAM on Loop 20

Figure A.5: Edge-related cracking on Loop 20

Figure A.6: Shoving of CAM underlayer at intersection between SH 21 and SH 6 in Bryan

Figure A.7: CAM surface irregularities apparent on FM 60 in Bryan

Figure A.8: Slick CAM surface and reflections on FM 60 in Bryan

Figure A.9: CAM paved opposite the Texas A&M Research Park building on FM 60 in Bryan

Figure A.10: CAM Rutting at an intersection on FM 2154 in Bryan

Figure A.11: CAM shoving at an intersection on FM 2154 in Bryan

Figure A.12: CAM on FM 2154 in Bryan

Figure A.13: Shoving of CAM on FM 1179 in Bryan

Figure A.14: Shoving of CAM on FM 2347 in Bryan

Figure A.15: Shoving of the CAM at an intersection on FM 1179 in Bryan

Figure A.16: Shoving of CAM at another intersection on FM 1179 in Bryan

Figure A.17: Surface irregularities of CAM on FM 1179 in Bryan

Figure A.18: Cracked surface on FM 499 overlaid with CAM (Hopkins County)

Figure A.19: Transverse reflection cracking of new CAM on FM 499 in Hopkins County

Figure A.20: More transverse reflection cracking of new CAM on FM 499 in Hopkins County

Figure A.21: Longitudinal cracking of CAM on US 69 in Denison

FigureA.22: Transverse cracking of CAM on US 69 in Denison

Figure A.23: Shaving of CAM at intersection on US 69 in Denison

Figure A.24: Flushing of CAM paved on US 90 in Uvalde County

Figure A.25: Uniformity of bleeding patterns suggests tack coat striping

Figure A.26: Rutting of CAM on BU 59 in Angelina County, Lufkin

Figure A.27: Shoving and shear failure of CAM on US 281 in Burnett County, Austin

Appendix B: AIMS Flakiness Distribution Results

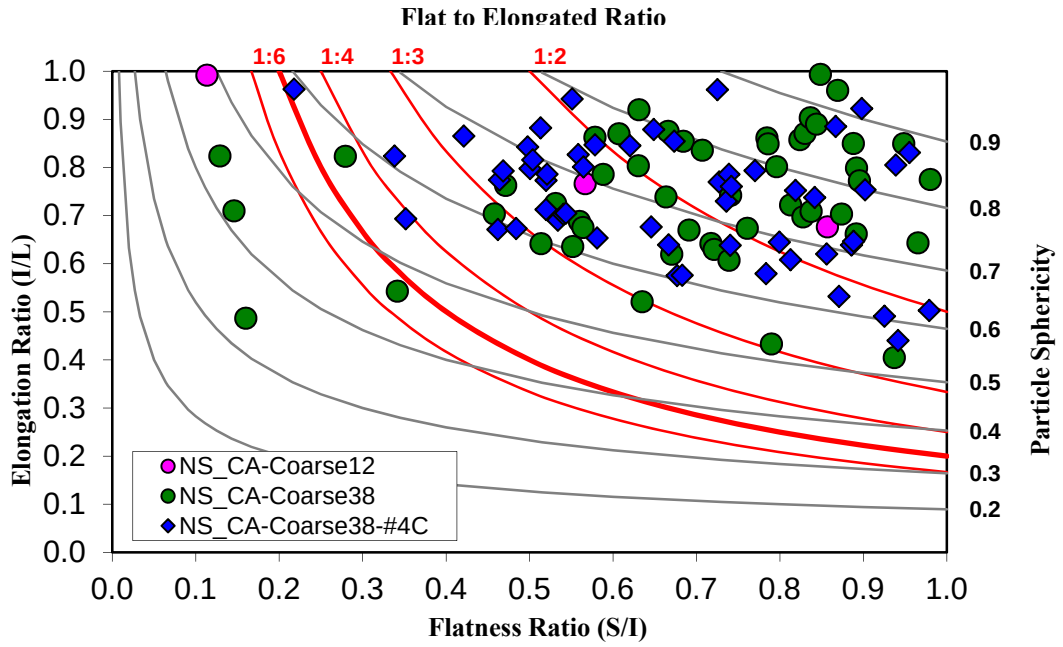

Figure B.1: Flakiness distribution of Fordyce gravel

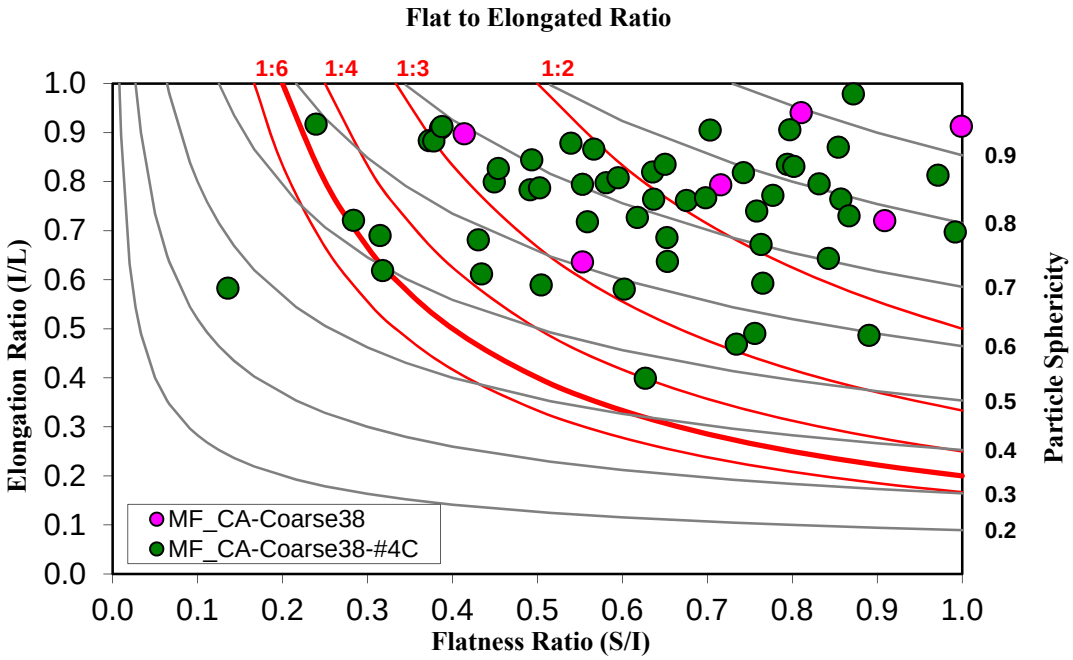

Figure B.2: Flakiness distribution of Marble Falls limestone

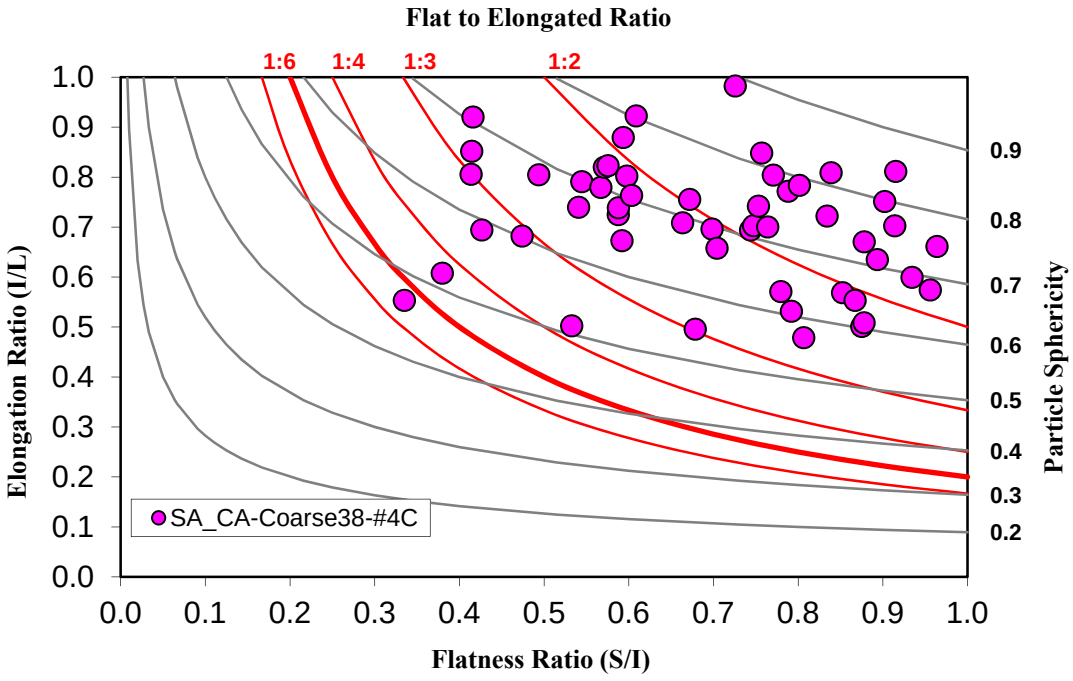

Figure B.3: Flakiness distribution of Beckmann limestone

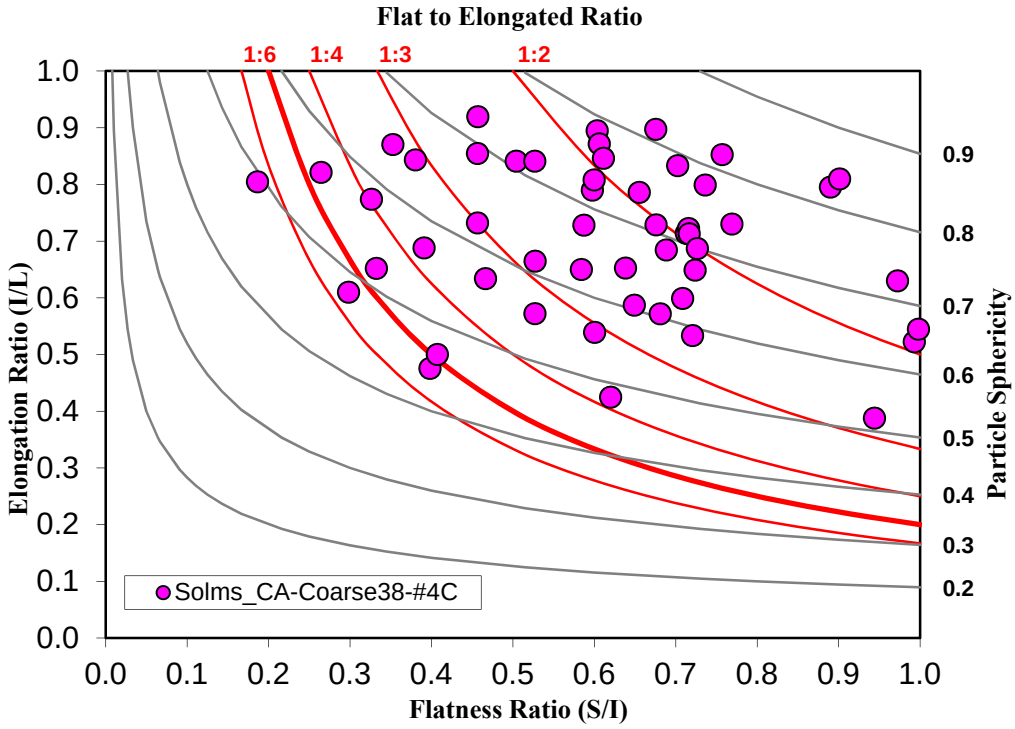

Figure B.4: Flakiness distribution of Solms Road limestone

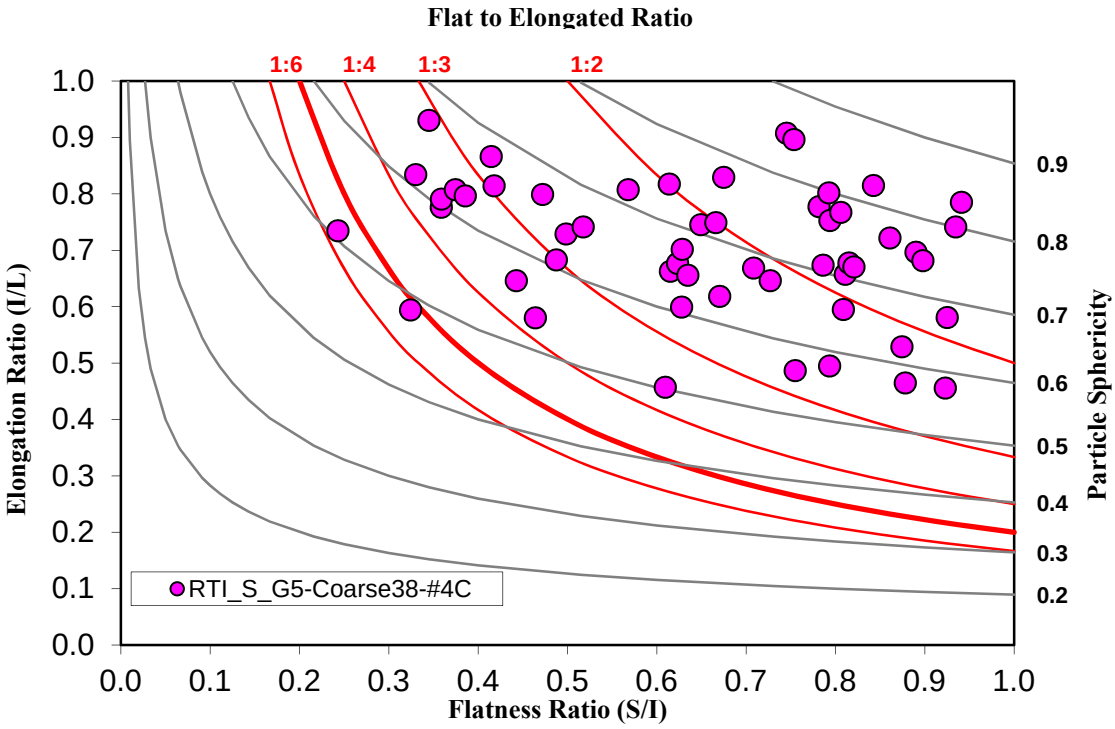

Figure B.5: Flakiness distribution of RTI limestone

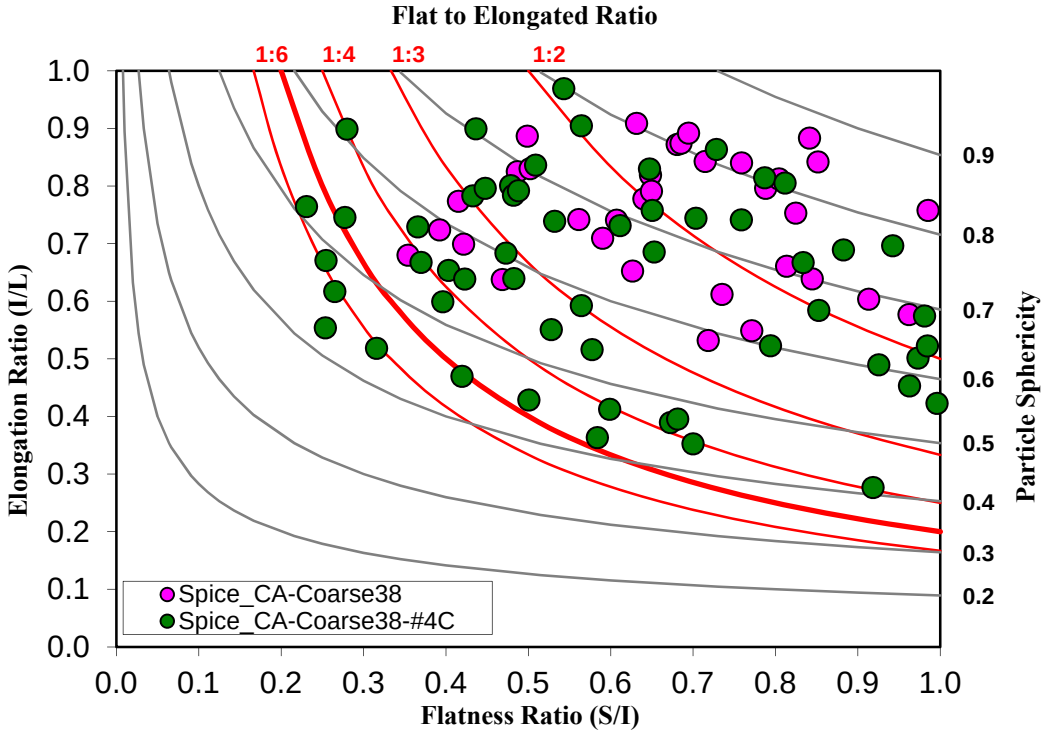

Figure B.6: Flakiness distribution of Spicewood limestone

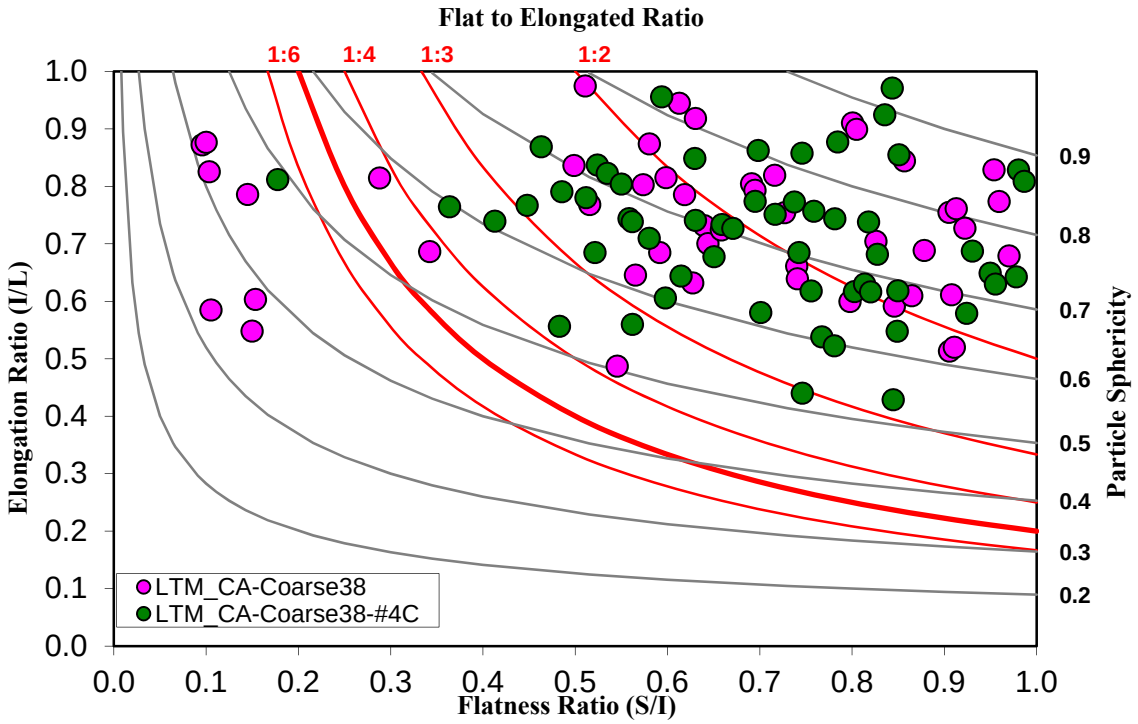

Figure B.7: Flakiness distribution of Lattimore limestone

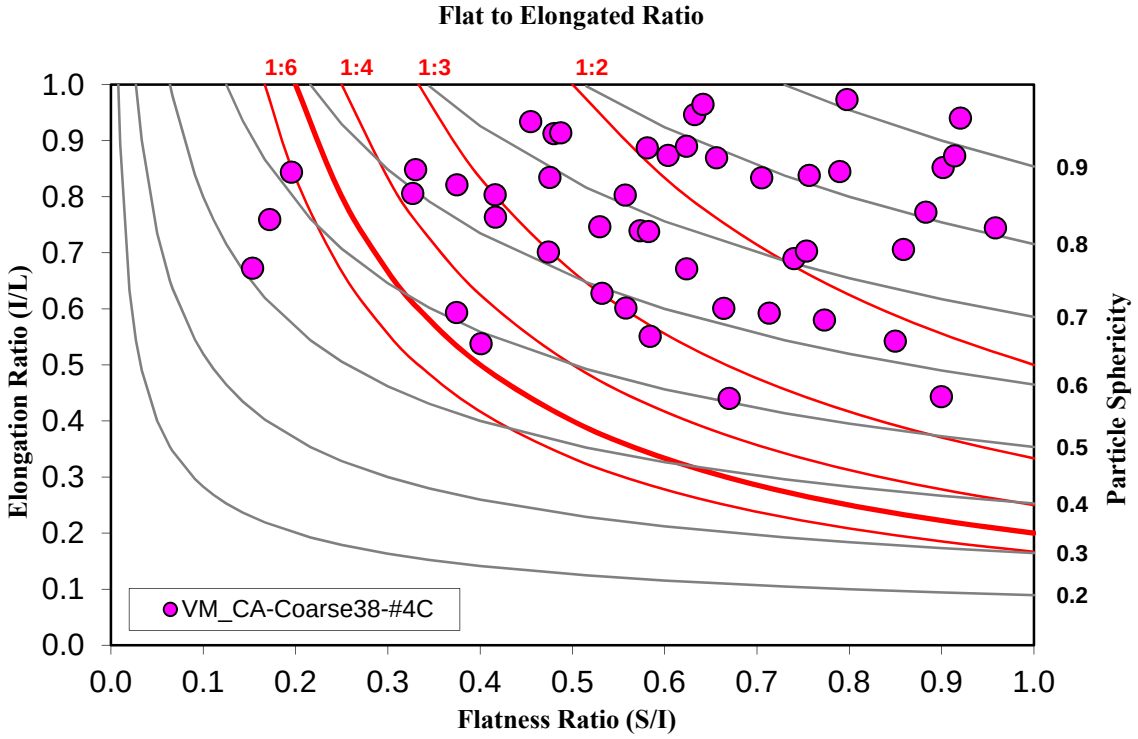

Figure B.8: Flakiness distribution of coarse aggregates from Vulcan in 1604 loop

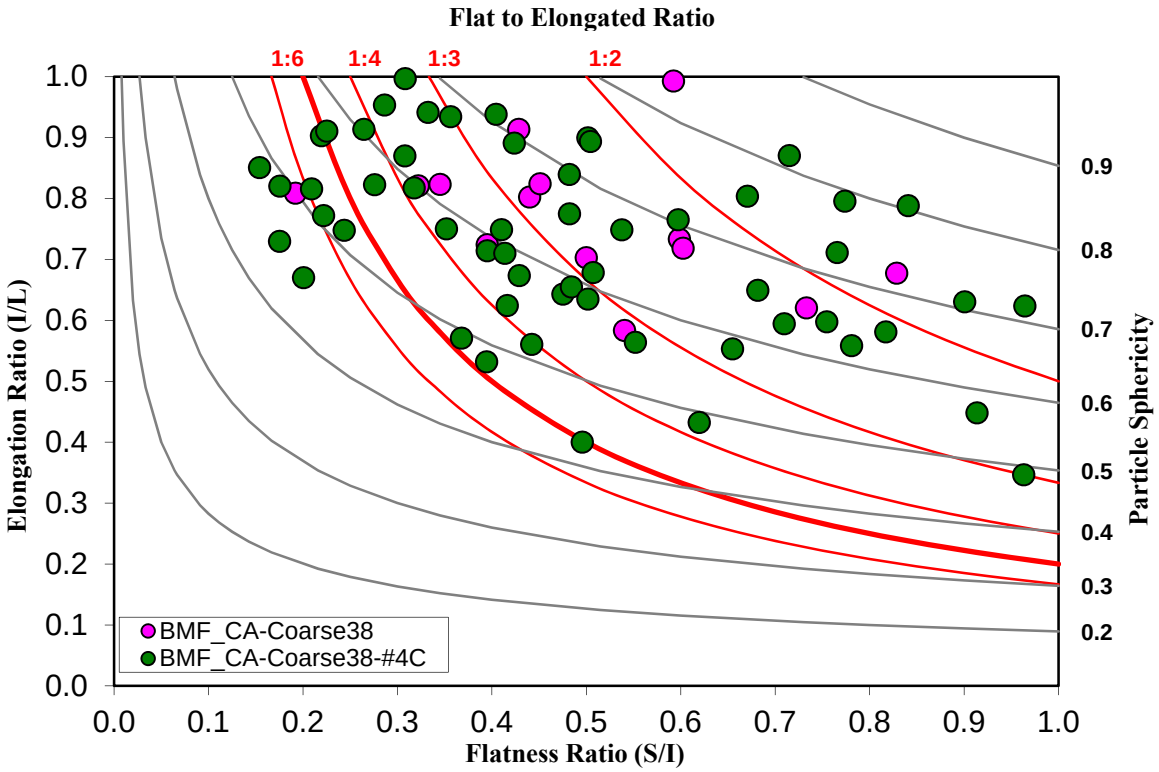

Figure B.9: Flakiness distribution of coarse limestone from Burnet

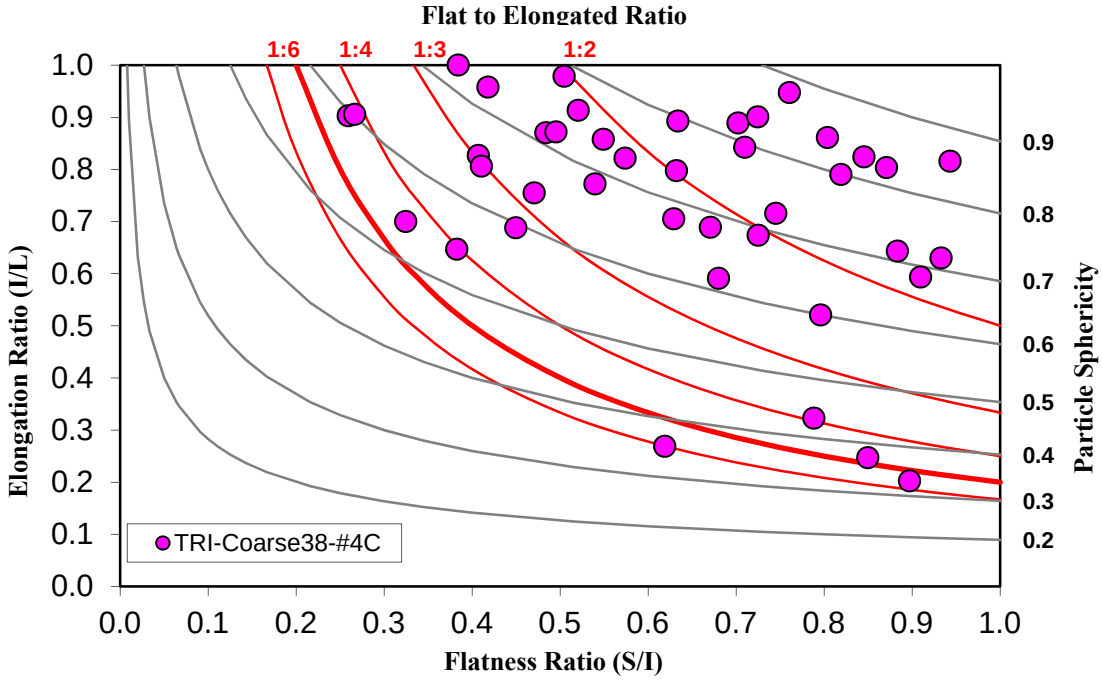

Figure B.10: Flakiness distribution of coarse aggregates from Trinity

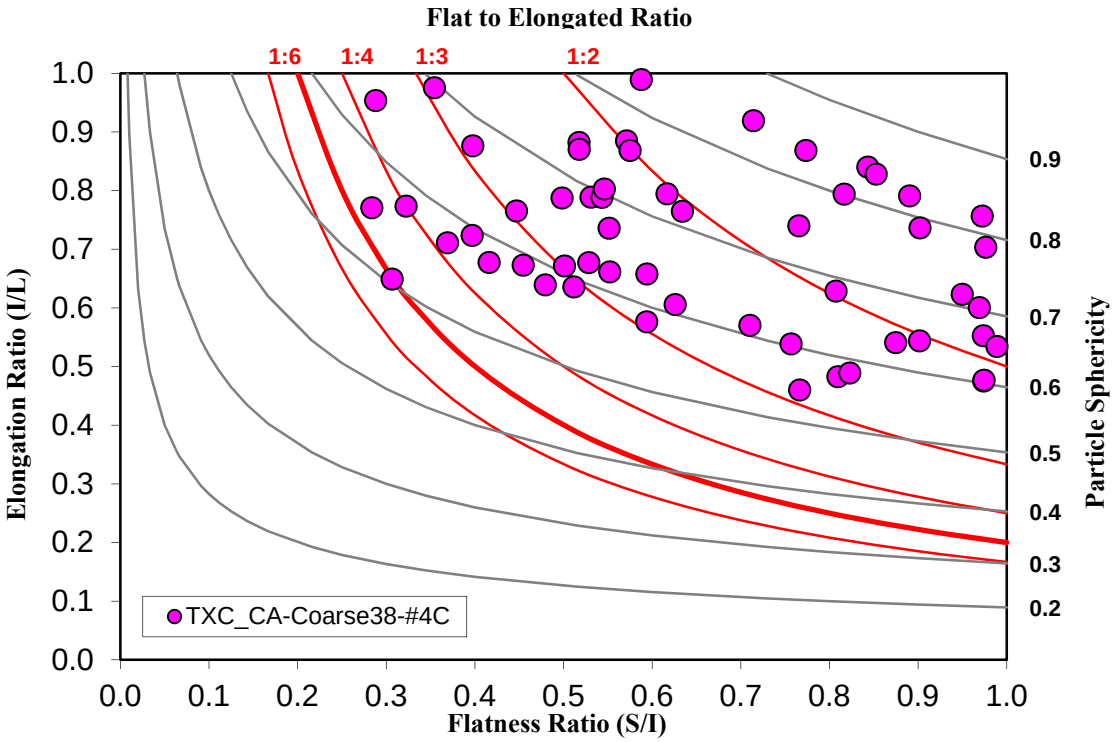

Figure B.11: Flakiness distribution of coarse aggregates from Texas Crushed Stone

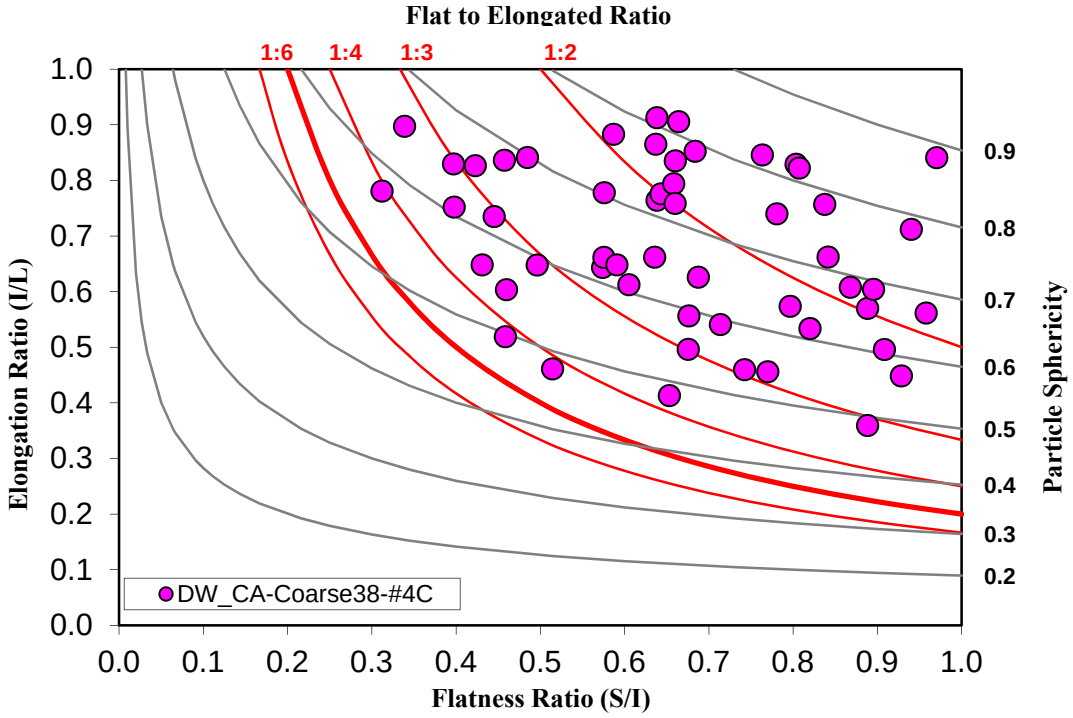

Figure B.12: Flakiness distribution of coarse aggregates from Dean Word

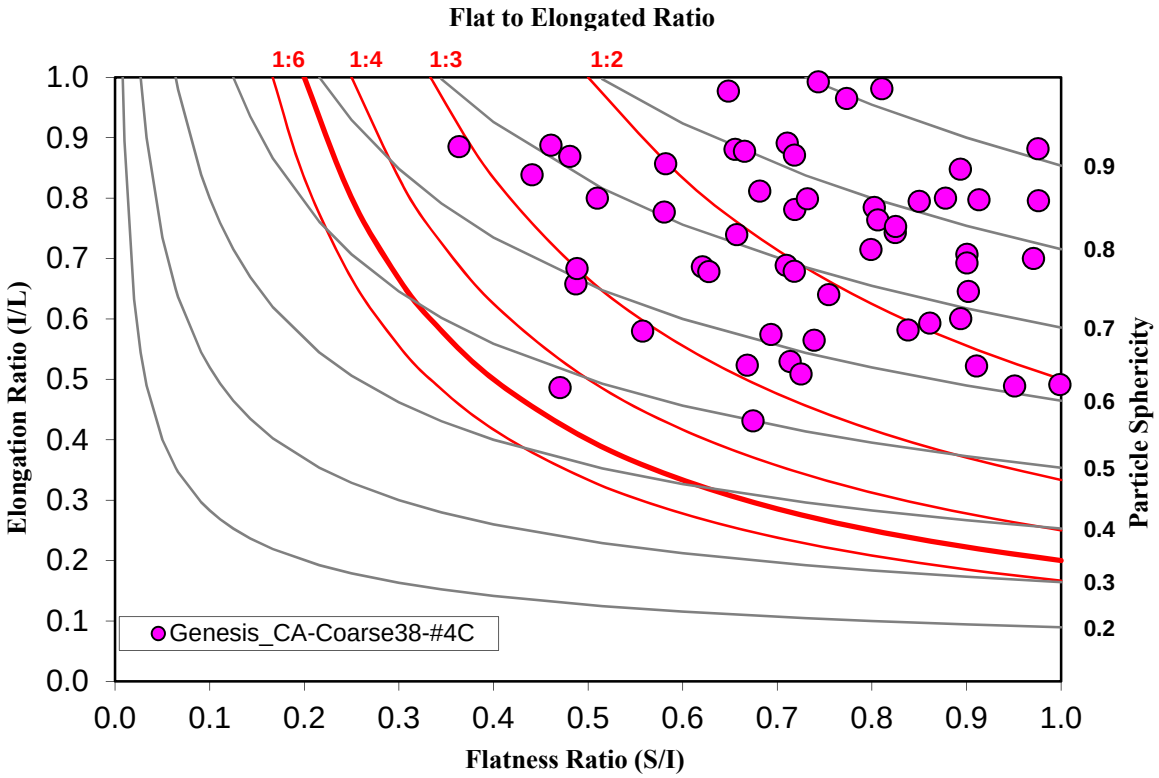

Figure B.13: Flakiness distribution of coarse aggregates from Genesis

Appendix C: SGC Volumetric Plots

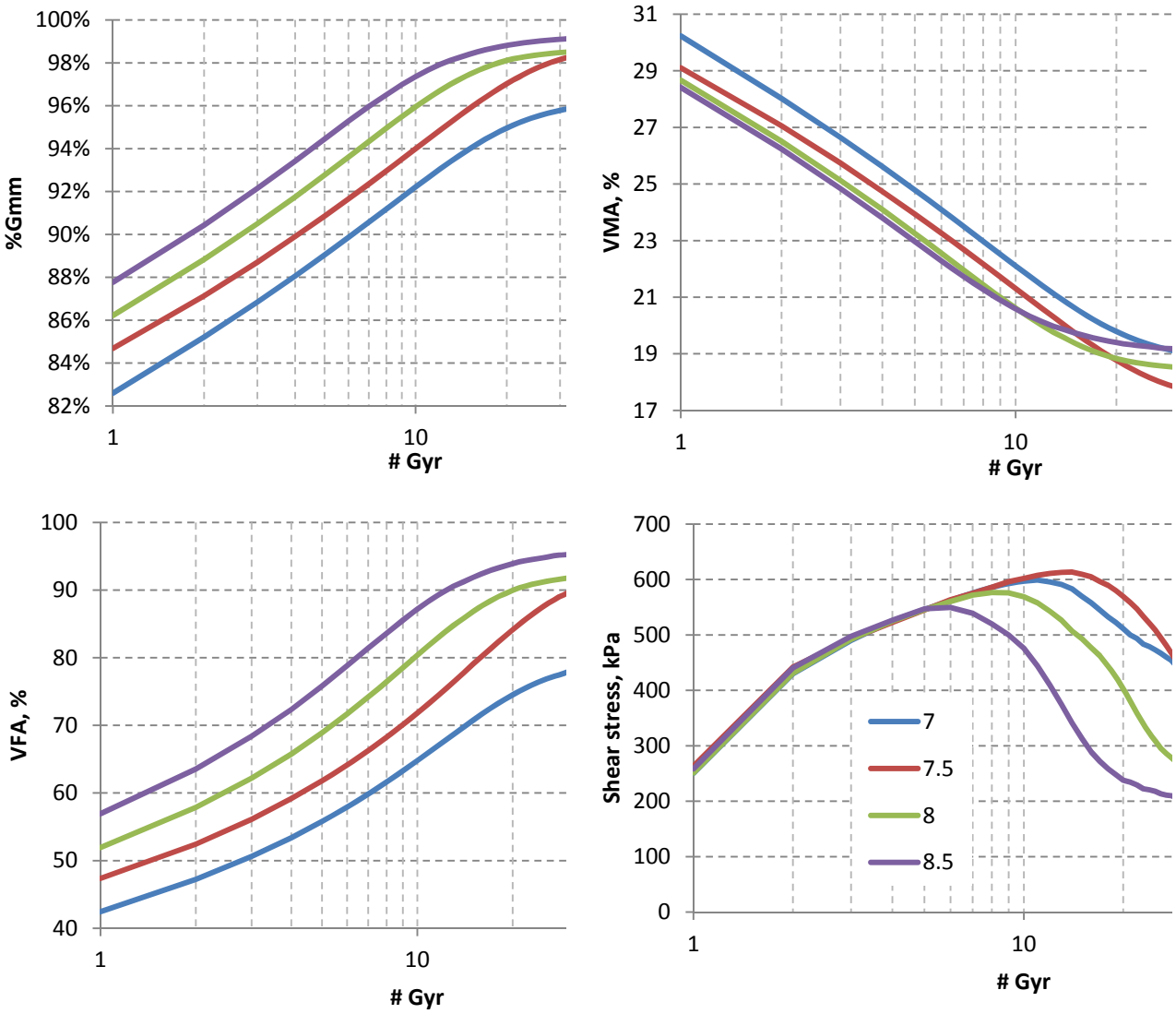

Figure C.1: Volumetric and shear stress properties of Fordyce gravel PG76-22 mix

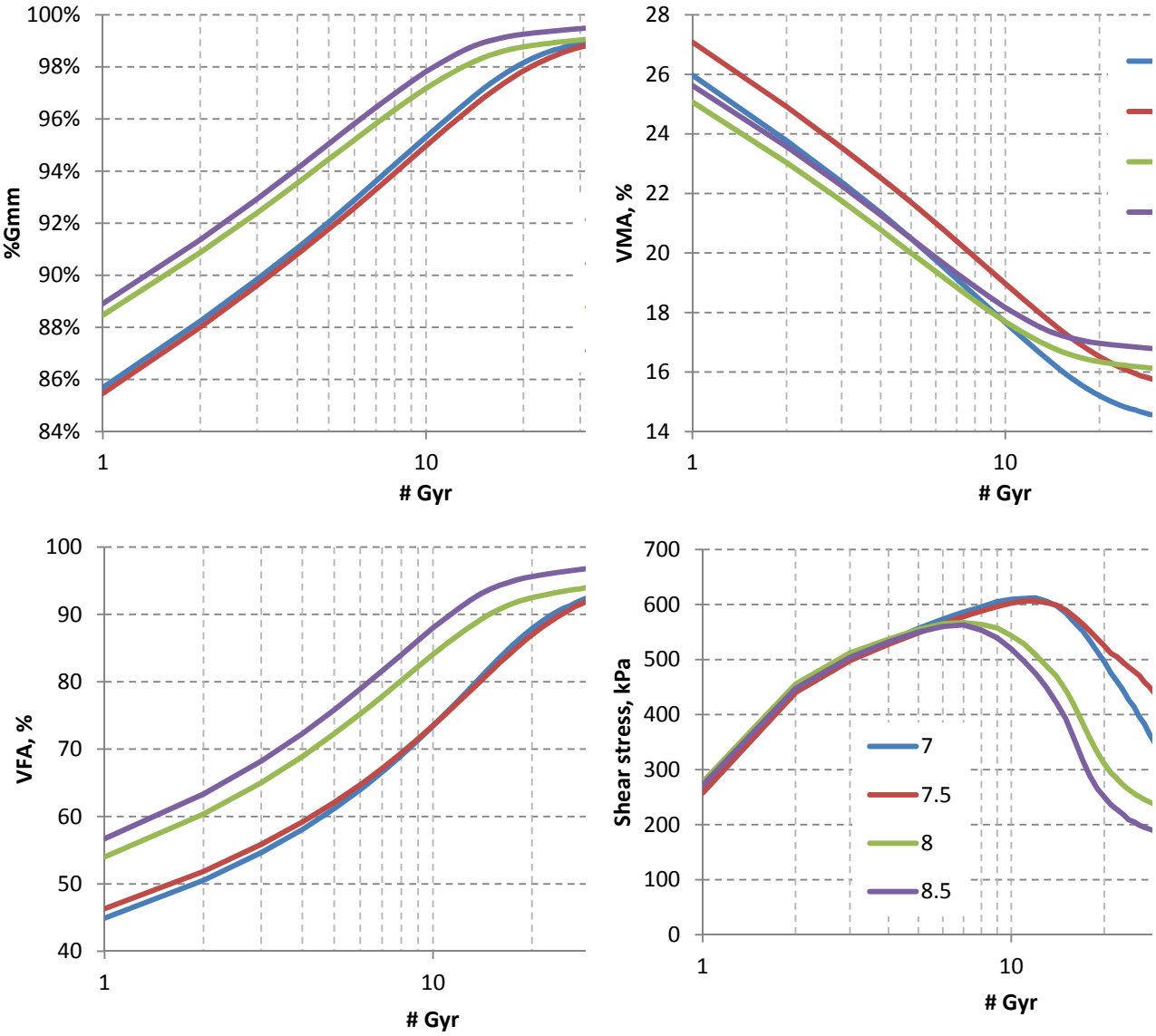

Figure C.2: Volumetric and shear stress properties of Fordyce gravel PG70-22 mix

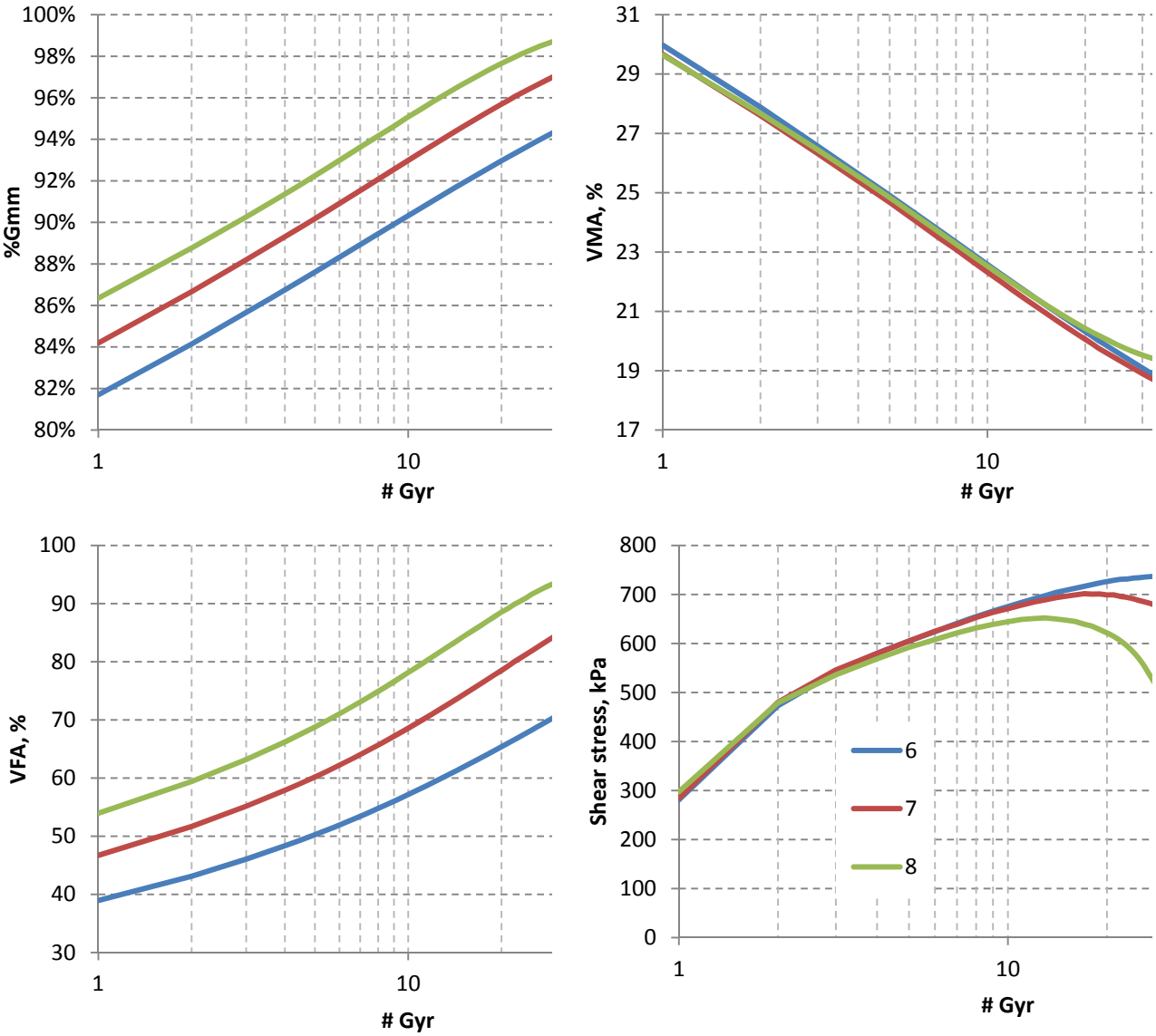

Figure C.3: Volumetric and shear stress properties of Marble Falls I mix

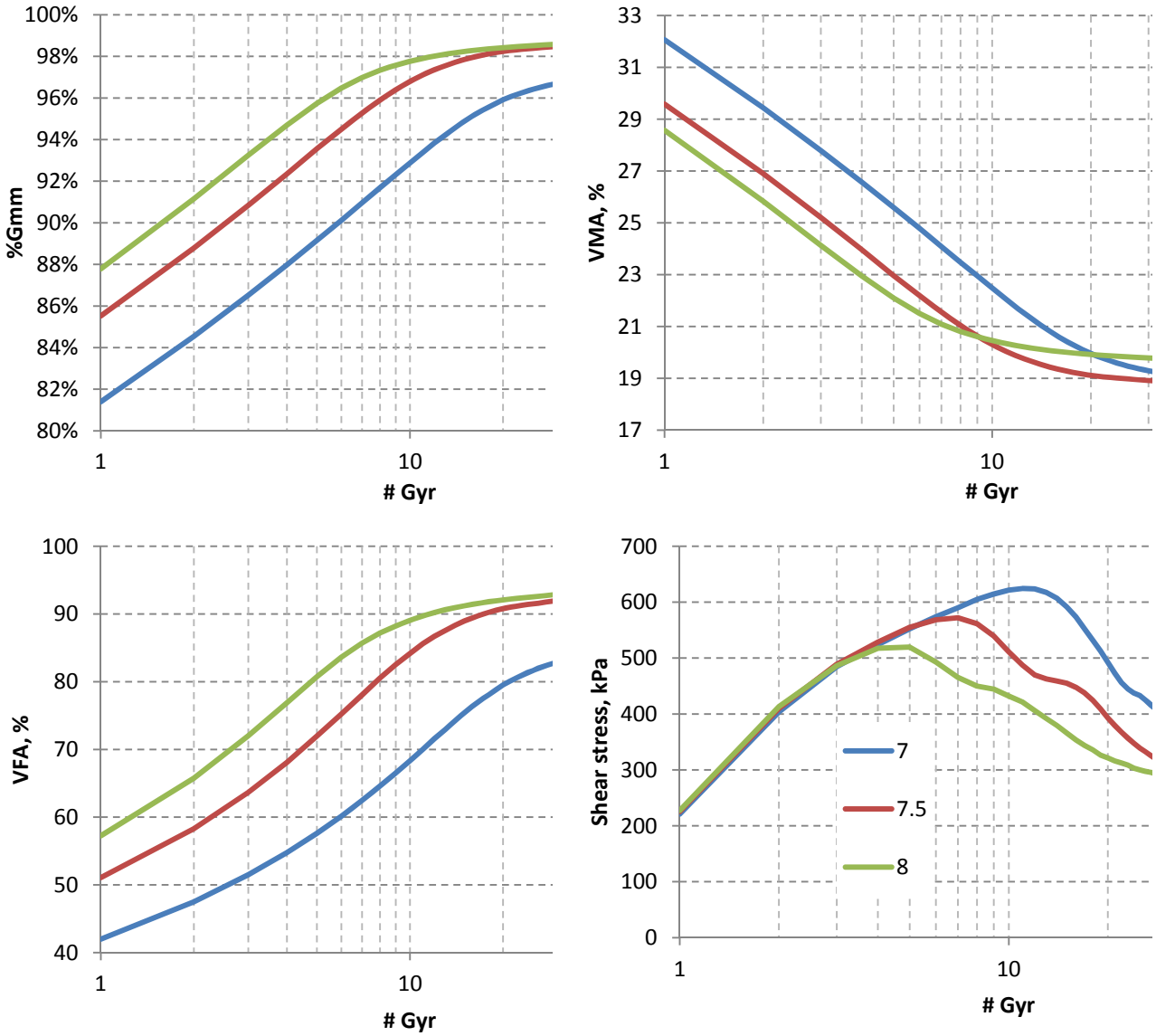

Figure C.4: Volumetric and shear stress properties of Marble Falls II mix

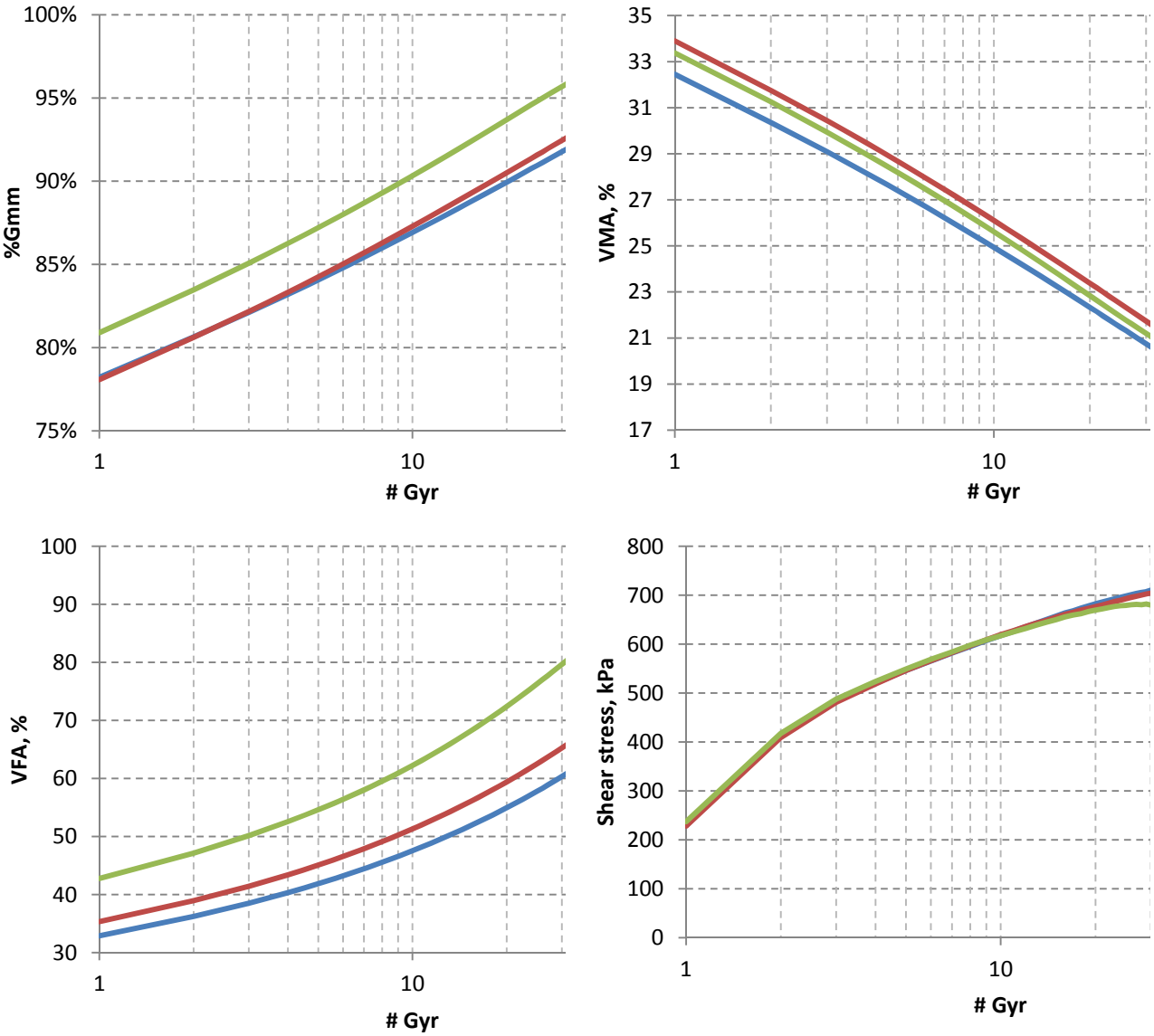

Figure C.5: Volumetric and shear stress properties of Beckmann mix

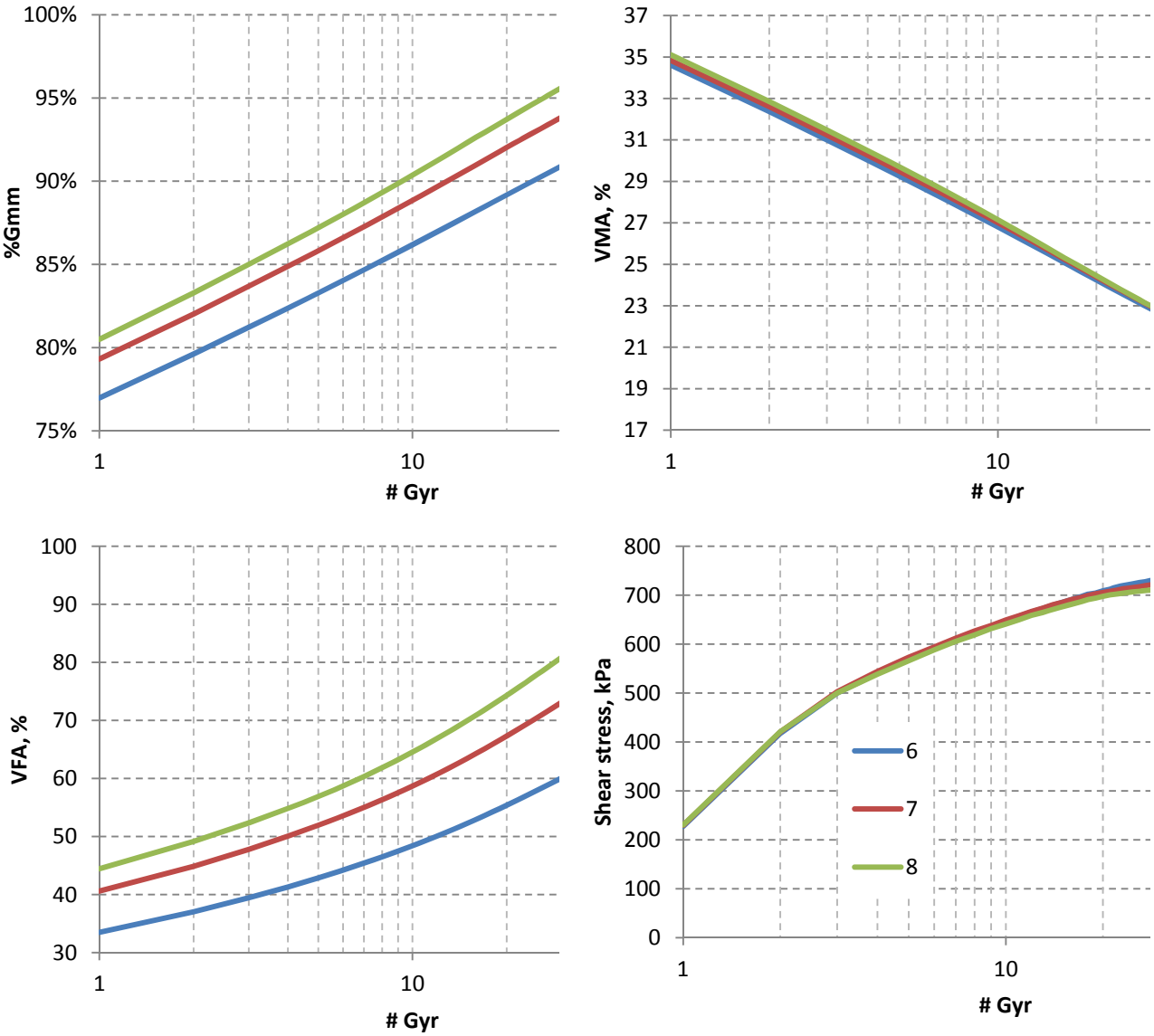

Figure C.6: Volumetric and shear stress properties of Solms Road mix

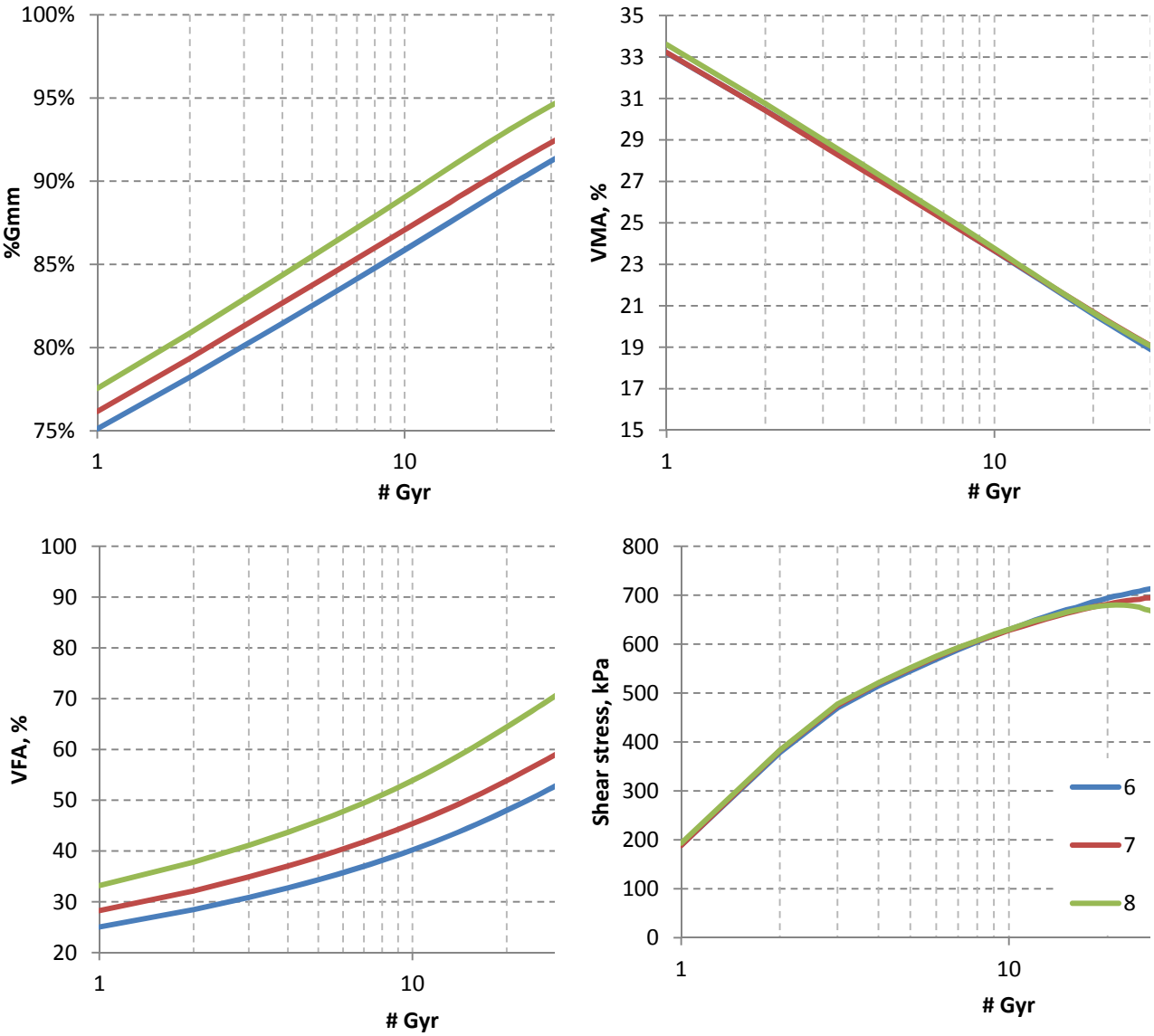

Figure C.7: Volumetric and shear stress properties of RTI mix

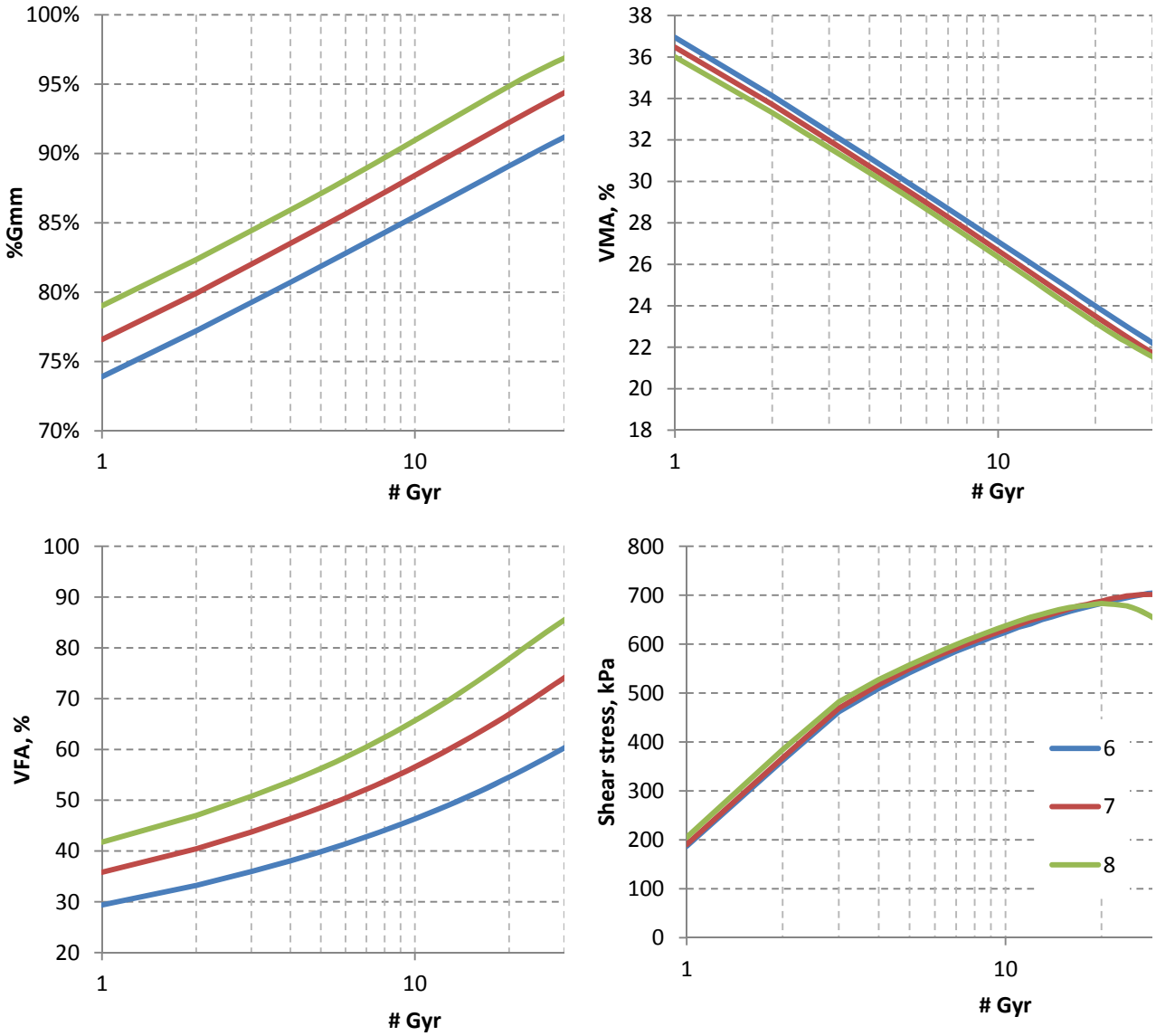

Figure C.8: Volumetric and shear stress properties of Spicewood mix

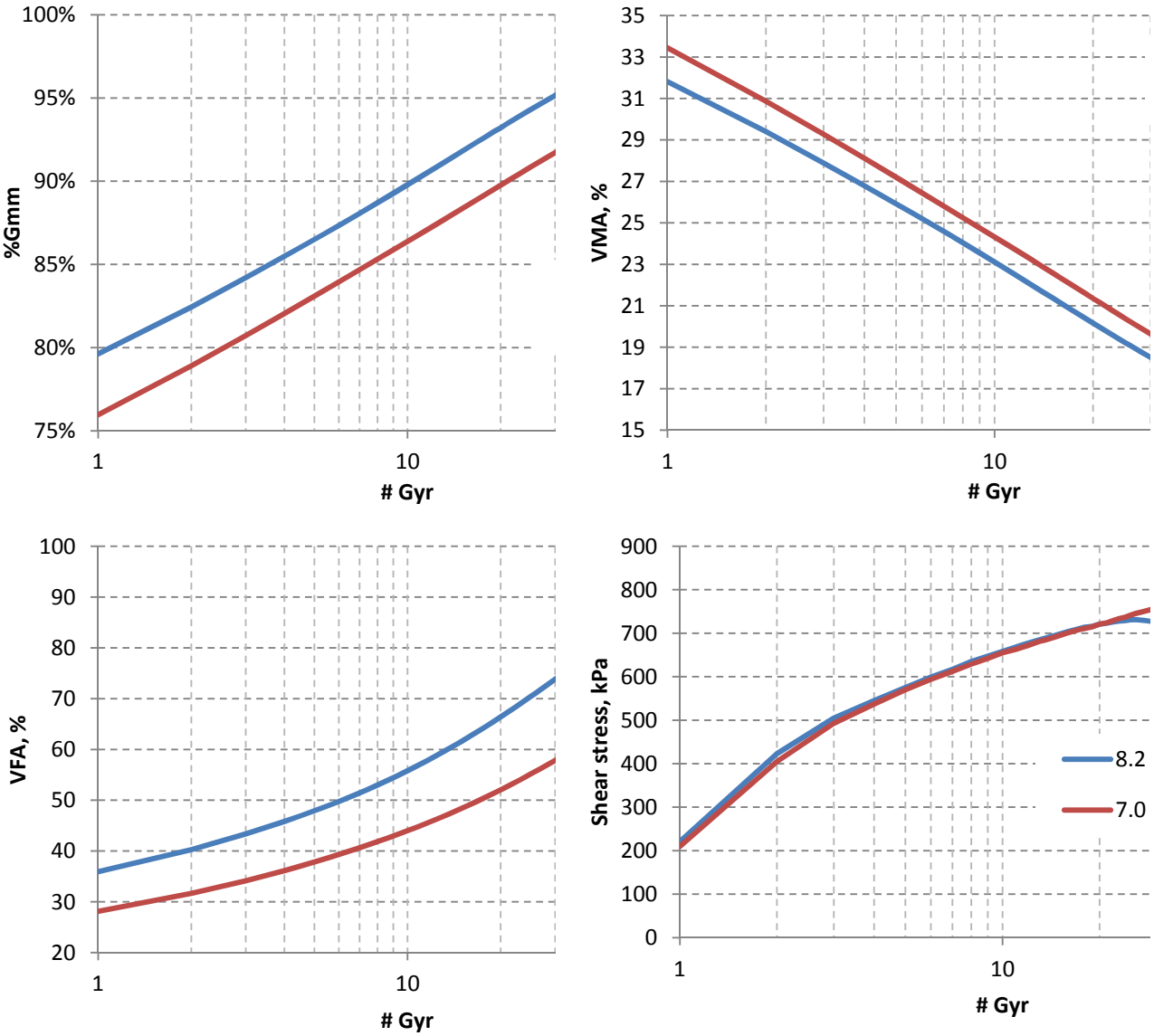

Figure C.9: Volumetric and shear stress properties of Lattimore mix

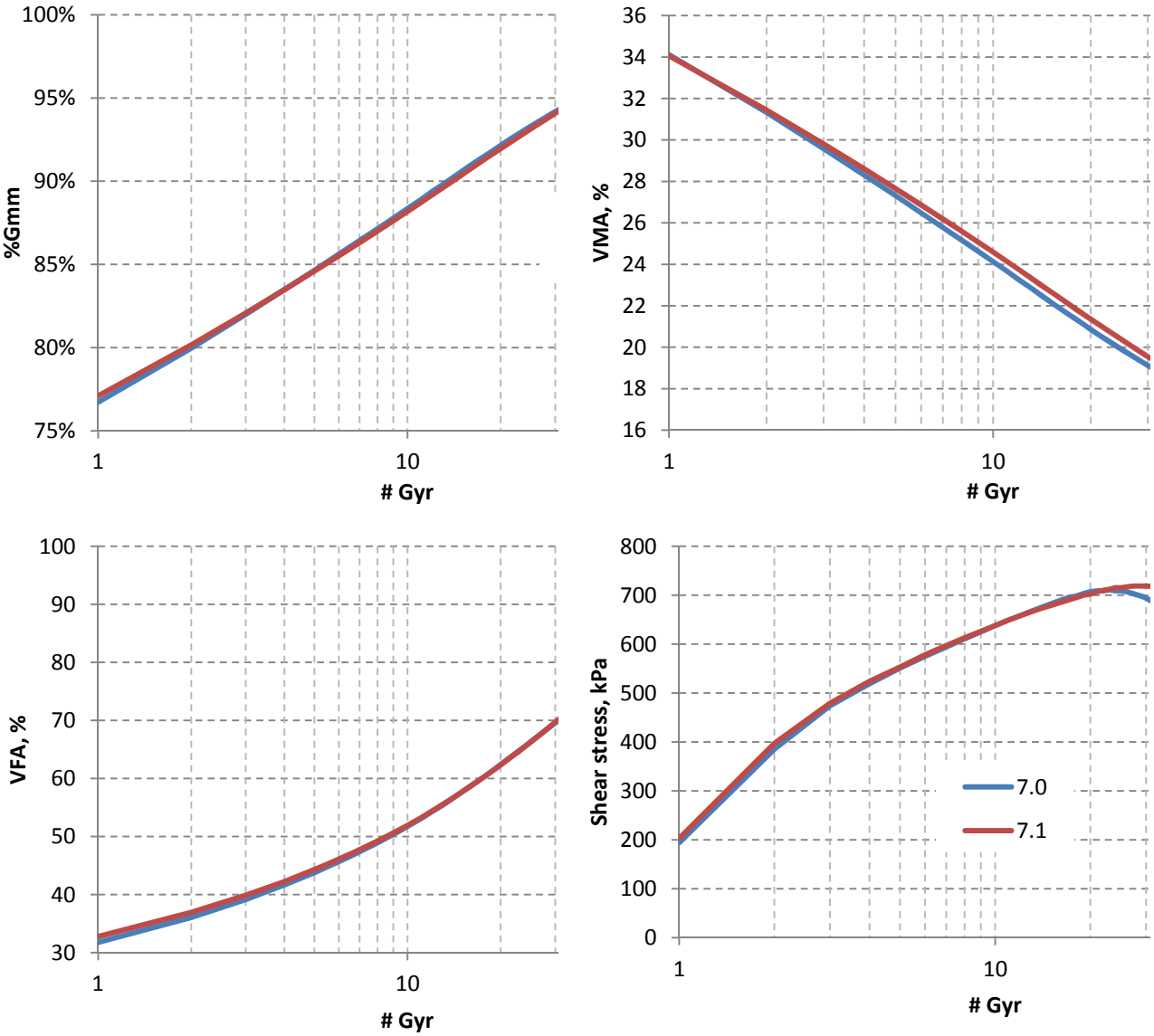

Figure C.10: Volumetric and shear stress properties of 1604 mix

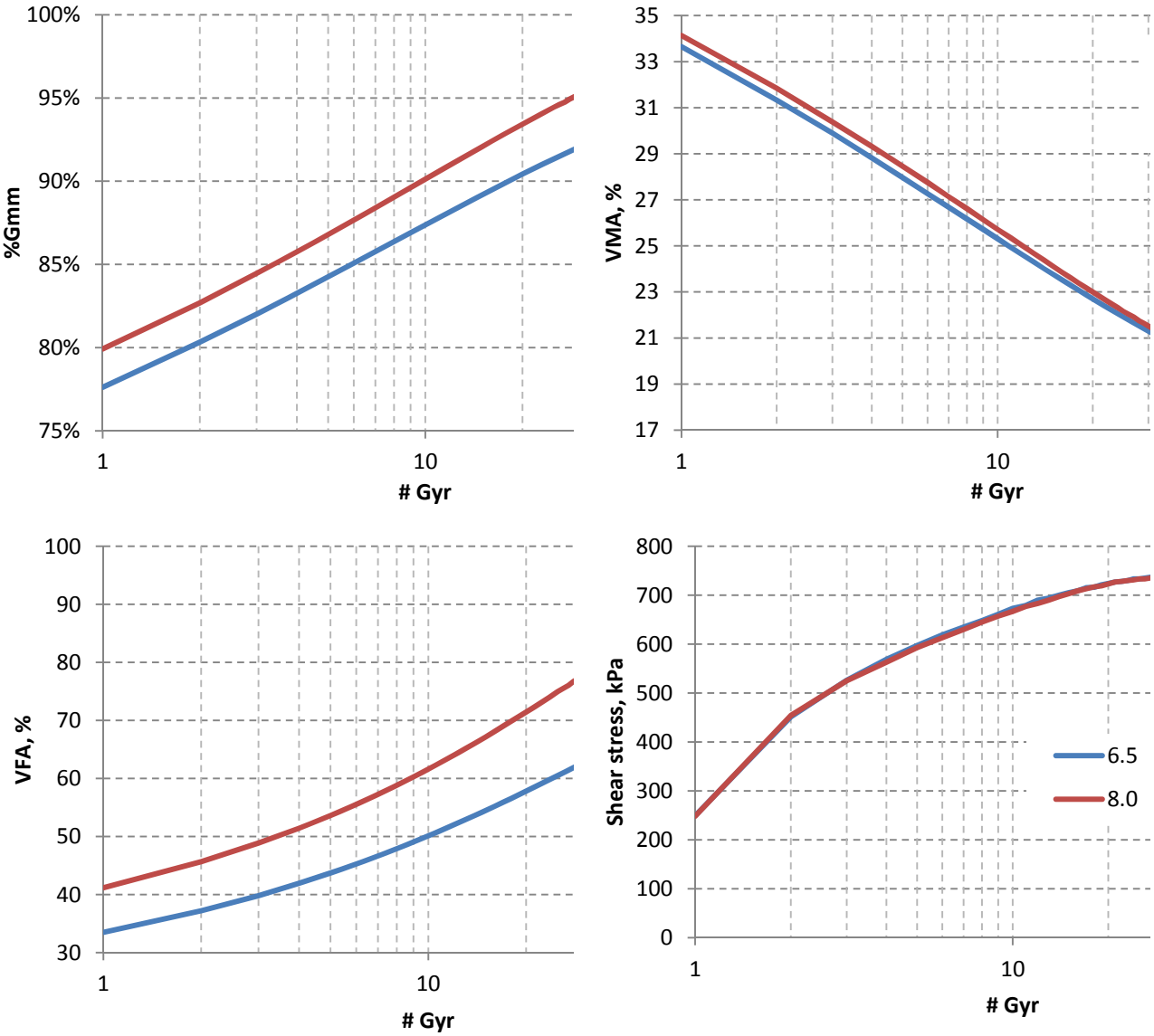

Figure C.11: Volumetric and shear stress properties of Burnet mix

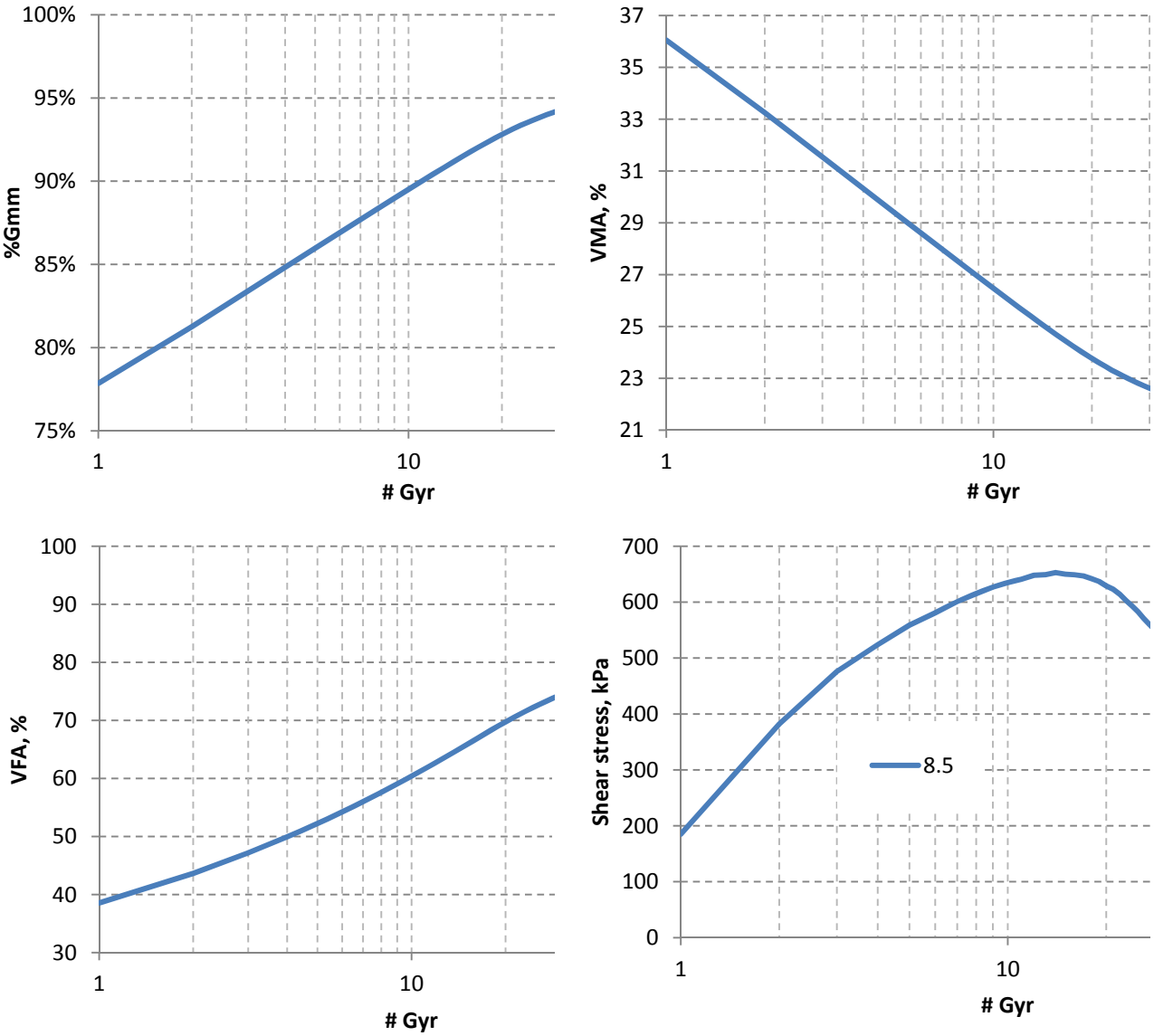

Figure C.12: Volumetric and shear stress properties of Pit 365 mix

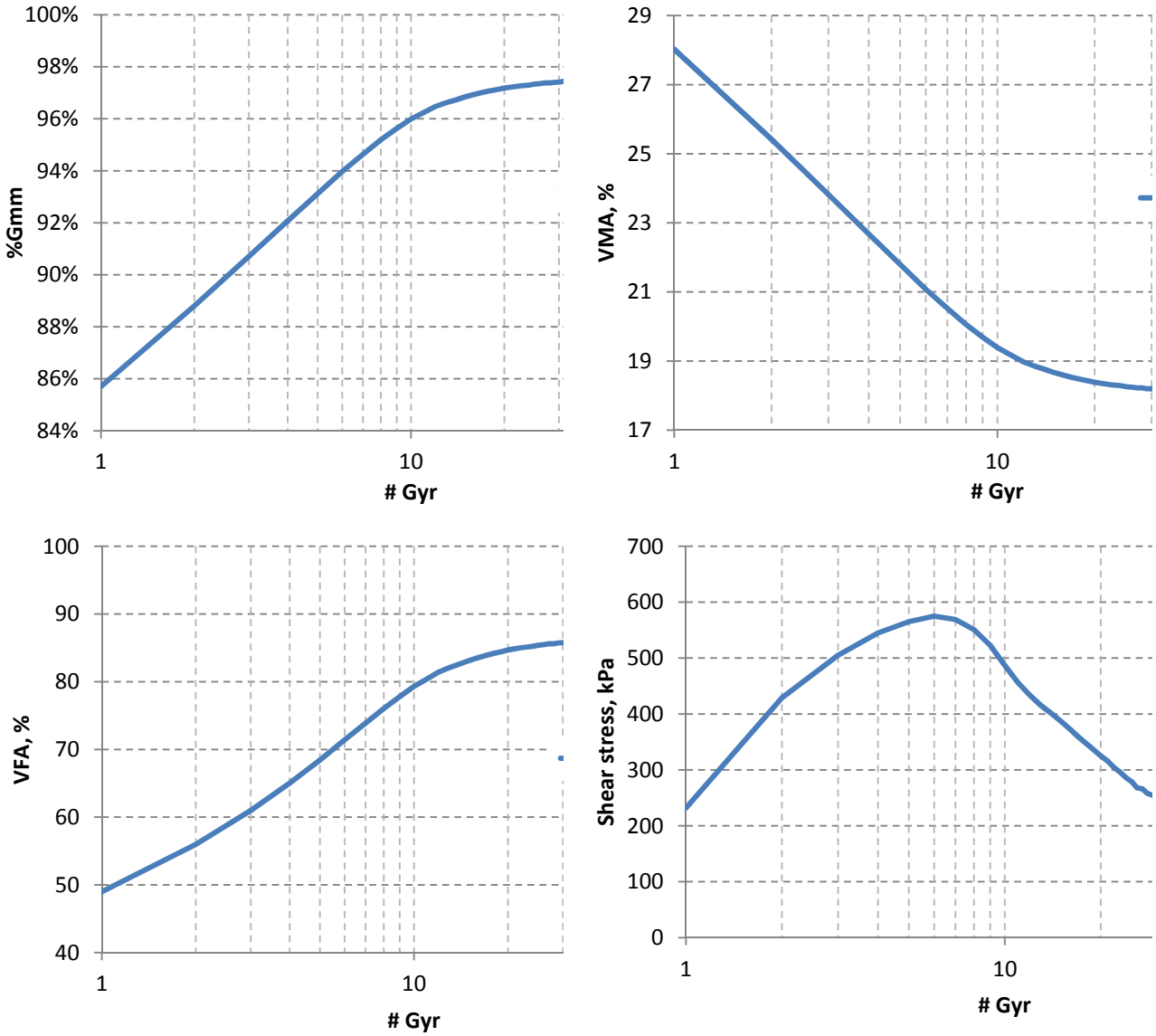

Figure C.13: Volumetric and shear stress properties of Luckett/Tehuacana mix

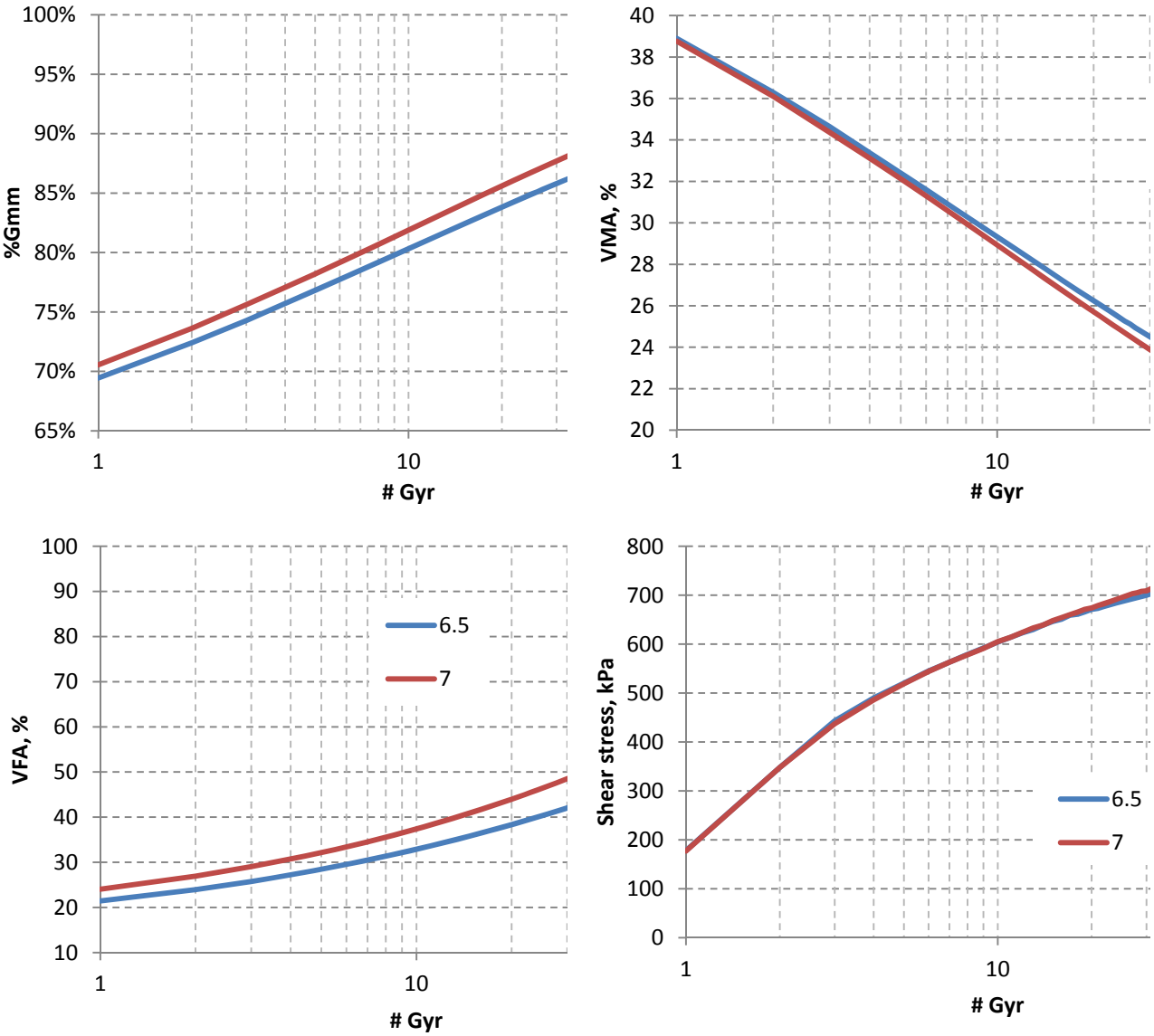

Figure C.14: Volumetric and shear stress properties of Feld/Tehuacana mix

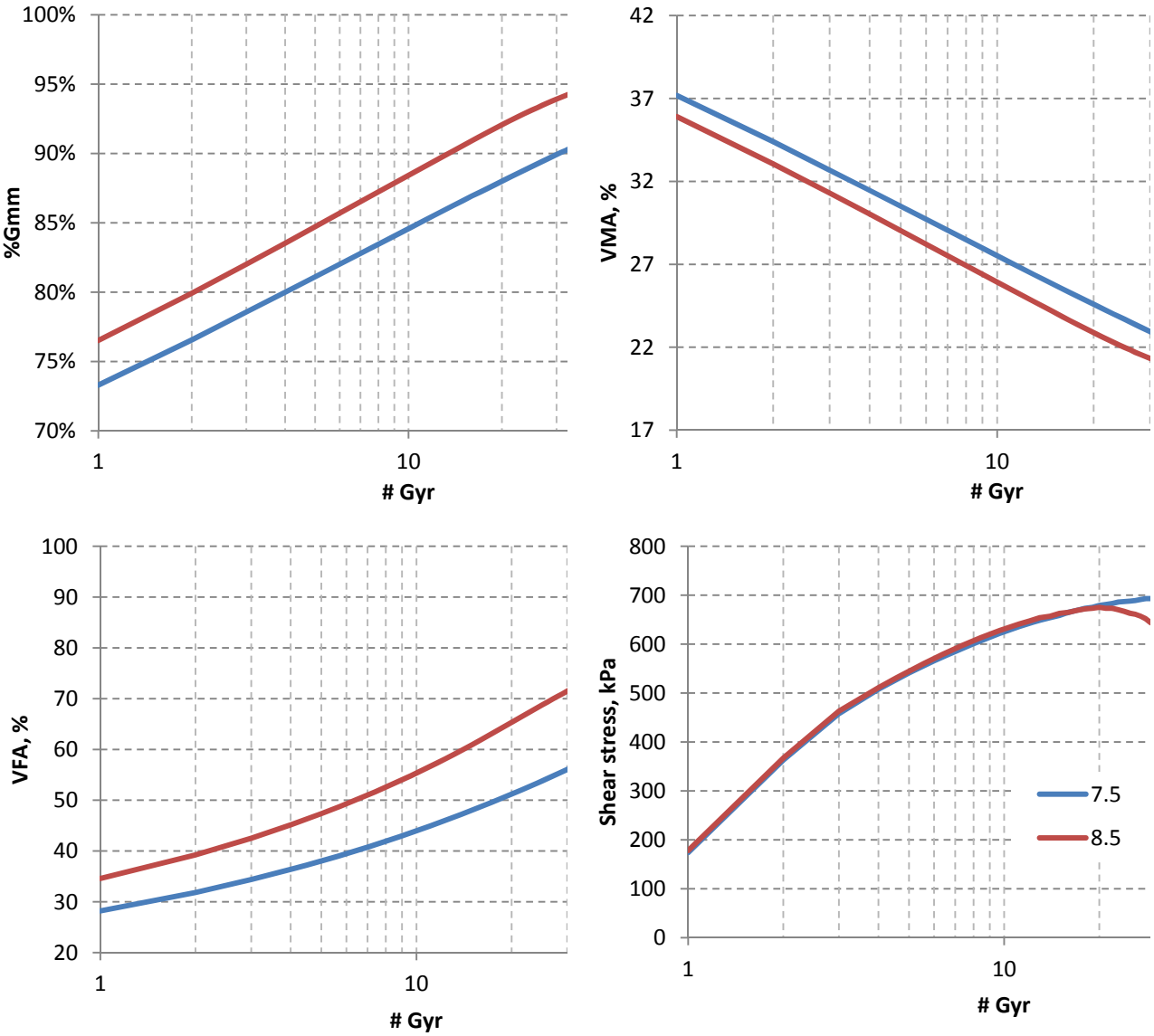

Figure C.15: Volumetric and shear stress properties of Lone Star/Pit 365 mix

Appendix D: HWT Plots

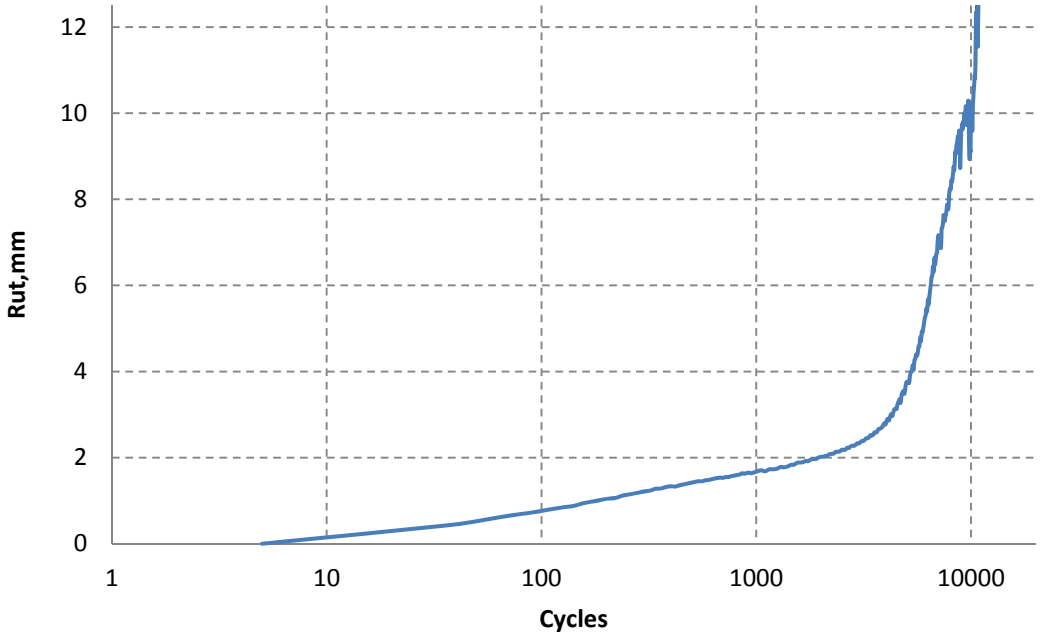

Figure D.1: HWT of Fordyce mix at 6% AC

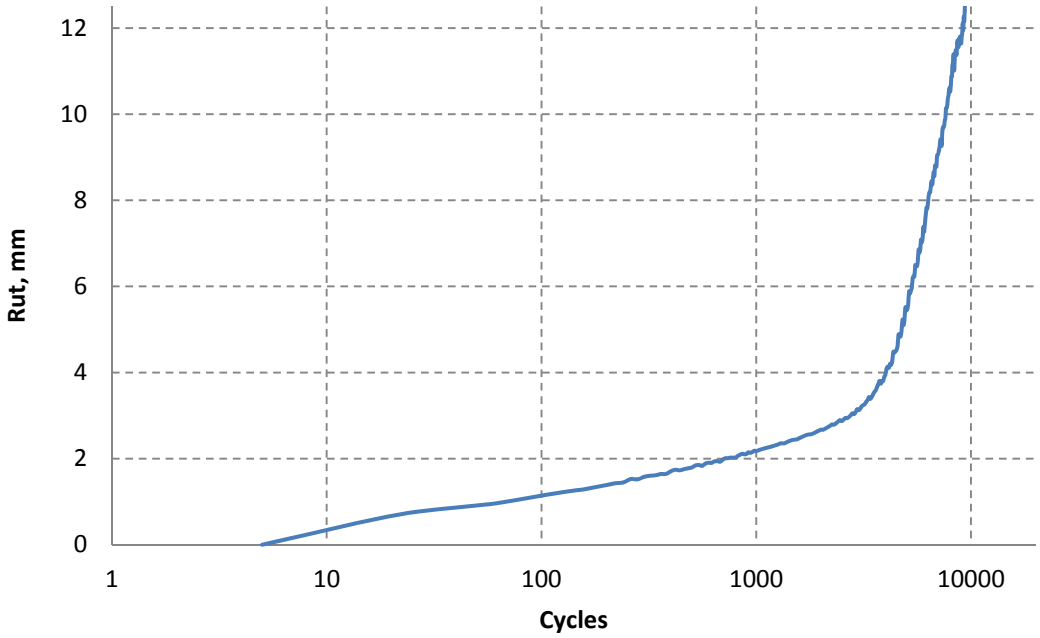

Figure D.2: HWT of Fordyce mix at 7% AC

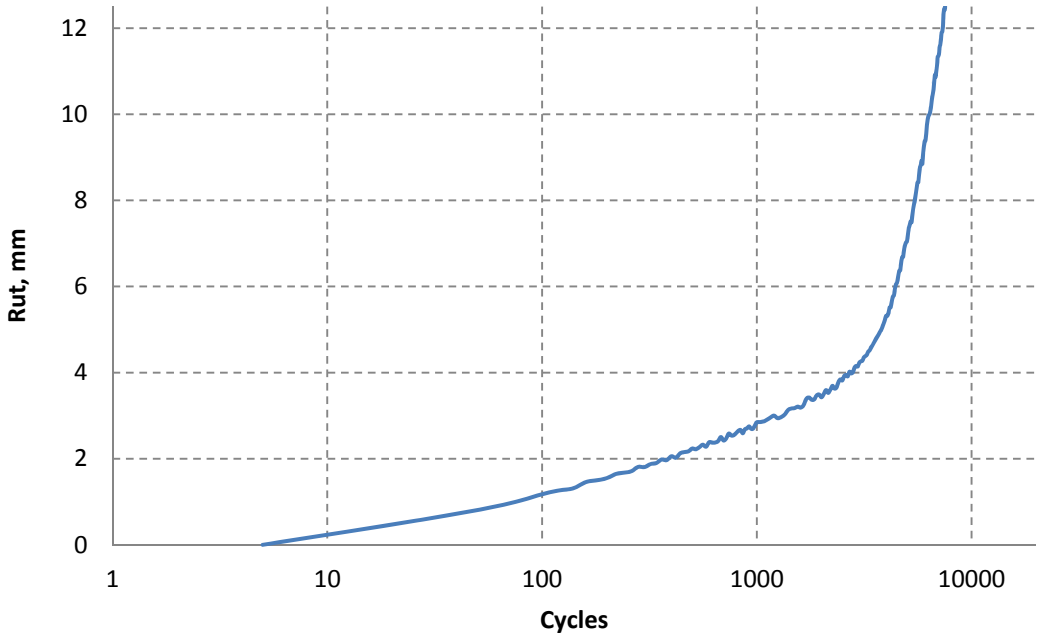

Figure D.3: HWT of Fordyce mix at 8% AC

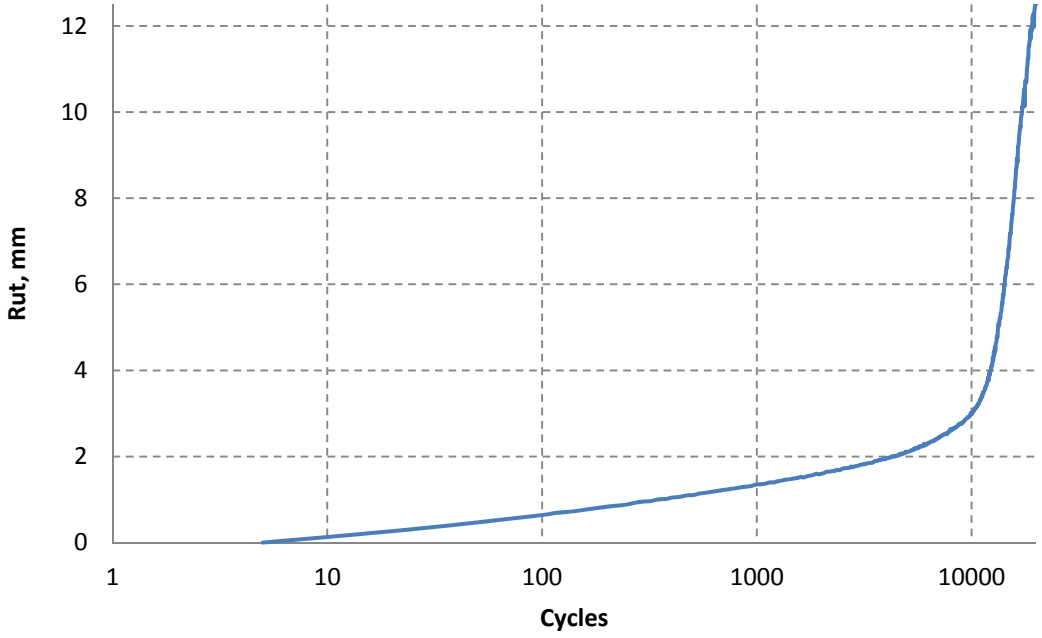

Figure D.4: HWT of Marble Falls I at 6% AC

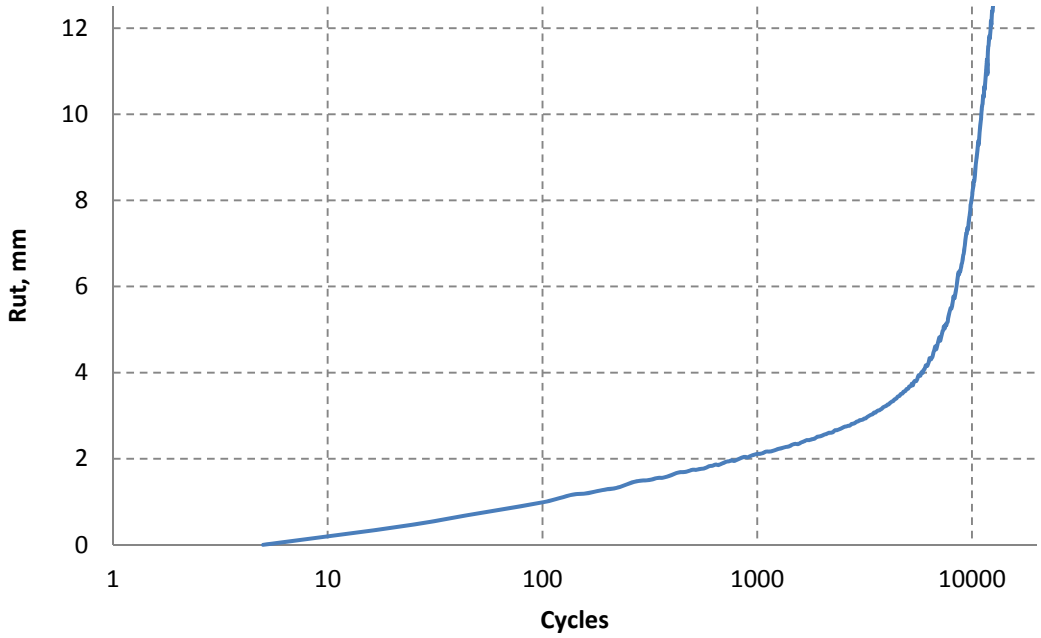

Figure D.5: HWT of Marble Falls I at 7% AC

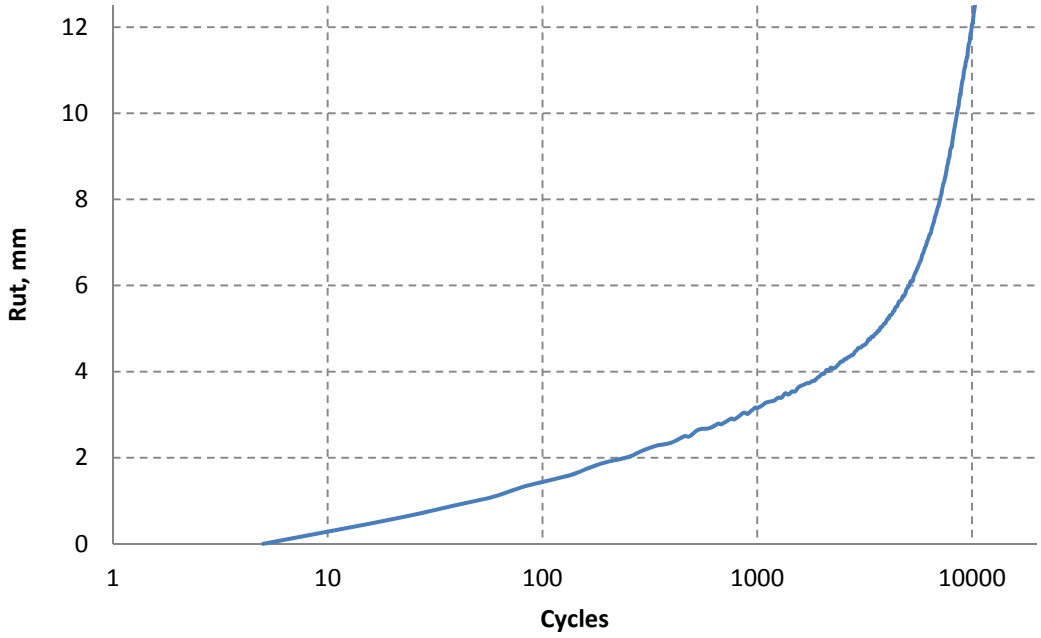

Figure D.6: HWT of Marble Falls I at 8% AC

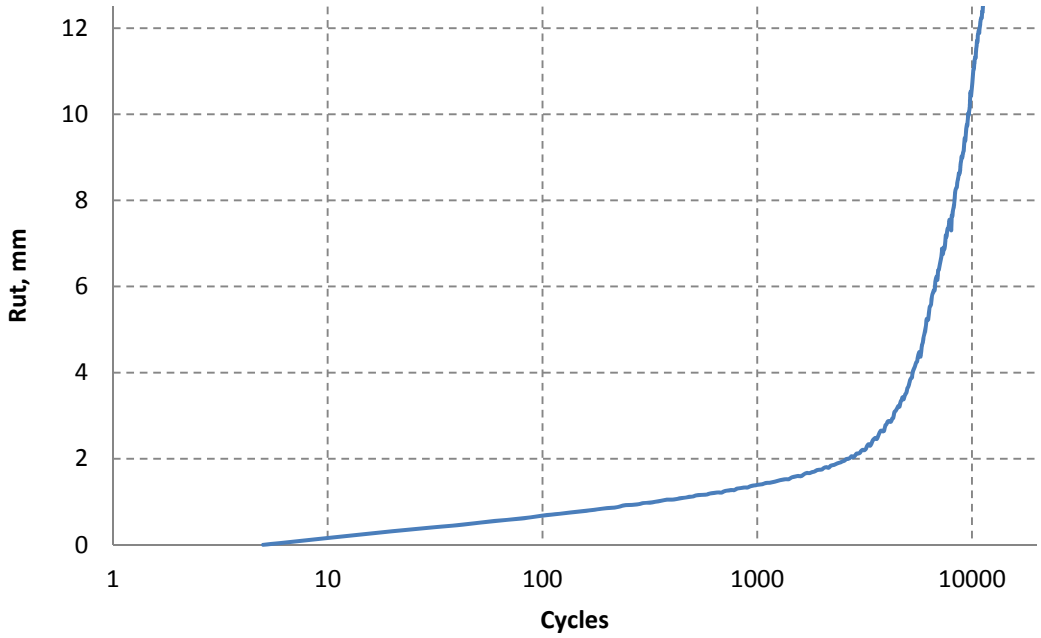

Figure D.7: HWT of Beckmann at 6% AC

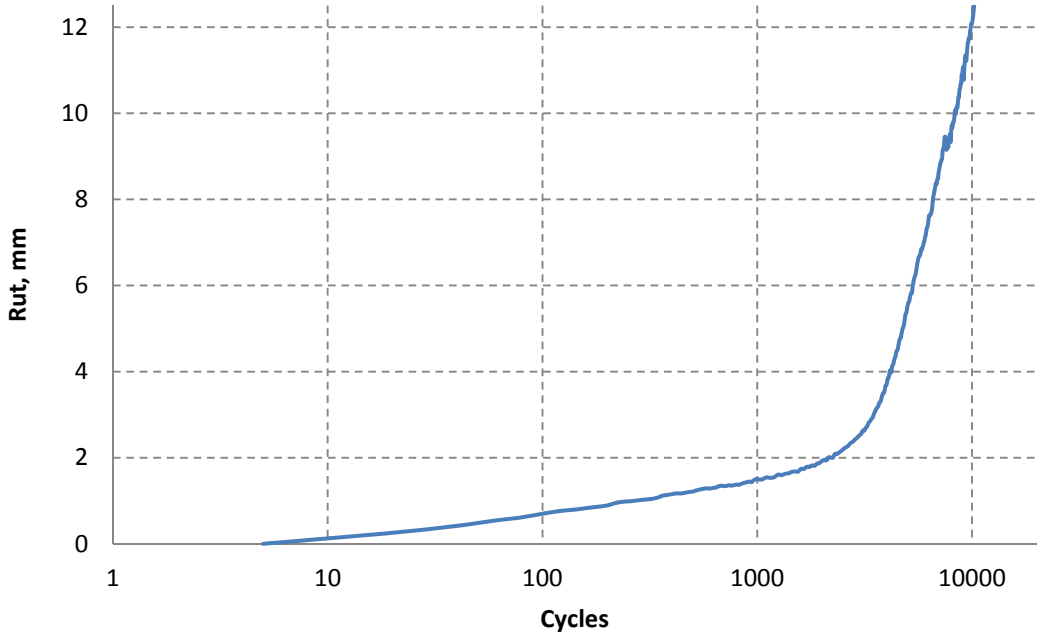

Figure D.8: HWT of Beckmann at 7% AC

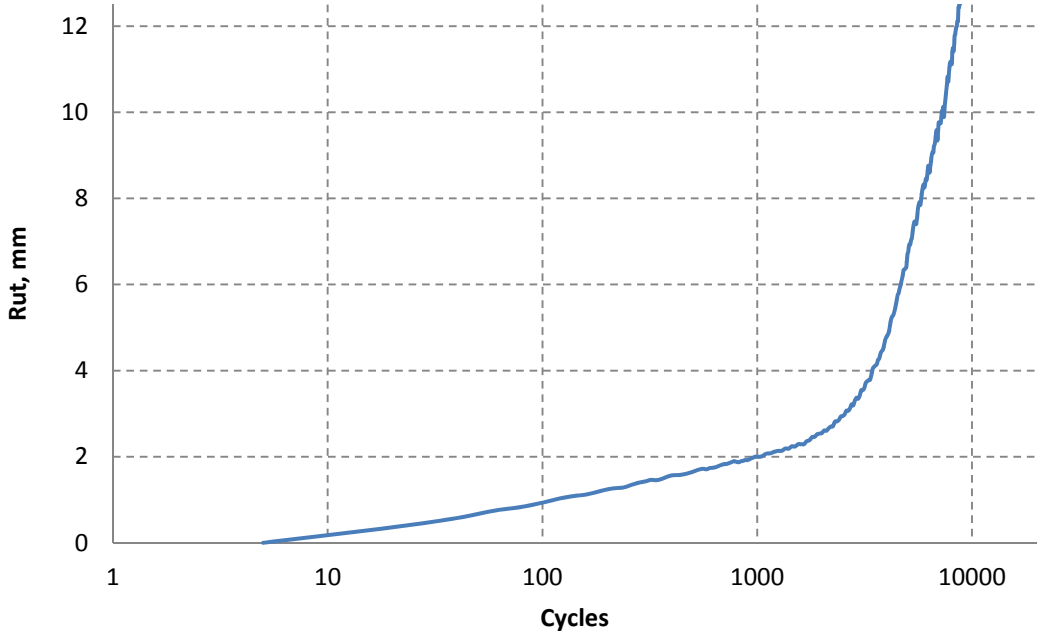

Figure D.9: HWT of Beckmann at 8% AC

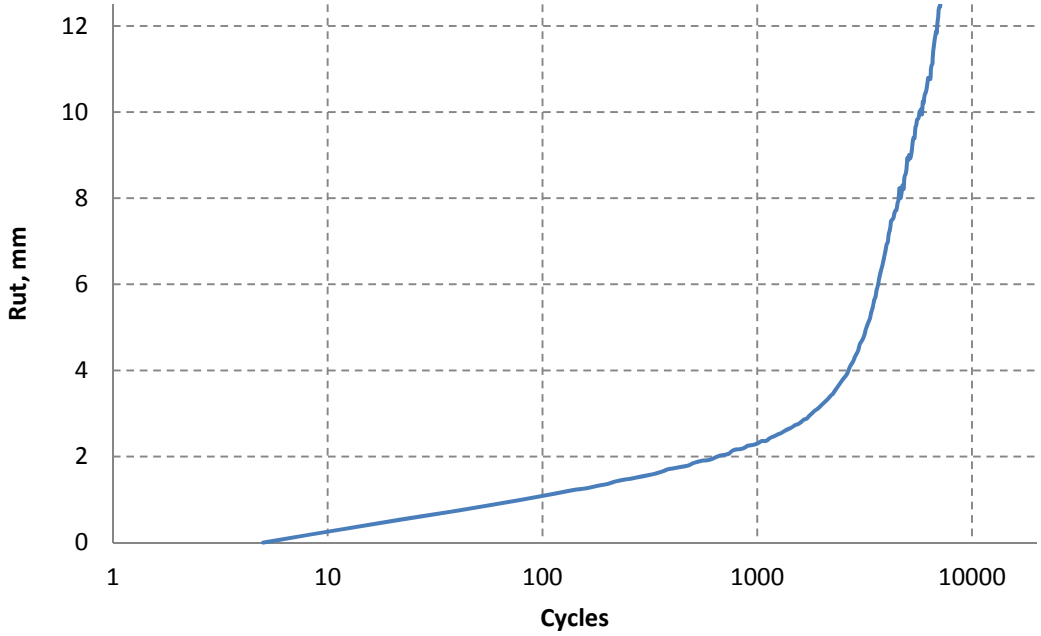

Figure D.10: HWT of Solms Road at 7.2% AC

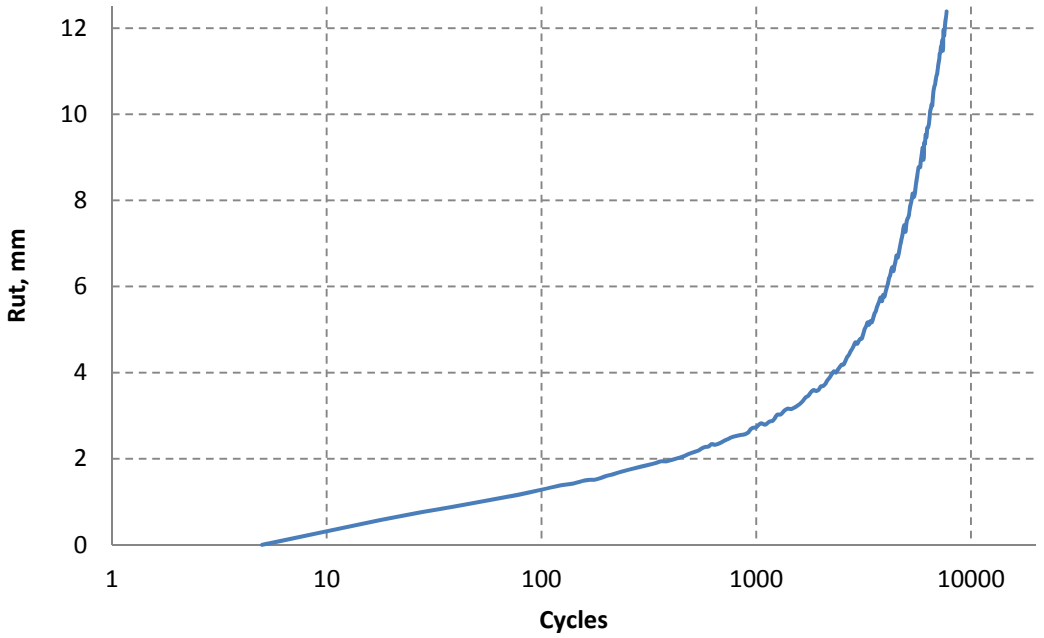

Figure D.11: HWT of Spicewood at 7.1% AC

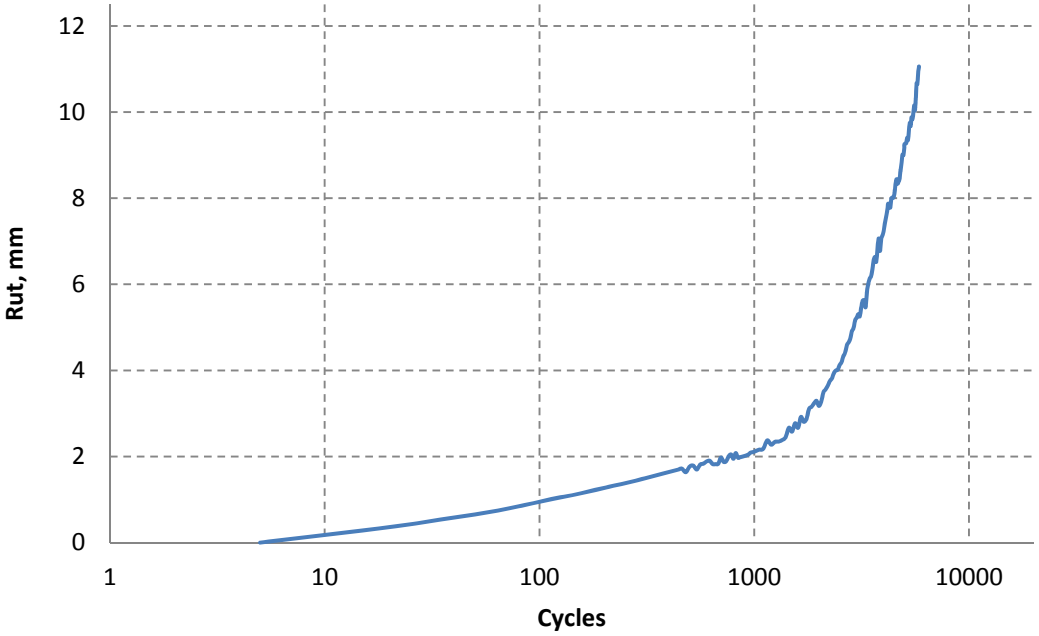

Figure D.12: HWT of RTI at 8.4% AC

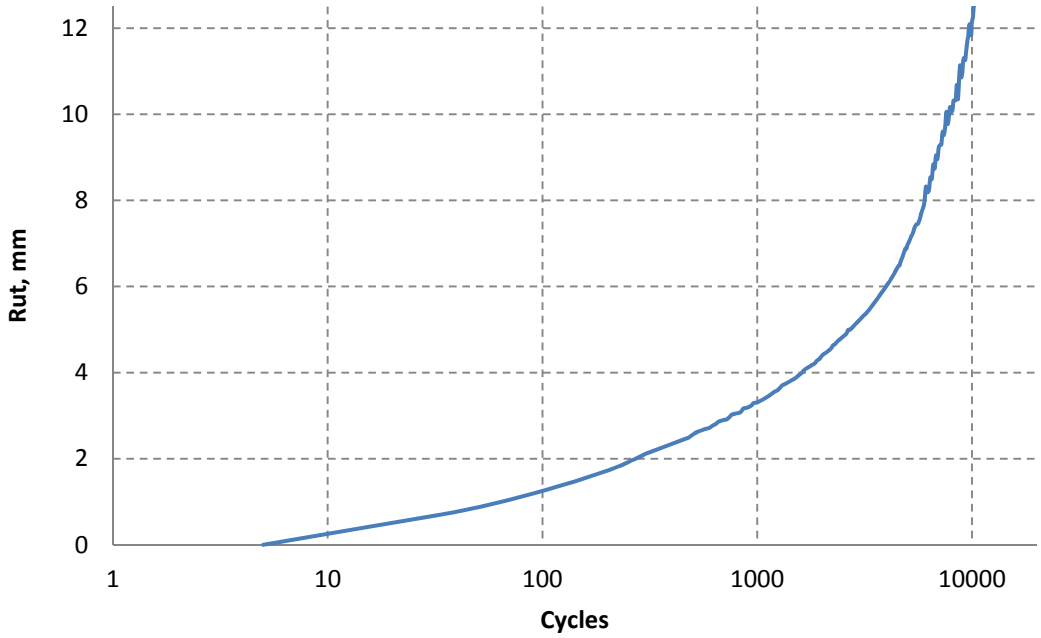

Figure D.13: HWT of Luckett/Tehuacana at 7.3% AC

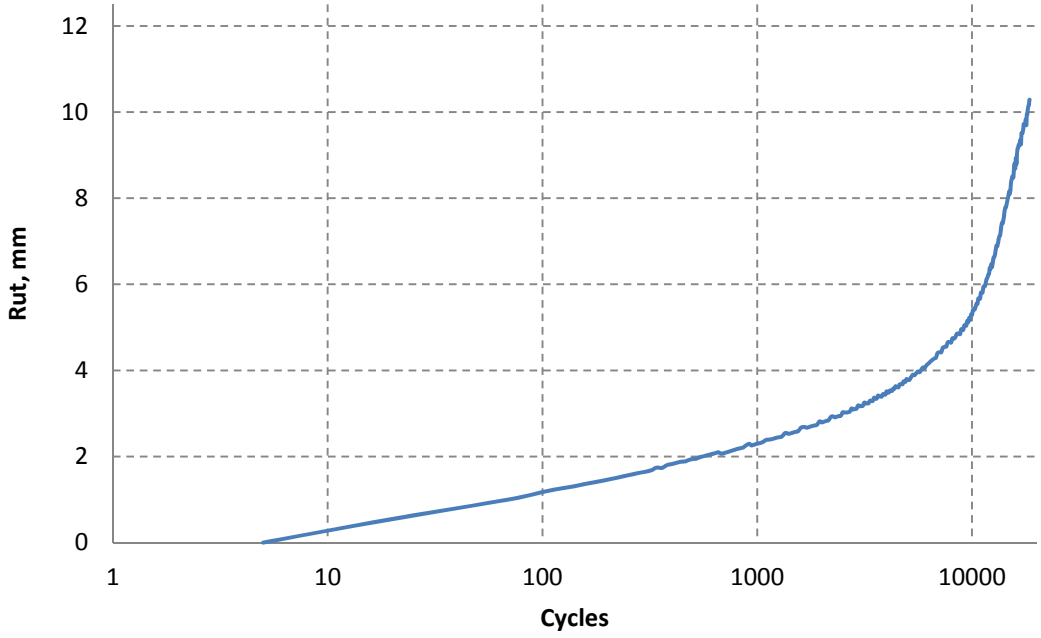

Figure D.14: HWT of Burnet at 7.6% AC

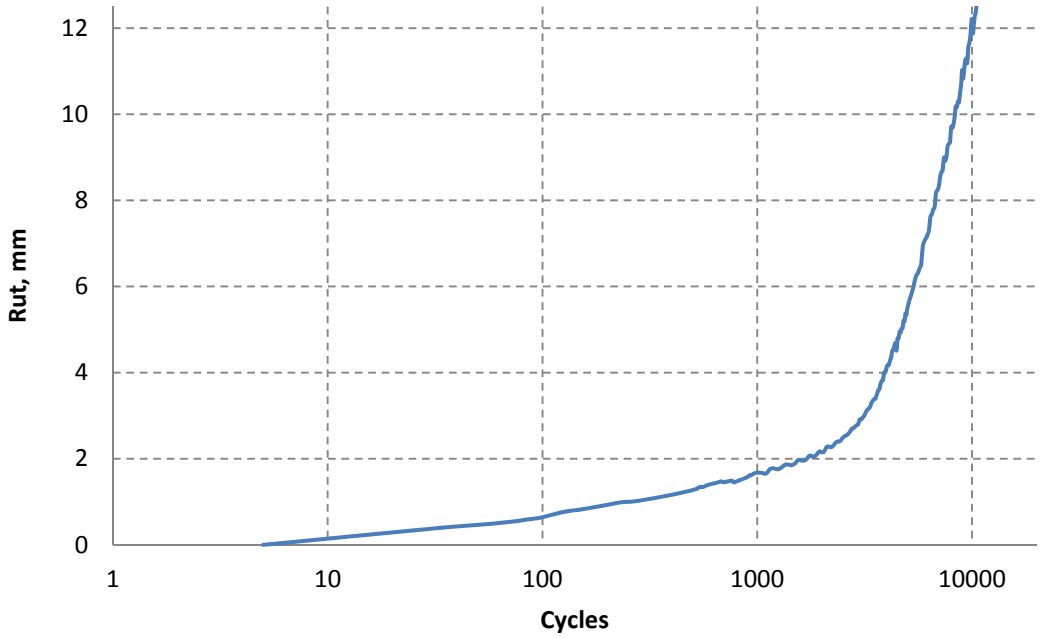

Figure D.15: HWT of 1604 at 7.1% AC

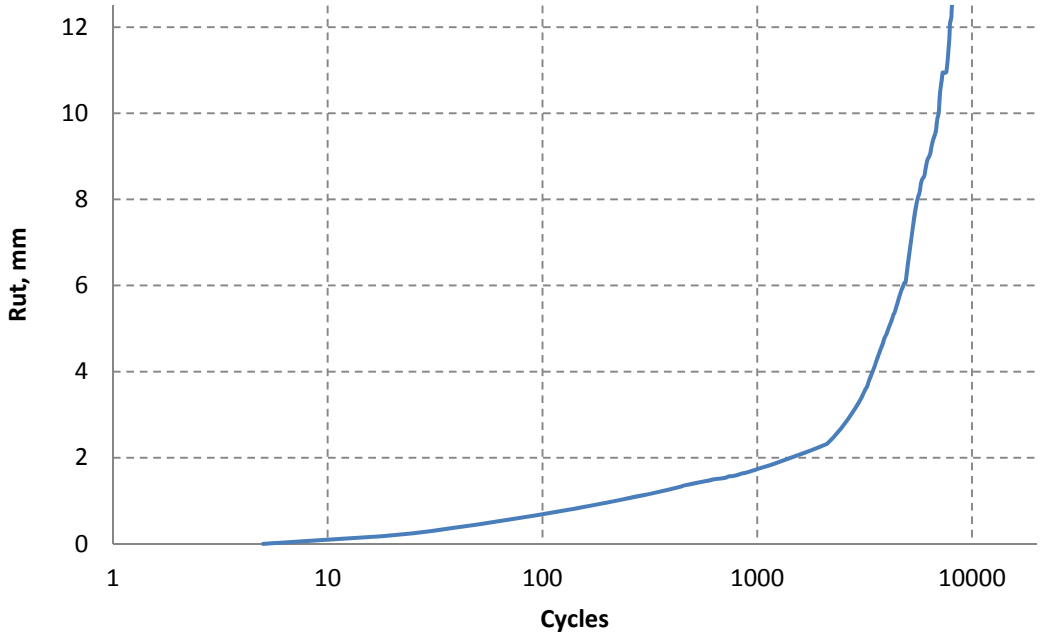

Figure D.16: HWT of Lattimore at 7.8% AC

Appendix E: Aggregate Properties vs. Performance Correlation Plots

Los Angeles Abrasion

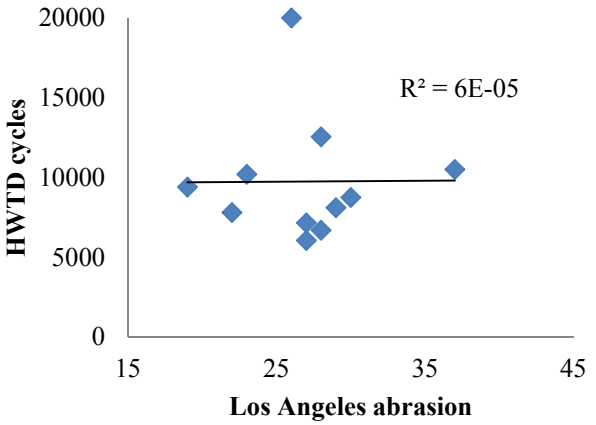

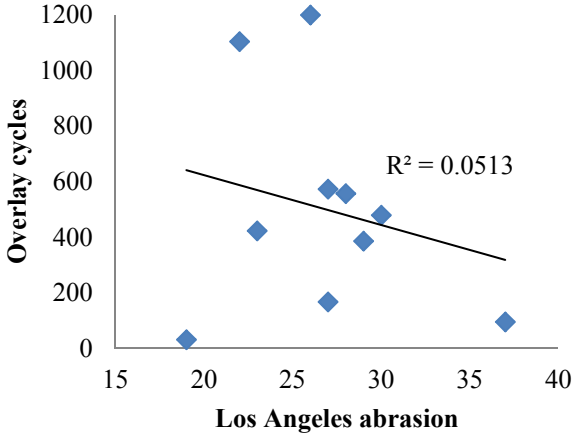

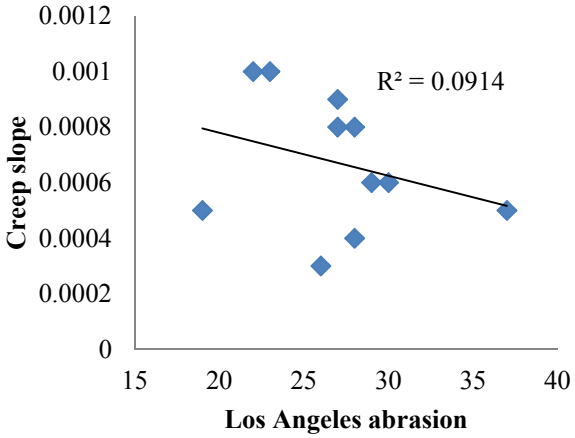

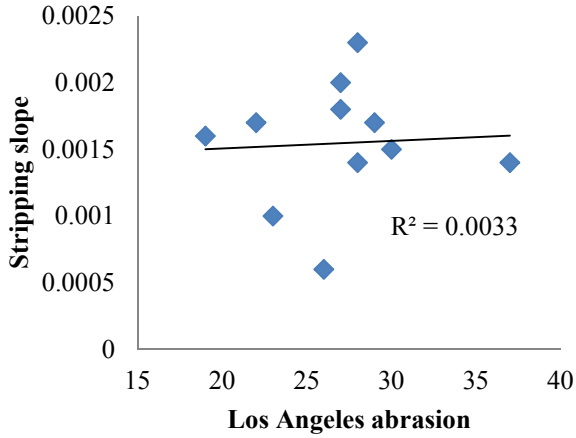

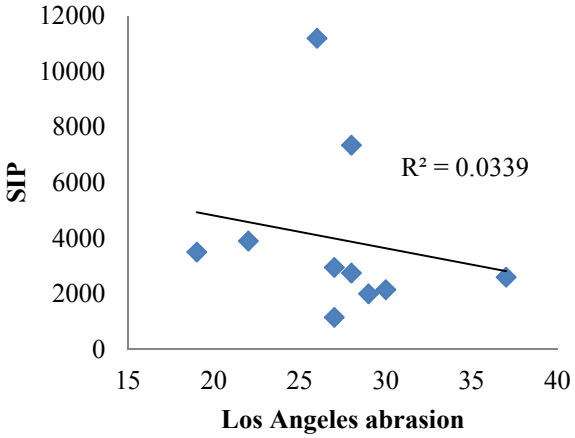

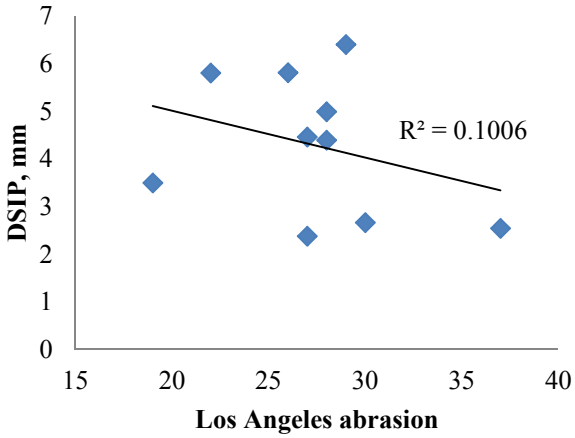

Magnesium soundness

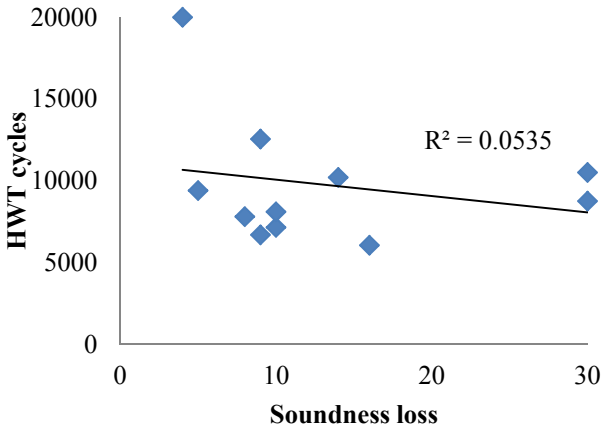

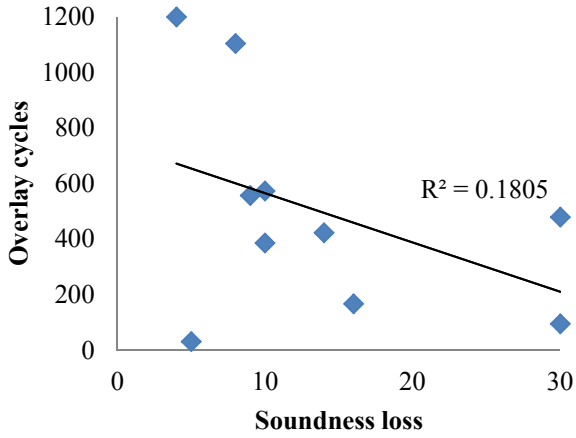

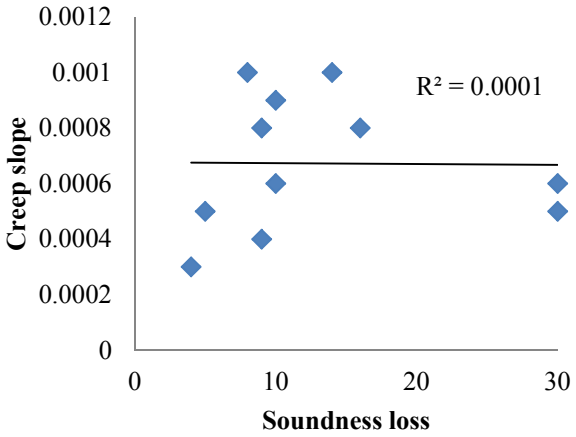

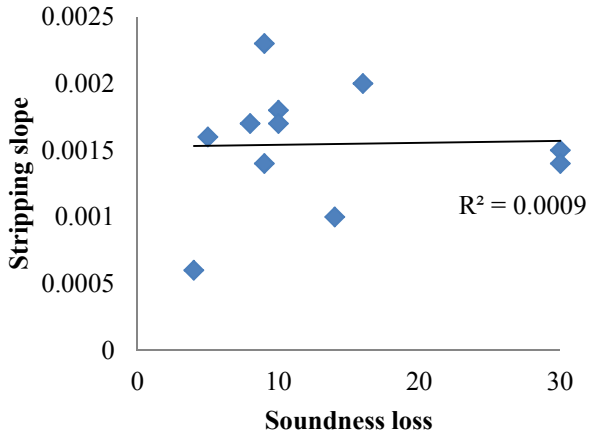

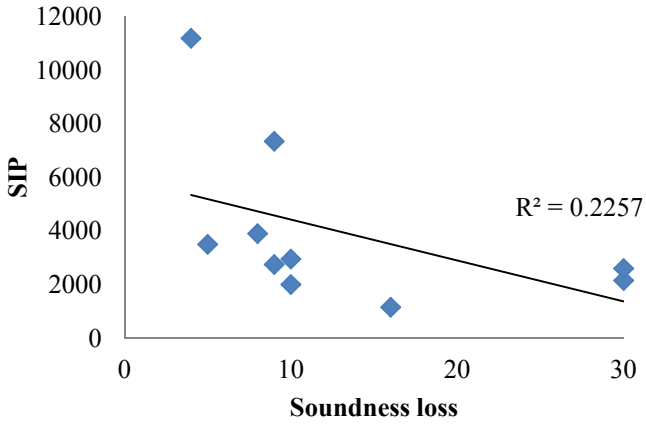

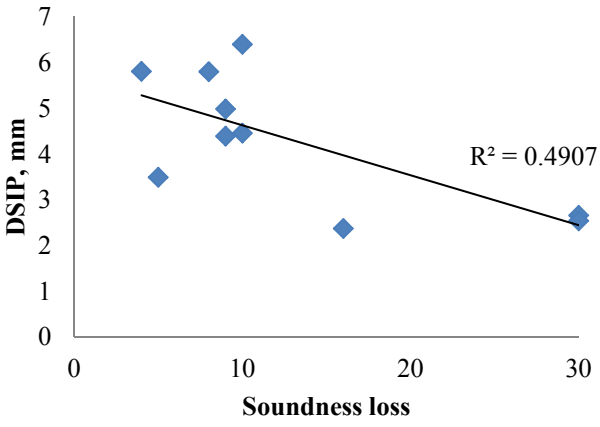

Micro-Deval

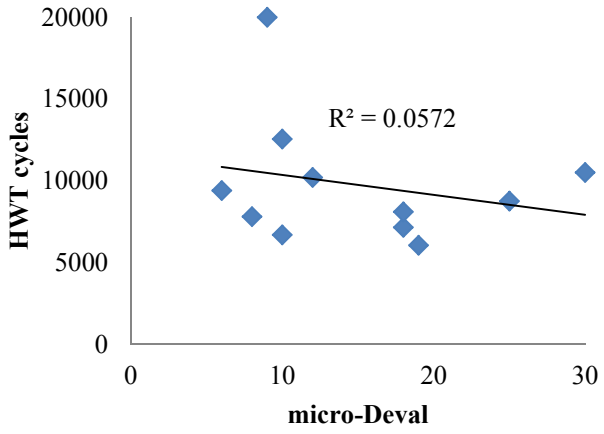
HWT cycles
micro-Deval
R² = 0.0572
20000
15000
10000
5000
0
0
10
20
30

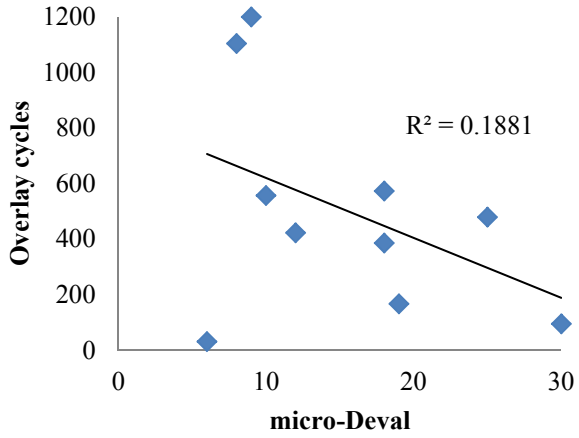
Overlay cycles
micro-Deval
R² = 0.1881
1200
1000
800
600
400
200
0
0
10
20
30

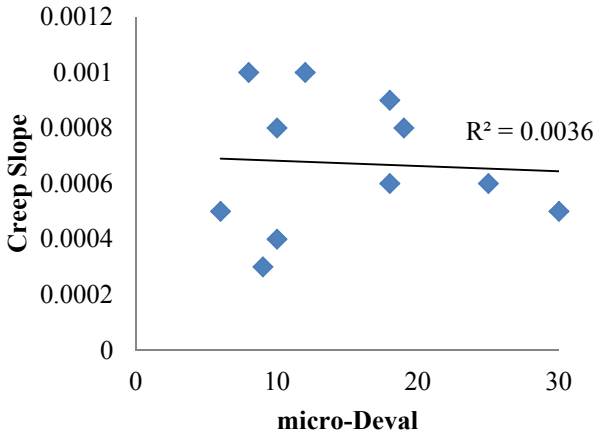
Creep Slope
micro-Deval
R² = 0.0036
0.0012
0.001
0.0008
0.0006
0.0004
0.0002
0
0
10
20
30

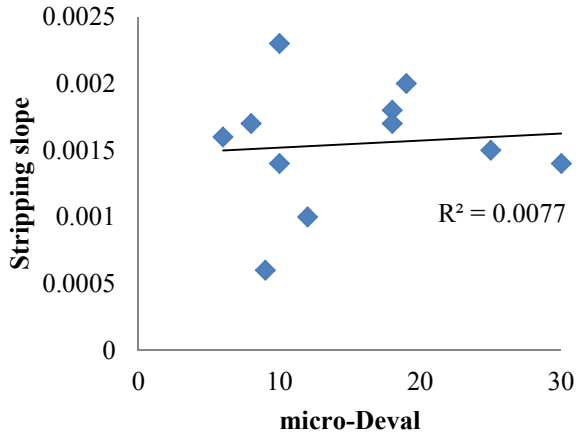
Stripping slope
micro-Deval
R² = 0.0077
0.0025
0.002
0.0015
0.001
0.0005
0
0
10
20
30

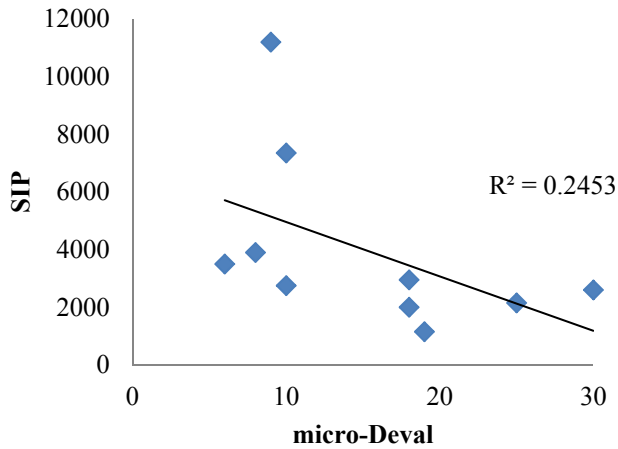
SIP
micro-Deval
R² = 0.2453
12000
10000
8000
6000
4000
2000
0
0
10
20
30

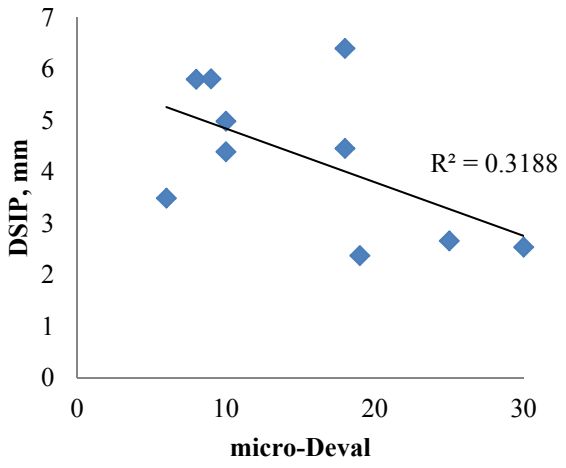
DSIP, mm
micro-Deval
R² = 0.3188
7
6
5
4
3
2
1
0
0
10
20
30

Acid Insolubility

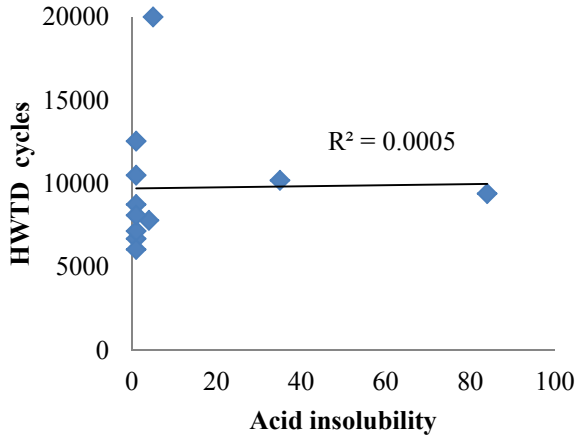

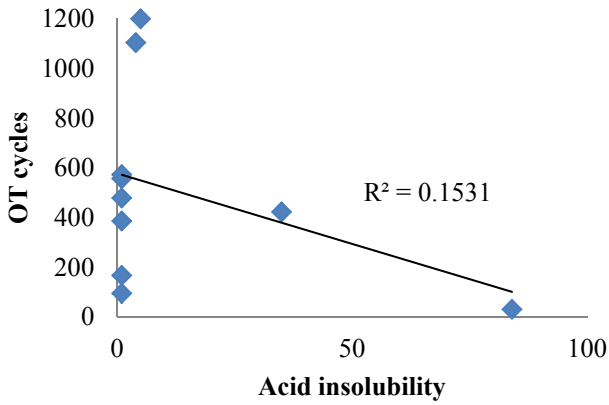

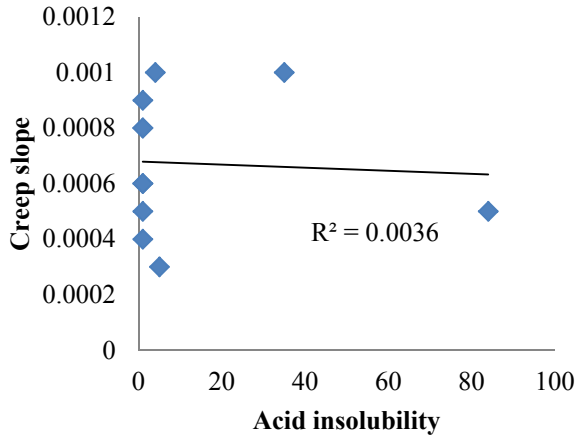

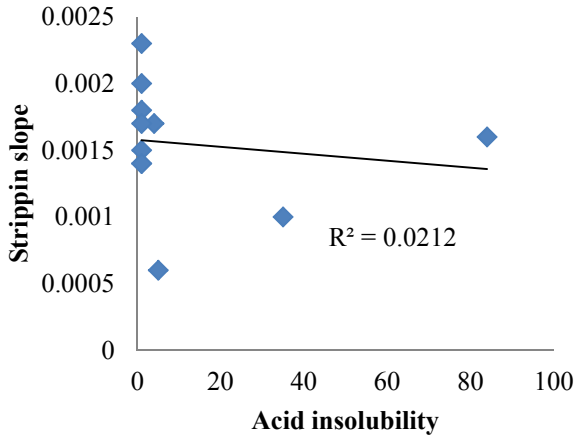

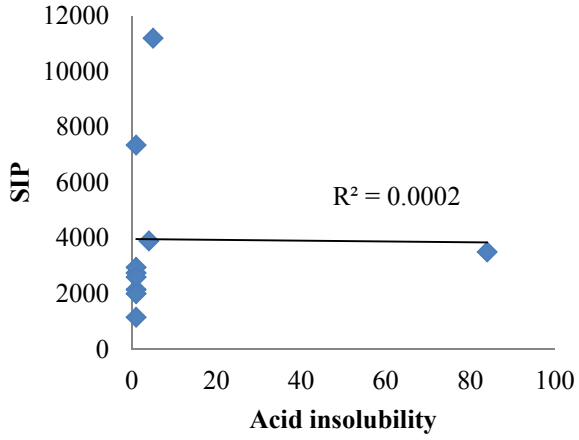

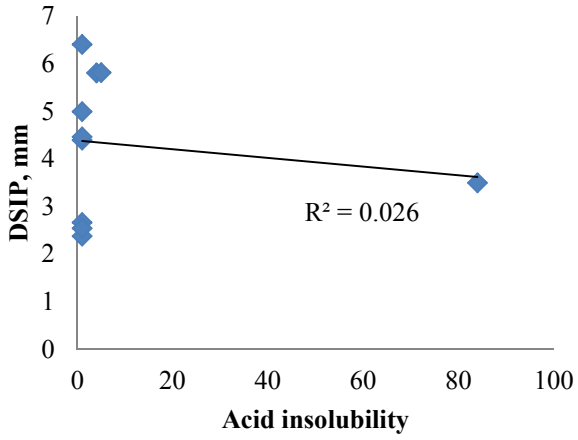

AIMS sphericity

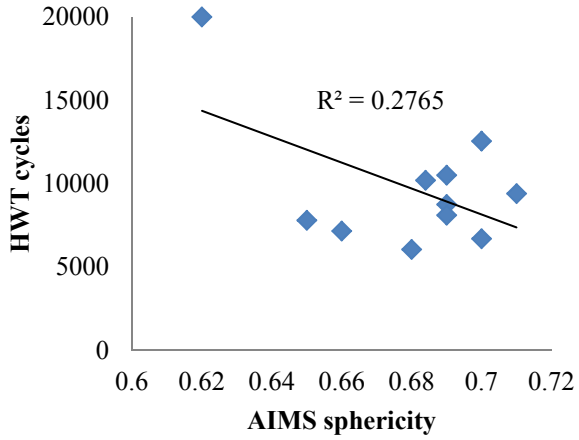

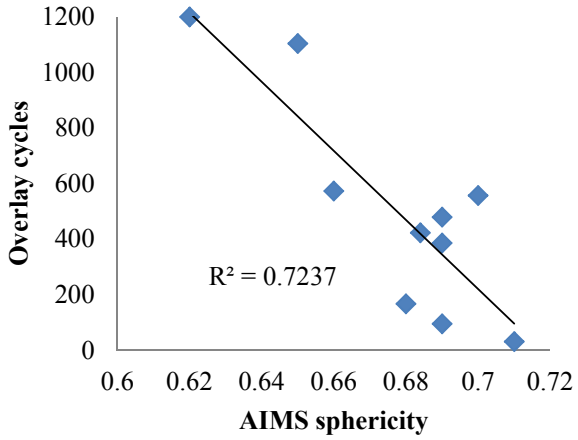

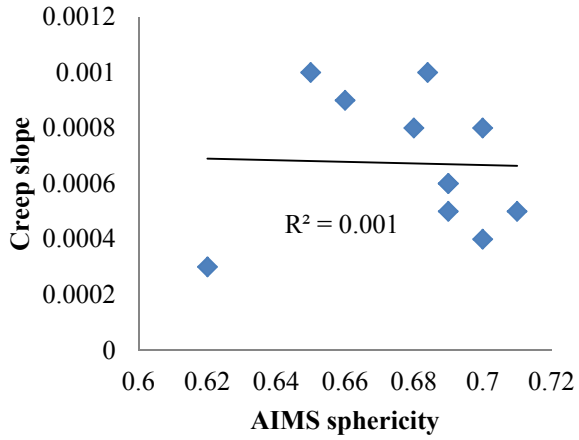

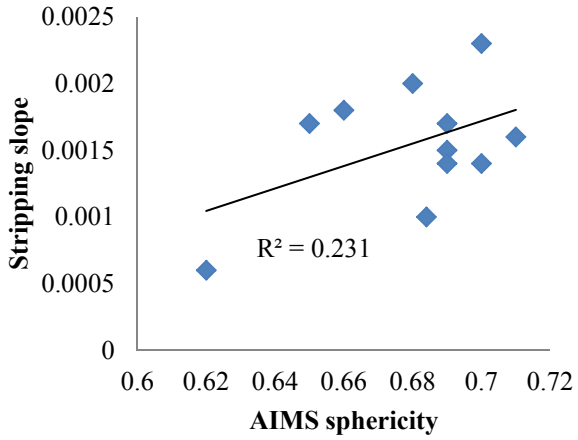

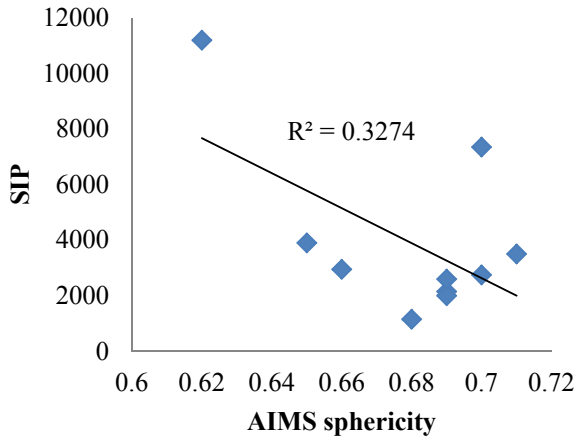

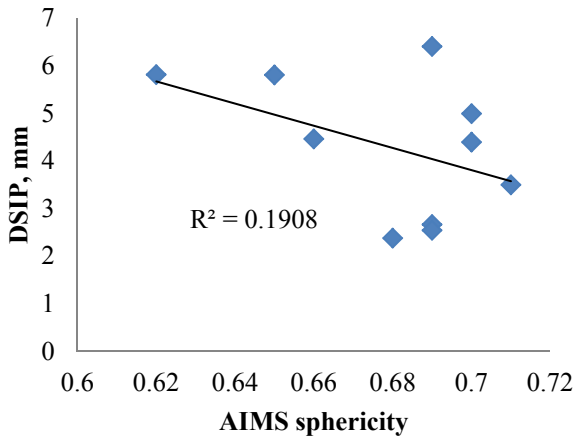

AIMS surface texture (coarse aggregate)

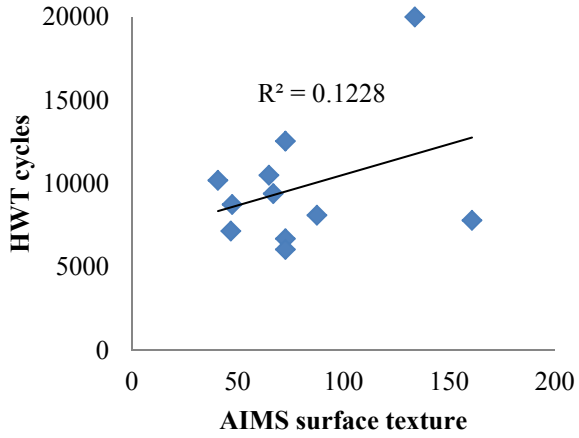

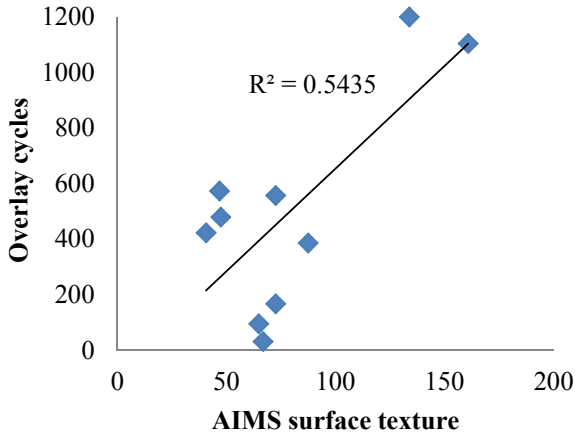

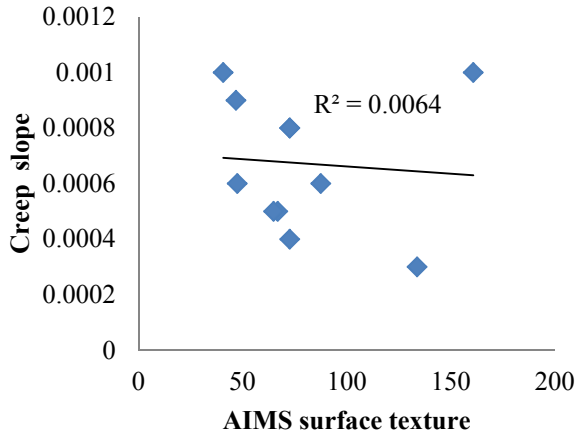

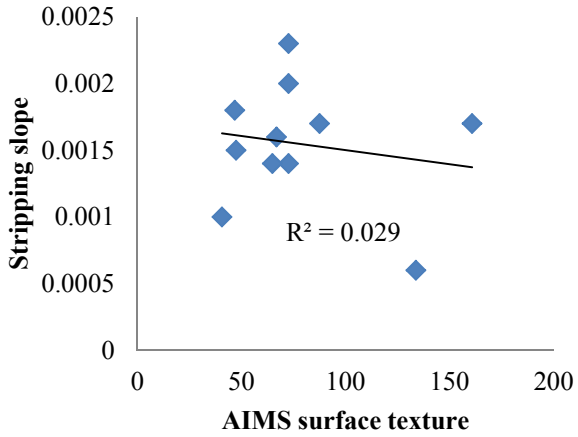

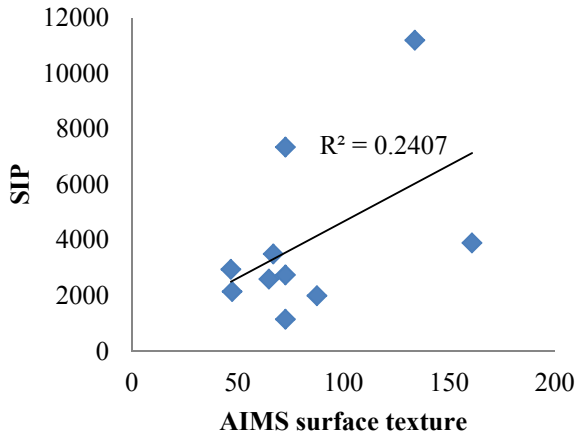

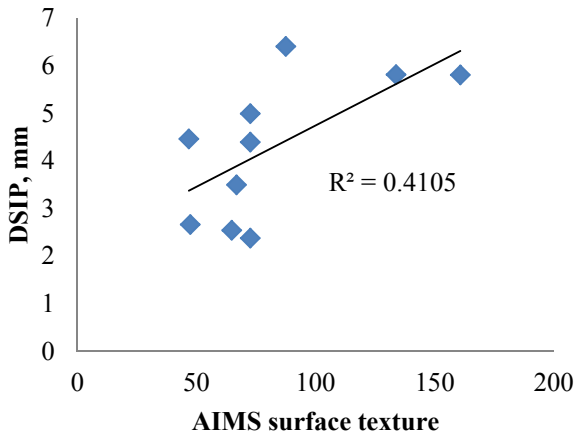

AIMS angularity (coarse aggregate)

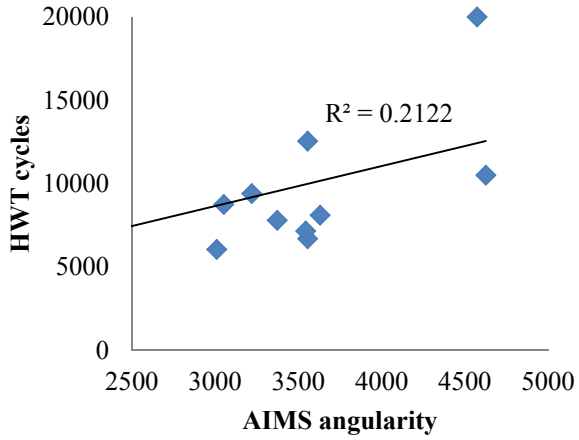

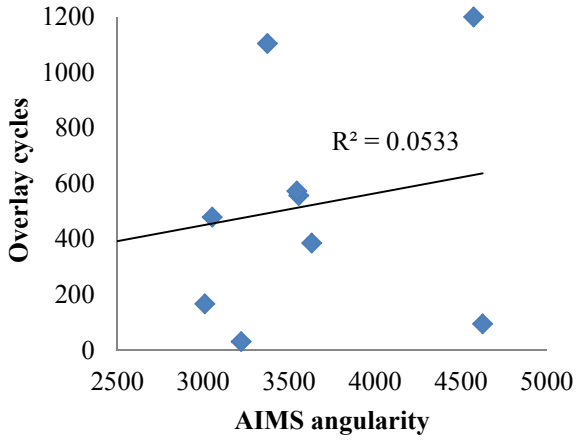

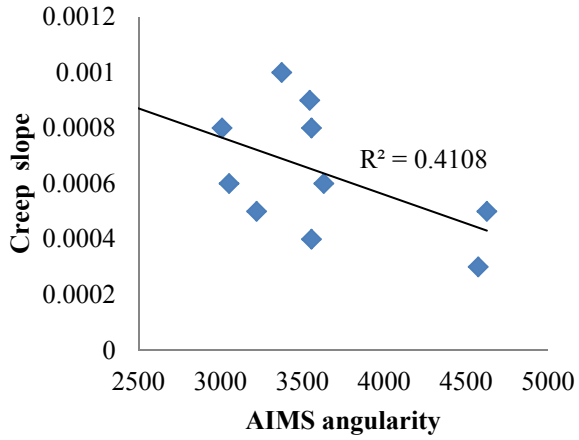

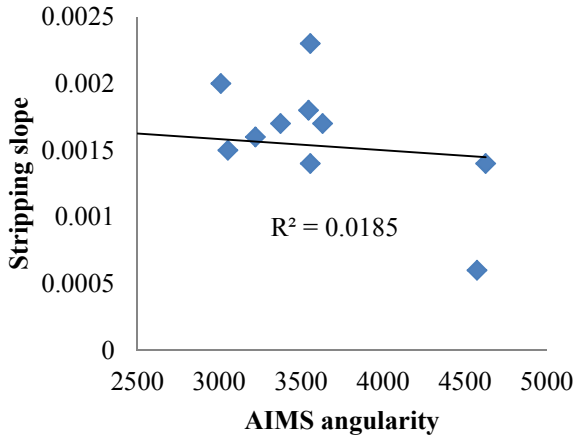

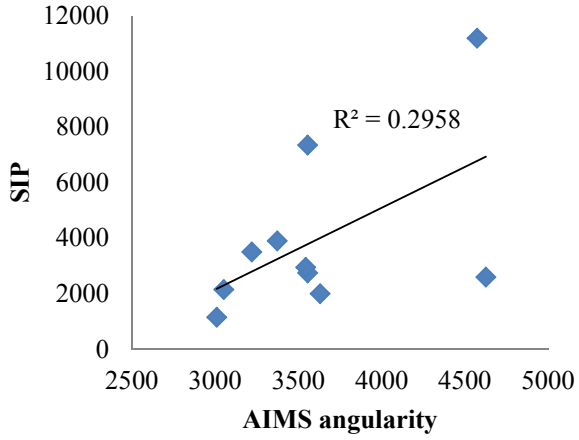

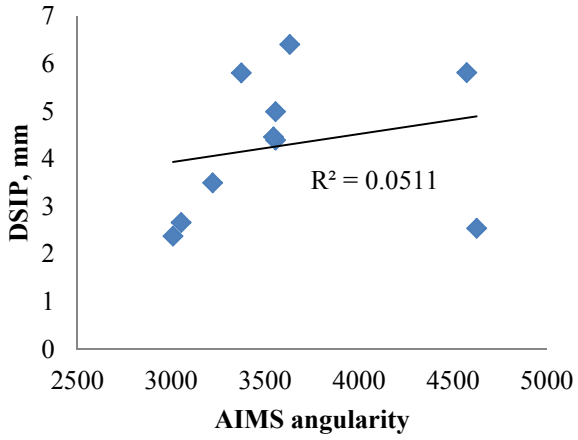

AIMS fine aggregate angularity

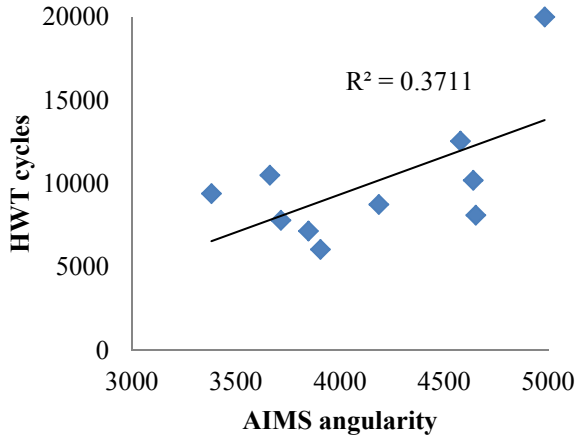

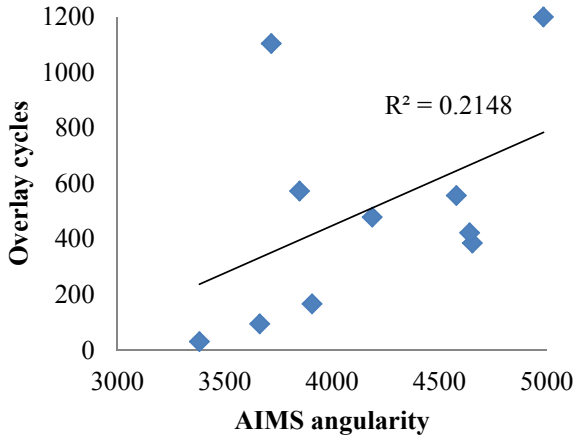

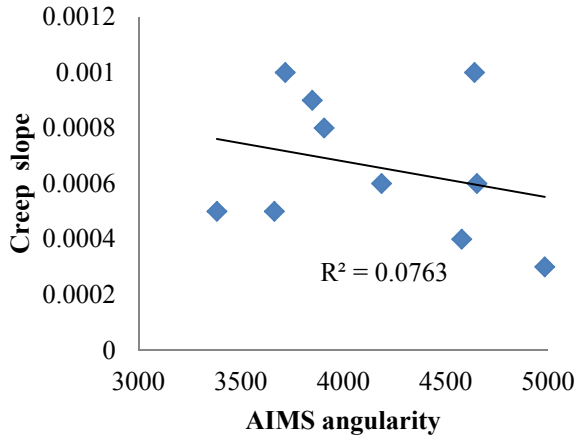

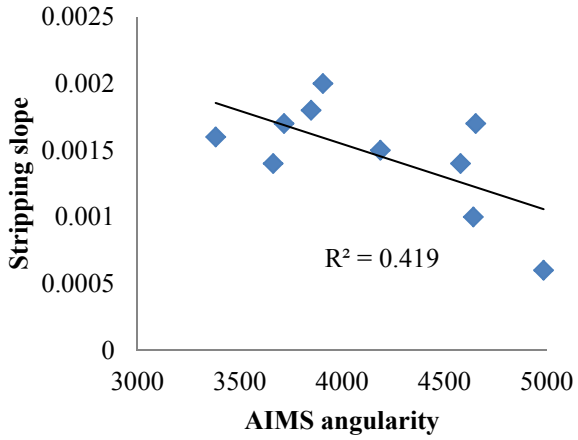

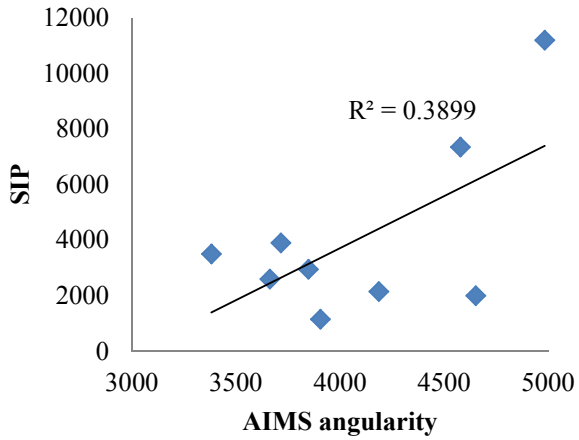

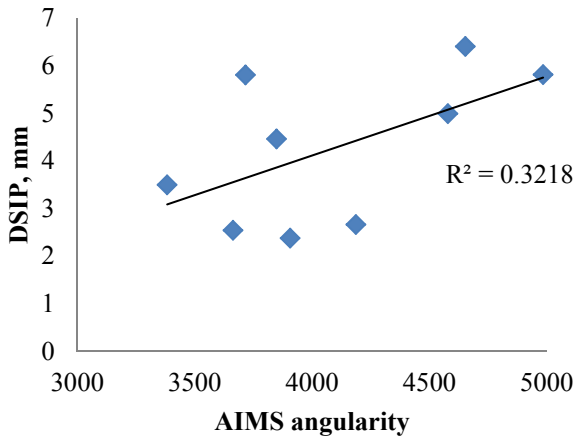

Superpave fine aggregate angularity (FAA)

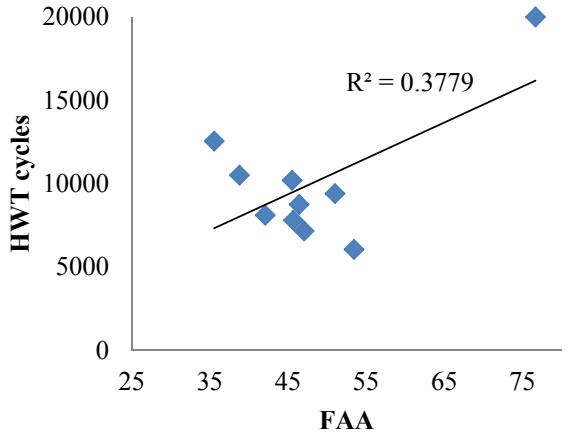

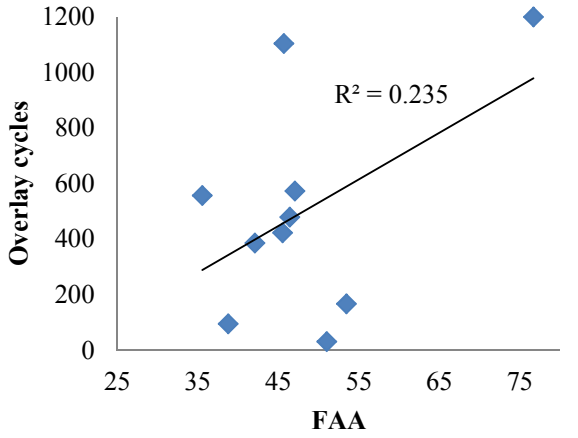

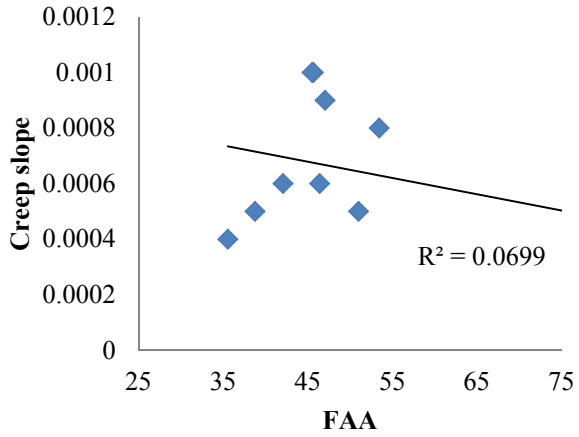

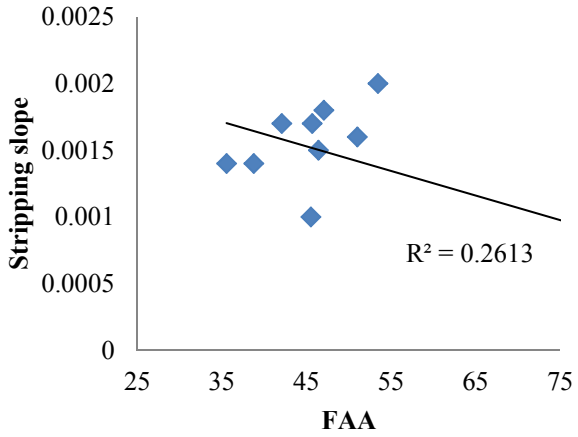

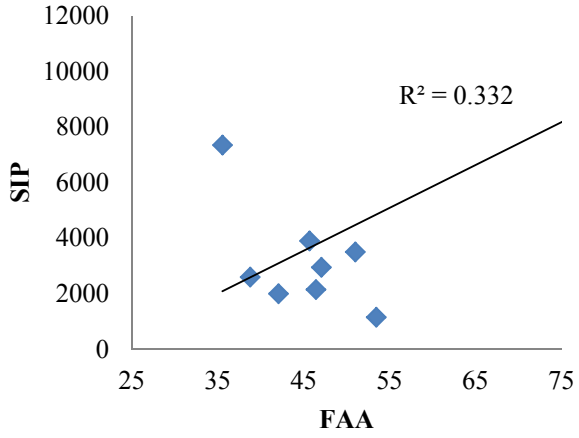

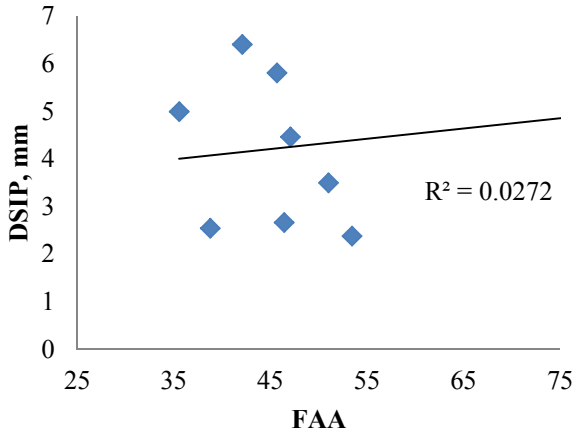

Rigden voids

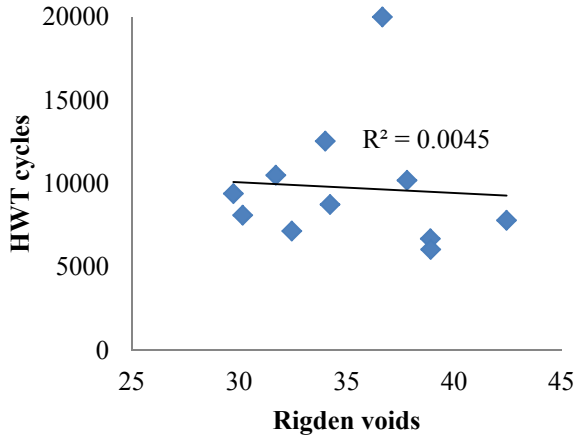

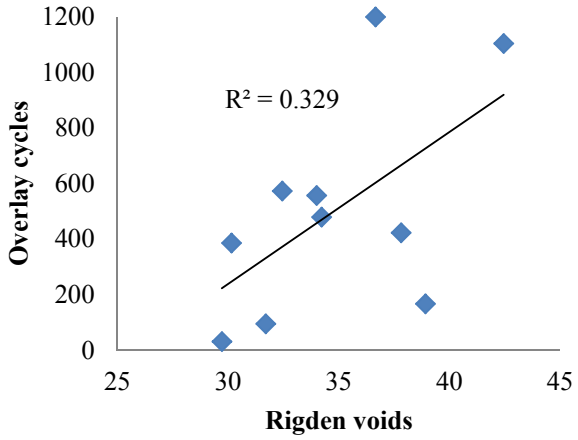

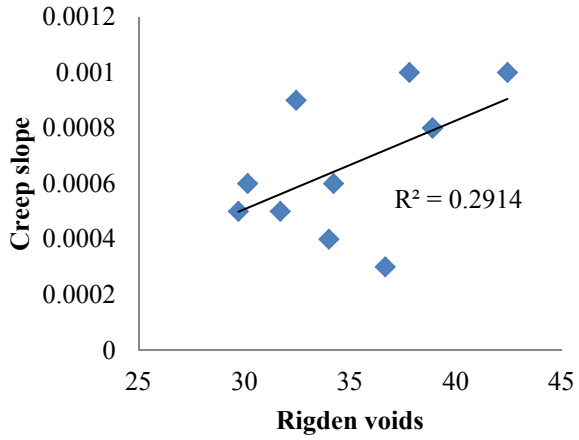

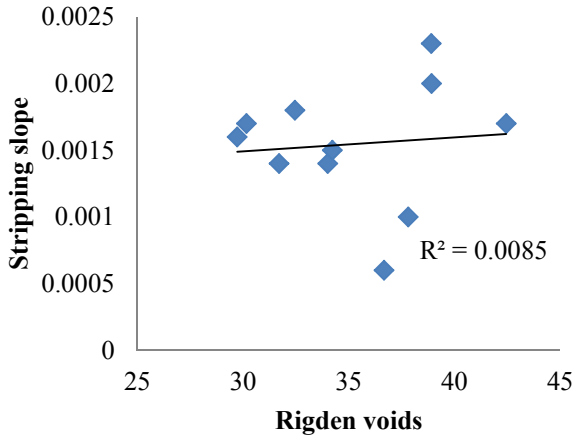

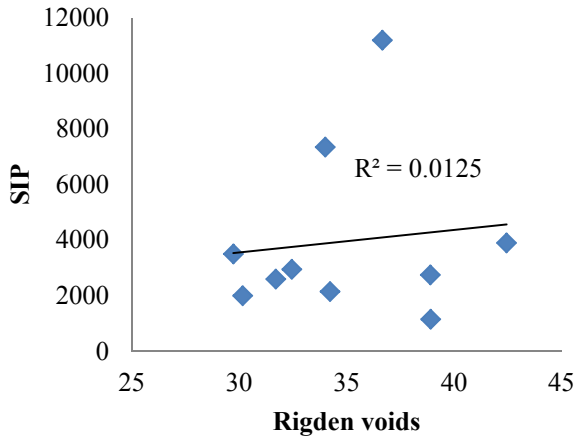

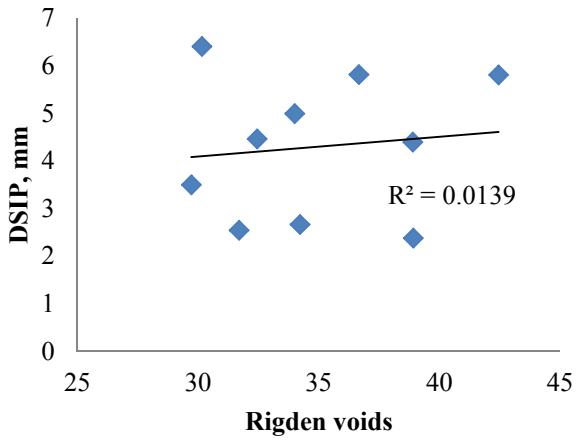

Hydrometer 10 micron passing

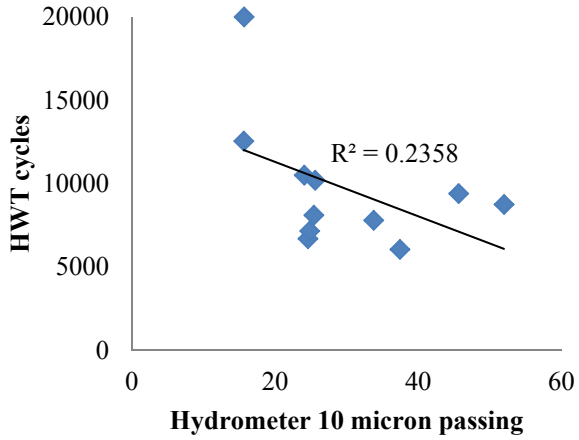

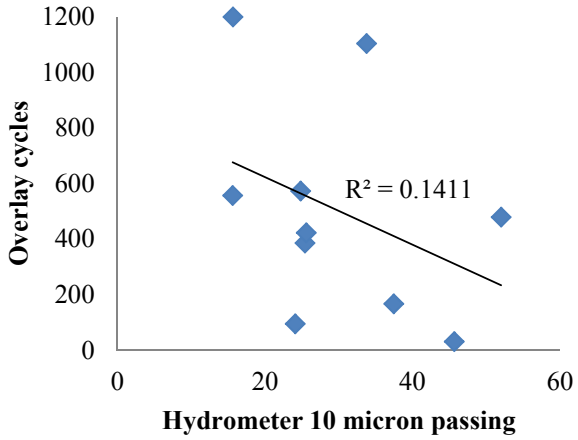

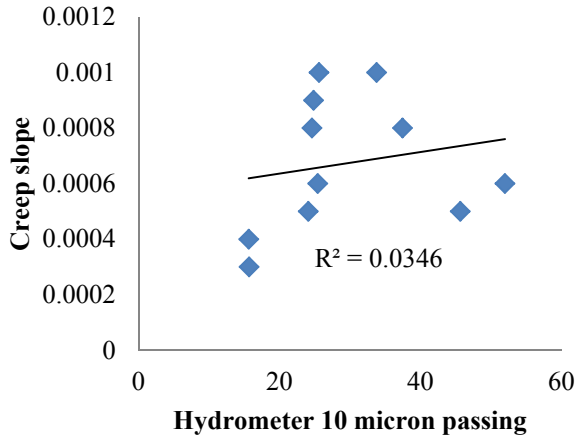

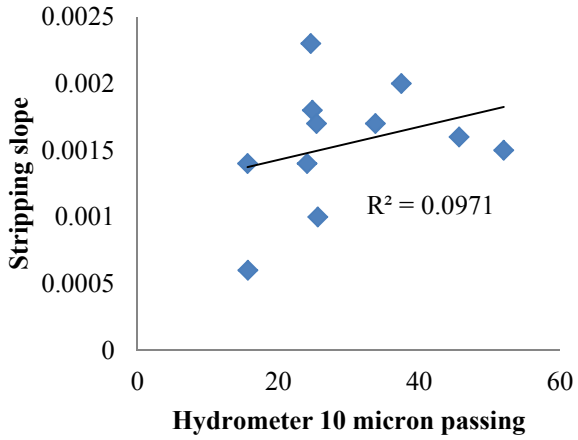

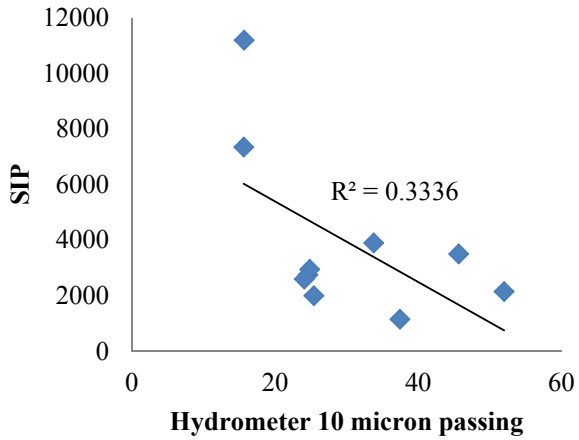

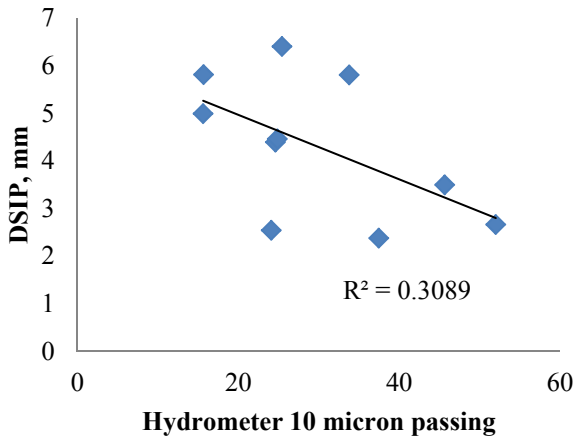

Fineness modulus

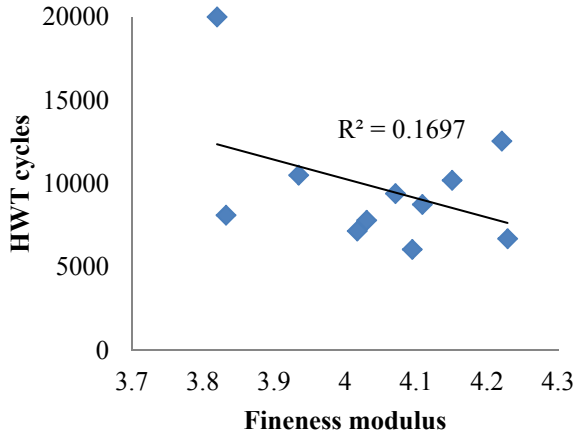

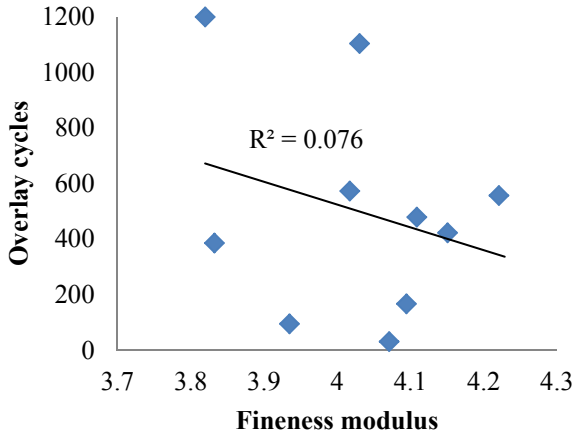

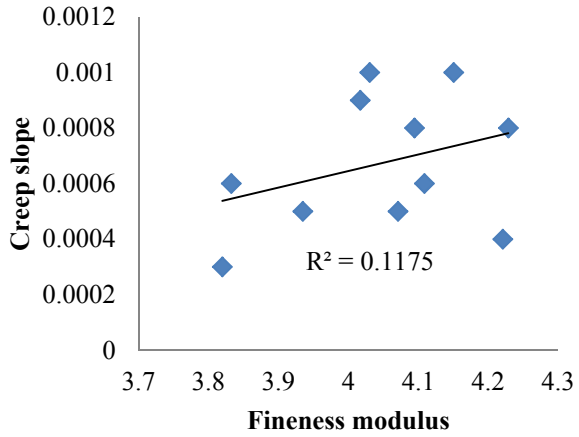

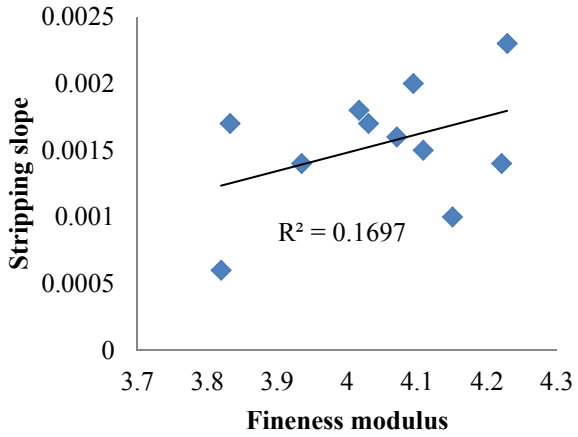

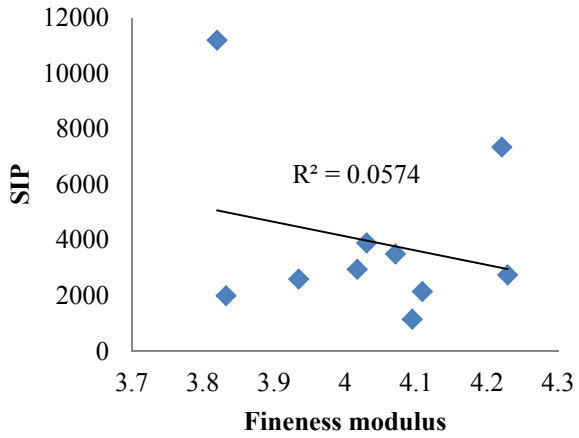

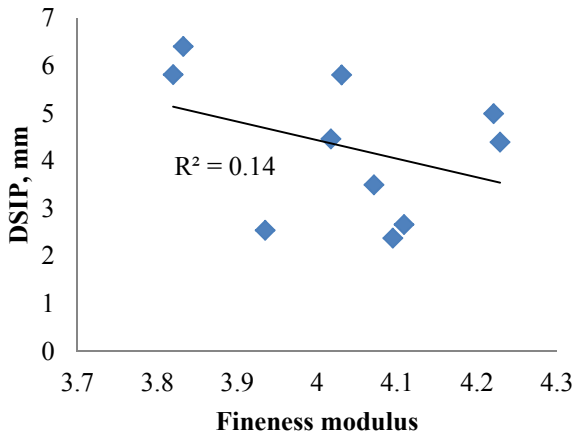

Coarse aggregate proportion

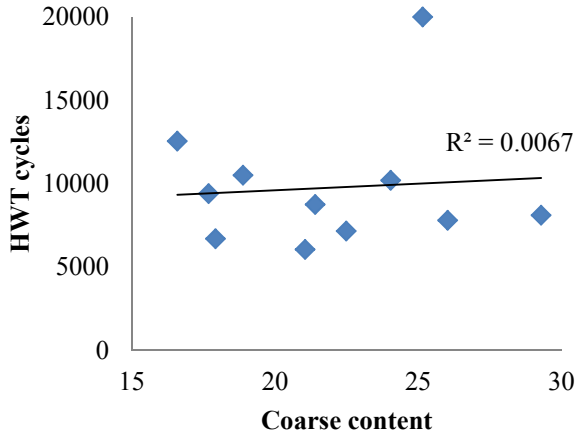

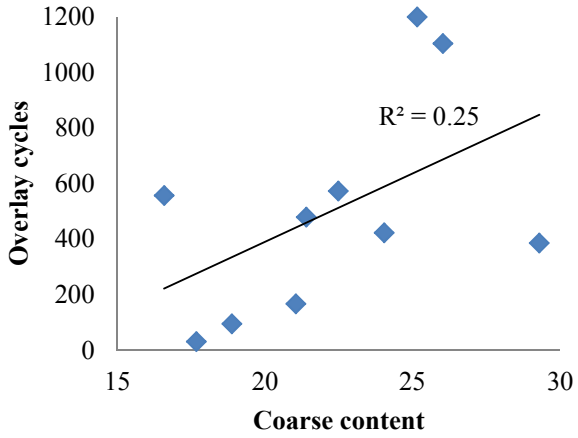

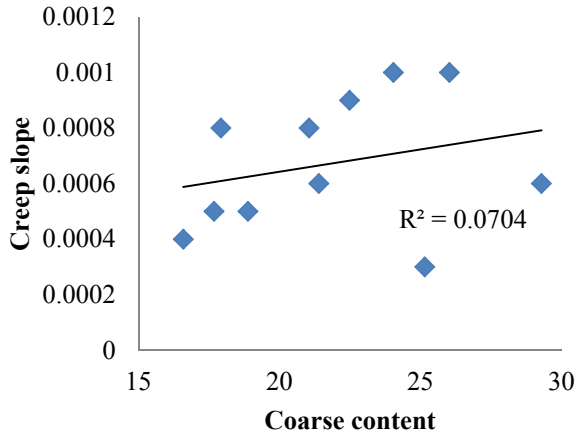

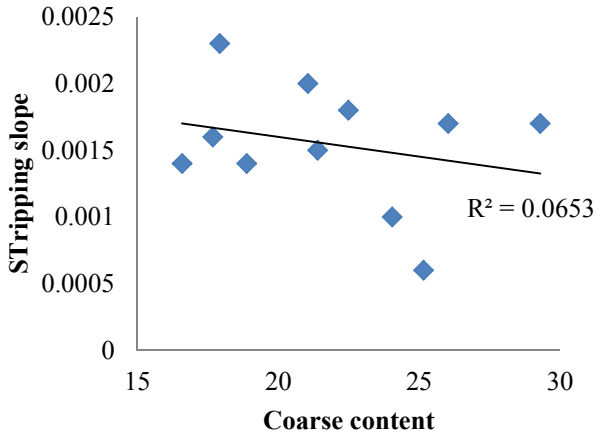

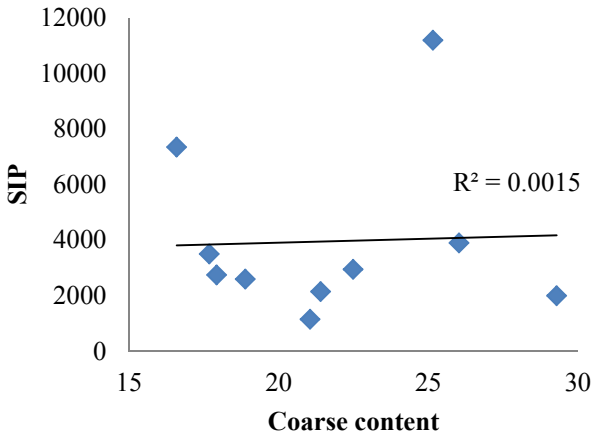

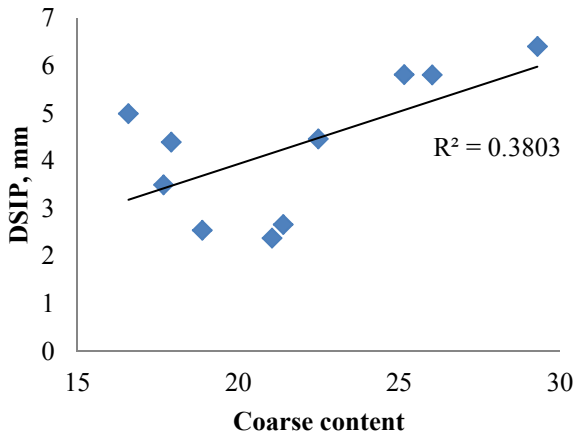

Sand proportion

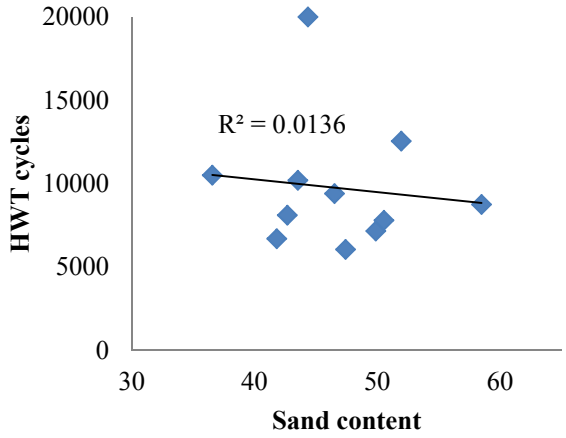

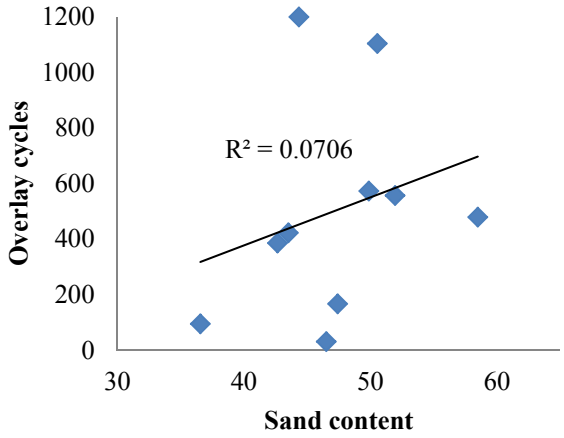

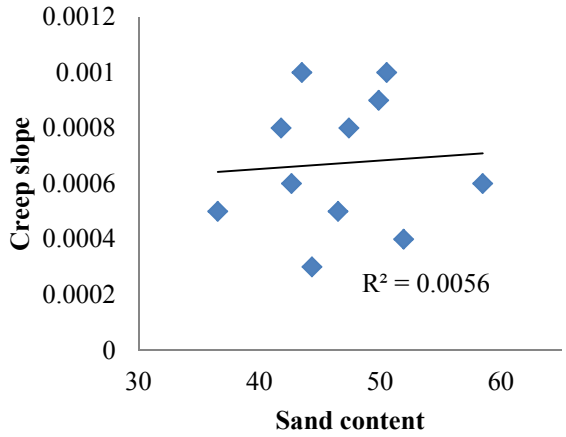

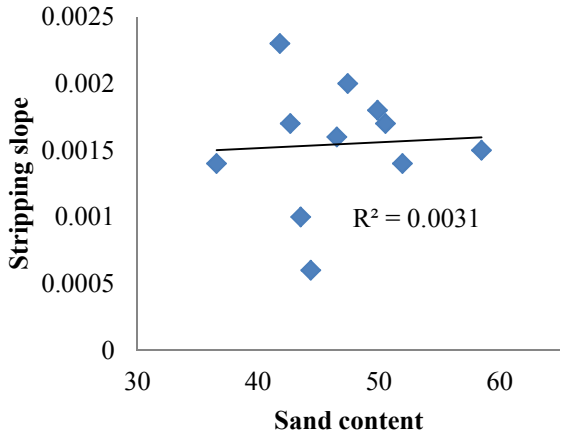

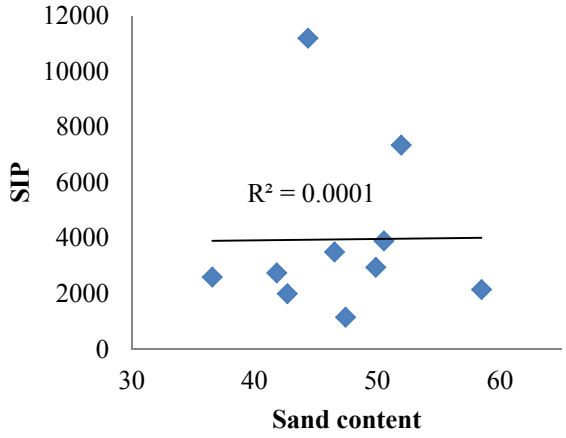

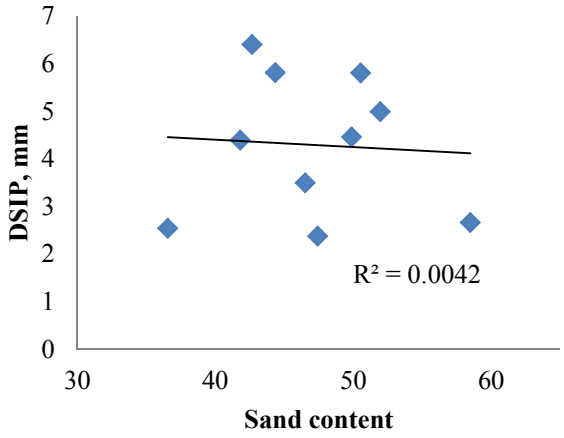

Filler content

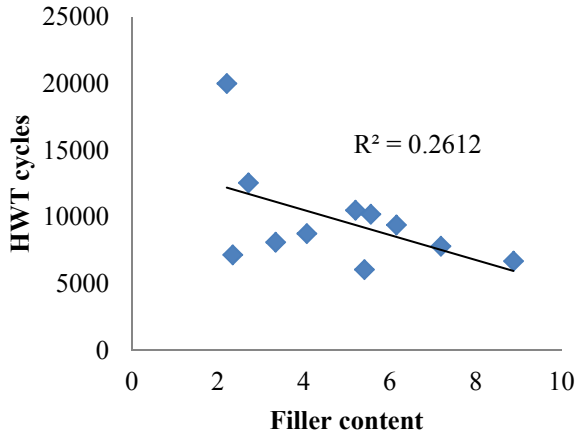

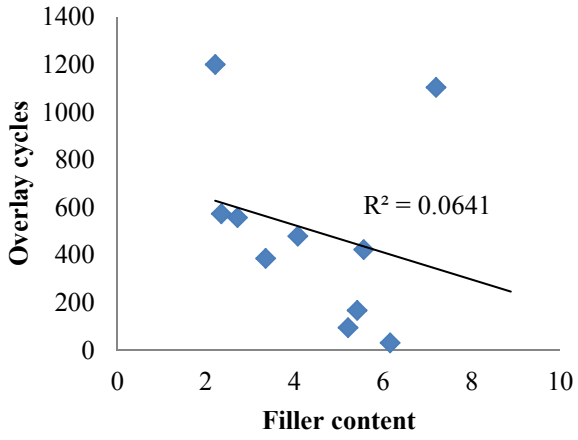

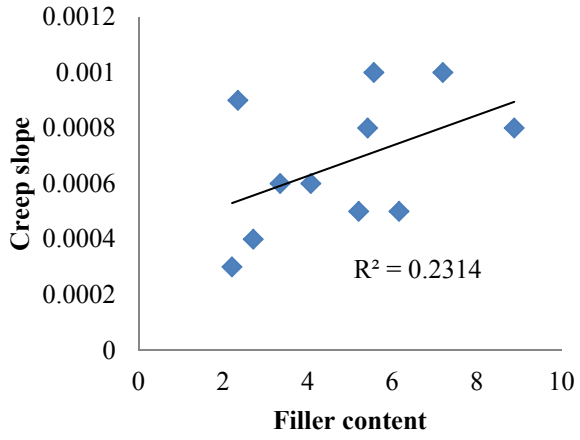

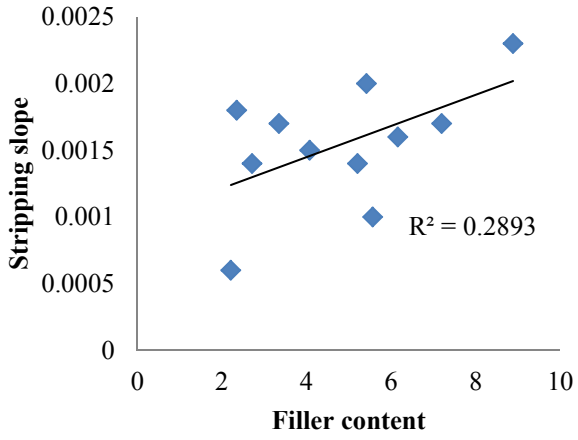

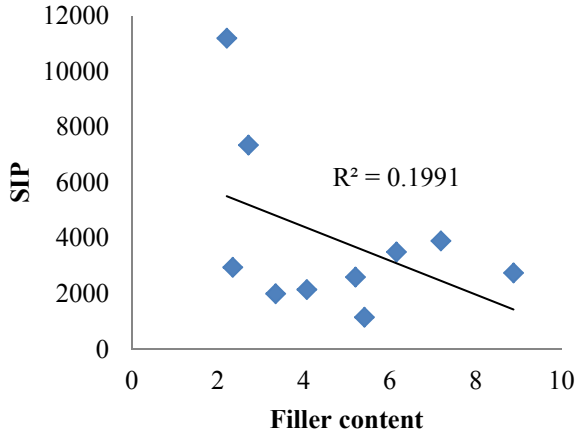

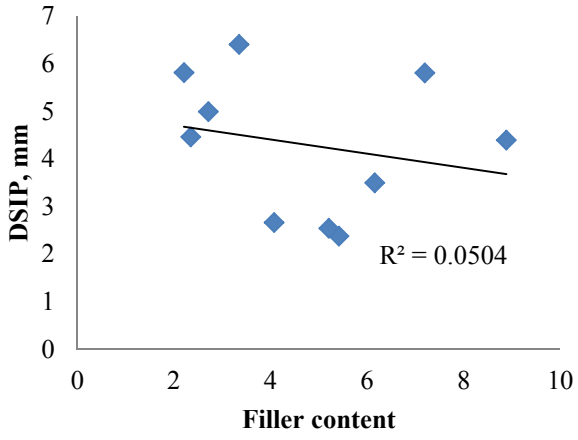

Filler-binder ratio

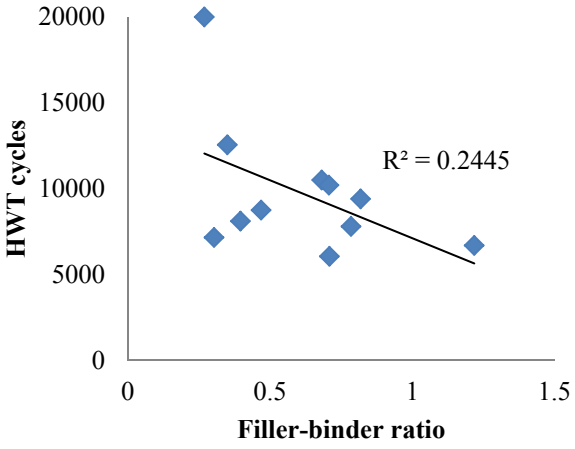

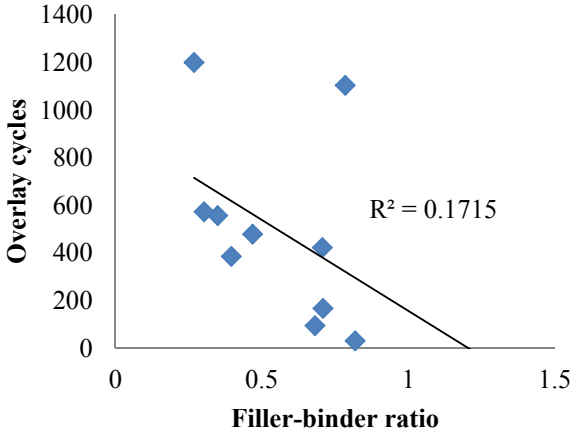

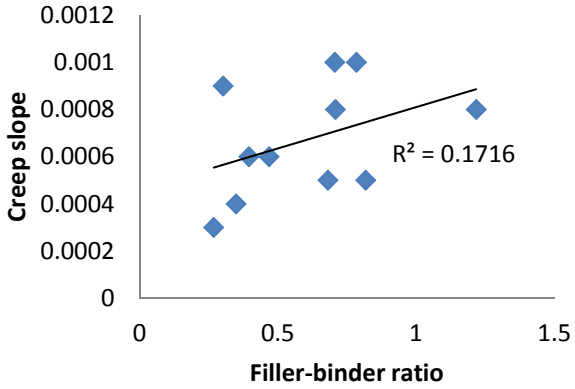

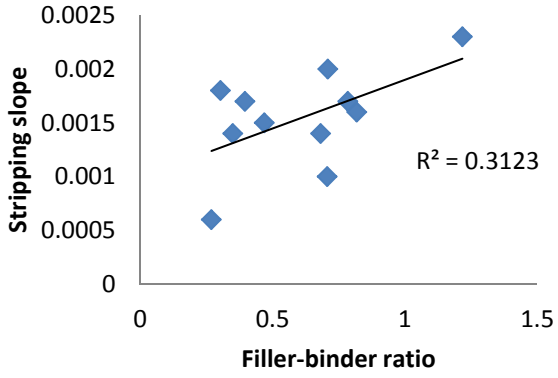

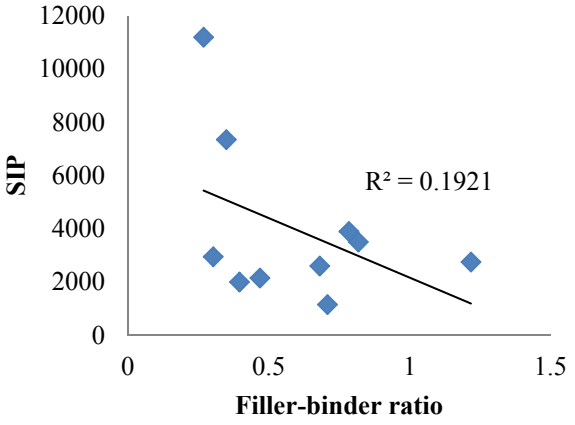

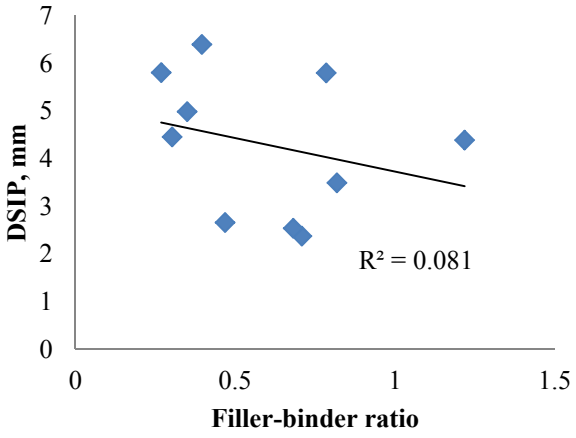

Free binder content

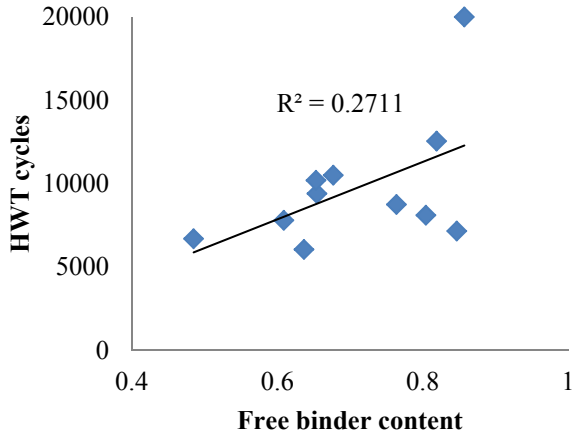

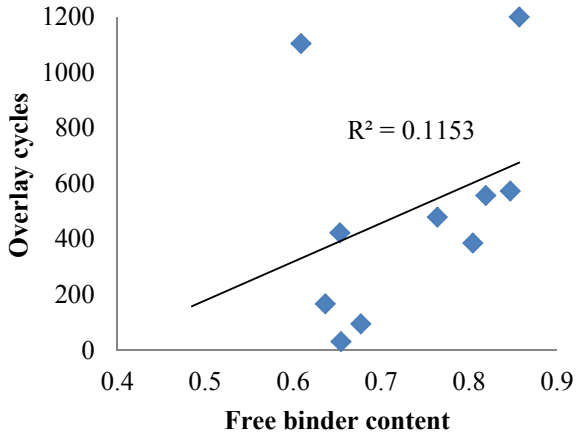

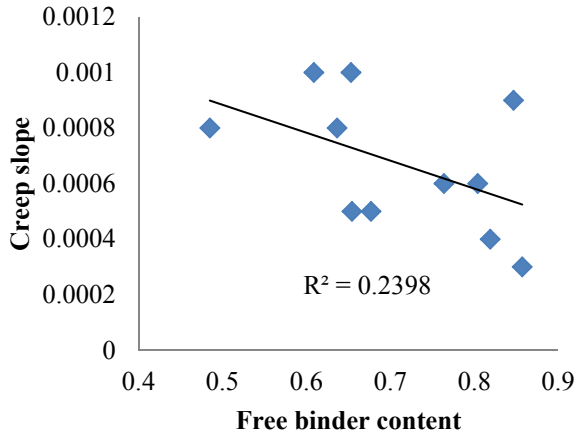

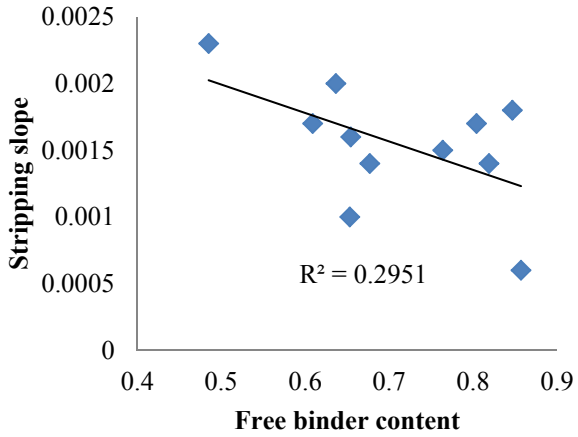

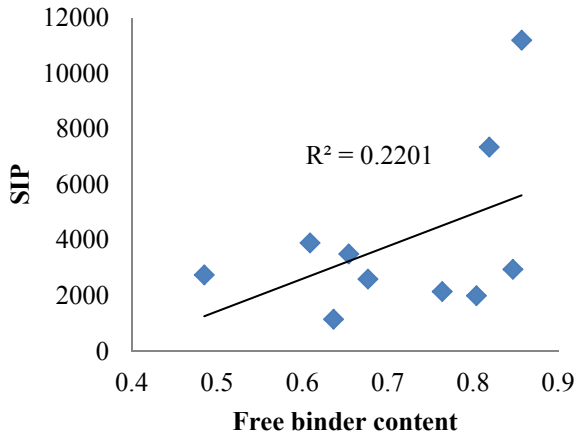

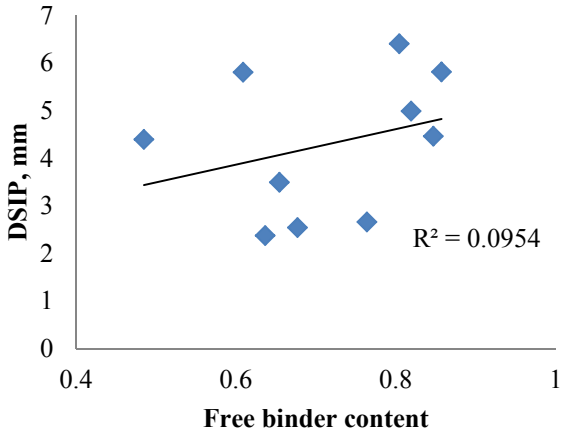

%